TECHNISCHE UNIVERSITÄT DARMSTADT

Department for Renewable Energies
Institute of Electrical Power Systems

RISØ
Wind Energy Department
Risø National Laboratory

PhD thesis

Gabriele Michalke

Variable Speed Wind Turbines - Modelling, Control, and Impact on Power Systems

Variable Speed Wind Turbines - Modelling, Control, and Impact on Power Systems

Vom Fachbereich 18
Elektrotechnik und Informationstechnik
der Technischen Universität Darmstadt
zur Erlangung des Grades eines Doktor-Ingenieurs (Dr.-Ing.)
genehmigte Dissertation

vorgelegt von
Dipl.-Ing. Gabriele Michalke
geboren am 21.09.1978
in Dillenburg

Referent:	Prof. Dr.-Ing. Thomas Hartkopf
Korreferent:	Dr.-Ing. Anca Daniela Hansen
Tag der Einreichung:	04.01.2008
Tag der mündlichen Prüfung:	24.04.2008

D 17
Darmstadt 2008

Erklärung zur Dissertation

Ehrenwörtliche Erklärung zu meiner Dissertation mit dem Titel:
„Variable Speed Wind Turbines -Modelling, Control, and Impact on Power Systems"

Hiermit erkläre ich, dass ich die beigefügte Dissertation selbstständig verfasst und keine anderen als die angegebenen Hilfsmittel genutzt habe. Alle wörtlich oder inhaltlich übernommenen Stellen habe ich als solche gekennzeichnet.

Ich versichere außerdem, dass ich die beigefügte Dissertation nur in diesem und keinem anderen Promotionsverfahren eingereicht habe und, dass diesem Promotionsverfahren keine endgültig gescheiterten Promotionsverfahren vorausgegangen sind.

Gabriele Michalke

Darmstadt, 20.12.2007

Preface

The present PhD thesis deals with the modelling, control, and the impact of variable speed wind turbines on the power system. Due to increasing wind power penetration the power system impact of wind power is a relevant aspect of research. Comprehensive dynamic simulation models of wind turbines are required in order to simulate their interaction with the power system. In the present report dedicated control strategies are developed, which improve the wind turbines´ impact on the power system.

The PhD project was carried out in a co-operation between the Institute of Electrical Power Systems - Department of Renewable Energies at Darmstadt Technical University (Germany) and the research group Wind Energy Systems at the Wind Energy Department of Risø National Laboratory/DTU (Denmark). The duration of the project was from November 2003 to October 2007. The work was mainly funded by the “Stiftung Energieforschung Baden-Württemberg”. Within the project four 3-months research periods were carried out at Risø National Laboratory funded by the scholarship “Herbert-Kind-Preis” of the ETG (German Power Engineering Society) and the DAAD (German Academic Exchange Service).

Summary

Due to the increasing penetration of wind energy in the transmission system modern wind turbines are required to take over the control tasks, which were traditionally aligned to conventional power plants, and to contribute to power system stability. In countries with high amount of wind power, as e.g. Germany and Denmark, such control requirements are specified in grid codes for wind turbines. Goal of the present PhD work is thus the development of dedicated control strategies for variable speed wind turbines, which enable the turbines to act as active components in the power system and to comply with various grid code requirements.

The most promising wind turbine concepts for the future market are investigated in the presented work, namely the doubly-fed induction generator wind turbine (DFIG) and the direct driven wind turbine using a permanent magnet excited synchronous generator (PMSG) connected via a full-scale converter. In a first step, comprehensive dynamic simulation models of both wind turbine concepts are developed. The models represent the aerodynamical and mechanical behaviour of the turbine as well as the entire electrical system including generator, converter and grid connection. The models are implemented in the power system simulation software DIgSILENT Power Factory

In a second step, based on the simulation models advanced control strategies are designed for each considered wind turbine concept. The control is subdivided into two stages: a control for normal operation and a superimposed control for grid faults. The control for normal operation assures variable speed operation at maximum aerodynamic efficiency. However, on demand the turbine can provide active and reactive power according to requests of the power system operator. In case of a grid fault the superior control for grid codes is used. Protection equipment prevents damaging of the turbine under grid faults and facilitates thus fault ride-through. Meanwhile a voltage controller assures reactive power supply for faster voltage re-establishment in the surge of a fault. The basic control principle is the same for both wind turbine concepts, but differs internally due to the different system configuration.

The presented case studies verify the effectiveness of the control strategies. It is shown, that both wind turbine concepts can contribute to power system stability when equipped with such a control system. Comparing the PMSG and DFIG wind turbine it turns out, that the PMSG wind turbine has a slightly better grid support capability, which is due to the full-scale converter.

A promising result of the presented work is, that modern variable speed wind turbines can even help nearby connected conventional stall wind turbines to ride-

through a grid fault by means of the developed control strategies. A high loss of active power production in the surge of a fault due to turbine tripping can thus be avoided.

Zusammenfassung

Aufgrund der zunehmenden Penetration der Windenergie im Übertragungsnetz, wird von modernen Windkraftanlagen gefordert, sich wie konventionelle Kraftwerke zu verhalten und zur Unterstützung der Netzstabilität beizutragen. In Ländern mit hohem Anteil an Windenergie, wie beispielsweise Deutschland oder Dänemark, haben Netzbetreiber solche Forderungen in Netzanschlussregeln für Windkraftanlagen formuliert. Ziel der vorliegenden Arbeit ist daher die Entwicklung geeigneter Regelungsstrategien für drehzahlvariable Windkraftanlagen, um diese zu befähigen, sich als aktive Teilnehmer beim Netzbetrieb verhalten zu können und die Anforderungen der Netzanschlussregeln erfüllen zu können.

In den vorliegenden Studien werden zwei zukunftsträchtige Windkraftanlagenkonzepte untersucht: die Windkraftanlage mit doppelt gespeister Asynchronmaschine (DFIG) sowie die direktangetriebene Windkraftanlage mit hochpoligem permanenterregtem Synchrongenerator und Vollumrichter (PMSG). In einem ersten Schritt werden detaillierte Simulationsmodelle beider Anlagenkonzepte entwickelt. Die Modellbildung umfasst das gesamte aerodynamische und mechanische Verhalten der Windkraftanlage sowie daran anschließend den elektrischen Teil des Systems mit Generator, Umrichter und dem Anschluss ans Übertragungsnetz. Die Modelle werden in der Netzberechnungssoftware DIgSILENT Power Factory implementiert.

Auf Basis dieser Modelle werden dann in einem zweiten Schritt geeignete Regelungsstrategien für die jeweiligen Windkraftanlagen entwickelt. Die Regelung ist unterteilt in eine Regelung für den Normalbetrieb und in eine übergeordnete Regelung für den Fehlerfall. Die Regelung für den Normalbetrieb garantiert drehzahlvariablen Betrieb und maximale Energieausbeute. Nach Bedarf kann die Anlage jedoch auch ihre Wirk- und Blindleistungsbereitstellung nach Vorgaben des Netzbetreibers anpassen. Im Falle eines Netzfehlers kommt die übergeordnete Regelung für den Fehlerfall zum Einsatz. Schutzeinrichtungen sichern ab, dass die Anlage einen Fehlerfall unbeschadet durchfahren kann und eine Spannungsregelung ermöglicht, dass die Anlage Blindleistung bereitstellt, um das Spannungsniveau wiederherzustellen. Das grundlegende Regelungsprinzip ist für beide Anlagentypen gleich. In der Umsetzung der Regelungsstrategien ergeben sich jedoch aufgrund des unterschiedlichen Aufbaus beider Konzepte starke Unterschiede.

Zahlreiche Fallstudien belegen die Wirksamkeit der Regelung. Es wird gezeigt, dass beide Anlagenkonzepte, ausgestattet mit den entwickelten Regelungen, zur Unterstützung der Netzstabilität beitragen können. Aus technischer Sicht kann die PMSG Windkraftanlage aufgrund des Vollumrichters im Vergleich zur DFIG Anlage einen größeren Beitrag zur Netzstützung leisten.

Ein besonderes Ergebnis der vorliegenden Arbeit ist, dass moderne drehzahlvariable Windkraftanlagen mit Hilfe der entwickelten Regelung sogar benachbarten konventionellen Windkraftanlagen ein Durchfahren von Netzfehler ermöglichen können und damit große Einspeiseausfälle vermieden werden können.

Contents

1 Introduction

1.1 Motivation

In the recent public discussion conventional energy production based on fossil energy resources is seen more and more critically. Conventional electrical energy production generally involves CO_2 emissions influencing the global warming negatively. Moreover, at the one hand fossil energy sources are limited while at the other hand an enormous energy demand is expected especially by newly industrializing countries, e.g. India or China. Due to these reasons, in Europe an increasing tendency towards renewable energy sources exists. Wind power, one of the most popular renewable energy sources, has reached a higher percentage as hydropower in countries like Germany and Denmark [BMU 2007]. Denmark has the highest share of wind power in the power system world wide, while Germany has the highest wind power capacity according to amount [AWEA 2004], [BWE 2006]. In future, an increased wind power installation is also expected offshore, e.g. in the European North Sea or the Baltic Sea. Especially offshore wind power installation will take place in larger units.

Wind power, as most of the renewable energy sources, is naturally fluctuating. It possesses thus a different role in the power system compared to conventional power generation units. As long as only single and small wind power units are installed in the power system, wind power does not influence power system operation and can easily be integrated. However, when wind power penetration reaches a significant high level and conventional power production units are substituted, the impact of wind power on the power system becomes noticeable and must be handled.

The increased penetration of wind power into the power system generates new challenges for power system operators, who have to ensure reliable and stable grid operation. In countries with large amount of wind power e.g. in Denmark, Germany or Spain, this has resulted in the power system operators introducing grid codes [E.ON 2006], [Energinet.dk 2004]. These grid codes specify technical grid connection requirements of wind turbines connected to the power system. Wind turbines are requested to act as active components in the grid and have to take over control tasks, which are traditionally aligned to conventional power plants. Basically, these grid code specifications require fault ride-through capability of wind turbines, which addresses primarily the design of the wind turbine controller and the turbine's protection system in such a way, that the wind turbine is able to remain connected to the network during grid faults. Moreover, modern wind turbines are demanded to assist the power system, by supplying ancillary services. This includes primarily reactive power supply to support the voltage level and active power adjustment to maintain the system frequency.

Due to the aspects mentioned above, control equipment enabling both power and voltage control becomes increasingly important [Tande 2003]. Appropriate control strategies for wind turbines must be developed to enable the wind turbines to comply with the grid code specifications. Moreover, advanced control of wind turbines facilitates, that wind turbines can actively support the grid and contribute to power system stability.

Recently, increased research activities all over the world consider those aspects. At the present time wind power research addresses primarily wind power grid integration and power system operation with high amount of wind power. This includes the control and monitoring of wind turbines/wind farms and improvement of actual technologies. In terms of power system operation wind power forecast becomes an important issue. In some research projects the capacity credit of wind power in the power system is estimated. Wind energy research also includes prediction and estimation of future development of wind power production and expected changes of the power generation mix. Questions like “how much wind power will be installed in the next decades”, “how large is the future energy demand”, “which kind of power plants will dominate the power generation mix” and “is the power system capable for such changes” are discussed. Such questions are e.g. considered in detail in the so called “dena study” initiated by both counterparts the German utility partners and the wind power industry [dena 2005]. In addition to that wind energy research focuses on economical issues e.g. the macro economical benefit of wind power or on market mechanisms and market incentives to increase renewable power generation. Especially in new fields like offshore wind power production research activities are required. New challenges have to be faced as e.g. foundation and construction of wind turbines under maritime conditions and grid connection of wind farms over large distances.

The PhD report at hand deals with variable speed wind turbines, their modelling, control and impact on power systems. Due to the increased grid code requirements the tendency of modern wind turbines will be towards variable speed wind turbine concepts with power electronic interface. The presence of power electronics increases control possibilities and enables wind turbines to actively support the grid. Two auspicious variable speed wind turbine concepts are considered in this work, namely the doubly-fed induction generator wind turbine concept and the multipole permanent magnet synchronous generator wind turbine concept with full-scale frequency converter. These wind turbine concepts represent precisely the two chosen wind turbine concepts of the first German offshore wind farm “alpha ventus” [alpha ventus 2007] to be erected in 2008. This underlines the actuality of the present research.

1.2 Objectives and outlines of the thesis

The intention of this PhD project titled "Variable Speed Wind Turbines – Modelling, Control and Impact on Power Systems" is to develop advanced control strategies for variable speed wind turbines, which improve the wind turbine's impact on the power system. As indicated in the title, three main issues form the kernel of the research work: (i) Modelling, (ii) Control and (iii) Impact on power systems.

Modelling

In order to investigate the power system impact of wind turbines, it is essential to use accurate dynamic simulation models of wind turbines and power system. The models must correctly represent the dynamic behaviour of the wind turbines in order to predict critical operation conditions at the one hand and to improve their dynamic performance at the other hand. Hence, those wind turbine models have to be developed and implemented in dedicated power system simulation tools in order to facilitate study on the wind turbines´ interaction with the power system. Power system software tools build the basis for power system simulations and allow steady state load flow analysis as well as dynamic computation of the system. Power system elements as busbars, lines, cables, transformers or conventional generation units are generally built-in elements in such power system simulation software. In contrast to this new renewable power generation units like wind turbines are normally not part of the tools. One focus of the present work is therefore, to develop comprehensive dynamic simulation models of wind turbines, which can be included into the power system tool in order to analyse and to improve the wind turbine's power system impact. The simulation tool chosen for this purpose is the dedicated power system tool "DIgSILENT Power Factory".

The trend in modern wind turbines is clearly the pitch controlled variable speed wind turbine concept with power electronic interface [Hansen 2007b]. Such concept offers enlarged control capabilities, which enable the wind turbine to provide power system ancillary services. As mentioned above, the doubly-fed induction generator (DFIG) wind turbine and the multipole permanent magnet synchronous generator (PMSG) wind turbine, as two representative variable speed wind turbine concepts, are selected for investigation. The modelling is done in a modular structure, which means that all turbine components are modelled separately. The models of the mechanical parts of the wind turbine can be used for both concepts, while the electrical system and its control are modelled specifically for each concept.

The comprehensive simulation models serve to analyse the turbines´ dynamic behaviour. Based on this, advanced control strategies are developed to enhance the wind turbines´ dynamic performance and to improve their power system impact.

Control

In the present work the control system to be developed for the considered wind turbines is divided into two parts: (i) a basic control strategy for normal undisturbed operation and (ii) a specific control for grid faults and grid code accomplishment.

The basic control strategy is designed to optimize the wind turbine's energy capture. The control interacts with the power electronic interface, i.e. the frequency converter, and the pitch mechanism of the turbine. The control is designed and optimized by means of analytical considerations and verified by simulations.

This basic control strategy is then extended with a specific control strategy for fault ride-through and grid support tasks. Today, wind turbines are required to participate as active components in the power system, similar to conventional power plants. Although there are various aspects related to this problem, in this project the focus is limited to fault ride-through and grid support capability of wind turbines. Fault ride-through addresses the control and protection of the turbine in case of grid faults, so that the wind turbine can remain connected to the grid during grid faults. Moreover, dedicated control strategies are developed which enable the considered wind turbines to actively support the grid voltage by reactive power supply.

Impact on Power systems

Grid codes are generally more detailed and more stringent for the high and extra high voltage network. Moreover, the installation of larger units and especially of large offshore wind farms will always require connection to the high voltage grid. As wind power is generally connected to the grid in remote areas, where the network is weaker, the power system impact of wind power is of special importance. An objective of the present work is thus to analyse grid code accomplishment and voltage grid support of the considered wind turbine concepts. Hence, various case studies are performed by means of a generic transmission power system model, to which the wind turbine models are connected. By means of this, the impact of modern variable speed wind turbines on conventional stall and active stall wind turbines is investigated, too. Finally, the grid support capability of DFIG wind turbines and PMSG wind turbines will directly be compared.

The PhD report is organized as follows:

Chapter 2 "Wind power integration issues" presents the current status of wind power production. The problematic of wind power integration in terms of power system stability is addressed and the most important grid code requirements are summarized.

Chapter 3 "Wind turbine concepts" introduces all marketable wind turbine concepts at present and their different characteristics are emphasized. Moreover, the different wind turbine concept's market penetration over the last years is shown.

In Chapter 4 titled “Mechanical system and control of variable speed wind turbines” the modelling process of all mechanical parts of the wind turbine system is explained. The mechanical model can be used for both considered wind turbine types and comprises models for the wind, the aerodynamic rotor and the drive train. A control acting on the blade pitching mechanism is described.

Chapter 5 “DFIG wind turbine – Electrical system and control” focuses on the doubly-fed induction generator wind turbine concept. The theory of the generator’s steady state as well as dynamic performance are presented. Based on this an advanced control of the frequency converter is developed. The control is designed and optimized based on the wind turbine’s response to deterministic and stochastic wind speed changes.

In Chapter 6 “DFIG wind turbines´ grid support capability” the control system of the DFIG wind turbine is extended by a specific control strategy for fault ride-through and grid support capability. First, the dynamic behaviour of DFIG wind turbines in case of grid faults is analysed in detail. Based on this, a control and protection system is implemented, which enables wind turbines to ride-through faults and to support power system stability in order to comply with grid code requirements.

Similarly investigations to those presented in Chapter 5 and 6 are presented in Chapter 7 “Multipole PMSG wind turbine - Electrical system and control” and Chapter 8 “Multipole PMSG wind turbines´ grid support capability” but this time for the permanent magnet synchronous generator wind turbine concept. First, a model of the PMSG wind turbine is implemented and a control for normal undisturbed operation is developed. Then, in Chapter 8 a control for fault ride-through and grid support is presented.

Finally, Chapter 9 analyses the “DFIG and PMSG wind farm’s impact on the power system”. The models for these wind turbine concepts are included into a generic power system model and four case studies are carried out, in order to assess the interaction between wind farms consisting on such wind turbine concepts and the power system during grid faults. A direct comparison of the performance of DFIG and PMSG wind turbines is presented.

Each chapter closes with a short summary. “Conclusions” and a summary of the total report are given in the last Chapter 10.

2 Wind power integration issues

In some countries such as Germany and Denmark wind power has reached a significant level in electrical power production. Due to the increased penetration of wind power and its growing impact on the power system wind power integration issues become more and more important in those countries. Moreover, the role of wind power in the power system has changed in the last years. Traditionally, wind turbines where connected decentralised to the distribution system. Today large-scale wind farms are directly connected to the transmissions grid. Thus, large wind farms must adopt the tasks of conventional power generation units, such as the control of active and reactive power flow. In several countries the required control tasks of wind turbines, connected to the power system, are specified in grid codes, introduced by the transmission system operators. In order to comply with the grid codes and to assess and improve grid integration of wind power, dynamic wind farm models as part of power system simulation tools are necessary [Tande 2003].

In the present chapter wind power integration issues are examined. First, the current status of wind energy and its anticipated development in the next decades is briefly presented. Then the wind power impact in power system stability is discussed and an overview over German and Danish grid codes is given. Finally, relevant aspects in terms of wind turbine modelling in appropriate power system simulation software are addressed.

2.1 Current status of wind energy

In Germany and Denmark wind power is today the biggest renewable energy source for electrical energy production with a share of approx. 5.7% [BWE 2006] and 20 % [AWEA 2004], respectively, of the annual energy production. With 3,136 MW installed wind power capacity Denmark has today the highest share of wind power in the power system world wide, while Germany has the highest wind power capacity according to amount with 20,622 MW [EWEA 2007] in 2006. Figure 2.1 shows the accumulated wind power of the whole world with a forecast up to the year 2014. The share of Europe and Germany is illustrated in Figure 2.1 as well. According to this forecast the world-wide installed wind power will increase enormously in the next years and decades.

Figure 2.2 [DEWI 2006] gives a separate overview over the wind energy development in Germany from 1990 on and presents a forecast up to the year 2030. From the year 2010 on, wind power development in Germany is presumed to be mainly affected by offshore installations or repowering of old turbines. According to Figure 2.2 and to the outlines of the German government published in “Strategie der Bundesregierung zur Windenergienutzung auf See” [dena 2002] an ongoing growth of wind

power installations and further development of the wind power technology can be expected. The dena-Study [dena 2005], a well-known study about grid integration of onshore and offshore wind energy in Germany, forecasts 48,200MW installed wind power in Germany for 2020. The target of the European Union for the year 2020 is to cover the energy demand by 20 % renewable energy sources, with a major contribution coming from wind energy [EU 2007].

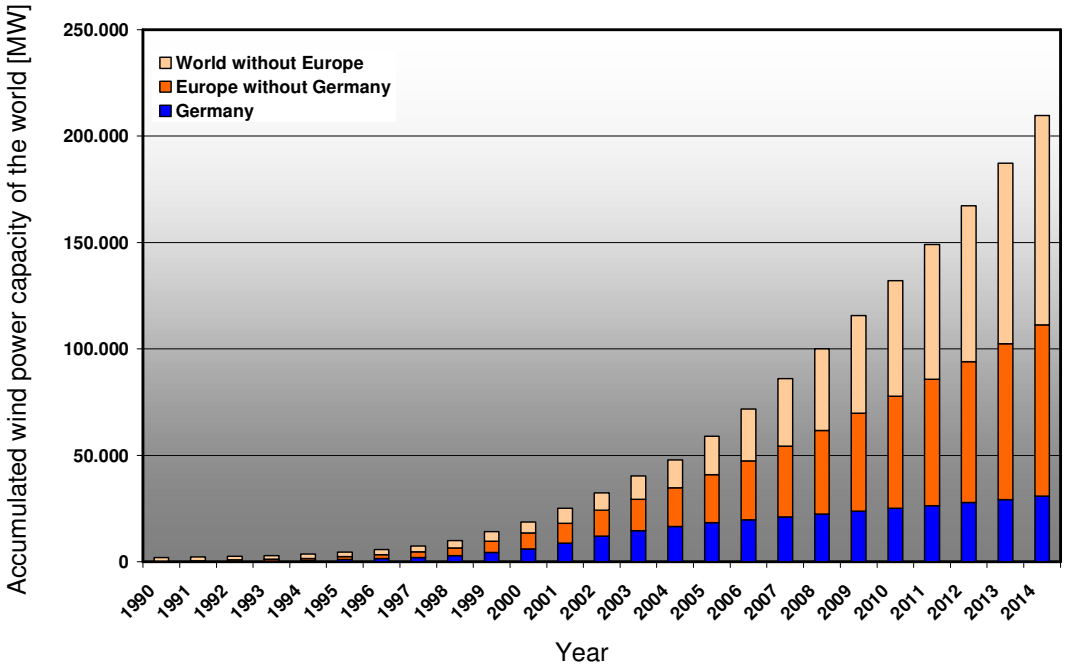

Figure 2.1: Accumulated wind power capacity of the world, Europe and Germany [DEWI 2006]

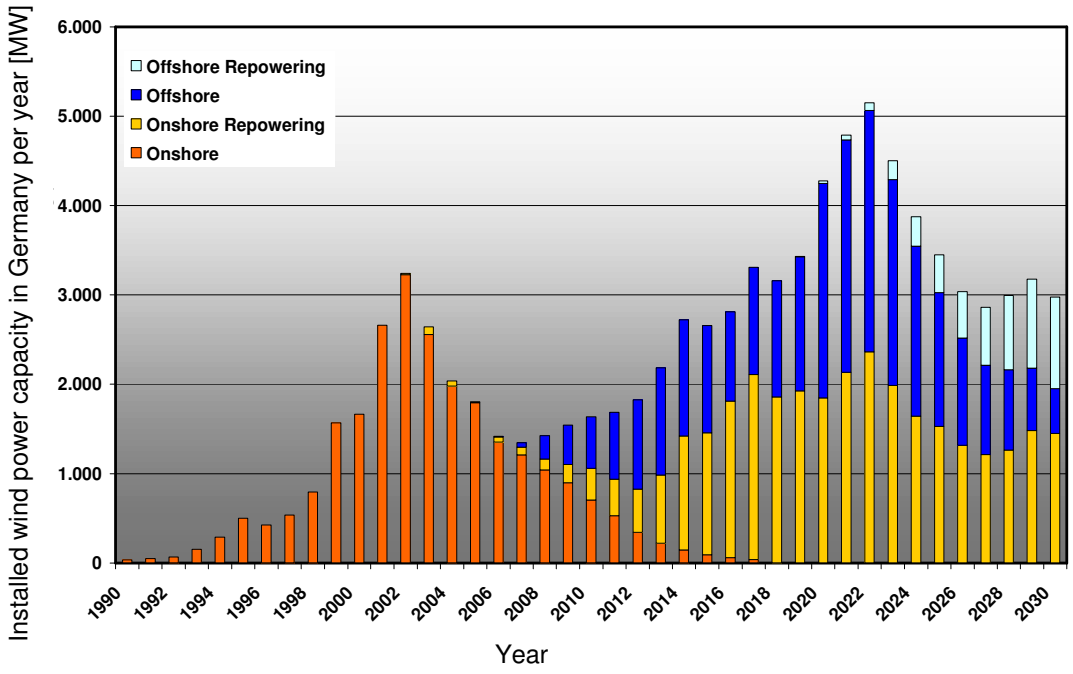

Figure 2.2: Installed wind power capacity in Germany per year [DEWI 2006]

The eminent increase of wind power capacity is due to both the increased number of installed wind turbines at the one hand and the increase in wind turbine size at the other hand. Figure 2.3 demonstrates the change of wind turbine size concerning turbine power, rotor diameter and hub height over the years from 1980 until 2005. Today modern wind turbines have a power of generally 1 MW - 3 MW and a rotor diameter of more than 60 m. Moreover, 5 MW prototype turbines already exist, which indicates that there is a clear tendency to even larger units. In the present PhD report wind turbines of 2 MW power with a rotor diameter of 40 m are considered in the investigations as they are representing the recent state of the art.

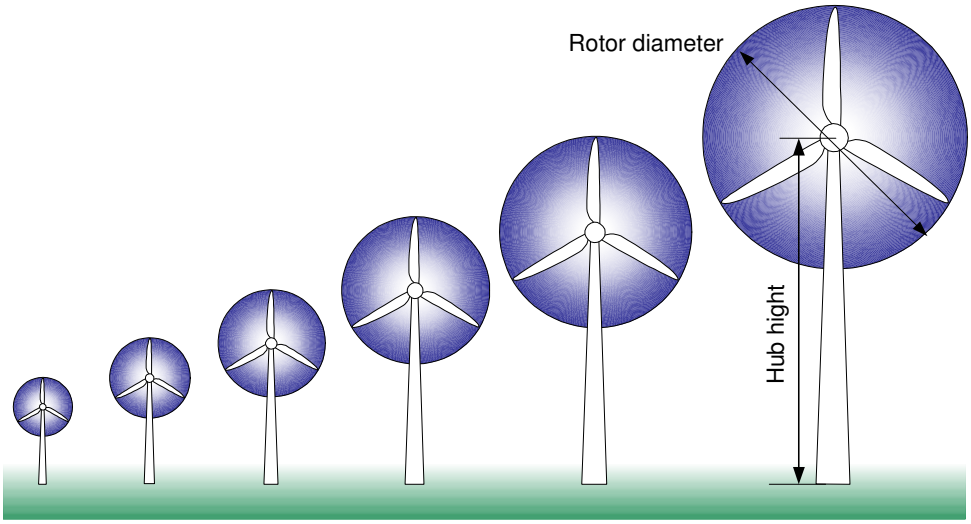

	1980	1985	1990	1995	2000	2005
Rated power	30 kW	80 kW	250 kW	600 kW	1500 kW	5000 kW
Rotor diameter	15 m	20 m	30 m	46 m	70 m	115 m
Hub height	30 m	40 m	50 m	78 m	100 m	115 m
Annual energy yield	35 mWh	95 mWh	400 MWh	1250 MWh	3500 MWh	approx. 17000 MWh

Figure 2.3: Development of wind turbine size [BWE 2007]

Due to the increasing wind power penetration and the larger installed units, the characteristics of wind power in power systems have also changed. As mentioned above wind turbines were traditionally connected to the distribution system, while today large wind farms are directly connected to the transmission system, replacing capacity, which was originally provided by conventional centralised power plants. Thus, power system operation and power system stability is significantly influenced by this development. This aspect is discussed in the following subsection.

2.2 Impact on power system stability

As stated in [Tande 2003] basic experience has been gained concerning wind power in distribution systems. Up to now, small wind power units were connected to the distribution system without any concern about the impact on power system stability and voltage quality, as their influence was little. However, today wind farms are of larger size (several 100 MW) and therefore connected to the transmission system, causing a significant impact on the power system. This is due to the following reasons [Ackermann 2005]:

- The contribution of conventional power plants to power system control is decreasing due to unbundling, decentralisation and replacement of conventional power plants by renewable energy sources, especially wind power.
- Wind power is installed in larger units, e.g. offshore wind farms, and therefore the impact of wind power becomes significant.
- Wind power is often installed at remote places and in weak grids, e.g. at coastal areas far away from the consumption centres.
- Wind power is a fluctuating power source depending on the prevailing wind and must be balanced.
- Larger variation in generation and consumption causes larger current fluctuations and node voltage variations, which must be balanced.

Power system stability is thus a matter of interest in terms of large wind power penetration or wind power in very weak grids and needs to be investigated. Power system stability addresses primarily two tasks:

(i) voltage control - reactive power compensation
(ii) frequency control – active power dispatch

(i) In order to keep the system voltage constant at each busbar in the grid, the reactive power production and consumption must be equalized at each point in the system. This task was traditionally performed by large centralized power plants placed in vicinity to the grid nodes at which reactive power compensation was necessary. A problem occurs if this task is today assigned to wind turbines located at remote places in distance to the consumption centres. Furthermore, some wind turbine concepts have reactive power demand by themselves, which varies depending on the wind speed and which must be compensated, too. The ability of wind turbines to supply reactive power is also a very important issue in respect of short term voltage stability, e.g. after voltage dips due to grid faults. Thus, voltage control capability of wind turbines becomes an increasingly important aspect regarding wind power grid integration and the wind turbine's market potential. [Ackermann 2005]

(ii) As wind energy is naturally a fluctuating power source, frequency regulation and active power dispatch become a challenging factor when the available power production is uncertain [Tande 2003]. Another aspect in this context is, that wind turbines until now were allowed to disconnect in case of grid faults. In areas with high wind power this could cause a significant loss of electrical power production due to disconnection of large wind turbines, which could negatively influence system stability and lead to major blackouts. Thus, transmission system operators require of wind turbines to be able to ride-through temporary faults, so that large losses of active power supply can be avoided. It must furthermore be investigated to which extend wind

power can contribute to primary and secondary control. A proposed solution to this problem is e.g. to curtail wind power and to release the power reserves when needed.

Due to the increasing impact of wind power on the power system, countries with a high share of wind power, such as Germany and Denmark, have introduced grid codes, specifying control tasks for wind turbines in order to assure safe and stable operation of the power system. An overview over the present grid code requirements in Germany and Denmark is briefly presented in the following subsection.

2.3 German and Danish grid codes

Up to 5-6 years ago, most grid codes did not require wind turbines to support the power system during a grid disturbance – wind turbines were only required to be disconnected from the grid when an abnormal grid voltage was detected. With the increased capacity of wind power in the power system over the years, a sudden high loss of power during grid faults, due to wind turbines´ disconnection, could generate control problems of frequency and voltage in the system, and as worst case a system collapse. The increased penetration of wind energy into the power system over the last decade has therefore lead to a serious concern about its influence on the dynamic behaviour of the power system. It has resulted in the power system operators revising nowadays the grid codes in several countries, such as in Germany and Denmark [E.ON 2006], [Energinet.dk 2004]. Basically, for wind power these grid codes require an operational behaviour more similar to that of conventional generation capacity and more responsibility in network operation. An overview of existing grid connection codes is given in [Jauch 2004.] and [Bolik 2003]. These regulations are generally determined for wind farms connected to the transmission grid but some power system operators also specify grid codes for distribution systems. The attention in these requirements is drawn on both the wind turbines fault ride-through capability and on wind turbine grid support capability, i.e. their capability to assist the power system, by supplying ancillary services [Hansen 2007b]. These ancillary services concern today generally the following issues [Milborrow 2005]:

Fault ride-though

The fault ride-through demand requires of wind turbines to stay connected to the grid during faults in order to avoid significant losses of active power production in systems with high amount of wind power. Before the fault ride-through requirement was introduced wind turbines had to disconnect in case of a fault. As most of the wind turbines were predominantly conventional fixed speed wind turbines with direct grid connected generator they could cause large inrush currents at voltage recovery [Soerensen 2007]. With installation of the anticipated wind power of 48,200MW in Germany for 2020 such disconnection could however cause a sudden loss of several thousand megawatts.

Thus, wind turbines, which are connected to the power system today, are requested to ride-through grid faults.

The fault ride-through requirement addresses both an advanced design of the wind turbine controller [Hansen 2007b] and the development of new technologies/equipment in wind turbines [Erlich 2006], which both enable the wind turbine to remain connected to the network and to continue normal operation and power production directly after fault clearing. The fault ride-through requirement defines rules of how long and how deep a voltage drop must be at which the wind turbines are allowed to disconnect [Milborrow 2005].

Reactive power supply

During grid faults the system voltage drops in vicinity to the location of the fault. In order to support the voltage level and voltage re-establishment, voltage control and reactive power supply are required by transmission system operators. The ability to deliver reactive power to the grid is strongly dependent on the wind turbine technology. Grid codes require not only compensation of the wind turbine's own reactive power demand but also additional reactive power supply in dependency of the voltage dip. The requirement can however be met by means of capacitor banks and power electronics connected close to the wind turbines. Moreover, modern variable speed wind turbines with frequency converters can accomplish the demand by means of advanced control.

Frequency stability

Another issue related to system stability is the operation of the generation units under deviating frequency. First, it must be assured that the generation unit stays connected to the system even if the frequency varies. Second, the frequency response of the generation unit, i.e. the ability to contribute to primary and secondary control, is important. Thus, the grid codes specify rules to adapt the wind turbine's active power production according to frequency changes in the system. This, however, can cause problems, as wind is naturally fluctuating so that active power is not necessarily available on demand. Nevertheless, some grid codes, e.g. the Danish grid code [Energinet.dk 2004], precisely specify to which extend wind turbines must contribute to adjust their power output. On demand of the transmission system operator the wind power production must be reduced below its optimal output (delta control) and the gradient of the power production is specified and limited (gradient constraints).

Other aspects concerning a longer time frame are the contribution to active power supply on demand, the requirement to provide balancing power and to curtail wind power production in order to provide spinning reserve. In this respect wind power forecast and the introduction of incentive market mechanisms for wind turbine operators become important issues.

Additionally to the requirements mentioned above, transmission system operators demand modelling, simulation and verification of the wind turbine system. Communication and external control for the wind turbine especially for large wind farms are also required but represent anyway standard equipment in modern wind turbines. Other grid requirements as e.g. the contribution of wind farms to perform a "black start", which means to start and operate in an islanding system, are discussed but no yet specified [Milborrow 2005].

Grid codes are generally different for wind turbines connected to medium voltage grids or high/extra high voltage grids [Energinet.dk 2004], [E.ON 2006] and are more stringent for the high voltage network. Today, most of the wind turbines are still connected to the medium voltage grid. However, the installation of larger units and especially of large offshore wind farms will always require connection to the high voltage grid [Erlich 2006]. As stated in [Ackermann 2005], in contrast to distribution systems the R/X value of transmission systems is lower, which intensifies the need of reactive power control. Thus, the most rigorous grid code requirements for high voltage grids refer to fault ride-through capability and reactive power control especially during voltage sags [Robles 2007]. Focus in the present PhD work will therefore be on fault ride-through and grid support capability of wind turbine connected to the transmission system with voltages above 100 kV. As the Danish power system and the control area of the German transmission system operator E.ON Netz GmbH undergo the worldwide highest share of wind power in their systems, the respective grid code specifications of Energinet.dk [Energinet.dk 2004] and E.ON Netz GmbH [E.ON 2006] concerning fault ride-through and reactive power support are representatively illustrated in the following.

Energinet.dk

The Danish transmission system operator Energinet.dk requires of each wind turbine manufacturer to provide a simulation model of the wind turbine system in an appropriate power system software (e.g. DIgSILENT, PSSE). Based on this simulation model a test report must be delivered to the transmission system operator, which verifies the dynamic behaviour of the wind turbine under grid faults. The simulation of the grid fault must be performed under the following conditions. Before the fault incident the wind turbine must operate at a wind speed, which results in production of rated power and at nominal speed. Moreover, full compensation of the system is required before the short circuit happens. It is sufficient to simulate a three-phase short circuit, as this short circuit represents a worst case scenario. The electricity system must be modelled by a Thevenin equivalent as illustrated in Figure 2.4. The grid is characterized by an R/X ratio of 0.1 and has a short circuit power S_k of ten times the wind turbine power $P_{\text{wind turbine,rated}}$. The wind turbine is connected to the grid via the machine transformer. In order to simulate the short circuit, a predefined voltage profile must be applied to

the voltage source. The voltage profile is illustrated in Figure 2.5. The test report must state the RMS values of the wind turbine's characteristic quantities.

The fault ride-through requirement is specified by the voltage profile. The voltage profile simulates a voltage drop down to 25 % rated voltage lasting for 100 ms continuing with a linear increase of the voltage up to 75 % at 750 ms after the fault incident. 10 seconds after the fault incident the voltage recovers totally to above 90 %. The voltage profile defines a lower margin, above which the wind turbines are not allowed to disconnect. If a grid fault results in a voltage drop below the defined voltage profile, disconnection will be tolerated.

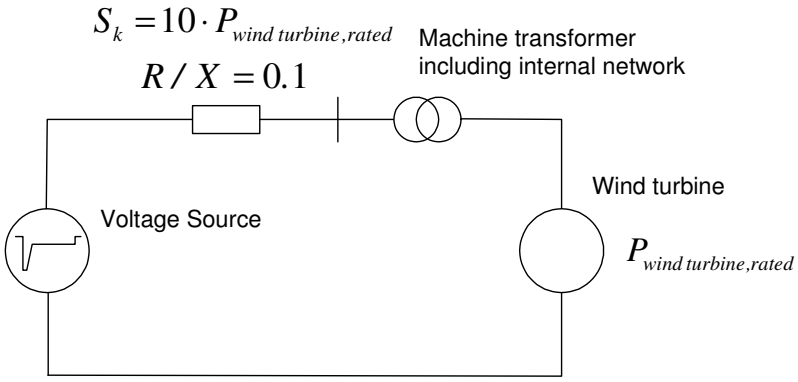

Figure 2.4: Single-phase diagram of the Thevenin equivalent applied for short circuit simulation [Energinet.dk 2004]

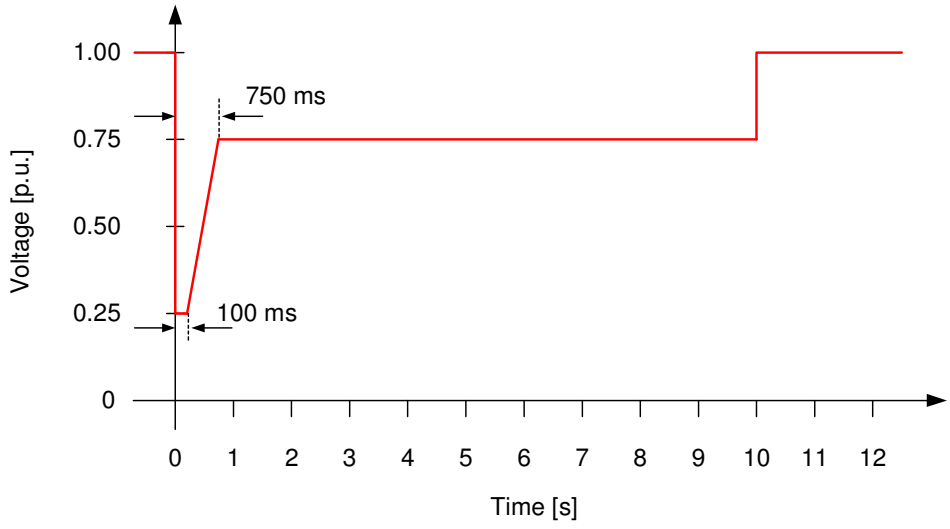

Figure 2.5: Voltage profile for fault ride-through requirement of Energinet.dk [Energinet.dk 2004]

The Energinet.dk grid code specifies furthermore the active and reactive power production of the wind turbine during the grid fault. During the voltage dip the active power in the connection point must meet the conditions of the following equation:

$$P_{current} \geq 0.4 \cdot P_{t=0} \cdot \left(\frac{U_{current}}{U_{t=0}} \right)^2 \quad (2.1)$$

with

P_{current}	Actual active power measured in the connection point (during fault)
$P_{\text{t=0}}$	Power measured in the connection point immediately before the fault
$U_{\text{t=0}}$	Voltage in the connection point immediately before the voltage fault
U_{current}	Actual voltage measured in the connection point (during fault)

In addition to that, the wind turbine can contribute to reactive power supply with the remaining reactive current. This means, that depending on the provided active power, reactive power supply can also be accomplished. The wind turbine must therefore be able to produce or absorb a maximum reactive current of 1 p.u. In contrast to the E.ON grid code the amount of reactive current, which must be provided, is not explicitly specified.

E.ON Netz GmbH

The German transmission system operator E.ON Netz GmbH was the first power system operator, who introduced grid codes for wind turbines and is followed now by many other network operators in several countries. Concerning fault ride-through and reactive power supply during grid faults the grid codes of E.ON Netz GmbH are similar to the specification given by Energinet.dk.

E.ON defines a slightly different voltage profile shown in Figure 2.6 defining the limiting curve, above which fault ride-through of wind turbines is required. The voltage profile is divided into 4 areas. Above the dotted line corresponding to area 1 no tripping of the generation unit is permitted. The solid line, defining area 2 requires also fault ride-trough but allows short term interruption of the generation unit in case of occurring instability. The voltage profile defines a voltage drop down to 0 % for 150 ms continuing with linear voltage recovery to 90 % at 1.5 s after the fault incident. The voltage drop defined by E.ON is thus deeper and longer compared to the Erngi-net.dk profile. However, on the other hand the requirement of Energinet.dk to ride-through a fault with a 75 % voltage level for 10 s is more severe than the E.ON requirement in terms of total voltage re-establishment. For area 3 and 4 in Figure 2.6 no fault ride-through is required.

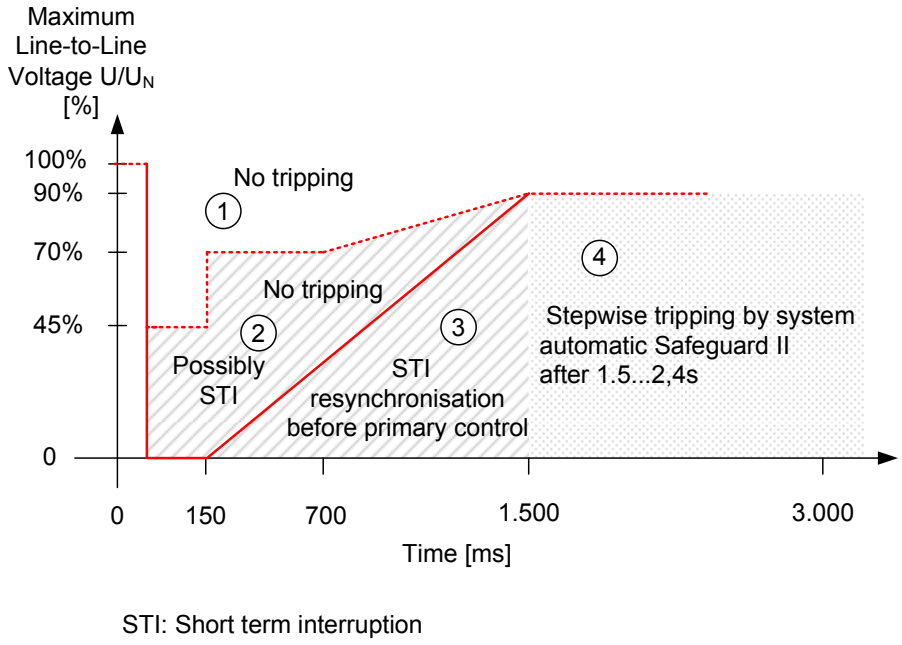

Figure 2.6: Voltage profile for fault ride-through requirement of E.ON Netz GmbH [E.ON 2006]

In contrast to the Energinet grid code E.ON Netz GmbH preferentially requires reactive power supply during voltage sags. Figure 2.7 specifies how much reactive current the wind turbine must deliver in dependency of the voltage level. Beyond a dead band of ± 10 % around rated voltage the reactive current must be increased according to the following equation:

$$\left(I_Q - I_{Q0}\right) \geq 2 \cdot \frac{\left(U - U_0\right)}{U_N} \cdot I_N \tag{2.2}$$

with

I_Q	reactive current
I_{Q0}	reactive current before the fault
I_N	rated current
U	current voltage
U_0	voltage before the fault
U_N	rated voltage

For voltage drops below 50 % of rated voltage maximum reactive current of 1 p.u. is required. In addition to that, E.ON specifies, that the voltage control must be able to provide the required reactive current within 20 ms rise time after fault detection. In contrast to the Energinet.dk grid code no active power production is specified during the fault. This means, that reactive power supply is prioritized and maximum reactive

power is required for voltage drops below 50 %. Thus, no current for active power production remains.

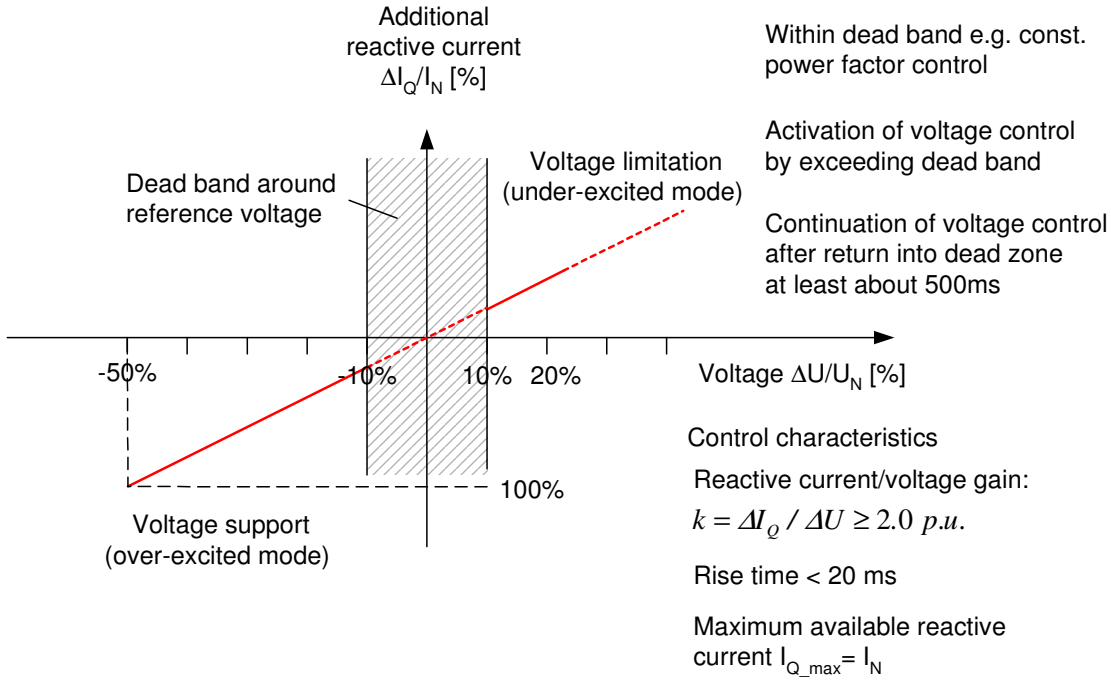

Figure 2.7: Principle of voltage support by reactive current injection during grid faults specified by E.ON Netz GmbH [E.ON 2006]

The compliance of variable speed wind turbines with the grid codes defined by Energinet.dk and E.ON will be presented in Section 6.4 and Section 8.4, respectively. The effect of wind farm integration in the power system depends both on the wind farm control ability to fulfil the grid requirements and on the power system design to which the wind farms are connected. This fact has challenged different wind turbine manufactures and initiated important research activity regarding the ability of different wind turbine concepts to comply with the power system operator's requirements. There is presently large research activity over the world, which carries out model simulation studies to understand the impact of system disturbances on wind turbines and consequently on the power system itself [Akhmatov 2003a], [Soerensen 2003] and also the present work aims to provide an important contribution to that.

2.4 Modelling issues

It has been shown, that power system stability is a concern in power systems with high amount of wind energy. In order to analyse the impact of wind power on the power system, appropriate power system simulation tools are required as well as wind turbine/wind farm models to be included into such simulation tools [Tande 2003]. Dynamic wind farm models as part of power system simulation tools facilitate investiga-

tions of wind power grid integration problems and enhance the development of innovative grid integration techniques [Tande 2003]. Modelling of the interaction between wind farms and the power system enables to predict critical operation conditions so that power system operation can be improved. In a broader sense modelling can be used to design and optimize the power system of the future, when even larger amounts of wind power must be integrated, so that investment risks can be minimized.

For this purpose several power system simulation tools, such as e.g. PSS/E, SIMPOW, PSCAD/EMTDC or DIgSILENT exist. These tools include built-in models of generators, network components etc. and allow for load flow simulations and dynamic simulation of power systems [Tande 2003]. However, as remarked in [Tande 2003], models for wind turbines and wind farms are not a standard feature within these power system simulation tools. It is thus essential to develop appropriate wind turbine and wind farm models for power system analysis and to incorporate these models into the power system simulation tool.

The model's level of detail is dependent on the chosen time frame of the simulation. The simulated time frame is in turn determined by the purpose of the simulation. If e.g. the contribution of balancing power of wind turbines is assessed, a much longer time frame must be taken into account than for investigations of transient stability. The presented work focuses on optimal control of variable speed wind turbines under fluctuating wind speed as well as on voltage grid support capability during faults, which yields a time frame from milliseconds to minutes. Figure 2.8 gives an overview over different wind turbine control tasks and their alignment to the respective time frame.

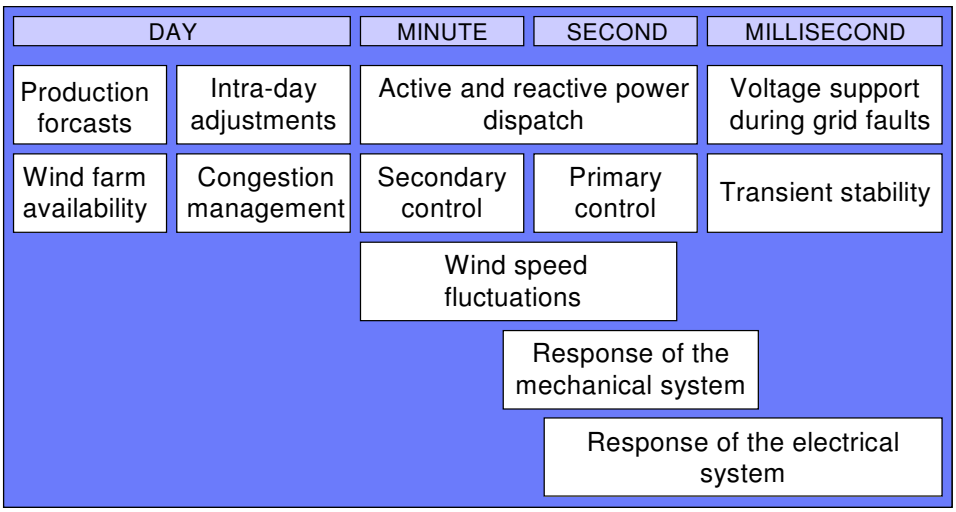

Figure 2.8: Classification of wind turbine performance according to time frame inspired by [Morales 2007] and [Holttinen 2007]

Days

The availability of wind power and the production forecast for wind farms is an important matter for power system operation and power flow. Such aspects concerning long term operation of wind turbines as e.g. wind power contribution to intra-day adjustments and congestion management are aligned to a time frame of days. However as the presented work focuses on wind turbine control for optimal turbine operation during fluctuating wind speeds and during grid faults this time frame is beyond the scope of the presented studies.

Minutes and Seconds

Wind speed fluctuations are a matter of seconds to minutes. Thus, wind turbine control for fluctuating wind conditions and the dynamics of their controllers need a response time of some milliseconds to seconds. The presented work also focuses on the wind turbine's capability to provide active and reactive power during fluctuating wind speeds. Thus, active and reactive power dispatch within seconds to minutes as indicated in Figure 2.8 is investigated in the presented work.

Milliseconds

In case of grid faults voltage support capability of wind turbines and their influence to transient stability becomes an important issue. A very small time frame of milliseconds must be considered when the impact of wind turbines on the power system during grid faults is investigated. This means, that a careful modelling of wind turbine performance according to a time frame of milliseconds is required. The response of the wind turbine's electrical system to grid faults will also be within a time span of milliseconds to seconds after the fault, while the mechanical system has a higher response time, due to larger time constants of mechanical components. As wind speed fluctuations are slow, compared to grid fault duration, wind speed changes must not be considered in grid fault investigations.

Another aspect concerning modelling of wind turbines is computation time and simplification of models. Today large wind farms can consist of several hundred wind turbines. This would results in a very high modelling effort together with too high computational time. However, as the impact of large wind farms to the power system is the kernel of the presented work it becomes necessary to represented the wind farm in a simplified way without confining the result's accuracy. A possibility to gain adequate simplification and reduction of computational effort, without decommissioning of accuracy, is to represent the wind farm as an aggregation model, a method, which is carried out in [Pöller 2003], and partly adopted in the here presented studies.

The necessity of wind turbine modelling and relevant modelling issues have been discussed in the present subsection. In accordance to [Tande 2003] it can be con-

cluded that application of dynamic wind farm models as part of power system simulation tools allows for detailed power system studies and enhances the development of appropriate control techniques for wind power grid integration. The continuous development of such analysis tools facilitates that improved technologies for wind power grid integration can be found and are necessary factor to ensure the worldwide growth of wind energy use.

2.5 Dynamic simulation tool

The present report focuses on modelling of wind turbines for power system studies. In order to investigate the interaction between wind power and the power system it is essential to integrate dynamic wind turbine models into power system simulation software. As the DIgSILENT Power Factory software package is a dedicated and approved power system simulation tool, which has been established for wind power modelling purposes in the last years, it is chosen to be the appropriate software for the objective of this work. Comprehensive wind turbine models for power system simulations have for example been developed and implemented at Risø National Laboratory in the DIgSILENT Power Factory software package [Hansen 2003]. Parts of those models are adapted and used in the present PhD work. As these models are documented extensively in a row of publications [Hansen 2002], [Hansen 2003], a brief documentation of the respective models is given in the thesis at hand.

DIgSILENT (DIgital SImuLator for Electrical NeTwork) is an object-oriented software and provides a vertically integrated model concept, which means that models can be shared for different categories as generation, transmission, distribution and industrial applications [DIgSILENT 2005]. It is therefore used by many utilities and power system operators, which underlines the benefits of including dynamic wind power models into the power system simulation software.

DIgSILENT provides a comprehensive library of built-in models for electrical power system components such as generators, motors, relays, circuit breakers, motor driven machines, dynamic loads and various other passive network elements as e.g. lines, cables, transformers, static loads and shunts, etc. Relevant for wind turbine modelling are dynamic built-in models for solid and salient pole synchronous generators, doubly-fed induction machines with integrated frequency converter and asynchronous generators with various rotor configurations (wound rotor, cage rotor, external rotor resistances etc.). The generator models are enhanced with saturation effects and slip dependent parameters. Furthermore, PWM converters, soft-starter and other power electronic elements are implemented in the power system simulation tool. The built-in models can refer to predefined types or user-defined data types. The so created types can be stored in a global or internal user database.

In addition to that, it is possible to create user-written models in a dynamic simulation language (DSL = DIgSILENT simulation language). The language includes mathematical descriptions of continuous linear and non-linear systems [DIgSILENT 2005]. Own sets of differential equations can be implemented. DSL models can interact with the provided built-in models from the database library and interface with all DIgSILENT functions as e.g. load flow, fault analysis and stability, etc. By means of provided built-in models from the database library together with the dynamic simulation language DSL it becomes possible to create comprehensive dynamic turbine models, which are interacting with the power system. Especially for the development of superimposed control systems, the DSL language is an appropriate instrument. The DSL language makes it possible to analyse the dynamic power system behaviour in the time domain.

Since DIgSILENT is a power system simulation tool, a main function is the load flow calculation. Active and reactive power dispatch can be analysed based on a Newton-Raphson algorithm. Furthermore, the load flow calculation is the first step of each dynamic simulation as it computes the initial values of the model. The initial values e.g. for generators are thus indirectly predefined by the power system to which they are connected. Based on a solved load flow calculation, the DIgSILENT simulation function determines the initial conditions of all power system elements, fulfilling the requirements that the derivative of all state variables of loads, machines, controllers, etc. are zero at simulation start, i.e. in a stationary operating point. In order to avoid transients, the initial conditions of the user defined models have to match with the DIgSILENT initialisation.

DIgSILENT provides two methods for dynamic simulation: a simulation with RMS values and with instantaneous values. The first method computes the RMS values of the simulated parameters and considers the electromechanical transients of the models, while the second method considers the model's electromagnetic transients (EMT) and thus computes the instantaneous values of each simulated signal. The EMT method is recommended for power system transient problems such as switching overvoltages, resonance problems or subtransient effects during grid faults [DIgSILENT 2005]. Since this method uses instantaneous values, it needs a longer simulation time than RMS simulation, however, only short time periods have to be considered. For power system studies as control analysis or power quality, the RMS method is more convenient. If e.g. the dynamic wind turbine behaviour in a time range over a few seconds and minutes must be analysed, electromagnetic transients are beyond the scope of the study. Longer periods have to be taken into account so that the simulation time must be significantly reduced. The RMS simulation is performed for either a balanced or un-balanced network representation. A dynamic simulation can manually or by schedule be interrupted and started again and events, such as short circuit or switching events can be defined.

2.6 Summary

The present chapter provides a survey of the relevant aspects related to wind power grid integration. The current status of wind energy and the recent state of the art is presented by assessing the most important statistics and forecasts. This analysis justifies, that research on the wind power's power system impact is of increasing importance. In some countries as Germany and Denmark, wind power has reached a significant penetration level in the power system. Due to this reason power system operators have introduced grid codes, which request wind turbines to act as active components in the power system similar to conventional power plants. The most rigorous grid code requirements for high voltage grids refer to fault ride-through capability and reactive power control especially during voltage sags. Hence, these issues are focus of the present PhD work.

In order to analyse the impact of wind power on the power system appropriate power system simulation tools are required. In addition to that, detailed dynamic simulation models of wind turbines/wind farm must be developed and included into such simulation tools. For this purpose, DIgSILENT Power Factory is assessed to be an appropriate power system software and its most important features are emphasized. The level of detail of the models, to be developed, is related to the time frame of the simulation. For analysis of power system stability and the wind turbine's response to grid faults or fluctuating wind loads a respective time frame from milliseconds to minutes is relevant.

3 Wind turbine concepts

Since the beginnings of wind turbine development (~1980) until today (2007), where wind energy is seen as a mature technology and has become an important participant in the power generation branch, various wind turbine concepts and designs have been developed. The marketable wind turbine concepts can be distinguished by different electrical design and control and can be classified by their speed range (variable speed, fixed speed) and power controllability (stall, pitch control) [Hansen 2007a]. In the following, a general overview about wind turbine components and topology is given. Then the characteristics of different wind turbine concepts are presented and their market penetration is evaluated. Finally the wind turbine concepts are assessed in respect to their controllability, grid code accomplishment and future market prospects.

3.1 Wind turbine components

The entire system of a grid connected wind turbine includes several components, which contribute with their specific function in the energy conversion process from wind energy into electrical energy. Figure 3.1 illustrates the main components of a modern wind turbine, which are to a greater or lesser extent common for all wind turbine concepts.

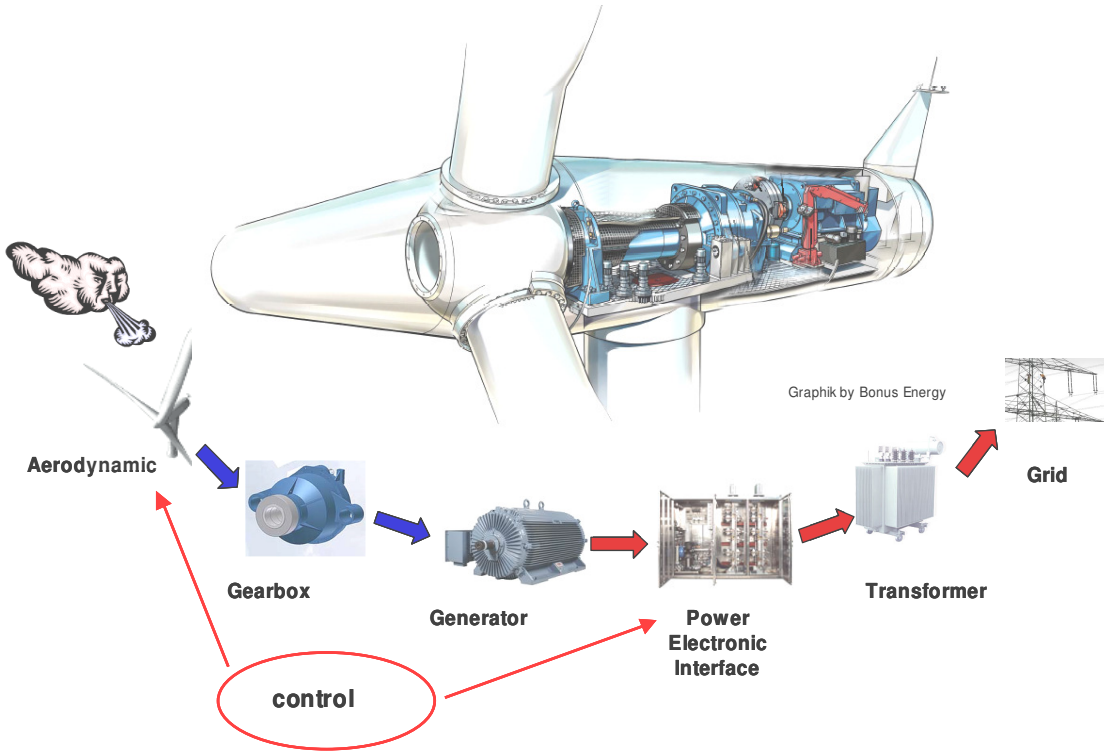

Figure 3.1: Wind turbine components [Risø/DNV 2007]

The figure illustrates from left to right the aerodynamical and mechanical part of the wind turbine (aerodynamic rotor and gearbox), the electrical system (generator, power electronic interface and transformer) and finally its connection to the grid. An interaction with the control system is indicated as well. The different turbine components can be subsumed under four main groups [Pierik 2004]:

1. ***Mechanical and aerodynamical components:***
   - Rotor effective wind
   - Turbine rotor
   - Blade pitching mechanism
   - Drive train (flexible shaft, bearings)
   - Emergency breaks
   - Gear
   - Tower

2. ***Electrical components***
   - Generator types
     - Squirrel cage induction generator
     - Wound rotor induction generator
     - Doubly-fed induction generator
     - Permanent magnet synchronous generator
     - Electrical excited synchronous generator
   - Power electronic interface
     - Softstarter
     - Capacitor bank
     - Static VAR compensator
     - Frequency converter
   - Protection system
   - Transformer
   - Cable

3. ***Control system***
   - Converter controller
   - Blade angle controller
   - Overall controller (TSO demand)

The fourth main group, called “grid components” contains components, which do not directly belong to the wind turbine itself; however, when the impact of wind

turbines with the power system is investigated the grid components play a major role.

4. Grid components – interacting with grid connected wind turbines

- Conventional power plants (synchronous generators)
- Frequency and voltage controller
- Consumer load
- Transformer
- Cable
- Busbars

3.2 Characteristics of different wind turbine concepts

Four different wind turbine concepts have predominated the global market in the last decade [Hansen 2007a]. These concepts are thus introduced in the following. For the sake of uniformity the same classification of concepts as presented in [Hansen 2007a] and [Ackermann 2005] is made.

Type A: Fixed speed wind turbine concept – Danish concept

Figure 3.2 shows the widely used and most conventional turbine concept. A stall or active stall controlled aerodynamic rotor is coupled via gearbox to a squirrel cage induction generator (SCIG), which in turn is directly (by transformer) connected to the power grid. A capacitor bank provides reactive power compensation and improved grid compatibility during grid connection is facilitated by means of a softstarter.

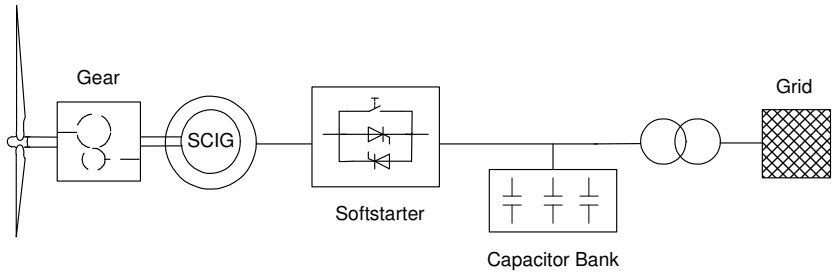

Figure 3.2: Squirrel cage induction generator concept with gearbox and "direct" grid connection –Type A

Due to its direct grid connection the generator operates at fixed speed. However, the slip of the generator allows very small speed variations and softens the torque-speed characteristic. Frequently, the generator is equipped with a pole changeable stator (e.g. 4-poles and 6-poles), so that the generator can operate at two speeds, which leads to a better aerodynamic utilization of the turbine at higher wind speeds. The turbine con-

cept excels in its cheap and simple design and robustness, while however its controllability is relatively poor.

Type B: Variable speed wind turbine with variable rotor resistance

A slightly more advanced wind turbine concept is sketched in Figure 3.3. The turbine setup is in principle the same as for Type A; however, now a wound rotor induction generator (WRIG) with external rotor resistance is used, which allows variable speed operation in a limited range of about 10 % above synchronous speed. The external rotor resistance enforces a higher slip, which on the one side enables variable speed operation but on the other hand increases ohmic losses, which are dumped in the resistance. As this also increases the reactive power demand of the generator a capacitor bank is used for this type as well. As the turbine operates with variable speed it is advisable to use pitch control instead of stall control for limitation of aerodynamic power above rated wind speed.

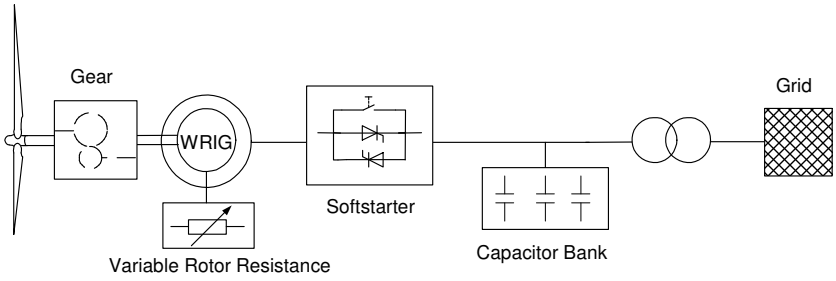

Figure 3.3: Wound rotor induction generator concept with variable rotor resistance - Type B

Type C: Doubly-fed induction generator wind turbine

Figure 3.4 shows the doubly-fed induction generator wind turbine concept, the most popular generator concept for wind turbines at the present time. The pitch-controlled aerodynamic rotor is coupled via gearbox to the generator. The doubly-fed induction generator (DFIG) provides variable speed operation by means of a partial-scale frequency converter in the rotor circuit. A wound rotor induction generator is used, in order to couple the converter via slip rings to the rotor. Depending on the converter size this concept allows a wider range of variable speed of approximately ± 30% around synchronous speed [Hansen 2007a]. Moreover, the converter system provides reactive power compensation and smooth grid connection. As the frequency converter only transmits the rotor power it can be designed for typically 25 % - 30 % of the total turbine power. This makes the turbine concept very attractive from an economic point of view compared to turbines with full-scale converter.

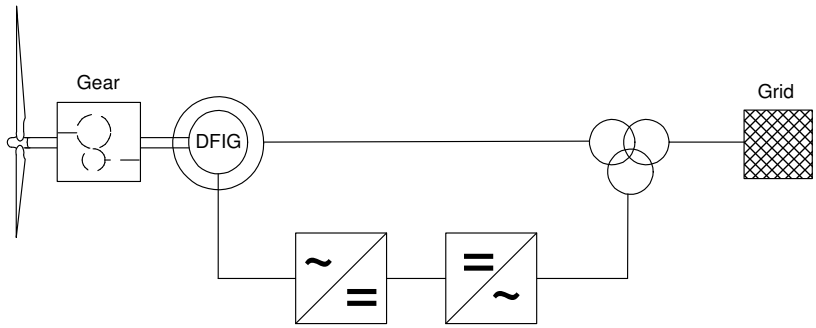

Figure 3.4: Doubly-fed induction generator concept with partial-scale frequency converter – Type C

Type D: Variable speed wind turbine with full-scale frequency converter

Type D, illustrated in Figure 3.5, represents the variable speed, pitch controlled wind turbine concept with the generator connected to a full-scale frequency converter. The full-scale frequency converter provides variable speed over the entire speed range of the generator. At the same time the converter guarantees reactive power compensation and smooth grid connection. The generator can optionally be an asynchronous or synchronous generator.

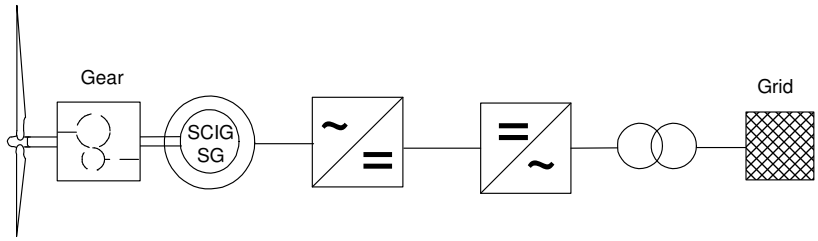

Figure 3.5: Induction or synchronous generator concept in combination with gearbox and full-scale frequency converter – Type D

A modification of this turbine concept is sketched in Figure 3.6. If a multipole synchronous generator is used instead of an induction generator, the generator can be built to operate at low speeds, so that a gearbox can be omitted. This reduces weight, losses and maintenance requirements. The generator can be excited electrically by a DC system (DCSG) or by means of permanent magnets (PMSG).

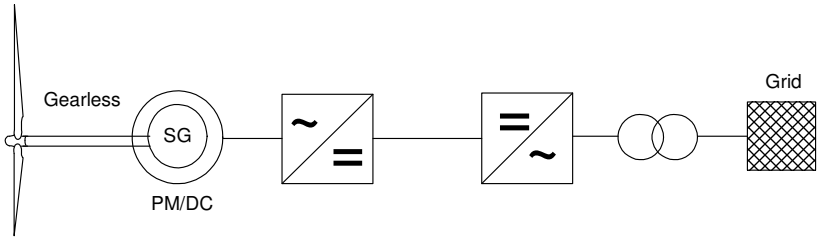

Figure 3.6: Gearless synchronous generator concept with full-scale converter - Type D

A resume of the wind turbine concept classification is given in Table 3.1, where the most important attributes of the wind turbine types are summarized and an assignment to the corresponding speed range is given.

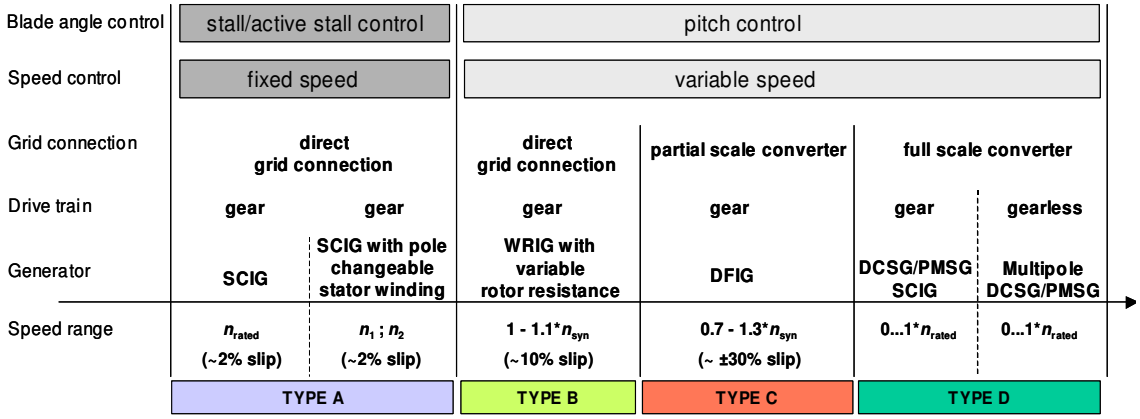

Table 3.1: Wind turbine concept classification

3.3 Market penetration

The most favoured technology among the four different introduced wind turbine concepts has changed within the last decade. In [Hansen 2007a] a detailed investigation of the wind turbine concept market penetration and its development over 10 years from 1995-2004 is presented and the most interesting outcomes are summarized here. Table 3.2 shows the results of the investigation of [Hansen 2007a], which is based on data provided by BMT Consults. The table reflects the market penetration of the four wind turbine types A-D from the top 22 wind turbine market suppliers over the years from 1995 to 2004. The total world market share of these 22 suppliers is listed as well. As this value is higher than 85 % for each year, it means that the statistical significance of the data collection is reliable.

Year / Concept	1995	1996	1997	1998	1999	2000	2001	2002	2003	2004
Type A (%)	69.5	62.7	53.5	39.6	40.8	39.0	30.6	27.8	19.2	24.7
Type B (%)	16.2	23.4	27.0	17.8	17.1	17.2	15.2	5.2	3.1	2.2
Type C (%)	0.0	0.1	3.1	26.5	28.1	28.2	37.3	46.7	59.8	54.8
Type D (%)	14.3	13.7	16.3	16.1	14.0	15.6	16.9	20.3	17.9	18.3
Installed power [%] (22 suppliers)	1161	1092	1483	2345	3788	4381	7175	7242	8084	8247
Total world market share of top 22 suppliers [%]	85.7	95.7	96.2	92.7	94.0	96.3	100.0	97.4	100.0	97.7

Table 3.2: Wind turbine concept market penetration - world market share of yearly installed wind power during 1995 – 2004 [Hansen 2007a]

The market penetration of the wind turbine types A-D in the years 1995-2004 is also shown graphically in Figure 3.7.

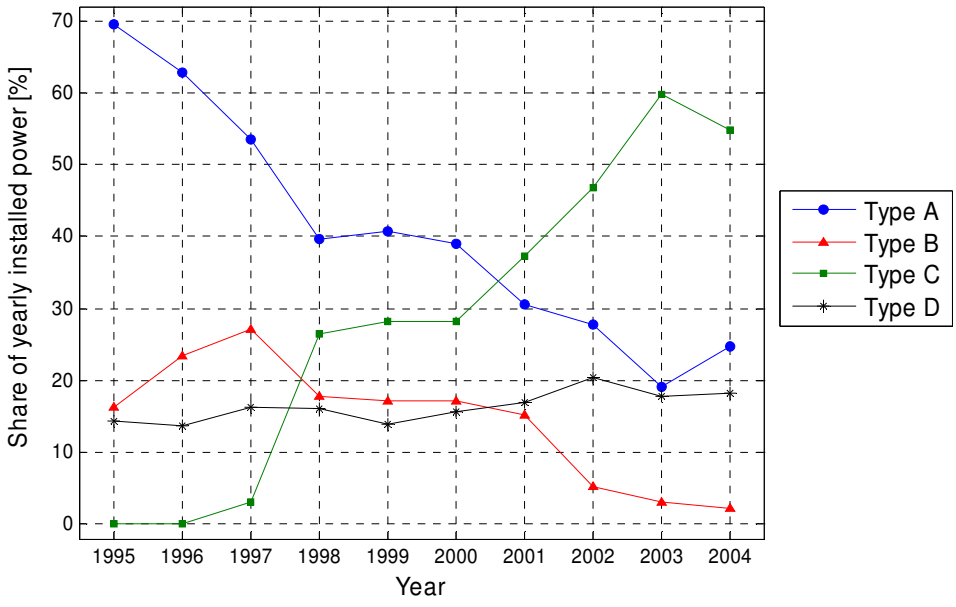

Figure 3.7: World market share of yearly installed wind power during 1995 – 2004 of the four different wind turbine concepts Type A-D [Hansen 2007a]

During the years 1995-1997 the fixed speed wind turbine concept (Type A) was the predominating wind turbine technology, which was due to the simplicity and robustness of the system. However, from 1997 the DFIG wind turbine (Type C) gained an

increasing market penetration, while the demand of Type A and B continuously decreased. The doubly-fed induction generator became thus the most used generator concept, and remains the primary choice for variable speed wind turbines of 1.5 MW and above. This is confirmed by the investigations of [ISET 2007], who assessed a market share of approximately 50 % for the doubly-fed generator on the German market in the years 2002-2005. The market penetration of the variable speed wind turbine concept with full-scale frequency converter – Type D – shows no considerable changes during these considered 10 years, as illustrated in Figure 3.7. However, [ISET 2007] predicates a share of 44 % of yearly new installed wind turbines with synchronous generators in Germany for 2004 and 2005, because of the high market penetration of the ENERCON concept on the German market. For the coming years an increasing trend of Type D wind turbines can therefore be expected, due to their good control and grid support capabilities.

3.4 Variable speed wind turbines versus fixed speed wind turbines

In the previous chapter it has been shown that fixed speed wind turbines were the most installed wind turbines in the early 1990s. The major advantages of this concept are its simplicity and robustness, as standard asynchronous generators can be used and power electronics can be omitted causing economical benefits and reducing maintenance requirements. However, its drawbacks are uncontrollable reactive power consumption, higher mechanical stress and limited power quality control [Hansen 2007a]. Fixed speed wind turbines are generally equipped with stall control, which implies again simplicity and robustness as no blade bearings or pitch system needs to be installed. On the other hand, stall control causes higher mechanical stresses and requires stronger blades, brakes and bearings. Moreover, a fixed blade angle entails losses in energy capture, as the point of maximum aerodynamic efficiency cannot be approached for any wind speed. A possibility to achieve power control for fixed speed wind turbines at high wind speeds is active stall control. A very slow control adjusts the pitch angle to larger angles of attack and smoothes the power limitation.

In contrast to this, variable speed wind turbines are generally equipped with pitch control. It is not advisable to combine pitch control with fixed speed generators as this would lead to large inherent power fluctuations at high wind speeds since the pitch mechanism reacts too slowly during fast wind speed changes. However, variable speed operation assures, that sudden power surplus of wind gusts is temporarily buffered in rotational energy of the turbine until the pitch control limits the excess power. At partial load variable speed operation assures that maximum aerodynamic efficiency can be adjusted for any wind speed. At wind speeds above rated wind speed the pitch control changes the pitch angle in order to limit the power to its rated value. In both

operational modes variable speed pitch controlled wind turbines achieve a better energy capture compared to stall controlled wind turbines.

Finally, the power curves of stall wind turbine, active stall wind turbine and pitch controlled wind turbine plotted for different pitch angle values can be compared in Figure 3.8. As indicated in the figure pitch control works in the opposite direction as active stall control.

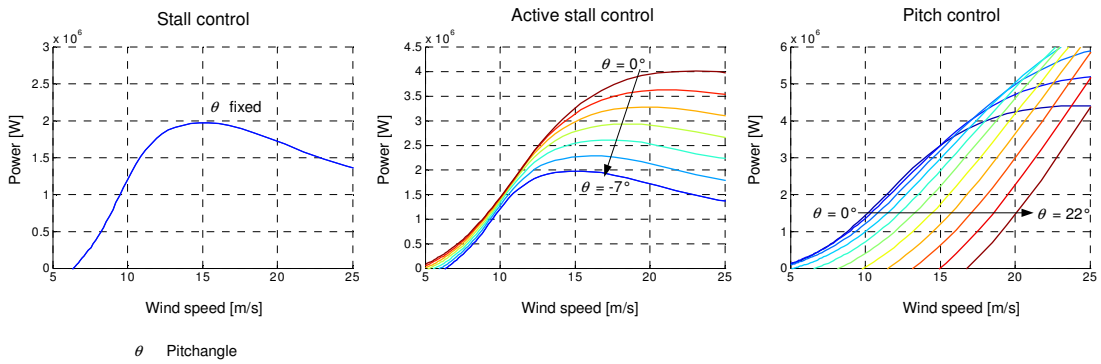

Figure 3.8: Wind turbine power curves versus wind speed for stall control, active stall control and pitch control

Variable speed pitch control wind turbines have become the predominating technology for wind turbines, which is confirmed by the investigations of [Hansen 2007a] and [ISET 2007]. As investigated in [ISET 2007] 92 % of the new installed wind turbines in 2005 were variable speed wind turbines. The main advantages are the increased power capture, reduced mechanical stress and minor acoustical noises as well as better controllability. The drawbacks of the variable speed pitch controlled concept are additional losses due to additional components as e.g. power electronics and pitch system, which in turn leads to higher capital costs of the system. However, it can be expected, that due to improved developments, costs for power electronics will further decrease in the future.

The main trend in wind turbine technology is recently also influenced by other factors. Especially in countries with high wind power penetration, wind power grid integration issues are very important in terms of which wind turbine concept can be applied. Wind power grid integration addresses at the one hand power control capability of wind turbines, which means that wind turbines must curtail or adjust their power output in order to contribute to the dispatch of power production and consumption. At the other hand grid codes require fault ride-through and reactive power supply from wind turbines. Thus, the wind turbine's controllability in terms of grid compatibility and compliance of grid connection standards has a great impact on future development. Due to this reason variable speed wind turbines using a frequency converter, as represented by wind turbine type C and D, will be the relevant technologies on the future market and they are therefore considered in the present PhD work. As fixed

speed wind turbines or variable speed wind turbines without power electronics are assessed to be incapable of fulfilling grid code requirements, these wind turbine concepts will withdraw from the market and will not be included in the investigations of the present work. The following chapters focus on (i) the doubly-fed induction generator concept – Type C, and (ii) the wind turbine with multipole permanent magnet generator and full-scale converter representing Type D.

3.5 Summary

Chapter 3 presents a general overview about the marketable wind turbine concepts and emphasizes their different characteristics. Four types of wind turbine concepts predominate the market at present. The most conventional wind turbine concept is the fixed speed stall controlled wind turbine with induction generator, the so-called Danish concept. A slight modification of this concept is to use an adjustable external rotor resistance in the rotor circuit to achieve variable speed. Both of these concepts show however a decreasing market penetration over the years from 1994 to 2005. In contrast to this, the variable speed pitch controlled wind turbine concept with doubly-fed induction generator and partial-scale frequency converter has increased its market penetration enormously, being the most popular generator concept in wind turbines today. The share of wind turbines using a full-scale frequency converter stayed relatively constant in the last decade, however, due to its good controllability and decreasing costs for power electronics, an increasing market prospect of this concept is anticipated. The conclusion is, that the main trend in wind turbine technology is recently the variable speed option using pitch control and power electronic interface. This development is due to increased grid requirements for wind turbines in systems with high amount of wind power. In the present work, two auspicious wind turbine concepts for the future market are therefore selected for investigation: the doubly-fed induction generator wind turbine concept and the wind turbine concept with multipole permanent magnet generator and full-scale converter.

4 Mechanical system and control of variable speed wind turbines

The main goal of the presented PhD work is to develop advanced control strategies for variable speed wind turbines and to investigate their interaction with the power system especially during grid faults. For this purpose it is essential to use realistic models for the electrical system as well as for the mechanical part of the wind turbine. The mechanical part of the wind turbine includes models for the rotor effective wind, the aerodynamic rotor, the blade pitching mechanism and the drive train with gearbox. The wind turbine tower itself is not important for power system studies, however the tower shadow affecting the aerodynamic torque must be considered. Elements like mechanical breaks will not be taken into account, as their action is not relevant for the here considered operational states. Moreover, a control of the mechanical system, i.e. the blade angle control, must be designed and coordinated with the control of the electrical system.

In the following the model of the mechanical system and a control strategy for the blade pitching mechanism are presented. This model was developed at Risø National Laboratory in Denmark and is provided and adapted for the here presented PhD work. Moreover, a variable speed wind turbine model of a 2 MW DFIG wind turbine was readily available at Risø National Laboratory at the beginning of this PhD work and was used as a basis for further investigation and modelling purposes presented in this work.

An overview over the modelling scheme is illustrated in Figure 4.1. DIgSILENT provides built-in models for all components of the electrical system, while all mechanical components (wind, aerodynamics, drive train model) as well as the total control system must be developed by the user. The models are implemented by means of the dynamic simulation language DSL of the simulation software DIgSILENT.

Wind turbines of 2 MW power with a rotor diameter of 40 m will be investigated. The wind turbine data is not linked to a specific manufacturer but is representative for all variable speed pitch controlled wind turbines. An overview over the technical wind turbine data can is provided in the appendix in Section 12.5. The model for the mechanical system of the wind turbine is valid for both wind turbine types, the DFIG wind turbine and the PMSG wind turbine, which are considered in Chapter 5 and Chapter 7, respectively.

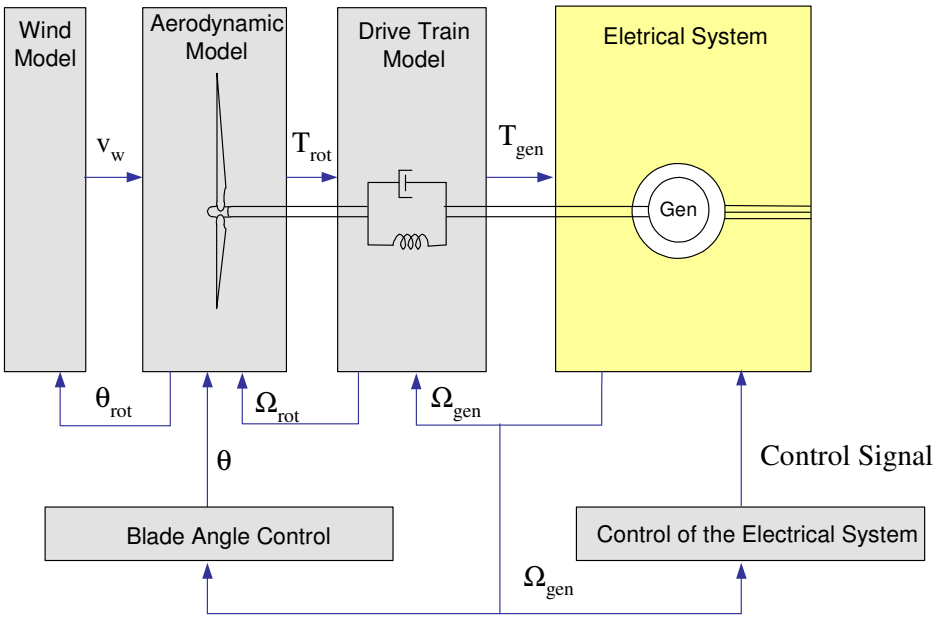

Figure 4.1: Modelling scheme of mechanical system and control

v_w	wind speed	θ	pitch angle
T_{rot}	aerodynamic torque	Ω_{rot}	mechanical speed of the rotor
T_{gen}	generator torque	Ω_{gen}	mechanical speed of the generator
θ_{rot}	rotor angle (rotor position)		

4.1 Wind model

Because a wind turbine is exposed to fluctuating wind speeds, to which the turbine's control has to respond, a realistic simulation model of the rotor effective wind is implemented. The wind model is described in detail in [Soerensen 2001] and [Langreder 1996] and is thus only briefly described in the following. A wind time series is generated based on the spectral energy distribution of the wind and a superposed noise signal. This method comprises both: (i) representation of the spectral energy distribution assures that the frequencies inherent in the wind are included according to their occurrence and their amplitude, (ii) the superposed noise signal reflects the stochastic character of the wind.

According to the specifications of the Danish Standard (DS DS 472 "Conditions for the construction of wind turbines in Denmark") [DS DS 472] or the IEC standard (IEC 61400-1 Wind turbine generator systems-Part 1: Safety requirements) [IEC 61400-1] the spectral energy distribution of the wind can be mathematically approximated by means of a Kaimal spectrum (equation (4.1)) [Langreder 1996].

$$\frac{f \cdot S(f)}{\sigma^2} = \frac{\frac{f \cdot L}{U_0}}{\left(1 + 1.5 \cdot \frac{f \cdot L}{U_0}\right)^{\frac{5}{3}}} \tag{4.1}$$

with

f	frequency of the turbulence [Hz]
σ^2	variance [m^2/s^2]
L	length scale in prevailing wind direction [m]
U_0	mean wind speed
S	Spectral energy distribution [m/s]

This spectrum represents the wind spectrum in a micrometeorological range (Figure 4.2), i.e. it reproduces the turbulence of wind in a time frame of approx. 5 minutes [Van der Hoven 1957]. This time frame is considered to be adequate for the performed studies.

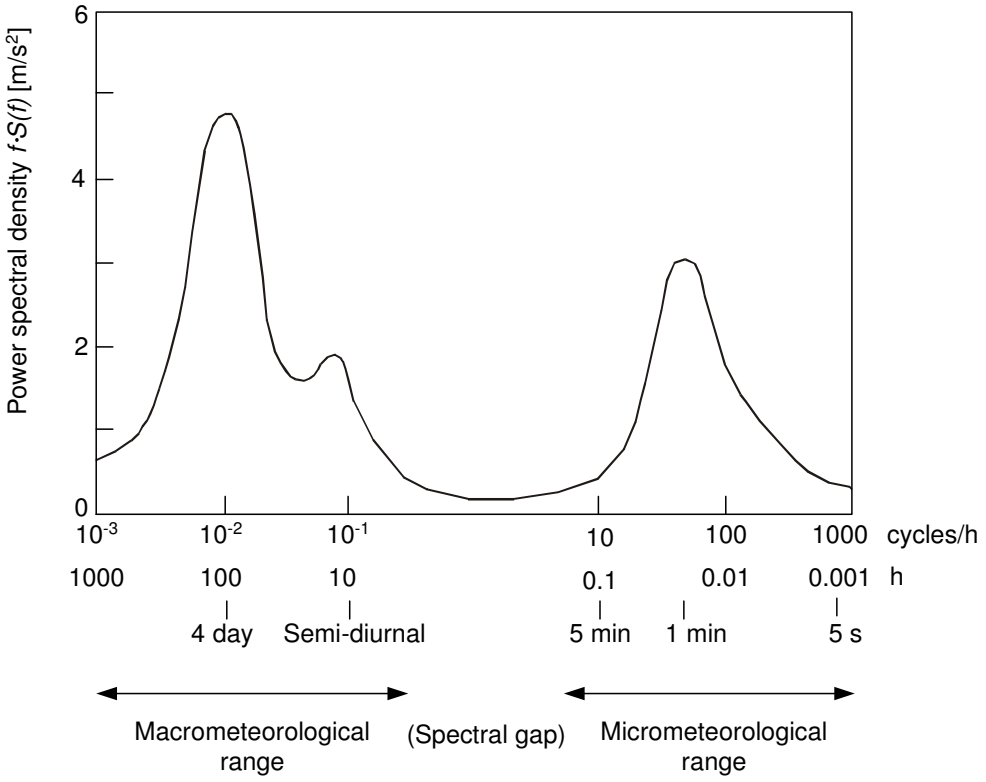

Figure 4.2: Van der Hoven Spectrum [Van der Hoven 1957]

In a second step the so gained wind speed is averaged over the whole rotor area, which considers the interaction of the wind stream and the rotating wind turbine rotor. By means of this the rotational sampling (3p effect), which represents wind speed

variations with an inherent excitation frequency of three times the turbine's rotational frequency especially caused by the tower shadow, is taken into account. The computed wind time series is thus a rotor effective wind speed including already aerodynamic effects of the rotor.

4.2 Aerodynamic model

The aerodynamic of the rotor is sufficiently modelled by means of a quasistatic aerodynamic model based on the aerodynamical equation (4.2). The power inherent in the wind, which is converted into mechanical power by the rotor blades, can be determined by the following equation:

$$P_{rot} = \frac{1}{2} \rho \, c_p \, \pi R^2 \, v_w^3 \tag{4.2}$$

P_{rot}	aerodynamic power
R	rotor radius
ρ	air density
v_{w}	wind speed
c_{p}	aerodynamic power efficiency

For a variable speed wind turbine the aerodynamic power efficiency c_{p} depends on the actual pitch angle θ and the tip speed ratio $\lambda = \frac{\Omega_{rot} \cdot R}{v_w}$, which is plotted in Figure 4.3.

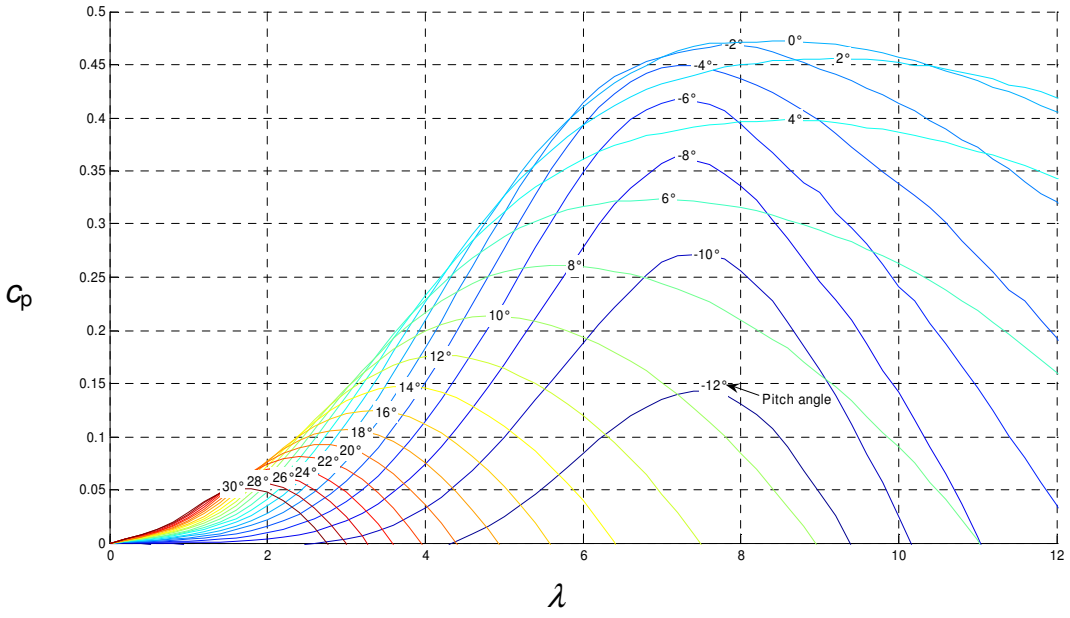

Figure 4.3: Aerodynamic power efficiency c_{p} depending on the tip speed ratio λ and the pitch angle

With the help of the proportional factor c_q, the aerodynamic torque T_{rot} can directly be computed.

$$c_q = \frac{c_p}{\lambda} \tag{4.3}$$

$$T_{rot} = \frac{P_{rot}}{\Omega_{rot}} = \frac{1}{2}\,\rho\, c_q\, \pi R^3\, v_w^2 \tag{4.4}$$

It is furthermore considered that the wind turbine will be shut down below the cut-in wind speed of 3 m/s and above the cut-out wind speed of 25 m/s. The output of the aerodynamical model is the aerodynamical torque and serves as an input for the drive train model.

4.3 Drive Train model

In stability analysis, when the system response to heavy disturbances is analysed, the drive train system must be approximated by at least a two-mass spring and damper model [Akhmatov 2003a]. This yields a more accurate response of the wind turbine's dynamic behaviour during fluctuating wind conditions or during grid faults and results in a more accurate prediction of the impact on the power system.

The drive train model, considered in the present report, is therefore a two-mass mechanical model, connected by a flexible shaft characterised by a stiffness K_{shaft} and a damping coefficient D_{shaft}, as described in [Hansen 2003] and [Iov 2004]. The flexible shaft can be understood as a torsion spring connected between two masses: one mass represents the turbine inertia J_{rot}, while the other mass is equivalent to the generator inertia J_{gen}. In case of a DFIG wind turbine (Type C Figure 3.4) an ideal gearbox with the exchange ratio 1:k_{gear} is considered. The stiffness and damping components are modelled on the low speed shaft, while the high speed shaft is assumed stiff. Figure 4.4 shows the two-mass-model, which is used to model the mechanical structure of the wind turbine.

For direct driven wind turbines with multipole synchronous generator as introduced in Figure 3.6 the gearbox can be omitted (k_{gear}=1). In this case the same model as illustrated in Figure 4.4 can be used with a gearbox ratio of 1:1. The turbine and shaft torque T_{shaft} and T_{gen} are then equal and in steady state operation the generator rotates with the same speed as the aerodynamic rotor.

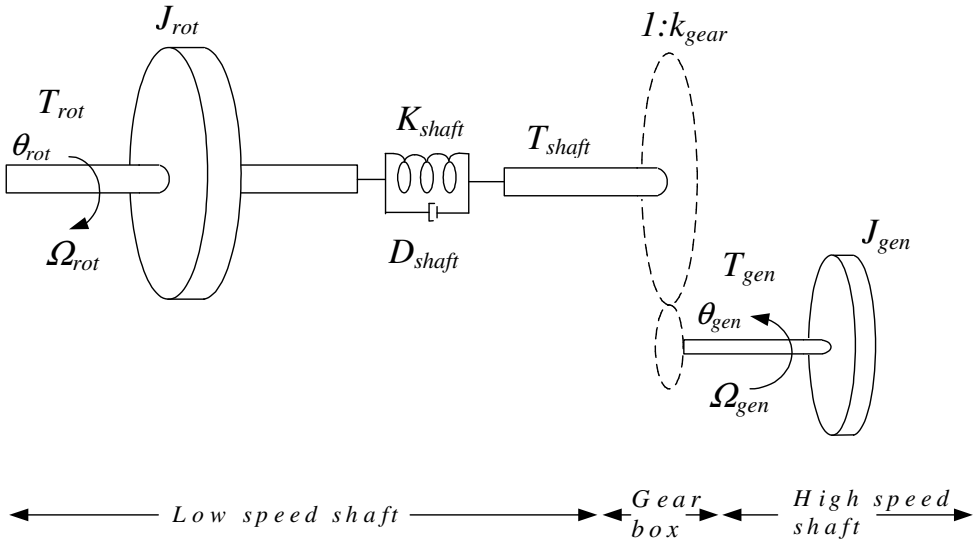

Figure 4.4: Two-mass-model for the drive train

J_{rot}	rotor inertia
T_{rot}	wind turbine rotor torque
Ω_{rot}	speed of the low speed shaft
θ_{rot}	low speed shaft angular position
K_{shaft}	shaft stiffness
D_{shaft}	damping coefficient of the shaft
T_{shaft}	shaft torque
$1{:}k_{\text{gear}}$	gearbox ratio
J_{gen}	generator inertia
T_{gen}	generator torque
Ω_{gen}	speed of the high speed shaft
θ_{gen}	high speed shaft angular position

In order to refer all terms to the high speed shaft the following transformations are used:

$$J'_{rot} = \frac{J_{rot}}{k_{gear}} \tag{4.5}$$

$$D'_{shaft} = \frac{D_{shaft}}{k_{gear}^2} \tag{4.6}$$

$$K'_{shaft} = \frac{K_{shaft}}{k_{gear}^2} \tag{4.7}$$

$$\Omega'_{rot} = k_{gear} \cdot \Omega_{rot} \tag{4.8}$$

$$\theta'_{rot} = k_{gear} \cdot \theta_{rot} \tag{4.9}$$

$$T'_{rot} = \frac{T_{rot}}{k_{gear}} \tag{4.10}$$

The mechanical model can then be described by the motion equations (4.11) - (4.14):

$$T'_{rot} = J'_{rot} \frac{d\Omega_{rot}}{dt} + D'_{shaft}(\Omega'_{rot} - \Omega_{gen}) + K_{shaft}(\theta'_{rot} - \theta_{gen}) \tag{4.11}$$

$$-T_{gen} = J_{gen} \frac{d\Omega_{gen}}{dt} + D'_{shaft}(\Omega_{gen} - \Omega'_{rot}) + K_{shaft}(\theta_{gen} - \theta'_{rot}) \tag{4.12}$$

$$\frac{d\theta'_{rot}}{dt} = \Omega'_{rot} \tag{4.13}$$

$$\frac{d\theta_{gen}}{dt} = \Omega_{gen} \tag{4.14}$$

The two-mass-model (Figure 4.4) uses the wind turbine torque T_{rot} and the generator speed Ω_{gen} as input. With the four equations (4.11) - (4.14) the four unknown, rotor speed Ω_{rot} and generator torque T_{gen} as well as rotor and generator angular position, θ_{rot} and θ_{gen}, can be computed. Optional also the shaft torque T_{shaft} can be calculated based on equation (4.15).

$$-T'_{shaft} = D'_{shaft}(\Omega'_{rot} - \Omega_{gen}) + K_{shaft}(\theta'_{rot} - \theta_{gen}) \tag{4.15}$$

The model has to be initialised with the values for rotor and generator inertia as well as the shaft stiffness and damping coefficient. The shaft stiffness represents an equivalent stiffness of high speed and low speed shaft [Iov 2004]:

$$\frac{1}{K'_{shaft}} = \frac{1}{\frac{K_{rot}}{k^2_{gear}}} + \frac{1}{K_{gen}} \tag{4.16}$$

The damping coefficient D_{shaft} can be computed with the help of the stiffness K_{shaft}, the rotor inertia J_{rot} and the damping ratio ξ [Hansen 2003]:

$$D_{shaft} = 2\xi\sqrt{K_{shaft} \cdot J_{rot}} \tag{4.17}$$

The damping ratio ξ can in turn be expressed as:

$$\xi = \frac{\delta}{\sqrt{\delta^2 + 4\pi^2}} \tag{4.18}$$

where δ denotes the logarithmic decrement of an oscillation, which is defined as:

$$\delta = \ln\left(\frac{a(t)}{a(t+t_p)}\right) \tag{4.19}$$

Here a is the amplitude of the oscillation with a period t_p.

4.4 Blade angle control

In variable speed wind turbines equipped with a pitch mechanism the mechanical system of the wind turbine can be controlled by means of blade pitching. For wind speeds below rated wind the absorbed aerodynamic power is optimized. According to Figure 4.3, this is done by adjusting the tip speed ratio λ to achieve the maximum power coefficient c_p. The pitch angle is kept constant while the turbine's rotational speed is adapted, when the wind speed changes. Variable speed operation is therefore assured by the control of the electrical system and the pitch control is inactive below rated wind speeds. In contrast to this, at wind speeds above rated wind the extracted wind power has to be limited by means of blade pitching. This is realized by a speed controller, regulating the speed $\omega_{gen,meas}$ to its rated value $\omega_{gen,rated}$ (Figure 4.5). The speed is controlled by a PI-controller, which outputs a reference pitch signal θ_{ref} to the pitch system. In order to get a realistic response in the pitch angle control system, a servomechanism model accounts for a servo time constant T_{Servo} and the limitation of both the pitch angle (0 to 30 deg angle limit) and its gradient (± 10 deg/s rate limit). The rate-of-change limitation is very important especially during grid faults, because it decides how fast the aerodynamic power can be reduced in order to prevent overspeeding during faults (see Chapter 6.2.1). In this work, the pitch rate limit is set to the typical value of 10 deg/s. The reference pitch angle θ_{ref} is compared to the actual pitch angle θ and then the error is corrected by the servo mechanism (Figure 4.5).

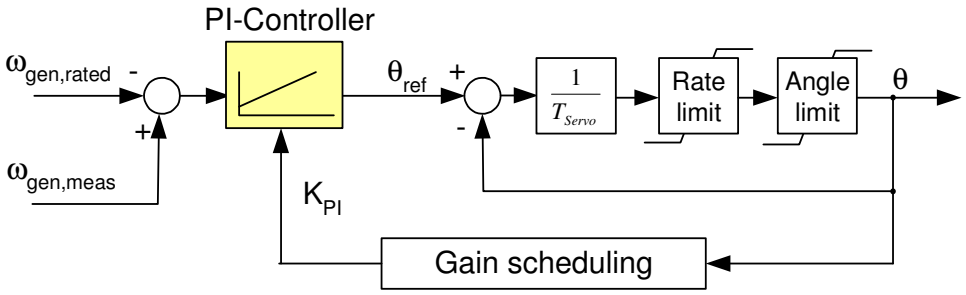

Figure 4.5: Blade angle control model

As mentioned above the blade angle control is only active, if the speeds exceeds rated speed. In other words the control task of the pitch controller is to limit the speed to its rated value, which indirectly implies that the power is limited to its rated value, too. This is due to the control of the electrical system where speed and power are linked by means of a maximum power point tracking table (MPP table). The MPP-table assures operation at maximum aerodynamic efficiency at partial load (see Chapter 5.2 or Chapter 7.2) and specifies that rated speed is achieved at rated power. By means of this a coordination between the control of the mechanical and the electrical system exists. The speed of the turbine and generator system is determined by the slow response time of the mechanical system and is therefore controlled by the slower acting pitch mechanism. Meanwhile the generator power, which is determined by the faster response time of the electrical system, is controlled with the faster converter control. As the servo mechanism reacts slowly compared to the electrical control, dynamic variations of the speed above rated speed occur. This has the advantage that the abrupt surplus power of momentary wind gusts is buffered in rotational power of the rotating masses, while the control of the electrical system keeps the output power constant. This in turn reduces the stress on the mechanical system.

A gain scheduling control of the pitch angle is also implemented, as illustrated in Figure 4.5. The gain scheduling compensates for existing non-linear aerodynamic characteristics [Hansen 2005]. The total gain of the system in the speed control loop K_{system}, can be expressed as a proportional gain K_{PI} in the PI-controller times the aerodynamic sensitivity of the system $\frac{dP}{d\theta}$:

$$K_{system} = K_{PI} \quad \frac{dP}{d\theta} = K_{basis} \quad \left[\frac{dP}{d\theta}\right]^{-1} \quad \frac{dP}{d\theta} \tag{4.20}$$

The aerodynamic sensitivity $\frac{dP}{d\theta}$ of the system depends on the operating conditions (the setpoint power value, the wind speed or the pitch angle). The sensitivity function

can be approximated to increase linear with the pitch angle. Thus, the more sensitive the system is, which is at higher wind speeds and so at larger pitch angles θ, the smaller the gain for the controller should be and vice versa. The total gain of the system K_{system} is thus kept constant by changing K_{PI} in such a way that it counteracts the variation of the aerodynamic sensitivity $\frac{dP}{d\theta}$ by the reciprocal sensitivity function $\left[\frac{dP}{d\theta}\right]^{-1}$:

$$K_{PI} = K_{basis} \left[\frac{dP}{d\theta}\right]^{-1} \tag{4.21}$$

The normalized sensitivity function $\left[\frac{dP}{d\theta}\right]^{-1}$ is plotted in Figure 4.6.

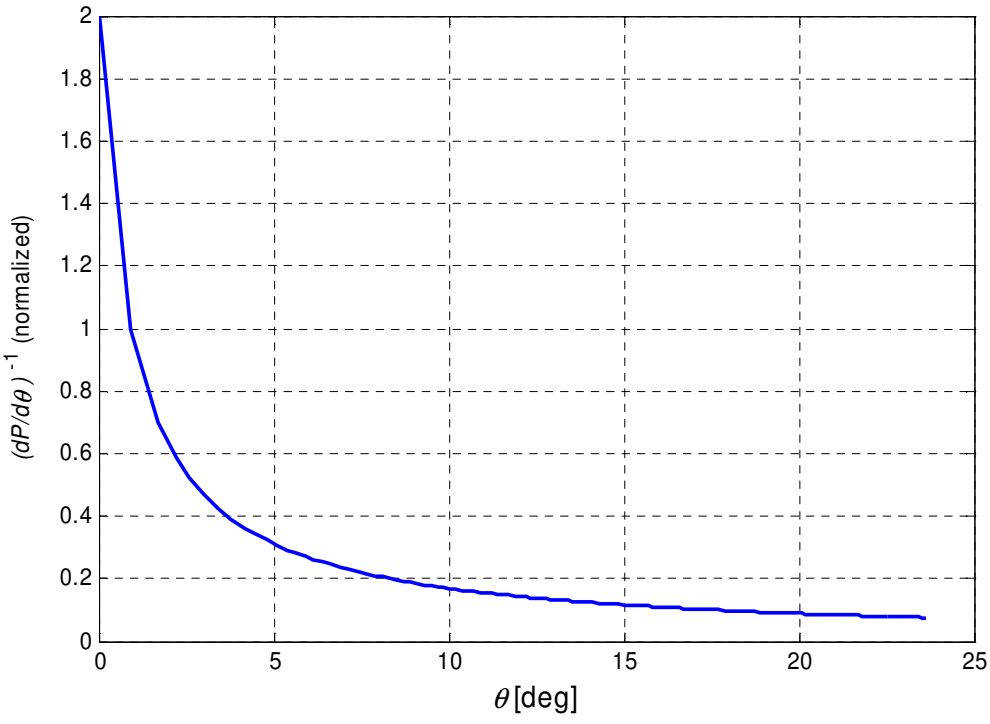

Figure 4.6: Sensitivity function $dP/d\theta^{-1}$ versus pitch angle

K_{basis} is the constant designed proportional gain of the PI- controller. The control parameters are found by means of the Ziegler-Nichols method [Co 2004]. However, the parameters can also be determined analytically, as it is carried out in [Hansen 2005].

4.5 Summary

In a first step of the wind turbine modelling process, a model for the mechanical system and its control is implemented. The challenge is to develop a model, which at the one hand simplifies the complex aerodynamical/mechanical behaviour, but at the other hand provides a sufficient representation of the turbine, necessary for power system studies.

The mechanical part of the wind turbine includes models for the rotor effective wind, the aerodynamic rotor, the blade pitching mechanism and the drive train with gearbox. Moreover a superposed control strategy for the mechanical system, a blade angle control, is implemented. The model for the mechanical system of the wind turbine is valid for both wind turbine types, the DFIG wind turbine and the PMSG wind turbine.

The wind model considers the spectral energy distribution of the wind in a micrometeorological range combined with a superposed noise signal to represent the wind's stochastic character. Moreover, the wind speed is averaged over the rotor area in order to include the interaction of the wind stream and the rotating wind turbine rotor e.g. noticeable as rotational sampling effect. The aerodynamics of the rotor can then be simplified by means of a quasistatic model based on the aerodynamic equation. In stability analysis when the system response to heavy disturbances such as grid faults is investigated it is essential to represent the drive train model as a two-mass spring and damper model. In case of the DFIG wind turbine model an ideal gearbox is included into the model.

The mechanical system is controlled by blade pitching. This is realized by a speed controller, which provides the reference pitch angle. A servomechanism model, adjusting the pitch angle, accounts for a servo time constant and the limitation of both the pitch angle and its rate of change. The control of the mechanical system of the wind turbine is coordinated with the control of the electrical system. At partial load, the pitch angle is kept constant to its optimal value, while the control of the electrical system assures variable speed operation. Above rated wind speed the pitch angle is increased to limit the absorbed aerodynamic power. Due to the slower response time of the pitch mechanism the speed controller permits dynamic variations of the speed in order to avoid mechanical stresses during wind gusts. Moreover, a gain scheduling is implemented in the controller in order to compensate for existing non-linear aerodynamic characteristics.

5 DFIG wind turbine – Electrical system and control

The variable speed doubly-fed induction generator (DFIG) wind turbine is today the most commonly used wind turbine concept [Hansen 2007a]. As assessed in [Hansen 2004a] the main trend of modern wind turbines is clearly the variable speed operation and a grid connection through power electronic interface. The presence of power electronics inside wind turbines offers enlarged control capabilities and accomplishment of grid connection requirements. The doubly-fed induction generator wind turbine concept uses a partial-scale frequency converter in the rotor circuit. This converter controls the rotor voltage and thus performs independent control of active and reactive power at a speed range of approx. ±30% around synchronous speed [Leonhard 2001]. Compared to wind turbine concepts with full-scale frequency converter, the partial-scale converter of the DFIG has the advantage of reduced converter size, costs and losses [Hansen 2004b], making the doubly-fed induction generator the most attractive generator concept in wind turbines at present. Figure 5.1 shows the doubly-fed induction generator concept applied in a wind turbine.

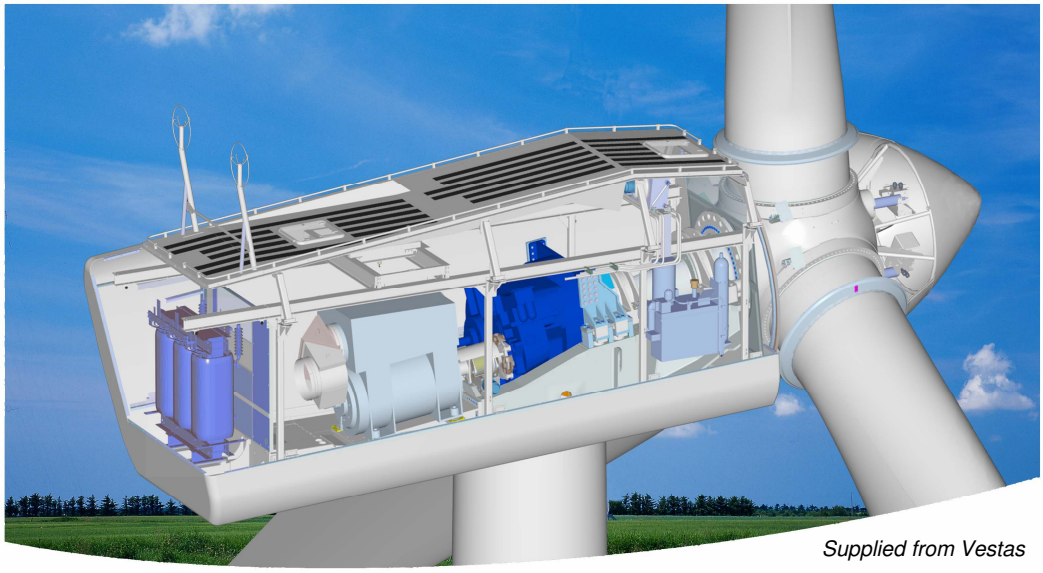

Figure 5.1: Wind turbine with doubly-fed induction generator concept

The present chapter focuses on modelling and control of the DFIG wind turbine's electrical system. A comprehensive dynamical model of this wind turbine concept had been developed at Risø National Laboratory in the power system simulation tool DIgSILENT and was available at the beginning of the present PhD work. During this PhD work an advanced control strategy has been further developed, which enhances the performance of the doubly-fed induction generator concept during normal

operation as well as during grid faults. The mechanical part of the DFIG wind turbine is modelled as shown in Chapter 4.

All components of the electrical system, i.e. generator, converter and transformer are provided as built-in models in the simulation tool DIgSILENT Power Factory. The data of the models is not linked to a certain manufacturer but representative for a 2 MW DFIG wind turbine. Relevant data of the electrical system is provided in the Appendix, Section 12.6.

5.1 The doubly-fed induction generator system

The doubly-fed induction generator wind turbine system is illustrated in Figure 5.2. The generator is an induction machine with a wound rotor, which is connected via a back-to-back voltage source converter, while the stator is directly connected to the grid. The converter supplies an additional rotor voltage with slip frequency to the rotor terminals. The variable rotor voltage assures variable speed operation of the generator and allows independent control of the generator's active and reactive power. Depending on the rotor voltage's amplitude and phase the generator operates in subsynchronous or oversynchronous operation. In subsynchronous operation the converter feeds power into the rotor, while in oversynchronous operation the rotor power is fed via the converter back to the grid. The power flow in the converter is thus bi-directional. The converter must therefore consist of active semiconductors, as e.g. IGBTs or GTOs, allowing power flow in both directions.

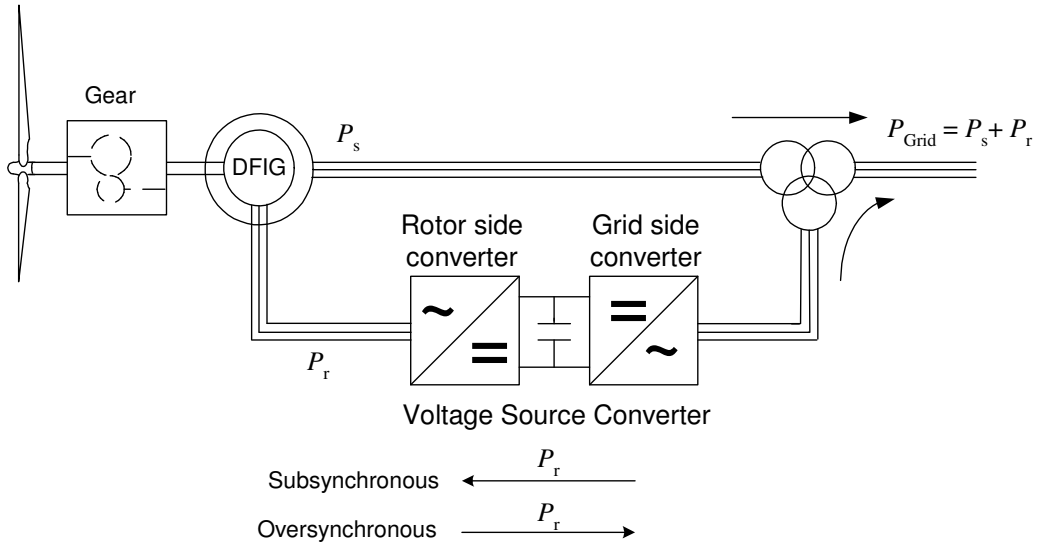

Figure 5.2: Scheme of the DFIG wind turbine system

5.1.1 Steady state theory

Figure 5.3 shows the equivalent circuit of the doubly-fed induction generator.

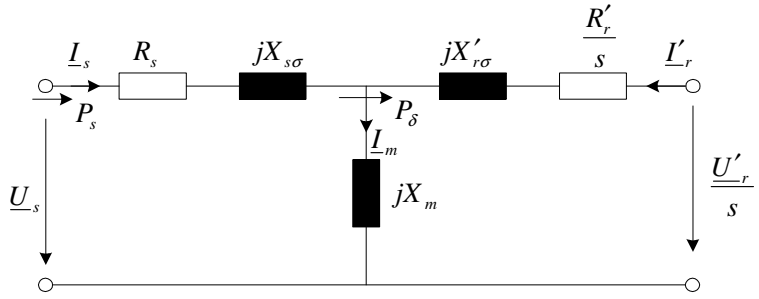

Figure 5.3: Steady state equivalent circuit of the DFIG

The equivalent circuit yields the following voltage equations:

$$\underline{U}_s = R_s \cdot \underline{I}_s + jX_{s\sigma} \cdot \underline{I}_s + jX_m \cdot \underline{I}_m \tag{5.1}$$

$$\frac{\underline{U}'_r}{s} = \frac{R'_r}{s} \cdot \underline{I}'_r + jX'_{r\sigma} \cdot \underline{I}'_r + jX_m \cdot \underline{I}_m \tag{5.2}$$

U_s stator voltage
I_s stator current
U_r' rotor voltage related to stator side
I_r' rotor current related to stator side
R_s stator winding resistance
R_r' rotor resistance related to stator side
$X_{s\sigma}$ stator leakage reactance
$X_{r\sigma}'$ rotor leakage reactance related to stator side
X_m main reactance
s slip

To enhance the understanding of the power flow in the machine the equivalent circuit can as well be arranged as shown in Figure 5.3.

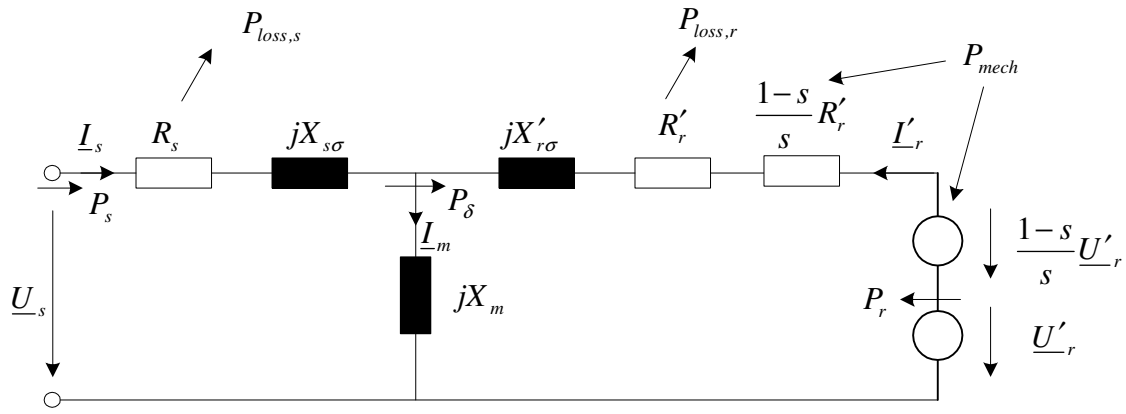

Figure 5.4: Power flow in the DFIG, illustrated with the equivalent circuit

$P_{\text{loss,s}}$	stator winding losses
$P_{\text{loss, r}}$	rotor winding losses
P_{mech}	mechanical power
P_δ	airgap power
P_r	rotor power

The power flow in the machine can then be derived from the equivalent circuit. The airgap power P_δ, which is transmitted from the stator over the airgap into the rotor, is:

$$P_\delta = P_s - 3R_s\left|\underline{I}_s\right|^2 \tag{5.3}$$

The equivalent circuit shows furthermore that the active power P_δ, which is converted in the rotor, must yield:

$$P_\delta = 3\frac{R'_r}{s}\left|\underline{I}'_r\right|^2 - 3\Re\left\{\frac{\underline{U}'_r}{s}\underline{I}'^{\,*}_r\right\} \tag{5.4}$$

The mechanical power P_{mech} can be expressed with:

$$P_{mech} = 3\frac{(1-s)}{s}R'_r\left|\underline{I}'_r\right|^2 - 3\Re\left\{\frac{(1-s)}{s}\underline{U}'_r\,\underline{I}'^{\,*}_r\right\} \tag{5.5}$$

Rearranging equation (5.4) yields:

$$s\cdot P_\delta = 3R'_r\left|\underline{I}'_r\right|^2 - 3\Re\left\{\underline{U}'_r\,\underline{I}'^{\,*}_r\right\} = P_{loss,r} - P_r \tag{5.6}$$

If now the stator winding losses $P_{loss,s} = 3R_s \left| \underline{I}_s \right|^2$ as well as the rotor winding losses $P_{loss,r} = 3R'_r \left| \underline{I}'_r \right|^2$ are neglected, Equation (5.7) gives the well known relation between stator power and rotor power in the DFIG.

$$P_r = -s \cdot P_s \tag{5.7}$$

However, this is only true in a little range around the operating point of the machine [Gail 2006]. This fact is exemplified in Figure 5.5 for the case of one specific rotor voltage, which is adjusted by the control system at 8 m/s wind speed. Figure 5.5 shows the steady state power curves of sP_s, $-P_r$ and the rotor losses $P_{loss,r}$. A zoom on the operating range is given in Figure 5.6. The curves of sP_s and $-P_r$ converge in a little range around the operating point.

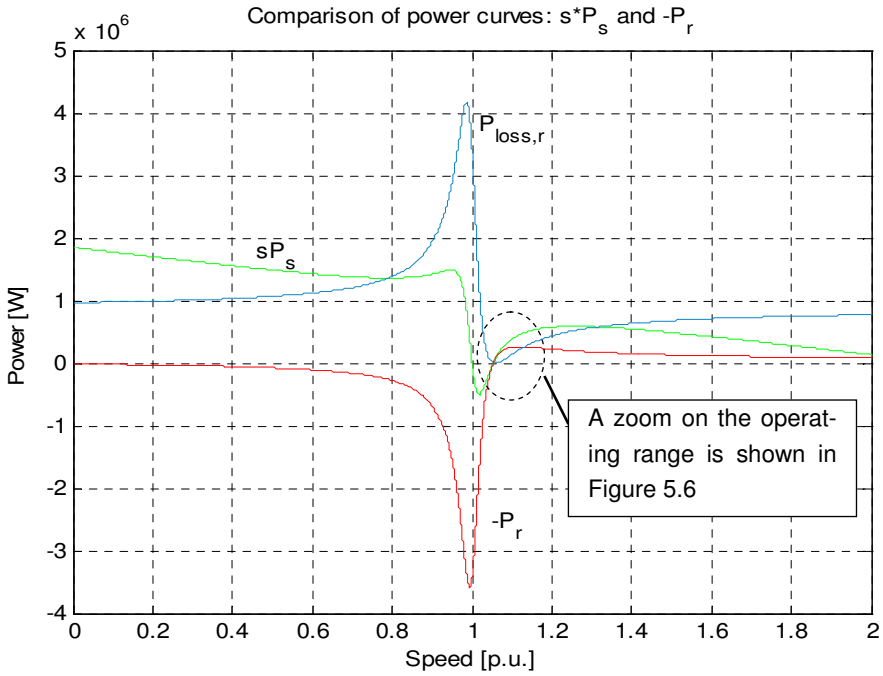

Figure 5.5: Comparison of steady state power curves of the DFIG [Gail 2006]

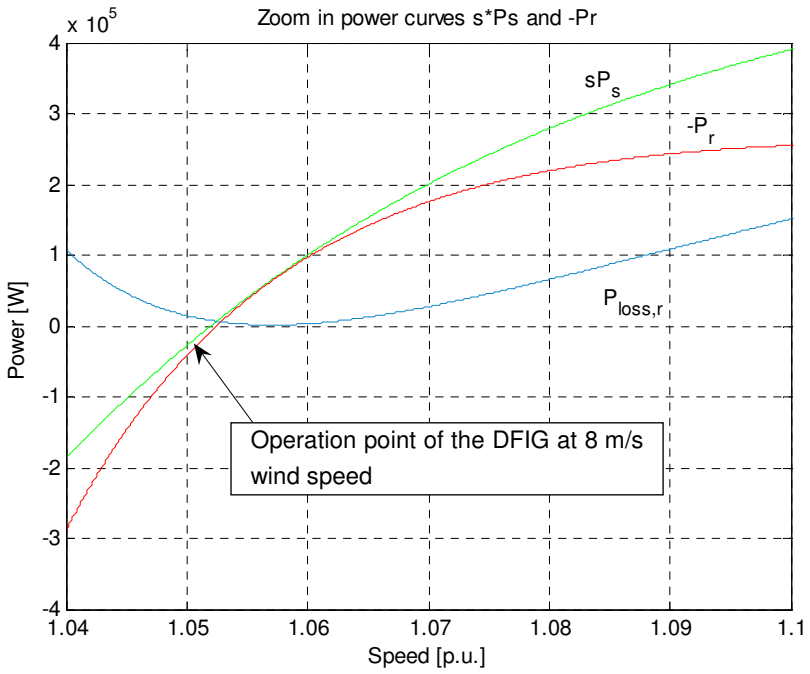

Figure 5.6: Zoom on the steady state power curves of the DFIG [Gail 2006]

The rotor power P_r can be fed back to the grid in oversynchronous operation instead of being burned in external rotor resistances. Moreover, the possibility of changing both the amplitude and phase of the rotor voltage U_r provides an additional degree of freedom for control. Figure 5.7 illustrates the torque-speed characteristics of the doubly-fed induction generator with different applied rotor voltages. For comparison the torque-speed characteristics of an asynchronous generator with variable rotor resistance is shown, too. According to [Binder 2006], the real part of the rotor voltage related to the stator voltage causes a parallel displacement of the DFIG's torque-speed characteristic. If the amplitude of the additional rotor voltage $\underline{U}_r'$ is expressed as a fraction or a multiple of the stator voltage $\underline{U}_s$ (the ratio of the in-phase component is *re*, of the reactive component is *im*) the following equation results:

$$\underline{U}'_r = \underline{U}_s \cdot (re - j \cdot im) \tag{5.8}$$

The no-load slip s_L is displaced towards lower or higher values depending of the real part of the rotor voltage $U'_{r,real}$ [Binder 2006]. The no-load slip s_L of the DFIG is defined as in (5.9). The displacement of the no-load slip is illustrated in Figure 5.7.

$$s_L = re = \frac{U'_{r,real}}{U_s} \tag{5.9}$$

If the real part $U'_{r,real}$ of the rotor voltage is positive or in phase with the stator voltage U_s the torque-speed characteristic is displaced to the left. The new no-load point at slip s_L is displaced to the subsynchronous region. Additional power is then fed into the rotor of the DFIG. In contrast, if the real part $U'_{r,real}$ of the rotor voltage is negative the torque-speed characteristic is displaced to the right and the new no-load point is displaced to oversynchronous region. The rotor power is then fed from the rotor into the grid. This means, that the real part of $\underline{U}_r'$ allows variable speed operation and control of the DFIG´s active power, while the imaginary part of $\underline{U}_r'$ allows control of the generator's reactive power.

As shown in Figure 5.7 a variable rotor resistance applied to an asynchronous generator causes instead a flatter torque-speed characteristic, while the no-load slip stays the same. In this case variable speed operation can only be achieved by a slightly increased slip due to the flatter torque-speed characteristic. Moreover, active and reactive power cannot be controlled independently and are determined by the generator speed.

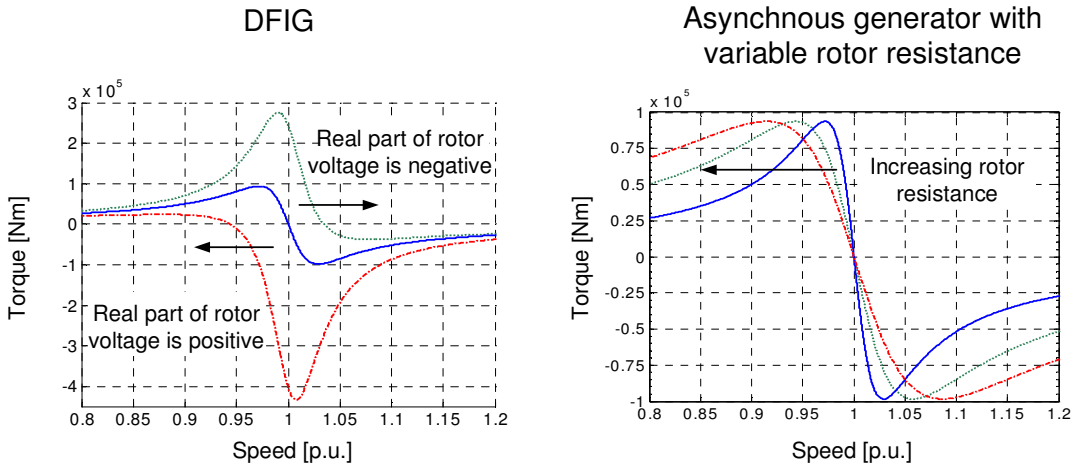

Figure 5.7: Comparison of the torque-speed characteristic for a doubly-fed induction generator with 3 different applied rotor voltages and an asynchronous generator with 3 different applied rotor resistances

5.1.2 Dynamic model of the DFIG

The dynamic model of the doubly-fed induction generator is based on the dynamic equations of stator and rotor voltage expressed corresponding to the steady state voltage equations (5.1) and (5.2). The dynamic voltage equations are given in equations (5.10) and (5.11)

$$\underline{u}_s = R_s \underline{i}_s + j\frac{\omega_{syn}}{\omega_n}\underline{\psi}_s + \frac{1}{\omega_n}\frac{d\underline{\psi}_s}{dt} \tag{5.10}$$

$$\underline{u}_r = R_r \underline{i}_r + j \frac{(\omega_{syn} - \omega_r)}{\omega_n} \underline{\psi}_r + \frac{1}{\omega_n} \frac{d\underline{\psi}_r}{dt} \tag{5.11}$$

$\underline{u}$, $\underline{i}$, and $\underline{\psi}$ are space vectors for the voltage, current and flux, respectively. ω_{syn} is the synchronous speed, ω_r is the electrical angular speed of the rotor, while ω_n is the nominal electrical frequency of the network. The equations are expressed in the per unit (p.u.) system because the p.u. representation is required in the modelling base DIgSILENT [DIgSILENT 2007a]. The p.u. system offers computational simplicity and is convenient for power system analysis [Kundur 1994]. The presented equations are expressed in the synchronous reference frame (defined in Chapter 5.2.1). Equations (5.10) and (5.11) represent a fifth-order generator model as stator transients are included. Applying the principle of neglecting the stator transients, the doubly-fed induction generator can be expressed by a third-order model [Hansen 2005]:

$$\underline{u}_s = R_s \underline{i}_s + j \frac{\omega_{syn}}{\omega_n} \underline{\psi}_s \tag{5.12}$$

$$\underline{u}_r = R_r \underline{i}_r + j \frac{(\omega_{syn} - \omega_r)}{\omega_n} \underline{\psi}_r + \frac{1}{\omega_n} \frac{d\underline{\psi}_r}{dt} \tag{5.13}$$

The dynamic model is completed by the mechanical equation:

$$J_{gen} \cdot \frac{\omega_r}{p} = T_e - T_{gen} \tag{5.14}$$

where J_{gen} is the generator inertia, T_e is the electromechanical torque of the generator, T_{gen} is the mechanical generator torque and $\frac{\omega_r}{p} = \Omega_{gen}$ is the mechanical speed of the rotor.

Ω_{gen}	mechanical generator speed
p	number of pole pairs

5.1.3 The frequency converter

The frequency converter of a DFIG is connected in the rotor circuit of the generator. Since the converter has to guarantee a bi-directional power flow it must consist of ac-

tive elements. The model uses an IGBT back-to-back voltage source converter as illustrated in Figure 5.8.

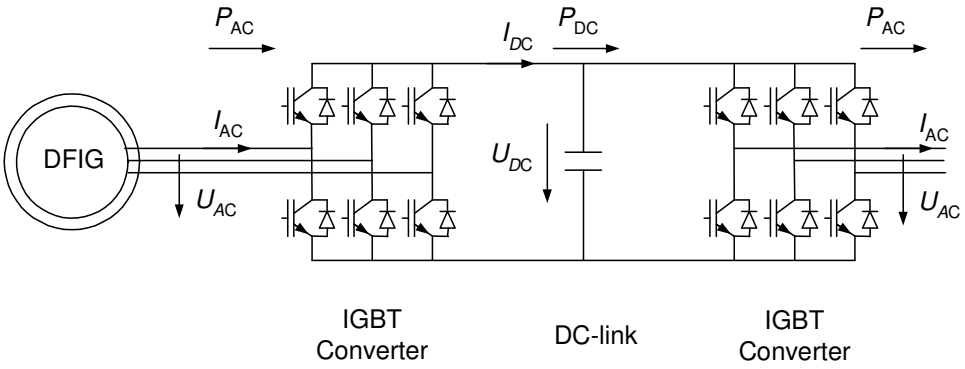

Figure 5.8: IGBT back-to-back voltage source converter in the rotor circuit of the DFIG

Like the DIgSILENT generator model, the converter model is also a built-in model in the DIgSILENT library. The fundamental equations are pre-defined in the model, while the user has to implement the characteristic data of the converter. Specific description of the converter model can be found in the technical documentation of DIgSILENT [DIgSILENT 2004]. The applied converter model represents a voltage source converter with sinusoidal pulse width modulation [DIgSILENT 2004]. The converter is modelled by a fundamental frequency approach, which is appropriate and sufficient for power system analysis. The relation between AC- and DC-voltages, which result from the PWM-converter, can be achieved with the following equations:

$$U_{AC,r} = K_0 \cdot PWM_r \cdot U_{DC} \tag{5.15}$$

$$U_{AC,i} = K_0 \cdot PWM_i \cdot U_{DC} \tag{5.16}$$

The PWM factors, separated into real and imaginary part PWM_r and PWM_i, are limited to 1 and –1 in order to avoid saturation effects. The factor K_0 depends on the modulation method, e.g. rectangular or sinusoidal modulation. Sinusoidal modulation is the standard modulation method in power applications resulting in a lower amount of harmonics [DIgSILENT 2004]. In case of sinusoidal modulation the factor K_0 is defined as:

$$K_0 = \frac{\sqrt{3}}{2 \cdot \sqrt{2}} \tag{5.17}$$

If a loss-less power conversion in the IGBT converter is assumed, the power at the AC side P_{AC} and the power at the DC side P_{DC} are equal, which is expressed by means of equation (5.18):

$$P_{AC} = \Re\left\{\underline{U}_{AC} \cdot \underline{I}^{*}_{AC}\right\} = I_{DC} \cdot U_{DC} = P_{DC} \tag{5.18}$$

Equation (5.18) can then be solved to determine the converter currents.

Nevertheless, losses can be modelled by specifying a series resistance to the converter. Moreover, as PWM converters are generally grid connected to the AC system through a reactance, the DIgSILENT built-in model of the converter includes a series reactance to the converter system.

As derived in equation (5.7) the power, which is transmitted via the converter, can be approximated by:

$$P_r = -s \cdot P_s \tag{5.19}$$

This means, that the size of the frequency converter decides about the speed range of the DFIG wind turbine. The larger the converter size, the more power can be transmitted via the converter and the larger the slip, which can be provided. However, a larger converter size means higher costs. Thus, there is a trade-off between financial benefits using a cheaper, smaller converter and the speed range, which can be provided. Generally, the DFIG converter size is designed for approximately 1/3 of the generator power, which results in a speed range of ±30 % around synchronous speed.

5.2 Frequency converter control

Control strategies and performance of the doubly-fed induction generator have been widely discussed in literature [Leonhard 2001], [Mohan 1996], [Novotny 1996] and [Pena 1996]. The control strategy, which is introduced in the following is inspired by the investigations of [Hansen 2004c] and [Hansen 2003]. The partial-scale frequency converter in the rotor circuit of the DFIG assures variable speed operation of the generator and allows independent control of the generator's active and reactive power. In the present chapter a control strategy is presented, which assures optimal energy capture of the DFIG wind turbine under fluctuating wind speed. An overview over the total dynamic simulation model of the DFIG wind turbine and the superposed control system is illustrated in Figure 5.9. The control system for normal undisturbed operation can be divided into two coordinated control blocks: the frequency converter control, which interfaces with the frequency converter, and the blade angle control interacting with the pitch mechanism of the turbine as explained in Chapter 4.4. A proper coordination between both controllers is required. As the blade angle control operates by means of the mechanical system the response time of this system is slower than the frequency converter control, which interfaces with the electrical system. The blade angle controller is only active for wind speeds above rated wind while the frequency

converter control assures optimized operation for lower wind speeds. The frequency converter control can furthermore be divided into two control blocks: the rotor side converter control and the grid side converter control. The control of the rotor side converter applies a variable rotor voltage to the generator, while the grid side converter control assures a constant DC-link voltage and controls the converter reactive power to zero. The control blocks and their operation are presented in detail in the following paragraphs.

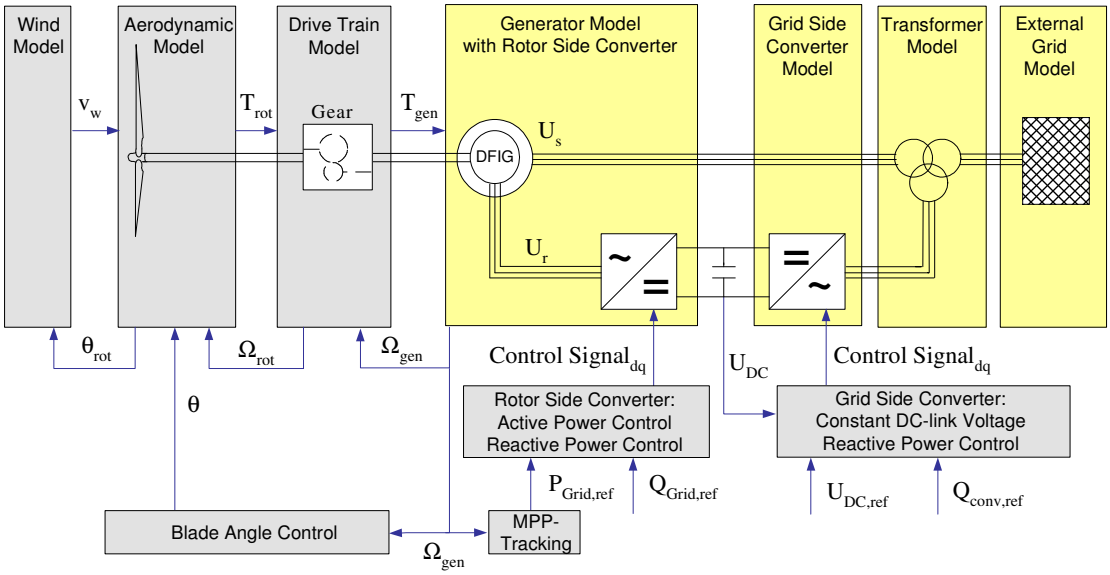

Figure 5.9: Modelling scheme and control concept of the variable speed wind turbine with DFIG

5.2.1 Reference frames for control

Control of generator systems is generally done by vector control techniques. These techniques are based on the concept of controlling the electrical quantities in their d- and q- components aligned to selected reference frames. The 3-phase generator quantities are transformed into d- and q-components of the according reference frame. Each reference frame is aligned to a state space vector of a specific generator quantity rotating with the vector's rotational frequency. This facilitates that the generator quantities become steady state terms instead of sinusoidal alternating so that control can easier be accomplished. Before the control strategy is explained, the conventions of the reference frames necessary for control of the electrical system are introduced.

Generally the space vectors are aligned to the magnetic flux of the generator, which is known as field oriented control. In this work stator flux oriented current control allowing decoupled control of active and reactive power is adapted [Novotny 1996]. The reference frames, which are used for this control, are illustrated in Figure 5.10 and are explained in the following.

Stator flux reference frame (SFRF)

The d-axis of the stator flux reference frame (SFRF) is aligned with the space vector of the stator flux. As the stator flux rotates with the electrical frequency of the stator all stator quantities (stator flux, current and voltage) become steady state quantities in the stator flux reference frame. Due to this reason the control of the rotor side converter is done in the stator flux oriented reference frame. Neglecting the stator resistance the stator flux represents the integral of the stator voltage. The stator voltage vector is then perpendicular to the stator flux. This yields, that the stator voltage consists of a q-component only in SFRF. Active and reactive power can then be determined by means of the following equations [Krause 2002]:

$$P = \frac{3}{2}\left[u_{sd}\ i_{sd} + u_{sq}\ i_{sq}\right] = \frac{3}{2} u_{sq}\ i_{sq}$$
$$Q = \frac{3}{2}\left[u_{sd}\ i_{sq} - u_{sq}\ i_{sd}\right] = -\frac{3}{2} u_{sq}\ i_{sd} \qquad \text{with } u_{sd} = 0 \text{ in SFRF} \qquad (5.20)$$

It has been derived in paragraph 5.1.1 that the rotor voltage component, which is in phase to the stator voltage, controls the active power, in this case the rotor voltage q-component, while the reactive power is then controlled by the d-component of the rotor voltage, respectively. As this reference frame rotates with synchronous speed it is sometimes referred to as the synchronous reference frame.

Rotor reference frame (RRF)

The d-axis of the rotor reference frame (RRF) is aligned with the mechanical axis of the rotor of the DFIG [Hansen 2003]. The rotor rotates relatively to the stator with the slip s. Thus, also the rotor reference frame rotates with slip frequency $\omega_r = s\omega_s$. In the DIgSILENT toolbox the generator model is e.g. implemented in the rotor reference frame [Hansen 2003]. The rotor quantities, e.g. the rotor current are therefore generally measured in the rotor reference frame. Since the rotor currents are used for control a proper transformation into the control reference frame (SFRF) is required.

Grid side converter voltage oriented reference frame (GVRF)

The control of the grid side converter is done in a grid side converter voltage oriented reference frame (GVRF). The d-axis of the reference frame is aligned with the space vector of the output AC- voltage of the grid side converter. In this case, the converter voltage u_{conv} consists of a d-component only, which yields the following equations.

$$P = \frac{3}{2}\left[u_{conv,d}\ i_{conv,d} + u_{conv,q}\ i_{conv,q}\right] = \frac{3}{2}\,u_{conv,d}\ i_{conv,d}$$
$$Q = \frac{3}{2}\left[u_{conv,d}\ i_{conv,q} - u_{conv,q}\ i_{conv,d}\right] = \frac{3}{2}\,u_{conv,d}\ i_{conv,q} \qquad (5.21)$$

with $u_{\mathrm{conv,q}} = 0$ in GVRF

The control task of the grid side converter is to maintain the DC-link voltage of the converter, while the reactive power of the grid side converter is typically controlled to zero. From equation (5.18) and (5.21) it results, that the DC voltage can be controlled by the converter current d-component, while the reactive power can be controlled by the q-current.

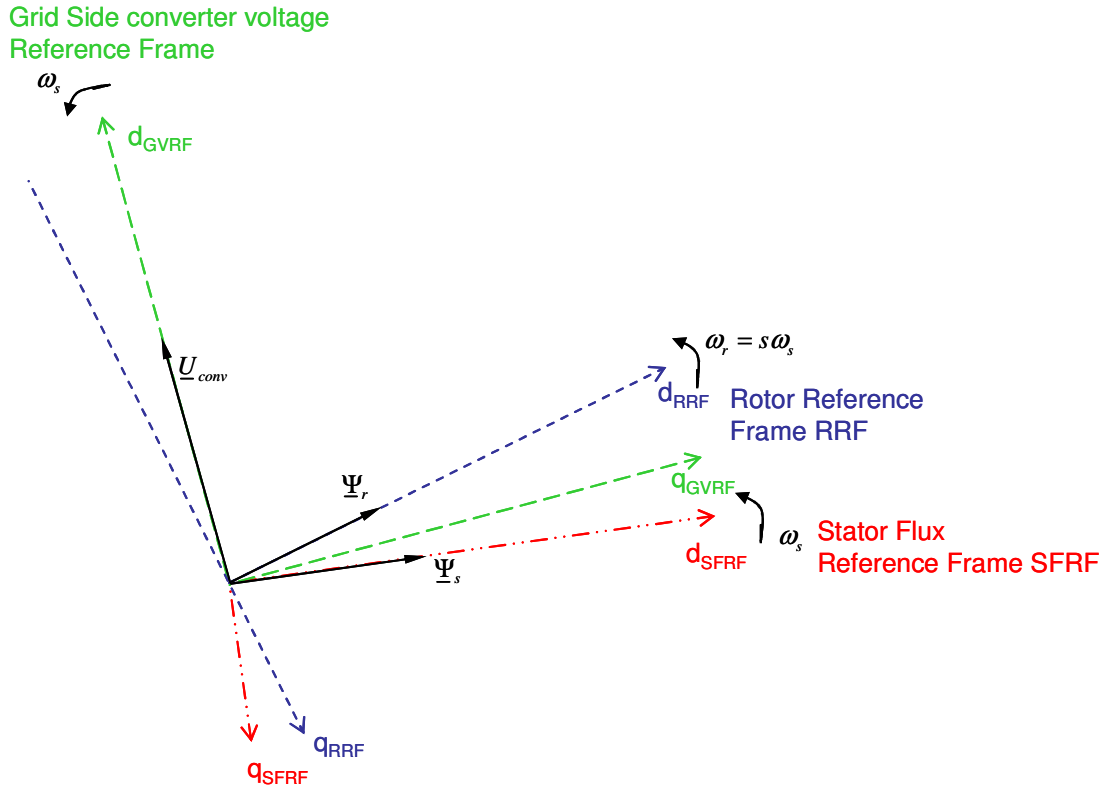

Figure 5.10: Reference frames of the DFIG used for control

5.2.2 Control of the rotor side converter

The rotor side converter provides a variable rotor voltage to the rotor terminals of the generator. The control adjusts the rotor voltage in its d- and q-components in order to control active and reactive power independently. Active and reactive power are not controlled directly but via the impressed rotor currents [Hansen 2004c]. As mentioned above, in this work the control of the rotor side converter is realized in the stator flux oriented reference frame (SFRF). In a SFRF the torque and thus the active power can be controlled by the q-component rotor current [Sun 2005], [Pena 1996].

$$T_e = \frac{3}{2} p \frac{L_m}{L_s} \frac{u_s}{\omega_s} i_{rq} \tag{5.22}$$

u_s	stator voltage	L_m	main inductance
i_{rq}	rotor current q-component	L_s	stator inductance
T_e	electromagnetic torque	ω_s	stator angular velocity

The reactive power can then be controlled by the rotor current d-component [Sun 2005] ,[Kayikçi 2005].

$$Q_s = \left(\frac{L_m}{L_s} i_{rd} - \frac{u_s}{\omega_s L_s} \right) \cdot \frac{3}{2} u_s \tag{5.23}$$

Q_s	stator reactive power	ω_s	electrical angular velocity
u_s	stator voltage	L_m	main inductance
i_{rd}	rotor current d-component	L_s	stator inductance

The generic control of the rotor side converter is illustrated in Figure 5.11. It contains two control loops: one for the active power and one for the reactive power.

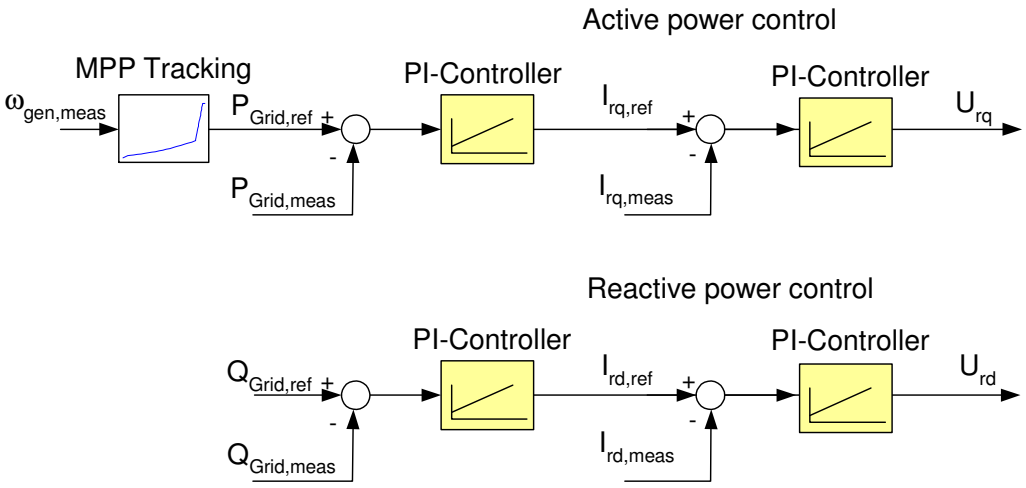

Figure 5.11: Active and reactive power control loops in the rotor side converter controller

Each control loop has a cascaded structure: a fast inner current control loop, controlling the rotor current in q- and d-axis combined with an outer slower control loop for active and reactive power, respectively. An MPP-tracking provides the reference signal $P_{\text{Grid,ref}}$ for the active power, while the reactive power $Q_{\text{Grid,ref}}$ is typically set to zero. The slower power control loop has as output a reference rotor current signal, which is further used by the fast inner current control loop. Finally two control signals for the

rotor voltage d- and q-components U_q and U_d are generated, which are sent to the PWM-controlled frequency converter.

The parameters of the controllers are determined based on the wind turbine response to steps in deterministic wind speeds. In case when the wind turbine has to support the grid, the reference signals for active and reactive power are imposed by the power system operator.

As mentioned before, the speed depends on the slow response time of the mechanical system and is therefore controlled by the slower acting pitch mechanism, while the electrical power, determined by the faster response time of the electrical system is controlled with the faster acting converter control. Nevertheless, a coordination between both controllers is necessary. Both, the blade angle control and the converter control use the generator speed signal as input. The blade angle controller uses the speed signal to limit the speed by means of blade pitching if rated speed is exceeded, while the power controller processes the speed signal in the maximum power point tracking (MPP-tracking)

The MPP look-up table predefines the points of maximum aerodynamic efficiency. By using this characteristic, below rated wind speed the turbine speed and power are automatically adapted in order to obtain the optimal tip-speed ratio λ_{opt} and the maximum power coefficient $c_{p,opt}(\theta_{opt}, \lambda_{opt})$. In this wind speed range the pitch mechanism is not active and the pitch angle is kept to its optimal value, which is zero for the considered wind turbine. The MPP-tracking look-up table is a $P \sim \omega^3$ characteristic for wind speeds lower than rated wind speed, as illustrated in Figure 5.12. The MPP characteristic continues as a ramp-function increasing P and ω linearly towards rated power. The reason for that is, that the generator reaches its rated speed, before the aerodynamic power reaches rated power. In addition to that, dynamic variations of ω around rated speed are allowed in order to absorb fast changes in aerodynamic power during wind gusts and to avoid large power fluctuation in the transition area between partial load and rated operation.

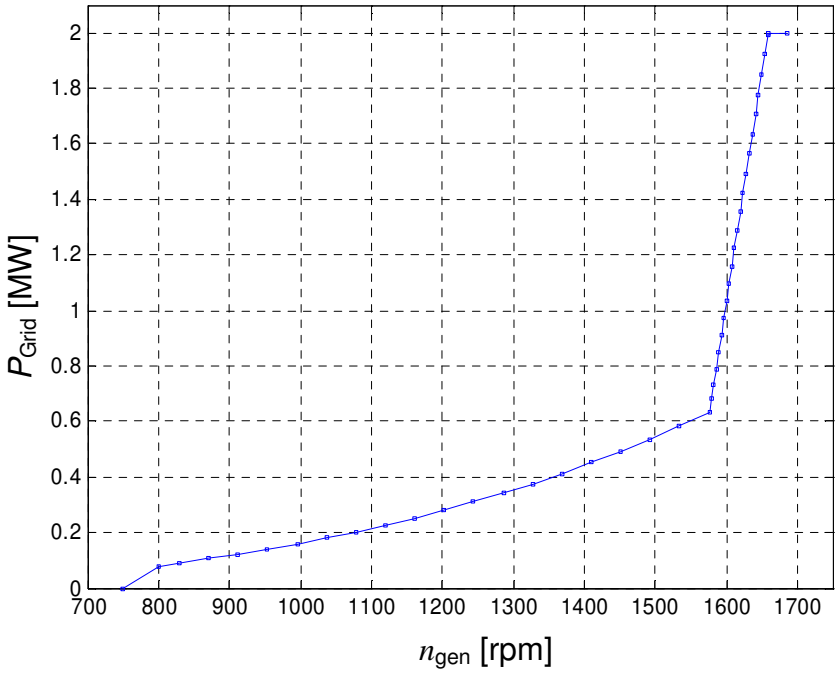

Figure 5.12: MPP-tracking characteristic

with

$$n_{gen} = \frac{\omega_{gen}}{2\pi \cdot p} \tag{5.24}$$

In order to enhance the understanding of the DFIG´s performance the P-ω characteristic is illustrated in Figure 5.13 together with the DFIG´s steady state power curves of the total produced power $P_{\text{Grid}} = P_{\text{s}} + P_{\text{r}}$ for 6 different rotor voltage vectors. The produced power of the generator is defined negative in this plot, since it also shows the steady state power curves of the DFIG, where motor operation is characterized by positive power. In order to drive the generator at the optimal operational point, which is determined by the MPP-characteristic, the control adjusts the d- and q-component of rotor voltage vector U_{r}. As derived above, the rotor voltage q-component determines the active power, while the reactive power is determined by the d-component. In the upper right corner of Figure 5.13 six different rotor voltage vectors are shown. These vectors are adjusted by the control for the wind speeds 5 m/s, 6 m/s, 7 m/s, 8.2 m/s, 10m/s and 12 m/s, respectively. The operational point at these wind speeds is marked by the circle • on the P-ω characteristic. Notice that both the rotor voltage d- and the q-component are decreasing with increasing speed. It is confirmed that in subsynchronous operation the rotor voltage q-component, controlling the active power, is positive, while it becomes negative for oversynchronous operation.

In addition to that the power curves of the DFIG are plotted, which result if the respective adjusted rotor voltage vector is applied. It exemplifies, how the steady state

power-speed characteristic of the generator changes when the rotor voltage varies. The operation point of the DFIG is thus specified by the intersection of the steady state power curve and the *P-ω* characteristic of the MPP-tracking.

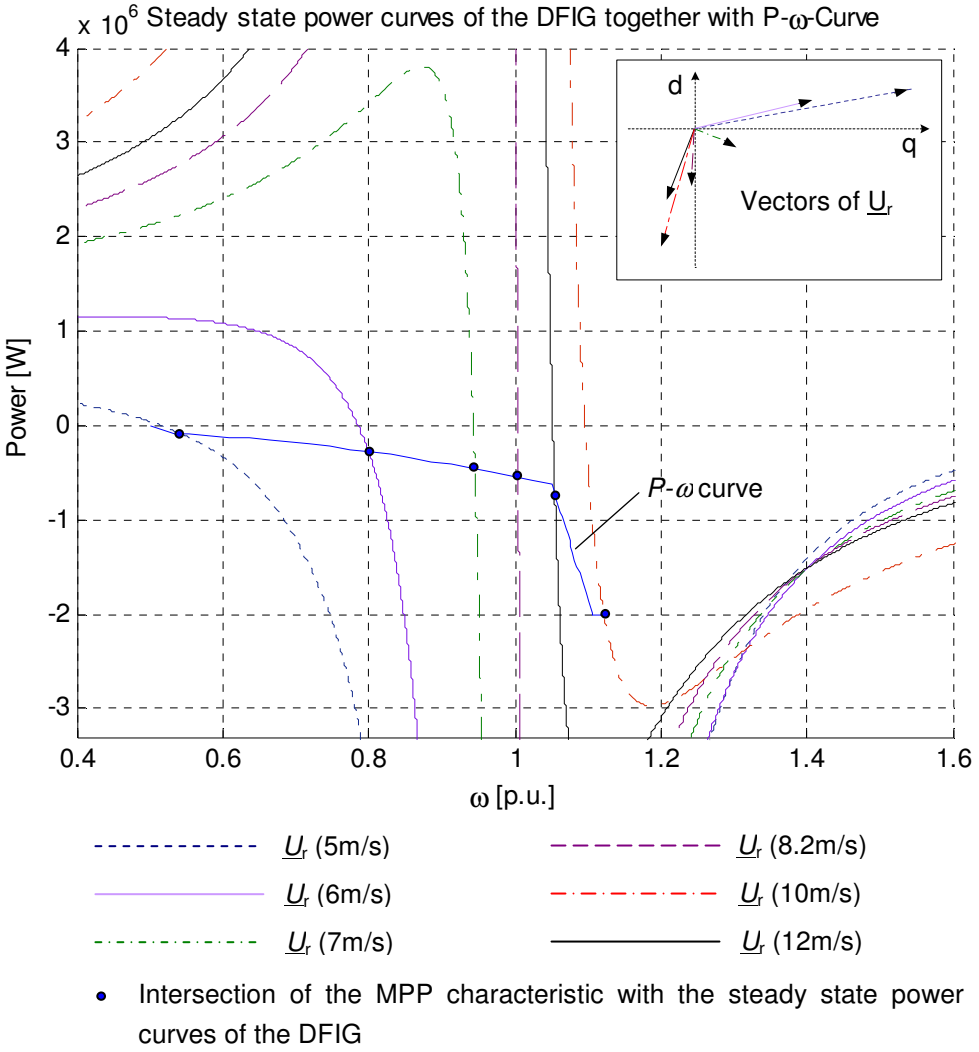

Figure 5.13: Intersections of the *P- ω* characteristic, specified by the MPP-tracking table, with the steady state power curves corresponding to the adjusted rotor voltage vector

5.2.3 Control of the grid side converter

The aim of the grid side converter control is both to maintain a constant DC-link capacitor voltage, regardless of the magnitude and direction of the rotor power, and to guaranty a converter operation with unity power factor. The reactive power in the rotor circuit is thus controlled to zero, so that any reactive power exchange is done only through the stator. Similar to the rotor side converter the grid side converter is current regulated. However, the control is now based on a converter voltage reference frame [DIgSILENT 2003]. As shown in Figure 5.14 a slower outer DC-link voltage control loop controls the DC-link voltage $U_{DC,meas}$ to a predefined value $U_{DC,ref}$. A faster inner

current control loop controls in turn the d-axis converter current $I_{conv,d,meas}$ to a reference signal $I_{conv,d,ref}$, which is provided by the slower DC-voltage controller.

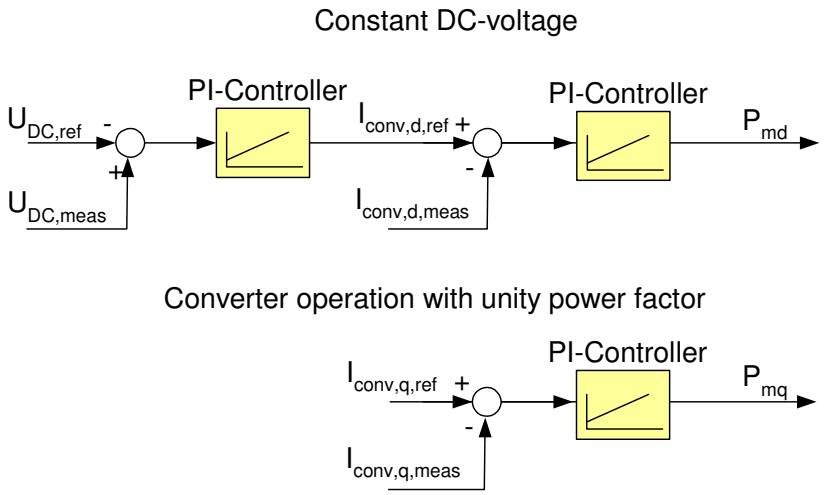

Figure 5.14: Control loops of the grid side converter controller

Simultaneously, the reactive power is controlled to zero by means of the converter current q-component. Since the grid side converter control is realized in a grid side converter voltage oriented reference frame [DIgSILENT 2003], in which the reference voltage vector has only a d-component, it becomes sufficient to control the q-current $I_{conv,q,meas}$ to zero, in order achieve converter operation at unity power factor. Hence, only the current control loop is necessary, in which the q-current is regulated to zero.

An overview over the whole control structure of the DFIG wind turbine for normal operation conditions is given in the appendix, in Section12.7.

5.3 Case studies

In order to evaluate the performance of the control system for the variable speed wind turbine concept with DFIG implemented in the power system simulation tool DIgSILENT, a set of step response simulations first with deterministic wind speed (no turbulence, no tower shadow) and then with stochastic wind speed are performed. Based on the step response analysis, the controller parameter can be designed and optimized. As specified in [Hansen 2005], this approach serves to verify the model under different operating conditions.

5.3.1 System performance under deterministic wind speeds

In Figure 5.15 typical quantities of the turbine system, as pitch angle, generator speed and power are shown for steps in wind of 1 m/s every 20 seconds. Figure 5.15 indicates, that for lower wind speeds below 12 m/s the pitch mechanism is passive and the

pitch angle is kept to its optimal value (i.e. zero for the considered turbine). Meanwhile, the power controller controls the active power to the active power reference signal provided by the maximum power tracking look-up table. The generator speed is continuously adapted to the wind speed, in such a way that maximum power is extracted out of the wind. Notice that the response time in the steps is bigger at lower wind speeds than at higher wind speeds. When the wind steps up to 12 m/s and exceeds rated wind speed (rated wind speed = 11.8 m/s) and the speed reaches its rated value of 1686 rpm, both speed controller and active power controller are active and the power is limited to the rated value of 2 MW.

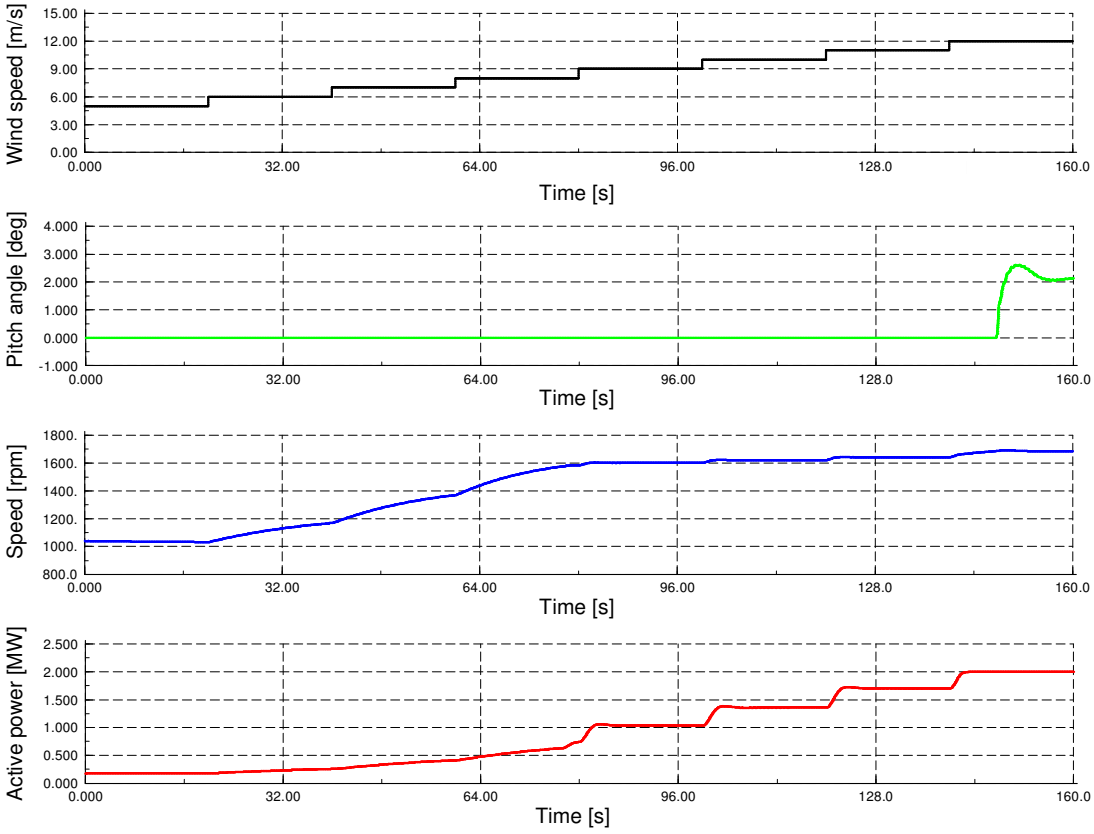

Figure 5.15: DFIG wind turbine: Wind speed, pitch angle, generator speed and active power for steps in wind of 1 m/s from 5 m/s up to 12 m/s

The step response of pitch angle, speed and power for wind speeds higher than 12 m/s is presented in Figure 5.16. The steps in wind speed yield changes in both the pitch angle and the generator speed. The step response of the pitch angle and generator speed does not present big overshoots and oscillations. Notice, that the response of the generator speed is almost identical over the whole speed range between 12 m/s and 20 m/s, a fact that indicates, that the gain scheduling controller, described in Section 4.4, is working properly. The power controller keeps the active power to 2 MW with a small deviation about 0.5 %. Since the pitch mechanism reacts slowly compared to the

power controller, dynamic variations in the generator speed and so in the rotational speed of the turbine rotor are allowed in order to absorb fast wind gusts and to temporarily store surplus power as rotational power in the turbine's inertia.

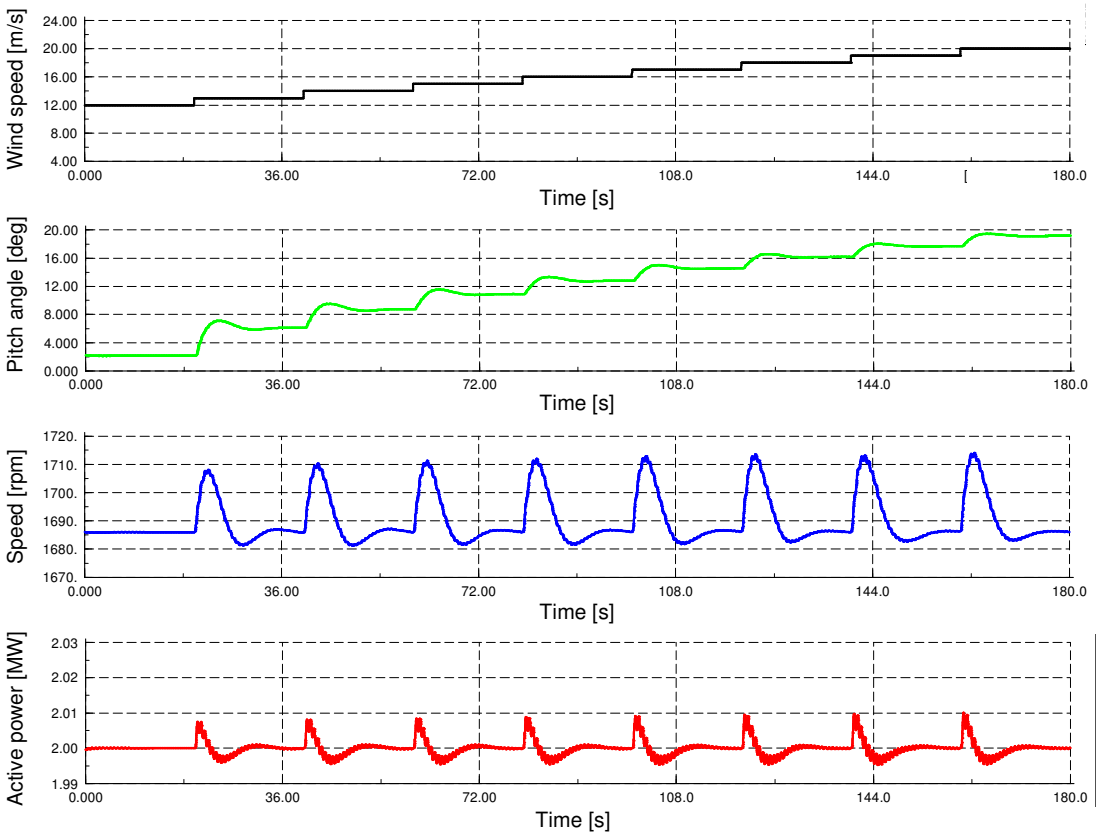

Figure 5.16: DFIG wind turbine: Wind speed, pitch angle, generator speed and active power for steps in wind of 1 m/s from 12 m/s up to 20 m/s

The simulation results confirm a good dynamic performance of the DFIG wind turbine model and of the developed control strategy during deterministic wind speeds.

5.3.2 System performance under stochastic wind speeds

In the following, simulations under stochastic wind speeds are performed. Three sets of simulations will be presented: (i) a simulation with a mean wind speed of 8 m/s, when the turbine operates at partial load only, (ii) a simulation with a mean wind speed of 12 m/s, when the operation of the turbine changes between partial and full load, (iii) a simulation with a mean wind speed of 20 m/s, where moreover the ability of the DFIG wind turbine to regulate its power to imposed reference values is underlined.

Figure 5.17 shows the turbine quantities pitch angle, rotational speed and active power for a fluctuating wind with a mean wind speed of 8 m/s and a turbulence intensity of 10 %. The turbine operates at partial load only, so that the pitch mechanism is passive. The pitch angle is kept to zero while the speed and the power are adapted to

capture the maximal power out of the wind. As expected the speed and the power are tracking the slow variations of the wind speed.

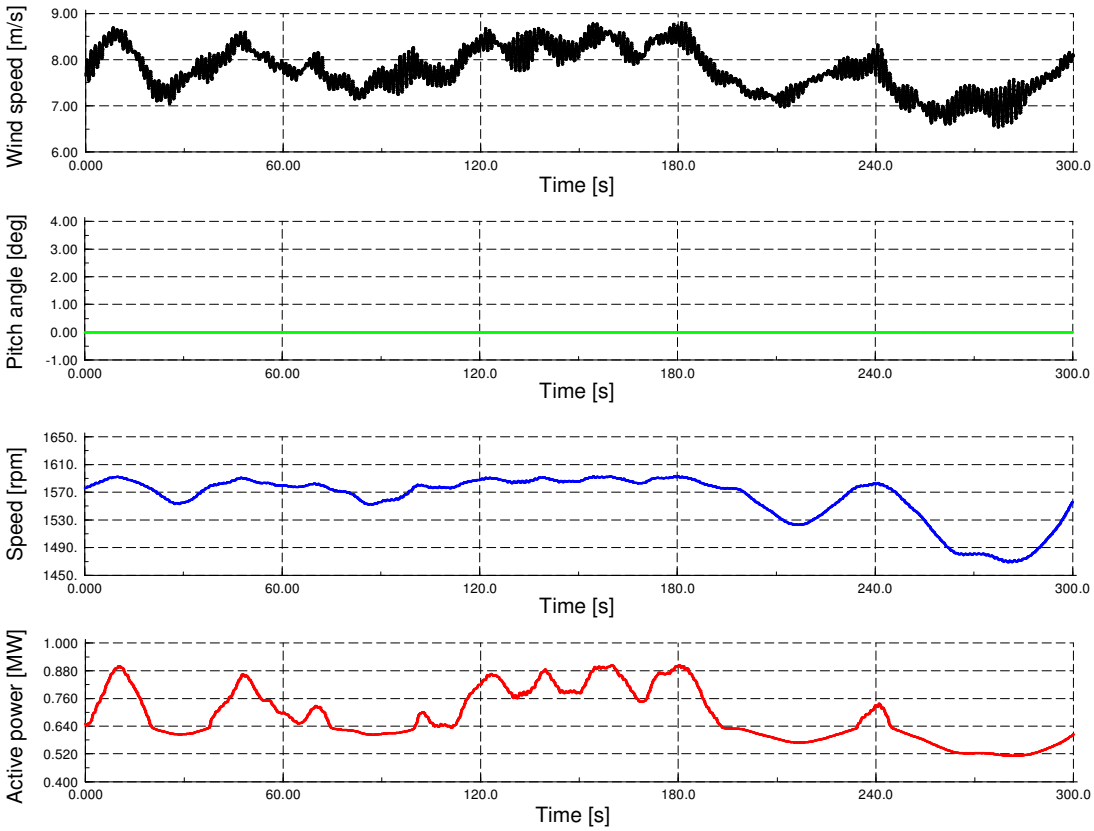

Figure 5.17: DFIG wind turbine: Wind speed, pitch angle, generator speed and active power under stochastic wind speed with a mean wind speed of 8 m/s

Figure 5.18 illustrates simulation case (ii) with a mean wind speed of 12 m/s. In this case the pitch mechanism is activated when the speed exceeds its rated value. Notice, that the power is limited to rated power as long as the pitch mechanism is active. Small dynamic variations of the speed above rated speed are allowed to absorb fast wind gusts and to reduce the mechanical stress on turbine and generator system.

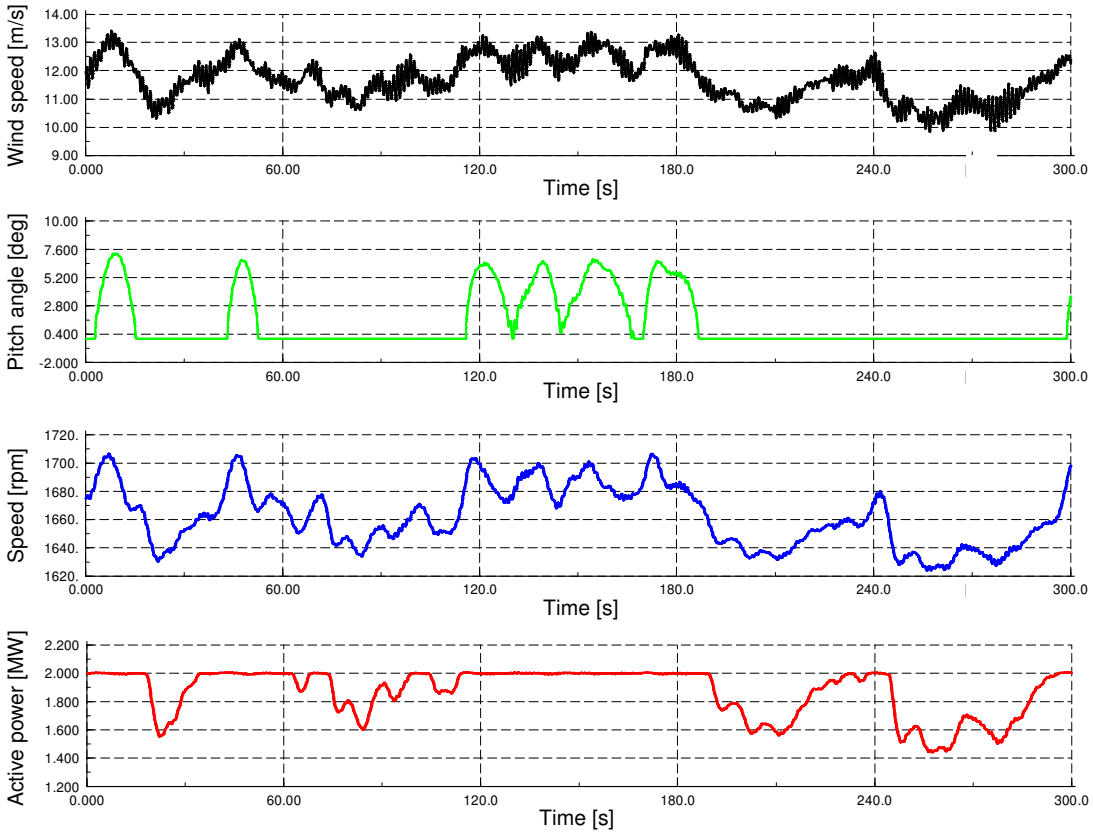

Figure 5.18: DFIG wind turbine: Wind speed, pitch angle, generator speed and active power under stochastic wind speed with a mean wind speed of 12 m/s

Finally, the simulation results of Figure 5.19 illustrate the ability of the variable speed wind turbine with DFIG to regulate its power production to an imposed reference value and moreover underline the feature of independent active and reactive power control. Figure 5.19 illustrates the pitch angle, the generator speed as well as the active and reactive power in case of turbulent wind with a mean wind speed of 20 m/s and a turbulence intensity of again 10 %. The pitch angle signal reflects the stochastic character of the wind and is tracking the slow variations of the wind speed. However, independent of the fluctuations of the wind, the active power can be controlled and limited to 2 MW. The reference power is reduced from 2 MW to 1 MW between 100 and 200 seconds and stepped up back again to 2 MW. Notice that the active power output is following this reference very well. This is however only possible, if the wind speed is sufficiently high. The reduced reference power of 1 MW implies higher pitch angles. The first 250 seconds the reactive power is controlled to zero. Then the same active power control sequence is repeated for a different reactive power reference of 0.5 MVar. Figure 5.19 points out, that the designed control strategy of the variable speed wind turbine model with DFIG is able to control active and reactive power independently to specific imposed values, exactly as a conventional power plant does.

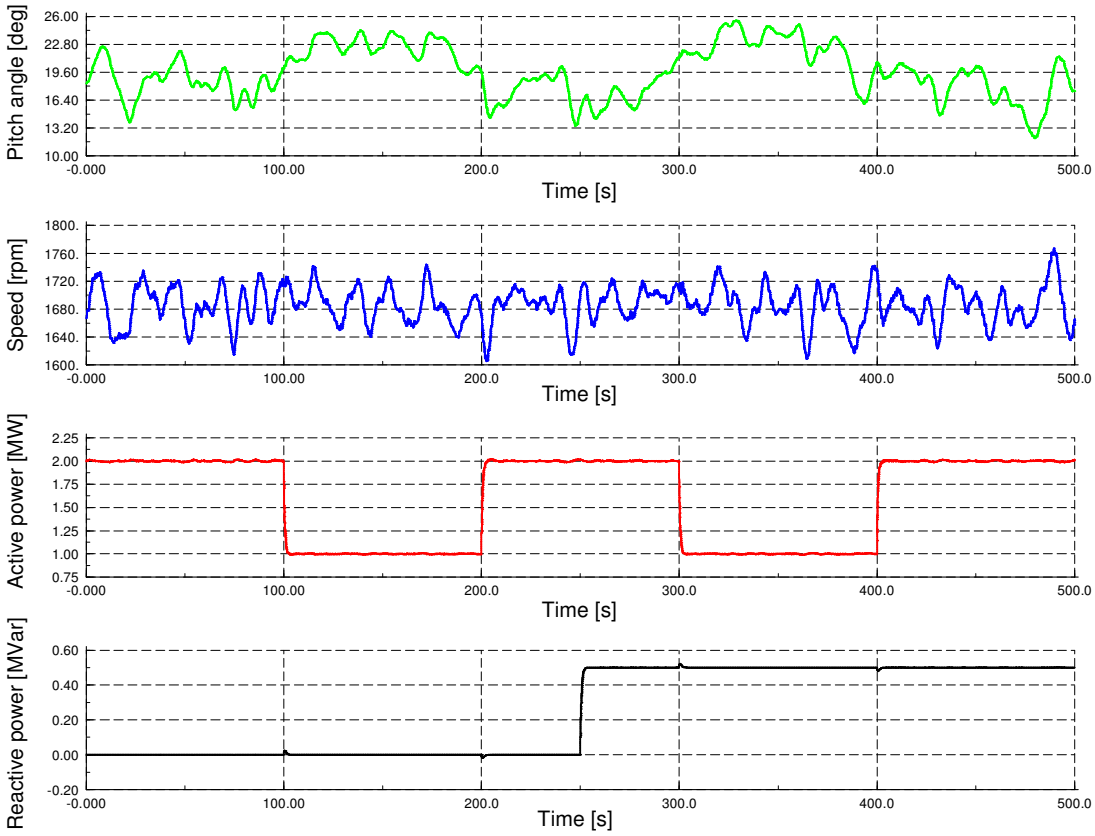

Figure 5.19: DFIG wind turbine: Pitch angle, generator speed and active and reactive power production under stochastic wind speed with a mean wind speed of 20 m/s

5.4 Summary

The goal of the present work is to develop dynamic simulation models of variable speed wind turbines and to design appropriate control strategies enabling the turbines to act as active components in the power system similar to conventional power plants. Chapter 5 focuses on the design and investigation of the entire control system for a variable speed wind turbine with doubly-fed induction generator, the most commonly used wind turbine concept today. A comprehensive dynamic simulation model is developed in the simulation tool DIgSILENT.

In a first step a detailed analysis of the doubly-fed induction generator's steady state behaviour is presented. The steady state power curves of the generator corresponding to different adjusted rotor voltage vectors are illustrated. Different rotor voltage vectors cause a significant change in the shape of the power curves, which in turn enhances the controllability of the generator and the turbine system.

In a second step a dedicated control strategy of the DFIG system is designed. The control is realized by vector control technique using appropriate reference frames. The control of the wind turbine is achieved by two coordinated controllers: a speed controller and a power controller. The turbine power is directly controlled by the converter, while the generator speed is regulated by the pitch angle. The converter control

is furthermore subdivided into rotor side converter control and grid side converter control. The rotor side converter controls the generator's active and reactive power production on the grid, while the grid side converter control maintains a constant DC-link voltage and assures converter operation at unity power factor. The controller parameter are designed and optimized based on a set of step response simulations.

A set of simulations is performed in order to illustrate that the presented control method successfully controls the variable speed DFIG wind turbine within a range of normal operational conditions. At wind speeds less than the rated wind speed the converter seeks to maximise the power according to the MPP-tracking. At large wind speeds the speed controller permits a dynamic variation of the generator speed in order to avoid mechanical stresses, while the converter keeps the power to the rated power. The control strategy facilitates furthermore independent control of active and reactive power to imposed reference values at variable speed. However, active power production is still dependent on the actual wind speed. Nevertheless, it can be concluded, that the DFIG wind turbine can operate in a similar manner as a conventional power plant does.

6 DFIG wind turbines´ grid support capability

Due to the increasing penetration of wind power as e.g. in Germany and Denmark the power system operators are revising nowadays the grid codes in those countries [E.ON 2006], [Energinet.dk 2004] (see Chapter 2.3). Basically these grid codes require newly installed wind turbines ride-through faults and to support directly the power system in case of grid faults. The attention in the present chapter is thus on both, the wind turbine's fault ride-through and grid support capability. The fault ride-through capability of wind turbines is required because otherwise a tripping of the large wind turbines in case of grid faults would cause a significant loss of electric power supply.

The variable speed wind turbine with doubly-fed induction generator is recently the most commonly used wind turbine concept and is already applied in large wind parks as e.g. the Danish offshore wind park Horns Rev [Horns Rev 2007]. The attractiveness of the DFIG for the use in wind turbines is due to the partial-scale frequency converter in the rotor circuit causing an important financial advantage compared to generator concepts with full-scale converter. The converter system offers also good potentialities for control, which can especially be exploited for fault ride-through and grid support purposes. However, the financial advantage turns into a technical disadvantage in case of grid faults, as the partial-scale frequency converter must be protected against high transient currents and voltages.

Focus of this chapter is to analyse the dynamic behaviour of the DFIG wind turbine during faults. Based on this an advanced control strategy is developed, which facilitates fault ride-through of DFIG wind turbines and enables them to support the power system stability.

6.1 Dynamic behaviour of DFIG wind turbines under grid faults

In the following the performance of a DFIG wind turbine equipped only with the standard control strategy for normal operation, as described in Chapter 5, is analysed during grid faults. In this first stage analysis, no additional controller for enhancing the DFIG fault ride-through capability is assumed yet.

A symmetric three-phase short circuit at the wind turbine's high voltage grid connection terminal is simulated. The simulation setup, illustrated in Figure 6.1, is according to the simulation description, presented in the grid code requirements [Energinet.dk 2004].

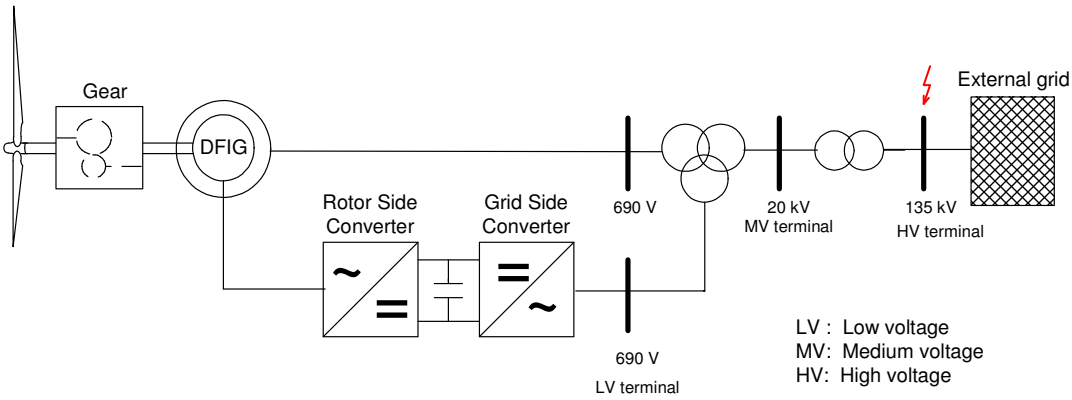

Figure 6.1: DFIG wind turbine subjected to grid fault at HV terminal

The external grid, to which the turbine is connected, is modelled by means of a Thevenin equivalent, which is sketched in Figure 6.2. The grid is characterized by a short circuit power S_k of approximately 10 times the rated wind turbine power $P_{\text{wind turbine, rated}}$ and an R/X ration of 0.1. The three phase short circuit happens at the high voltage grid connection terminal of the turbine and is represented with the short circuit impedance $R_f + j\,X_f$. It is assumed that the DFIG is initialized to operate at rated power. This represents a worst-case scenario as during a voltage drop the difference between the absorbed aerodynamical turbine power and output electrical power becomes maximum. The wind speed can be considered constant during the simulations, as fault durations are short compared to wind speed changes. A three-phase grid fault is however rare compared to other grid fault types (single-phase faults or two-phase faults). Nevertheless, the three-phase fault is considered to be a worst-case scenario, too, as it results in the most severe situation in the power system [Balzer 2006].

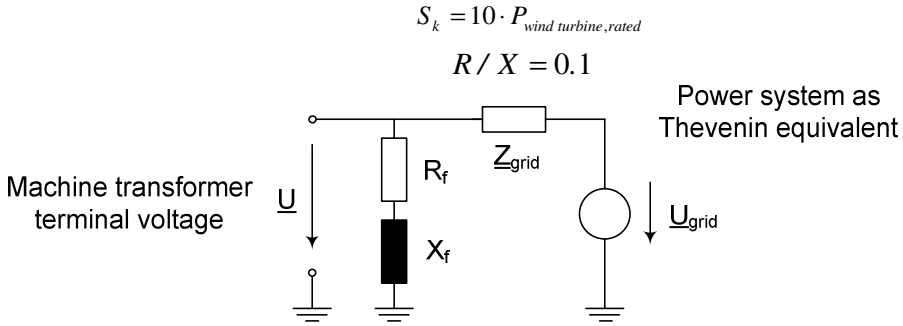

Figure 6.2: Single phase Thevenin equivalent of the external grid with short circuit impedance R_f+jX_f

6.1.1 Grid fault impact on the electrical system

As illustrated in Figure 6.3, the simulated grid fault results in a voltage drop down to approximately 20 % and lasts for 100 ms. The voltage at the MV terminal together with the turbine's active and reactive power production are plotted. The voltage drop at

the HV terminal implies also a voltage drop at the DFIG generator terminal. This in turn leads to a corresponding decrease of the stator and rotor flux in the generator, which results in a reduction of the electromagnetic torque and active power. As the stator flux decreases, the magnetization, stored in the magnetic field, has to be released. The generator starts thus its demagnetization over the stator, which is illustrated in Figure 6.3 by the reactive power peak in the moment of the fault.

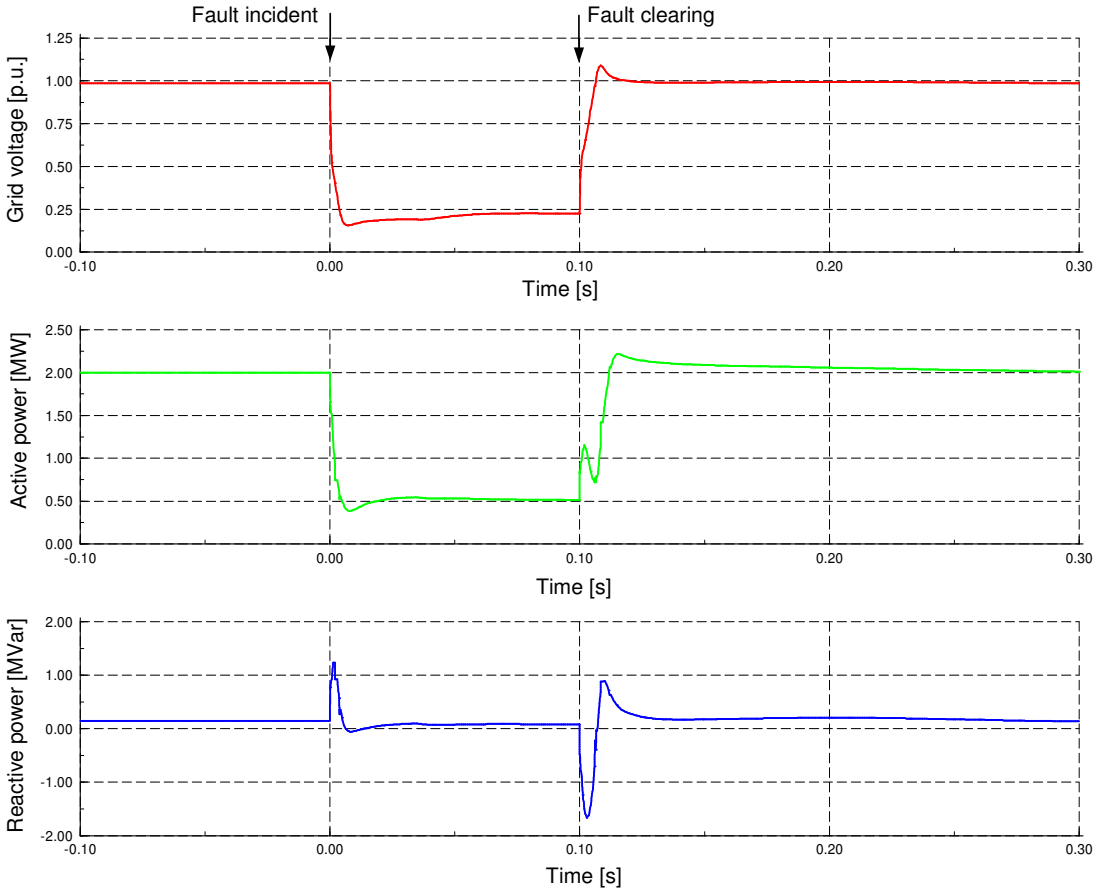

Figure 6.3: Simulation results at the medium voltage terminal: grid voltage, active and reactive power production for a three phase short circuit at the high voltage terminal, fault duration of 100 ms

Due to changing voltage and flux in the generator, high current transients appear in the stator and rotor windings, which can be expressed with as follows [Dittrich 2005]:

$$\underline{u}_s - \underline{u}_r - j\omega_{gen}\underline{\Psi}_r = R_s\underline{i}_s + L_{s\sigma}\frac{d\underline{i}_s}{dt} - R_r\underline{i}_r - L_{r\sigma}\frac{d\underline{i}_r}{dt} \qquad (6.1)$$

$\underline{u}_s$	stator voltage space vector	R_s	stator resistance
$\underline{u}_r$	rotor voltage space vector	R_r	rotor resistance
$\underline{i}_s$	stator current space vector	$\underline{\Psi}_r$	rotor flux linkage space vector

$\underline{i}_r$	rotor current space vector	$L_{s\sigma}$	stator leakage inductance
ω_{gen}	mechanical angular velocity	$L_{r\sigma}$	rotor leakage inductance

In order to compensate for the increasing rotor current, the rotor side converter control increases the rotor voltage, which implies a surge of power from the rotor terminals through the converter. On the other side, as the grid voltage has dropped immediately after the fault, the grid side converter is not able to transfer the whole power from the rotor through the converter further to the grid. The grid side converter's control of the dc-voltage reaches thus quickly its limitation. As a result, the additional energy goes into charging the dc-bus capacitor and the dc-voltage rises rapidly. This fact is illustrated in Figure 6.4, where rotor current and DC-link voltage are plotted. In this simulated fault case both, rotor current and DC-link voltage, reach very high transient values, which might damage the power electronics in the converter. Allowed limits for overcurrent and overvoltage of power electronics are generally specified individually by the manufacturer (e.g. [Semikron 2007], [Infineon 2007], [Woodward 2007]). As mentioned in [Akhmatov 2003a] the converter relay settings can also be determined by reasonable assumptions and evaluation of the frequency converter operation. [Akhmatov 2003a] proposes a maximum allowed rotor current of 2 p.u. and a maximum DC-link overvoltage of 25 % above its rated value. Both of these maxima are exceeded in the performed simulation. Therefore, a converter protection system, e.g. a crowbar protection, described in Section 6.2.1, is inevitable and must be implemented for the DFIG system.

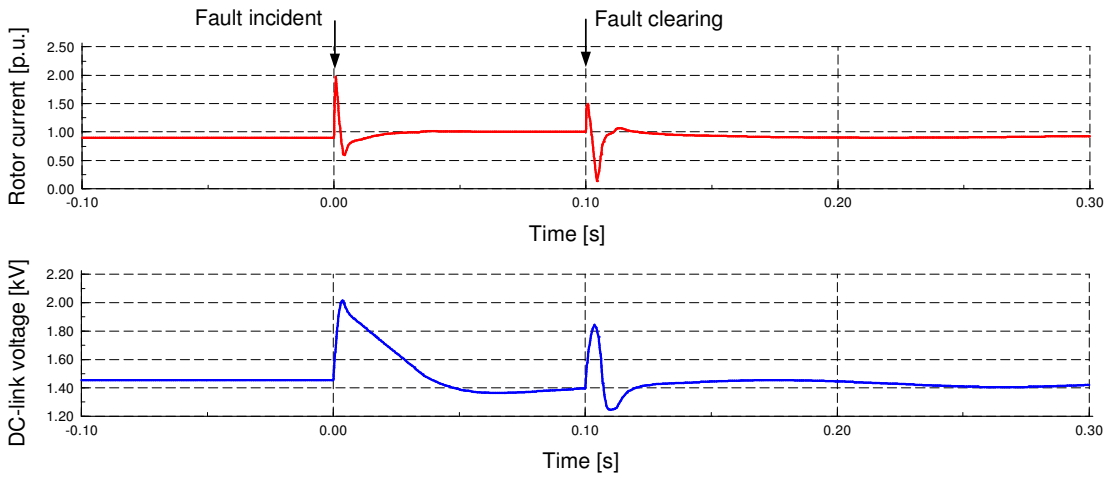

Figure 6.4: Simulation results: rotor current and DC-link voltage of the DFIG generator for a three phase short circuit at the high voltage terminal, fault duration of 100 ms

Immediately after the fault is cleared, the stator voltage is restored, the electromagnetic torque and active power start to increase. As the grid voltage and the flux

increase, the partly demagnetised stator and rotor oppose this change in flux leading thus again to rotor and stator current transients [Hansen 2007d] [Michalke 2007a].

6.1.2 Grid fault impact on the mechanical system

In stability analysis, when the system response to heavy disturbances is analysed, the drive train system must be approximated by at least a two-mass model [Akhmatov 2003a]. The idea of using a two mass mechanical model, described in Section 4.3, is to get a more accurate response from the generator and the frequency converter during grid faults and to have a more accurate prediction of the impact on the power system.

During a grid fault, as the electrical torque is significantly reduced, the drive train of the wind turbine acts like a torsion spring that gets untwisted. Due to the torsion spring characteristic of the drive train both the mechanical torque, the aerodynamical torque and thus the generator speed start to oscillate with the so-called free-free frequency of the system. In case of a grid fault, the drive train model can be reduced to a single eigenfrequency represented by the stiffness K_{shaft} and an equivalent inertia J_{eq} determined by:

$$J_{eq} = \frac{J_{rot} \cdot k_{gear}^2 \cdot J_{gen}}{J_{rot} + k_{gear}^2 \cdot J_{gen}} \tag{6.2}$$

The frequency of the drive train oscillations during grid fault can be estimated according to [Soerensen 2003] as:

$$f_{osc} = \frac{1}{2\pi} \cdot \sqrt{\frac{K_{shaft}}{J_{eq}}} \tag{6.3}$$

As these torsional oscillations may influence the converter operation during the grid fault and also a short while after the fault, their modelling by using at least a two-mass model for the drive train system is essential. These torsional oscillations can even be excited and become undamped at a fast converter control [Akhmatov 2002a].

Figure 6.5 shows the mechanical signals of the wind turbine under the same three-phase short circuit as performed in the previous subsection. The mechanical and electromagnetic torque of the generator are compared and shown together with the generator speed and the pitch angle. Since the mechanical quantities have larger time constants than the electrical quantities, the fault response is much longer in the mechanical system. Thus, the mechanical signals are plotted for 1.2 s although the fault clearing already happens at 100 ms.

When the electromagnetic torque of the generator drops in consequence of the voltage drop the mechanical torque of the generator drops, too. Thus, the torsion spring

in the drive train gets untwisted. However, the drop of the mechanical torque is slower than of the electromagnetic torque and therefore the generator starts to accelerate. The dynamic relation between the electrical torque, mechanical torque and the generator speed is reflected in Figure 6.5. Notice that the acceleration of the generator during the fault is counteracted by the pitch control system, sketched in Figure 4.5 and illustrated in Figure 6.5.

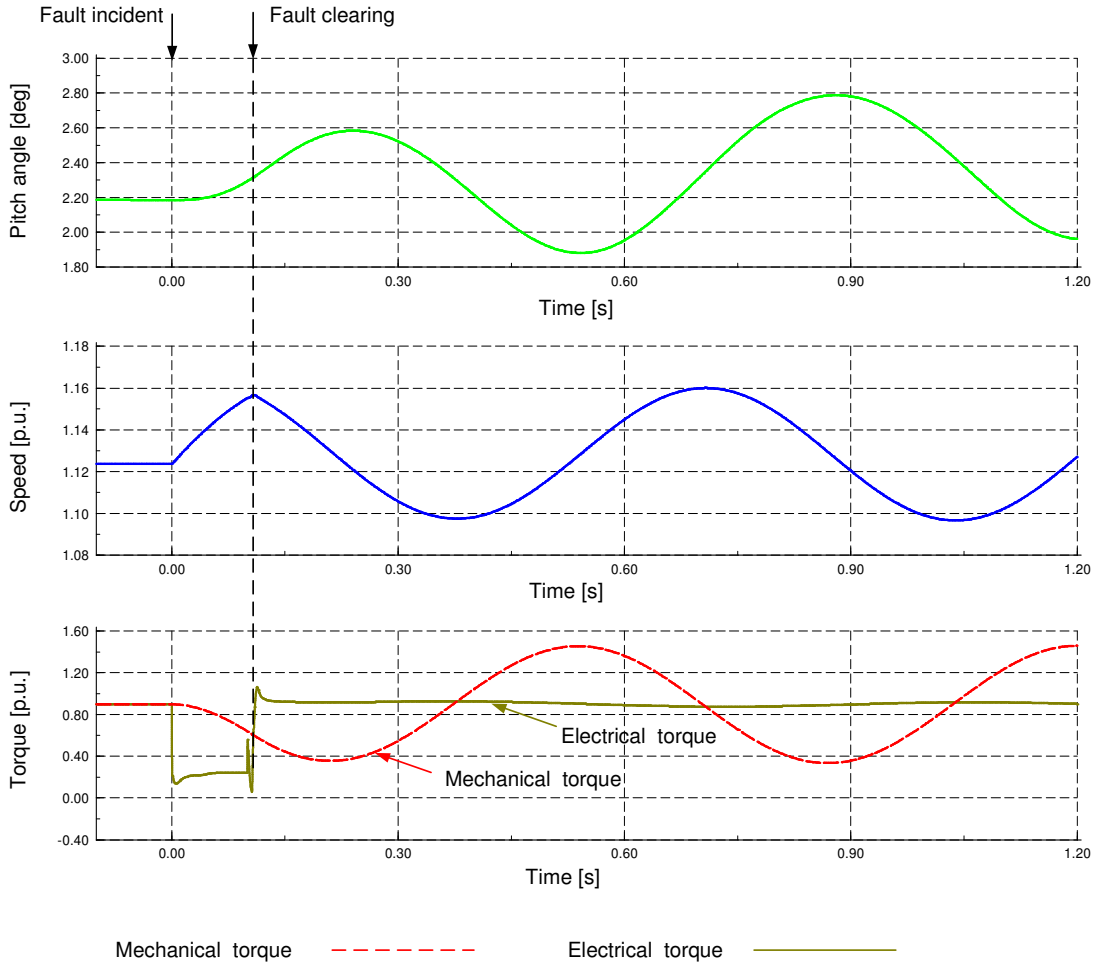

Figure 6.5: Simulation results: pitch angle, generator speed, electrical and mechanical torque of the DFIG generator for a three phase short circuit at the high voltage terminal, fault duration of 100 ms

Due to the torsion spring characteristic of the turbine drive train, the mechanical and aerodynamical torque and thus the generator and rotor speed start to oscillate. The mechanical system recovers more slowly compared to the electrical system, which is due to the high inertia of the turbine. Due to the big difference between the acting torques at the drive train and because of the long lasting oscillations, the system is exposed to big mechanical stresses. In the next chapter (Section 6.2.2) it will be shown how the mechanical stresses can be minimized by damping the oscillations by means of an appropriate fault control.

6.2 Fault ride-through capability

This section presents a control strategy, which enables the DFIG wind turbine for fault ride-through and facilitates reactive power supply and voltage re-establishment during grid faults. Figure 6.6 gives an overview over the total control structure of the DFIG wind turbine, which is extended by additional protection and control blocks for grid faults. The converter system is protected by a crowbar. The blade angle control assures overspeed protection. Acting on the frequency converter control, blocks for voltage control and reactive power boosting are implemented. Furthermore, an active damping controller is implemented in order to reduce the mechanical stresses of the turbine. In the following the presented protection and control blocks will be described in detail.

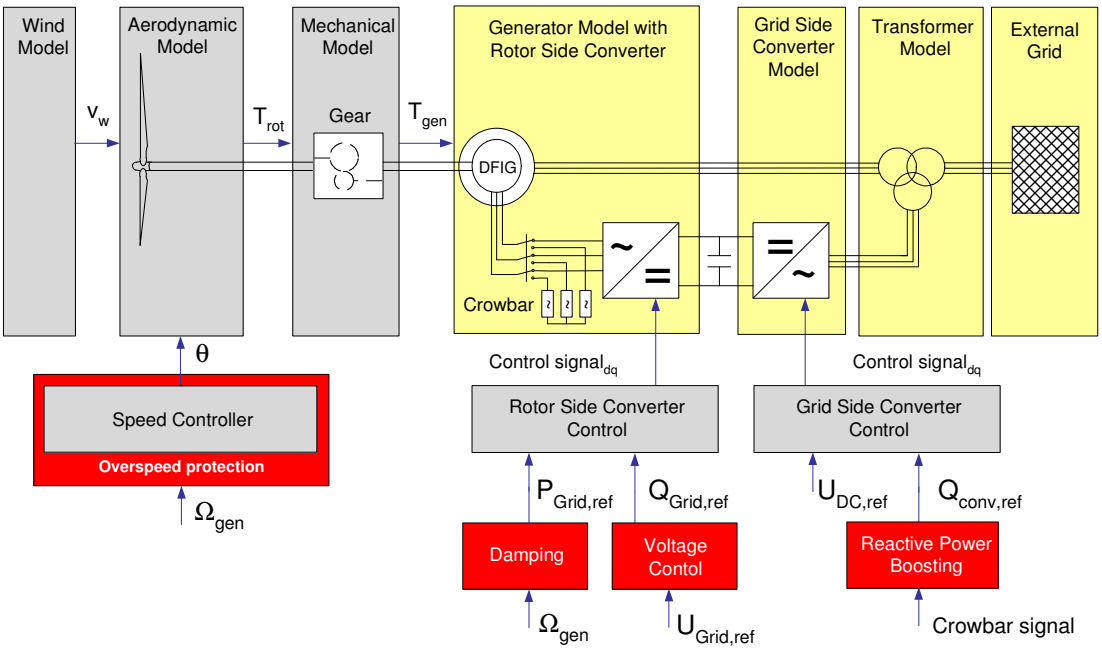

Figure 6.6: Control system of the DFIG wind turbine with additional control blocks for fault control

6.2.1 Protection system

Crowbar protection

In case of grid faults high transient rotor currents arise, implying a damaging risk for the power electronics of the rotor side converter. Moreover, the surge of power into the rotor side converter charging the DC link capacitor may cause overvoltages in the converter. Due to this reason a suitable protection of DFIGs is necessary. A simple protection method is to short-circuit the rotor via an external rotor resistant called crowbar (Figure 6.7) when high rotor currents are detected or the DC-link voltage exceeds the allowed limit [Akhmatov 2003a], [Akhmatov 2003b], [Seman 2006a]. In the present work a rotor current limit of 1.3 p.u is defined. According to [Akhmatov 2003a] maximum allowed DC voltage is set to 1.75 kV, which corresponds to a maximum

overvoltage of 25 % above rated voltage. The crowbar coupling protects the converter system and facilitates fault ride-through, which enables the DFIG to contribute to power supply directly after fault clearing. However, during crowbar coupling the rotor side converter is blocked and the generator's controllability in terms of active and reactive power production is temporarily lost. Figure 6.7 shows the DFIG with crowbar protection. Different crowbar types and crowbar control algorithms are possible [Niiranen 2004]. As an example in Figure 6.7 the crowbar impedances are coupled in each phase via an IGBT switch, which can be actively switched on and off by an activation control system. According to [Niiranen 2006] actual grid code requirements can only be accomplished by DFIG wind turbines if they are equipped with such "active crowbars" using fully controllable semiconductor switches, so that crowbar coupling and decoupling can be determined externally. In contrast to this "passive" crowbars are equipped with a thyristor switch, which allows closing the rotor circuit but not to open it until the crowbar current is extinguished [Rodriguez 2005]. The crowbar remains connected until the main circuit breaker is opened causing in the end a disconnection of the wind turbine. In order to accomplish fault ride-through the "active" crowbar type is applied in the present work so that the crowbar is externally decoupled, when transient currents and voltages have decayed, and the rotor side converter is restarted after crowbar disconnection.

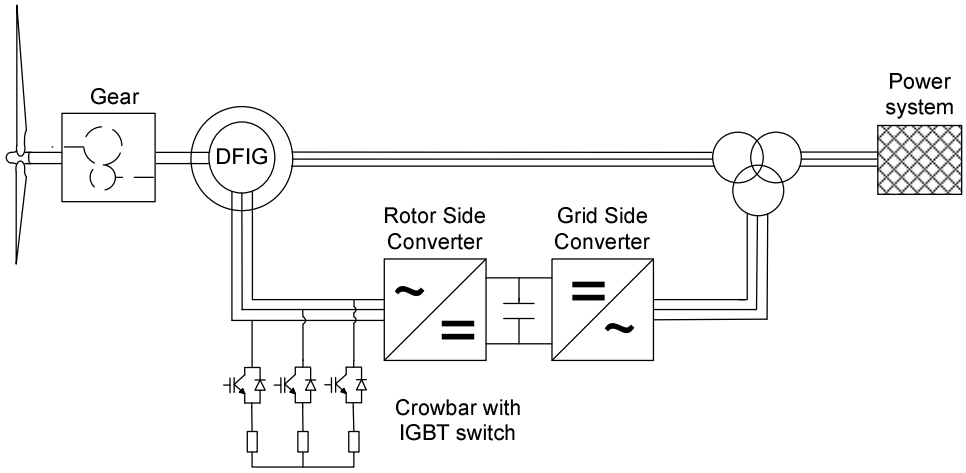

Figure 6.7: DFIG with crowbar protection

Figure 6.8 illustrates the static curves for the torque and reactive power as function of speed for different crowbar resistances R_{Crowbar}, applied for one 2 MW doubly-fed induction generator. When the crowbar is triggered, the rotor is short circuited over the crowbar impedance and therefore the DFIG behaves as a conventional squirrel cage induction generator (SCIG) with an increased rotor resistance. An increased crowbar resistance improves the torque characteristic and reduces the reactive power demand of the generator at a certain speed. By adding an external resistance in the ro-

tor circuit, the pull-out torque of the SCIG generator is moved into the range of higher speeds. During grid faults the dynamic stability of the SCIG generator is thus improved by increasing the external resistance [Akhmatov 2003a].

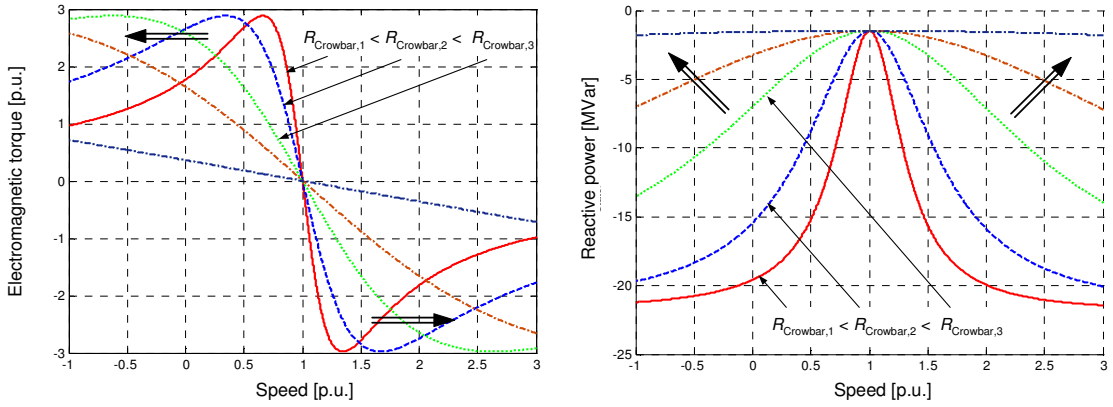

Figure 6.8: Static curves for torque and reactive power as function of speed for different crowbar resistances

Figure 6.9 shows the results of several dynamic simulations that have been carried out for different crowbar resistance values in case of a 100 ms three-phase fault at the high voltage terminal of the 3-windings transformer of the DFIG wind turbine. A similar study can be found in [Akhmatov 2002a], [Hansen 2007d]. The rotor current, the electromagnetic torque and the reactive power of the generator are illustrated in Figure 6.9. These electrical signals are determined using the full order transient generator model. In the moment of the short circuit fault, the rotor current starts increasing until the over current protection triggers the crowbar and inhibits the rotor side converter. In the simulation, the time delay due to switching of the shunt resistance is neglected.

Figure 6.9 depicts both the crowbar's function to limit the rotor current and the crowbar's influence on the reactive power demands of the generator. Small resistance values cause higher current and torque transient peaks in the fault moment. A higher crowbar resistance has an efficient damping effect both on the rotor current and on the electromagnetic torque. In accordance with Figure 6.8, it has also a positive effect on the dynamic stability of the power system, as it implies a reduced reactive power consumption in the fault clearance moment.

As illustrated in Figure 6.9, a too high crowbar resistance can however imply a risk of excessive rotor current, torque and reactive power transients when the crowbar is removed. Moreover, issues of thermal heating of the crowbar resistance, its size and its costs must be considered. A correct choice of the crowbar resistance must therefore take into account the previous aspects. Comparing the simulations results for different

crowbar resistance values, a crowbar resistance value of 0.5 p.u. is considered to be an appropriate trade-off for the present case study.

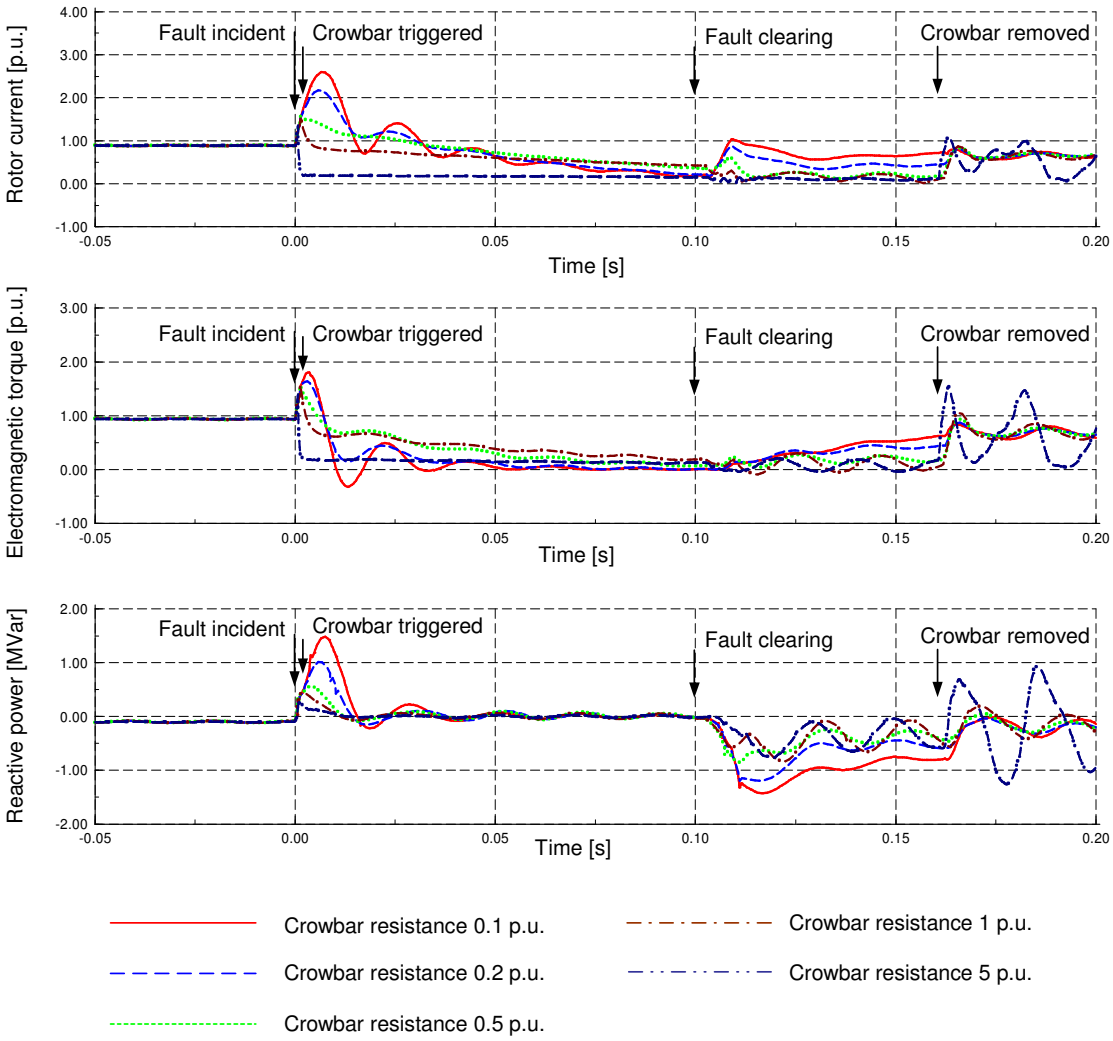

Figure 6.9: Dynamic performance of DFIG for different values of the crowbar

Another important aspect in terms of crowbar coupling is the crowbar coupling time. At the one hand, it is aimed to decouple the crowbar as fast as possible in order to regain the generator's controllability, when the rotor side converter is reconnected. However, in the moment of fault clearing high transient currents can again occur, which implies the risk that the crowbar may subsequently be triggered again. The crowbar coupling time is furthermore influenced by the dynamics of the power electronic devices e.g. the IGBTs. Moreover, the power electronics in the converter need some time to enable the converter restart. [Erlich 2007] assumes e.g. a crowbar connection time of minimum 60 -120 ms. In the present work the crowbar connection time is set to 100 ms, when transient currents and voltages have decayed. However, in order to avoid subsequent tripping of the crowbar, in some simulation cases the crowbar connection time is longer and the crowbar is removed after the fault is cleared.

In terms of crowbar coupling DFIG operation with undersynchronous speed needs special analysis. When the DFIG operates undersynchronous and the crowbar is triggered, the DFIG starts to behave as a SCIG. However, a SCIG with undersynchronous speed operates as a motor and would absorb electrical power from the grid. The fact is however not critical for stability as the voltage during the fault is low and thus also the power consumption. Furthermore, the asynchronous machine, now acting as a squirrel cage induction machine in motor operation, accelerates during the fault, which reduces the power of a SCIG in undersynchronous operation. The situation is however more critical if e.g. the fault is cleared, while the crowbar is still coupled. In this case much higher power consumption in motor operation would result. The sudden change of power causes also large torque differences, which stresses the mechanical system of the turbine. A proper damping provided by mechanical or electrical measures can however mitigate the problem. A detailed analysis of the crowbar coupling in under- or oversynchronous operation is carried out in [Bechtold 2007] and [Kayikçi, 2006a], [Kayikçi 2006b].

Different crowbar coupling sequences are analysed and suggested in literature [Erlich 2007], [Kayikçi 2006a], [Kayikçi 2006b], [Akhmatov 2002a] [Akhmatov 2003b] [Akhmatov 2003c], [Bechtold 2007], [Seman 2006a], [Seman 2006b], [Niiranen 2004] and [Fortmann 2003]. While generally fast crowbar decoupling is required it is pointed out in [Seman 2006b] that for the most severe unsymmetrical faults it is necessary to decouple the crowbar after fault clearing. This means, different control strategies depending on the fault characteristic are necessary. A detailed analysis of the subtransient behaviour of the converter and the crowbar coupling process is however out of the scope of the present work as it is circumstantial for power system studies.

In addition to that other protection methods are discussed today. [Erlich 2007] [Bechtold 2007] [Engelhardt 2007] suggest application of a chopper in the converter's DC-link. The chopper, a parallel ohmic resistance, could absorb the surplus power, which is transmitted into the DC-link. Such measures are suggested in combination with crowbar or even avoid crowbar connection totally [Woodward 2007].

Overspeed protection

A short circuit, as illustrated in Figure 6.1, causes a voltage drop at the generator terminal, which in turn provokes an active power drop in the stator. As this reduces the electrical torque, too, the generator starts to accelerate. Because the DFIG behaves as a squirrel cage induction machine as long as the crowbar is triggered, the acceleration causes an increased reactive power consumption of the generator in oversynchronous operation (see e.g. Figure 6.8). Both, increased speed and increased reactive power demand have a negative impact on power system stability. Furthermore, overspeeding of the generator could lead to a tripping of the whole turbine. It is thus necessary to prohibit a too strong acceleration by means of an overspeed protection. As the pitch

controller implemented in the presented model controls the generator speed, it acts directly as an overspeed protection. Notice that the pitch angle control, illustrated in Figure 4.5, prevents over-speeding both in normal operations and during grid faults, due to the fact that the pitch angle controls directly the generator speed. In case of over-speeding, the aerodynamic power is automatically reduced while the speed is controlled to its rated value. This means that there is no need to design any additional pitch control solution to improve the dynamic stability during grid faults. In constrast to this, in [Holdsworth 2004] and [Sun 2005] the reduction of the aerodynamic power and the prevention of the over-speed during grid faults, for both active stall wind turbines and variable speed wind turbines, are realised by implementation of an additional pitch control solution.

In the event of grid faults the pitch controller reacts to the acceleration of the drive train and increases the pitch angle. In this case the rate-of-change limitation of the pitch system's servo mechanism is very important, because it decides how fast the aerodynamic power can be reduced in order to prevent over-speeding during faults. The absorbed aerodynamic power of the turbine can so be reduced, which counteracts the acceleration process and reduces the reactive power absorption, respectively.

6.2.2 Damping

In order to reduce the large mechanical stresses on the turbine during grid faults, a damping controller as proposed in [Akhmatov 2003b], [Hansen 2007b] is implemented. This damps actively the speed fluctuations acting on the active power control (Figure 6.10).

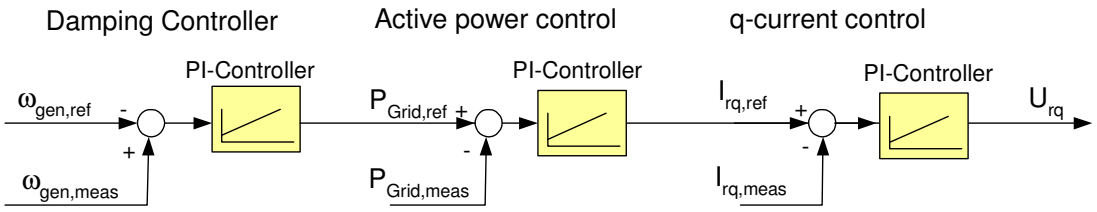

Figure 6.10: Damping controller

In order to illustrate the performance of the damping controller a 3-phase short circuit at the point of common coupling of the DFIG wind turbine as shown in Figure 6.1 is simulated. The short circuit happens at 0 s and has a duration of 300 ms. The DFIG wind turbine is connected to a grid, which is modelled as a Thevenin equivalent and the wind speed is kept constant during the simulation.

Figure 6.11 depicts the performance of the damping controller. It shows the signals of rotor speed and mechanical torque. Without the damping controller, the torsional oscillations are only slightly damped 10 s after the grid fault.

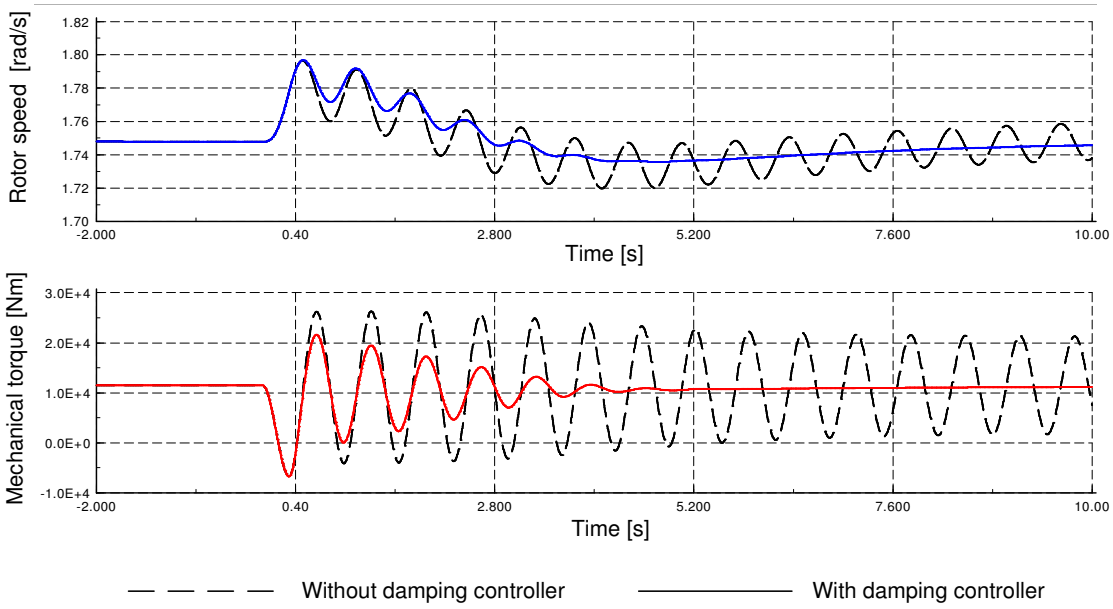

Figure 6.11: Performance of the damping controller

It is clearly visible that the oscillations decay very fast due to the included damping controller. Moreover the mechanical torque crosses only once through zero when the damping controller is used, which significantly reduces the mechanical stresses of the turbine. Hence the presence of the damping controller is very important for minimizing the grid fault effect both on the mechanical and on the electrical side of the turbine. The damping controller together with the protection system enhance thus the fault ride-through behaviour of the DFIG wind turbine.

6.3 Voltage control capability

To enable the DFIG wind turbine for grid support a co-ordinated voltage control of DFIG wind turbine for improved operation during grid faults is implemented. It is based on a strategy, where both DFIG converters, i.e. rotor side converter (RSC) and grid side converter (GSC) are used in a co-ordinated manner [Hansen 2007b]. The idea is that the rotor side converter is used as default reactive power source, while the grid side converter is used as a supplementary reactive power source when the protection system is triggered and when as a consequence the rotor side converter is blocked.

6.3.1 Voltage control of the rotor side converter

In order to utilize the good controllability of the DFIG for grid support in case of faults, the rotor side converter control is extended by a voltage control block. This controller regulates the voltage at the point of common coupling (PCC) of the wind turbine or the wind park by adjusting the reactive power supply. The generator can optionally provide inductive or capacitive reactive power. This can e.g. be utilized during

reactive power imbalance in the system, when an inductive load or generation unit is coupled to the grid. During grid faults, as long as the crowbar is not triggered, the voltage controller can control the grid voltage by providing or absorbing reactive power.

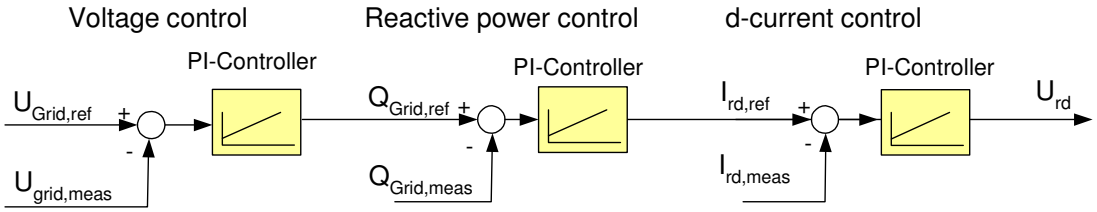

Figure 6.12: Voltage control by means of reactive power supply in the rotor side converter

Since the rotor side converter controller controls the reactive power fed into the grid via the stator circuit, this converter can compensate a bigger reactive power demand than the grid side converter. The goal of this control strategy is thus to control the reactive power demand mainly by means of the rotor side converter. This task is only temporarily assigned to the grid side converter, when the rotor side converter is blocked by the crowbar. A coordinated voltage control between both converters is thus important to assure [Hansen 2007b], [Kayikçi 2005], [Dittrich 2005].

Figure 6.13 illustrates as an example the voltage signal at the point of common coupling of the DFIG after an inductive load is connected to the grid. The voltage drops below 1 p.u. due to the reactive power demand of the inductive load. The voltage remains at the reduced level as long as no voltage control by the rotor side converter is enabled (dashed line). However, when the voltage controller is used, the voltage level is fast re-established (solid line).

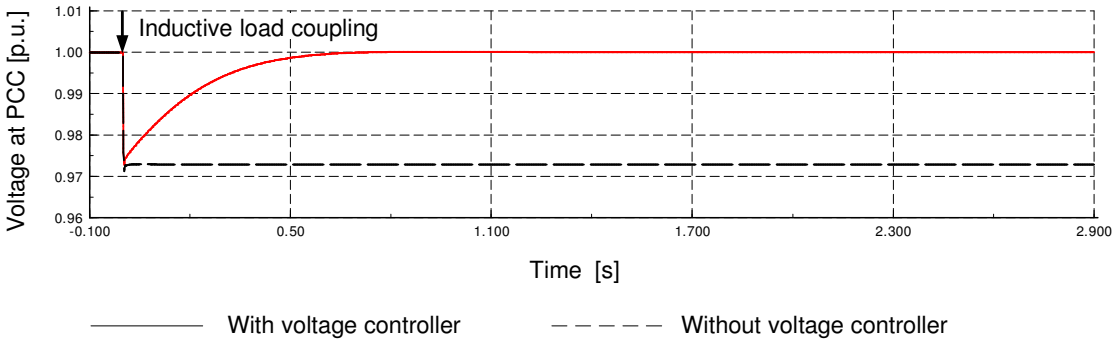

Figure 6.13: Performance of the rotor side converter voltage controller after inductive load coupling

6.3.2 Reactive power control of the grid side converter

In contrast to the rotor side converter the grid side converter can stay active during grid faults, when the rotor side converter is blocked by the crowbar. The grid side converter

can then be used as a STATCOM and contribute supplementary to reactive power supply. As shown in Figure 6.14 a reactive power boosting is implemented, which provides a reference reactive power signal to the grid side converter control. The reference reactive power for the grid side converter is set to its limits (+/-1 p.u.), so that the converter contributes always with its maximum reactive power to voltage re-establishment.

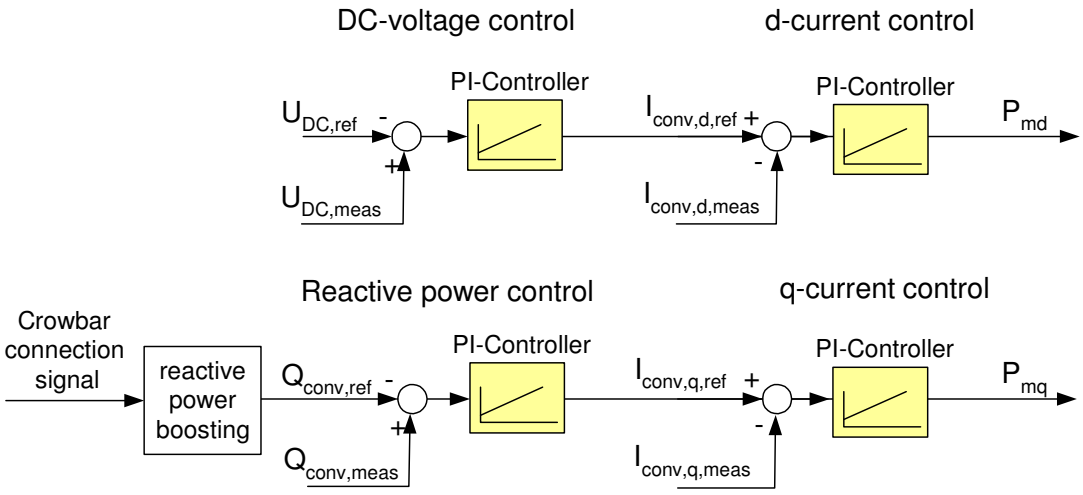

Figure 6.14: Grid side converter reactive power boosting during crowbar coupling

Figure 6.15 illustrates the signals of voltage at the point of common coupling (PCC) and the reactive power contribution of the grid side converter during a 3-phase short circuit at the PCC. The fault is followed by immediate crowbar coupling in the DFIG´s rotor circuit. In this simulation case the crowbar coupling time is set to 400 ms. After fault clearing, i.e. at 300 ms, the crowbar is still active for 100 ms. In Figure 6.15 a) the voltage is plotted for two cases: with and without reactive power boosting of the grid side converter. During crowbar coupling the grid side converter, working like a STATCOM, can contribute to reactive power supply and improve the voltage level. Figure 6.15 b) illustrates the reactive power, which is provided by the grid side converter. In this case the reference power of the reactive power boosting is set to –1 p.u., which denotes that the grid side converter must feed its maximum possible reactive power into the grid. However, since the voltage level is significantly reduced during the fault, the grid side converter's reactive power production capability is also reduced. It can be seen in Figure 6.15 b), that the reference reactive power cannot be provided during the fault. After fault clearing and thus after the voltage at the converter terminals has re-established, the grid side converter is able to provide the reference reactive power to the grid. Nevertheless, when the fault is cleared, the voltage does not recover completely immediately. This is due to the reactive power demand of the generator, which is used for magnetization. The generator continues to operate as a

squirrel cage induction generator and has an increased magnetization demand when the voltage level recovers. The generator absorbs thus reactive power from the grid, which delays the recovering process of the grid voltage. As soon as the crowbar is removed and the rotor side converter is restarted, the voltage controller of the rotor side converter provides for reactive power supply so that the voltage level is immediately re-established.

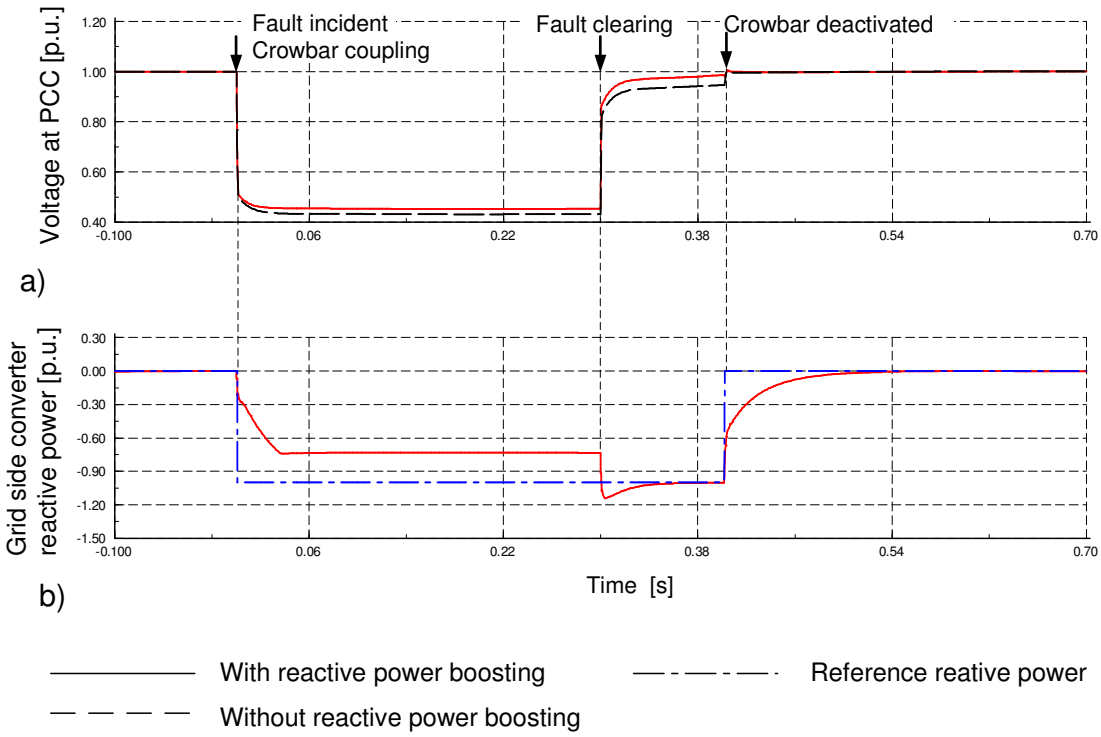

Figure 6.15: Performance of the grid side converter reactive power boosting
a) Voltage at the point of common coupling (PCC)
b) Reactive power boosting of the grid side converter

An overview over the whole control structure of the DFIG wind turbine for normal operation conditions and for grid faults is given in the appendix, Section12.7.

6.4 Case studies

This section finally illustrates and discusses the DFIG wind turbine's ability to comply with grid connection standards such as the E.ON and Energinet.dk grid codes presented in Chapter 2.3.

Two case studies are performed, one simulating the E.ON grid code requirements and the other the Energinet.dk grid code. The DFIG wind turbine model is connected to a grid characterized by the Thevenin equivalent, which is specified in the Energinet.dk grid code and illustrated in Figure 2.4. The voltage profile of the grid codes is applied to the voltage source of the Thevenin equivalent. For comparison the

voltage profile of the E.ON grid code is applied to the same Thevenin equivalent specified by Energinet.dk. Focus of this investigation is the fault ride-through and voltage support capability. A similar case study is also performed for the PMSG wind turbine and is presented in Section 8.4.

6.4.1 Compliance of DFIG wind turbines with the E.ON grid code

The simulation results of the DFIG wind turbine subjected to the voltage profile defined by the E.ON grid code are given in Figure 6.16. In the uppermost plot, the E.ON voltage profile applied to the voltage source is plotted together with the voltage characteristic at the wind turbine connection point (PCC). In addition to that, the active and reactive power production of the DFIG wind turbine are shown together with their corresponding reference values of the controller. The reactive current fed into the grid by the DFIG is also plotted.

According to the E.ON voltage profile for fault ride-through, a voltage drop down to zero for 150 ms is followed by a slow recovery of the voltage within 1.5 s. Due to the severe voltage drop the crowbar is coupled immediately at the fault incident. During this time the rotor side converter is blocked but the grid side converter provides a small amount of reactive current to the grid. After the crowbar is disconnected at 100 ms the rotor side converter contributes with reactive power. In this moment the active power decreases to zero as reactive power production is prioritized by the rotor side converter control. In the simulated case the DFIG contributes with its maximum reactive power. This results in an improvement of the voltage level compared to the E.ON voltage profile.

However, during the reduced grid voltage the DFIG is not able to provide the reference reactive power. The amount of reactive power a DFIG wind turbine is able to supply is to a certain extent limited. This is due to the following reasons. First, active and reactive power production are not totally independent as it is in contrast the case for a full converter connected generator. For full converter connected wind turbines the reactive power infeed into the grid is determined by the grid side converter only independent of the generator's operational point [Ackermann 2005] (see Section 7.2). Second, the rotor current of the DFIG is limited due to the smaller converter size of the DFIG´s frequency converter [Lund 2007], [Soens 2003]. Third, during crowbar coupling, reactive power supply is done only by the grid side converter, which has a smaller capability for reactive power supply.

In the simulated case study the rotor current, which is used for control, reaches its limitation, even if the reactive current supplied to the grid via the stator is still less than 1 p.u. In this case, the E.ON requirement, which requires 1 p.u. reactive current, cannot totally be met. Nevertheless, the reactive power supply supports and raises the voltage level slightly. Due to the crowbar protection fault ride-through can be accomplished and the turbine can stay connected. The only constraint in grid code accom-

plishment is the fact, that due to a limited rotor current capability reactive power production is limited, too, so that the reactive current infeed does not reach the specified requirement. However, for the simulated voltage profile, the E.ON grid code even allows short term interruption followed by fast resynchronisation of the wind turbine (see Figure 2.6 in Section 2.3). In this case reactive power supply would be limited or interrupted, too and is then tolerated by the power system operator. Considering this aspect it becomes apparent, that grid code accomplishment is a matter of correct interpretation of the defined requirements and approval of the responsible transmission system operator.

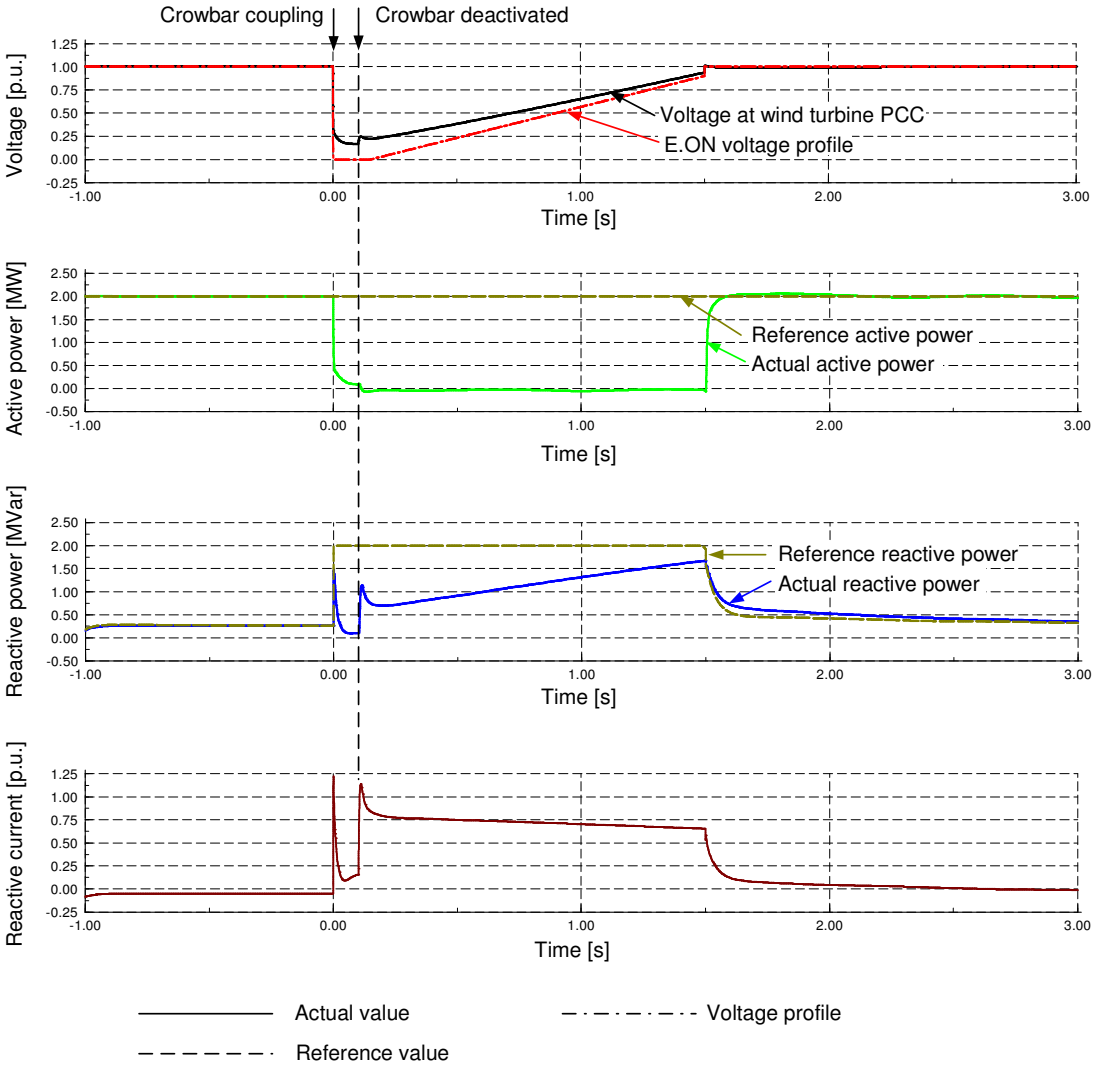

Figure 6.16: Voltage profile for fault ride-through of the E.ON grid code applied to a DFIG wind turbine: Voltage profile and Voltage at PCC, active and reactive power production, reactive current supply of the DFIG wind turbine

6.4.2 Compliance of DFIG wind turbines with the Energinet.dk grid code

A second case study is performed, in which the DFIG wind turbine is now subjected to the voltage profile specified in the Energinet.dk grid code. The same generator quanti-

ties, e.g. voltage at the wind turbine's PCC, active and reactive power production and the reactive current infeed of the wind turbine are plotted in Figure 6.17.

In contrast to the E.ON grid code the voltage profile specified by Energinet.dk is higher but the voltage reduction to 75 % lasts very long instead. The signals are therefore plotted for 12.5 seconds after the voltage drop. The voltage drops down to 25 % for 100 ms followed by linear increase of the voltage up to 0.75 p.u at 750 ms. Again, the voltage dip provokes crowbar coupling. In contrast to the E.ON grid code, Energinet.dk requires active power supply during the fault and the active power reference is defined by equation (2.1). The active power of the DFIG can follow this reference very well. Moreover, as the required active power is relatively small the reactive power capability is not totally constrained. This means that additional to the required active power supply the DFIG provides its maximum possible reactive power and reactive current, respectively. However, no specifications about the reactive current infeed are given in the Energine.dk grid code.

The rotor side converter voltage controller enables the DFIG for reactive power supply, which improves the voltage level at the PCC. After 10 seconds the voltage recovers totally and the DFIG reaches its pre-fault steady state. This investigation approves that fault ride-through of the applied voltage profile can be accomplished by DFIG wind turbines. Moreover, the Energinet.dk grid code requirements can totally be met.

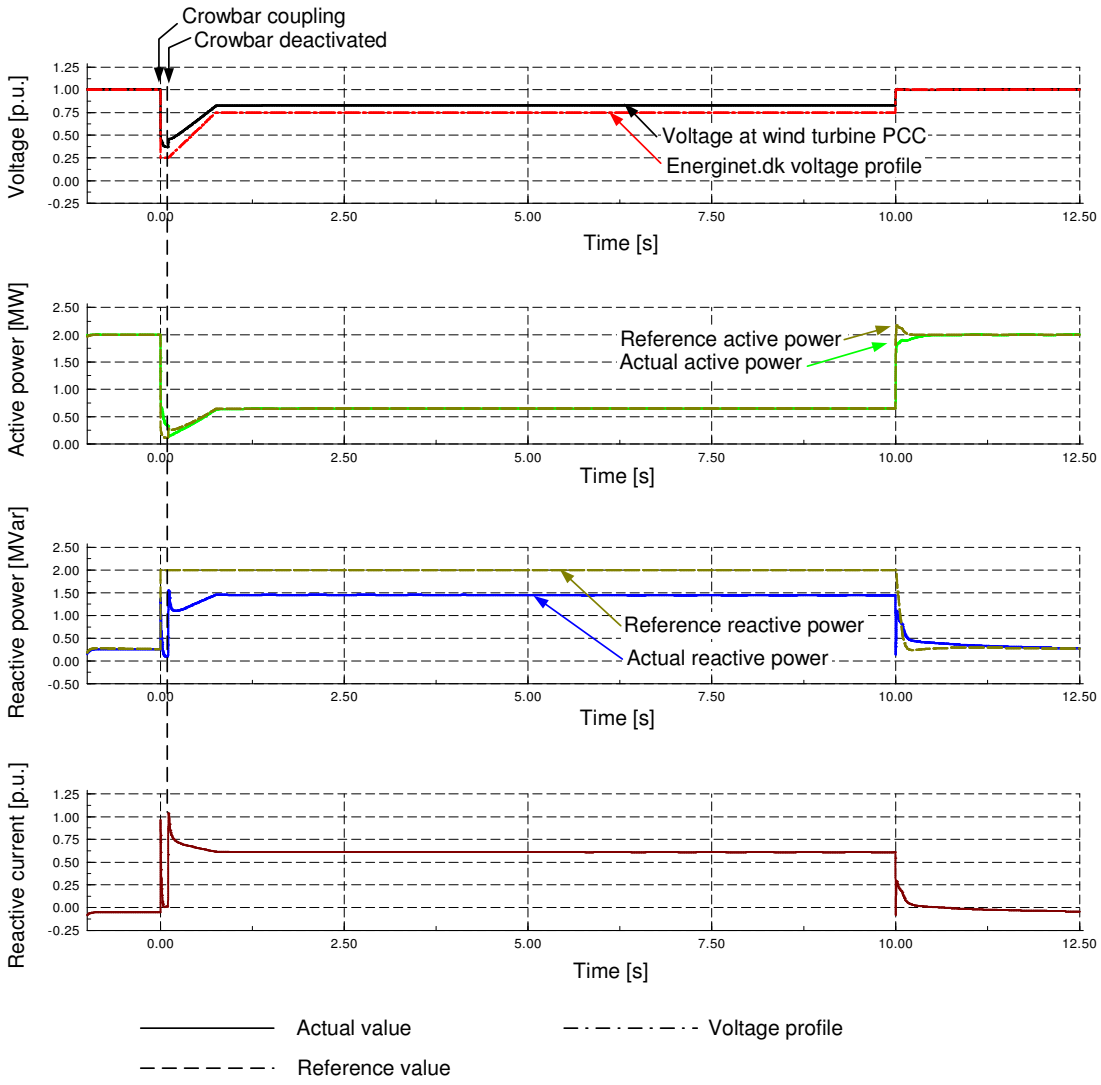

Figure 6.17: Voltage profile for fault ride-through of the Energinet.dk grid code applied to a DFIG wind turbine: Voltage profile and voltage at PCC, active and reactive power production, reactive current supply of the DFIG wind turbine

6.5 Summary

Grid codes require newly installed wind turbines to support directly the power system in case of grid faults. Focus of this chapter is therefore on the DFIG wind turbine's fault ride-through and grid support capability. An advanced control and protection system is developed, which facilitates fault ride-through of DFIG wind turbines and enables them to support power system stability.

In a first step the dynamic behaviour of DFIG wind turbines during grid faults is analysed. Due to the DFIG´s direct grid connection high transient currents arise in stator and rotor circuit, followed by a surge of power into the converter and DC-link, charging in turn the DC-link capacitor. A damage of the converter system due to such overcurrents and overvoltages must be prevented by a protection system.

In case of severe grid faults a crowbar is connected, which blocks the rotor side converter and reduces the transient rotor currents. The pitch control, controlling the speed, serves as an overspeed protection. The control is therefore assessed to be very advantageous for grid faults, as no additional pitch control solution needs to be implemented in contrast to the findings of other research works.

The presented control strategy for fault ride-through and grid support is based on the design of a proper coordination between three controllers: the damping controller, the rotor side converter voltage controller and the reactive power boosting of the grid side converter. A damping controller damps the mechanical oscillations excited by grid faults. The damping assures reduction of large mechanical stresses and prevents turbine tripping due to excessive loads. The grid voltage is controlled by the rotor side converter as long as it is not blocked by the crowbar, otherwise the grid side converter is taking over the voltage control.

Simulation results in DIgSILENT Power Factory exemplify how DFIG wind farms with such control strategy participate to re-establish the voltage during grid faults. In addition to that, accomplishment of grid codes is verified based on specified voltage profiles for fault ride-through of E.ON and Energinet.dk grid codes applied to the wind turbine.

Due to the presence of the converter system, DFIG wind turbines are able to provide grid support. However, the financial advantage of using a partial-scale converter turns into a technical disadvantage in case of grid faults, as it must be protected against high transient currents and voltages.

7 Multipole PMSG wind turbine - Electrical system and control

Due to grid code specifications, as described in Chapter 2.3, wind turbines are requested to act as active components in the power transmission system equal to conventional power plants. The presence of power electronics inside modern wind turbines is therefore essential.

As e.g. the E.ON grid code [E.ON 2006] requires that rated reactive current must be provided in case of grid faults, wind turbines with full-scale frequency converter might be favoured in future compared to the doubly-fed induction generator (DFIG) concept using only a partial-scale frequency converter. Furthermore, it is assumed that fault ride-through can easier be realized with a full-scale converter. Due to these reasons the wind turbine concept with multipole permanent magnet synchronous generator (PMSG) and full-scale frequency converter will be investigated in the following.

The direct driven wind turbine concept with multipole permanent magnet synchronous generator (PMSG) and full-scale frequency converter is an auspicious but not yet very popular wind turbine concept for modern wind turbines. The wind turbine concept is illustrated in Figure 7.1

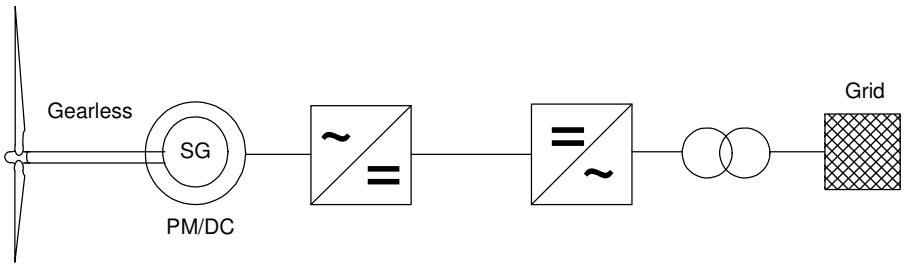

Figure 7.1: Gearless synchronous generator concept with full-scale converter

The generator is connected to the grid via a full-scale IGBT voltage source converter, which decouples the generator from the electrical frequency of the power system and allows variable speed operation. Furthermore, the reactive power provided by the converter to the grid is independent of the reactive power operational point of the generator. As the generator is a multipole synchronous generator, it can operate at low speeds and a gear can be omitted. Since a gearbox causes higher weight, losses, costs and demands maintenance [Westlake 1996] a gearless construction represents an efficient and robust solution, which could be very beneficial especially for offshore applications. Moreover, due to the permanent magnet excitation of the generator the DC excitation system can be eliminated reducing again weight, losses, costs and maintenance requirements [Polinder 2004]. The efficiency of a PMSG wind turbine is thus assessed to be higher than for other concepts [Grauers 1996a], [Jöckel 2002]. However the disad-

vantages of the permanent magnet excitation are the still high costs for permanent magnet materials and a fixed excitation, which cannot be changed according to the operational point.

In the following, the main features of a PMSG for the use in wind turbines are explained. A comprehensive dynamic simulation model of the PMSG wind turbine is implemented in the power system simulation software DIgSILENT Power Factory and a control strategy for the entire turbine system is developed. The model is representative for the variable speed wind turbine type with full-scale converter, specified as Type D in Chapter 3.2, Table 3.1.

7.1 The permanent magnet synchronous generator

The following subsection presents a brief overview over the features of synchronous generators. The PMSG is discussed in detail.

In order to emphasize the difference between DC excited synchronous generators used in large conventional power plants and the multipole PMSG used in a wind turbine, three different designs of synchronous generators (SG) are shown in Figure 7.2:

- **Salient pole SG**: The rotor windings are placed as a concentrated coil around the pole shoe. This causes a different magnetic resistance (reluctance) in the rotor oriented d- and q-axis, which results in different machine reactances x_d and x_q ($x_d > x_q$). A damper winding is placed in the pole shoe. Built with 8…16 poles and a respective speed of 750...375 rpm this kind of synchronous generator is generally used in hydro power plants, rotating with lower speed than round rotor SGs [Balzer 2001].
- **Round rotor SG**: The rotor windings are equally distributed in the rotor slots, which results in an equal reactance in d- and q-axis ($x_d = x_q$). 2-pole or 4-pole round rotor SGs are used in thermal power plants operating at very high speed (3000 rpm, 1500 rpm) [Balzer 2001].
- **Multipole permanent magnet SG**: In order to operate with low speeds, e.g. at 20 rpm, a high number of poles is used in PMSG wind turbines. Instead of electrical DC excitation the magnetic rotor field is provided by permanent magnets. Figure 7.2 shows a design with surface mounted permanent magnets. Due to the equal distribution of the surface mounted magnets and a permeability of the magnet material μ_m approximately as big as the airgap permeability ($\mu_m \cong \mu_0$) the reactances in d- and q-axis differ by only a few percent [Spooner 1996], [Binder 2006], so that surface mounted PMSGs can be considered as round rotor machines ($x_d = x_q$). Because the multipole PMSG is a converter connected low speed application (in contrast to high dynamic drives) no damper winding is necessary.

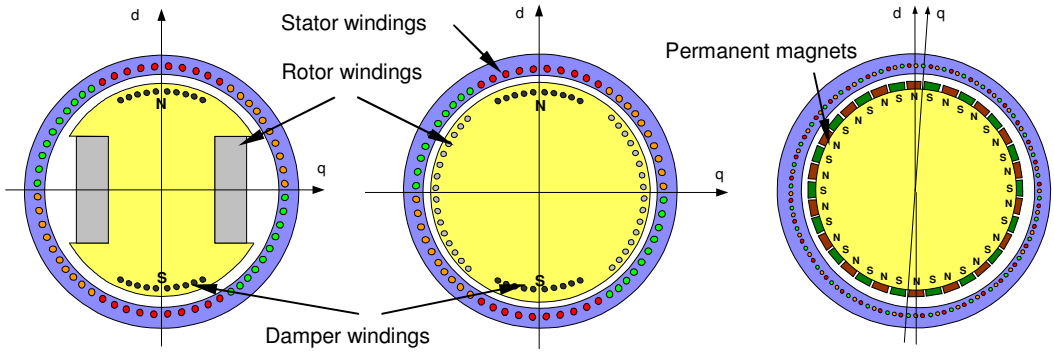

Salient pole SG	Round rotor SG	Multipole permanent magnet SG

Figure 7.2: Cross section of different synchronous generator types

Direct drive wind turbines, characterized as high efficient and low maintenance solutions, offer high potentials for future applications [Jöckel 2006], especially off-shore. In order to eliminate the gearbox the generator must be built for low speeds (max. 15-20 rpm). The generator needs thus a large rotor diameter for the high wind turbine torque and a large number of poles in order to get a suitable frequency at low speeds [Binder 2005]. As asynchronous generators cannot be built for low speeds (a small pole pitch together with a large airgap yields a too big reactive power demand of asynchronous generators) synchronous generators are required for low speed wind turbine applications. In a synchronous generator the magnetic field is provided by the rotor excitation. The excitation can either be provided by DC excitation (e.g. known from the German wind turbine manufacturer Enercon) or by means of permanent magnets. In case of DC excitation, the power factor of the machine can be adjusted so that operation with unity power factor becomes possible and the converter rating is reduced to the generator´s active power value [Binder 2005]. However, the use of permanent magnets eliminates the DC excitation system, which means a reduction of losses (high field ampere turns in multipole generators) and the omission of slip rings and thus maintenance requirements. A gearless wind turbine application with PMSG is e.g. known from the manufacturers “Vensys”, “Leitner” or “MTorres”, all of them using surface mounted permanent magnet generators [Binder 2005]. A 1.2 MW multipole permanent magnet synchronous generator from “Vensys” is shown in Figure 1.3.

Figure 7.3: A 1.2 MW multipole PMSG, Vensys [Jöckel 2006]

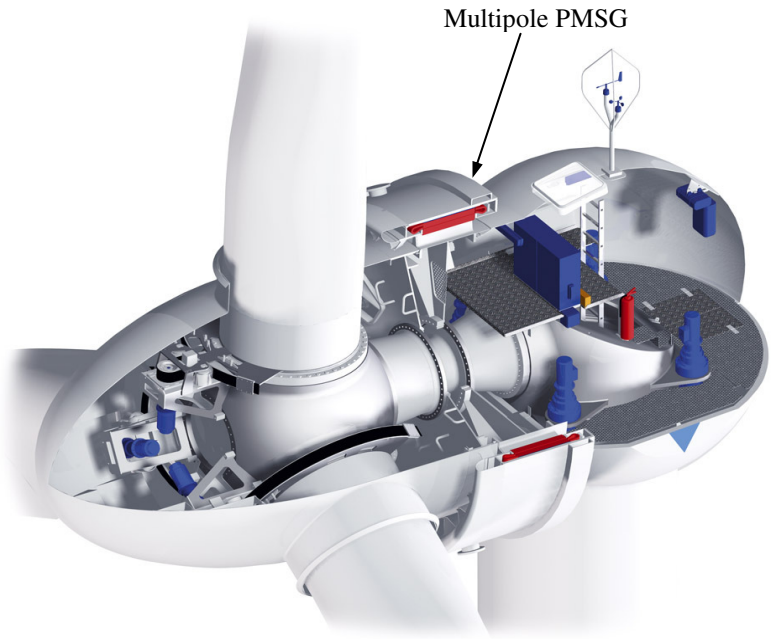

Figure 7.4: Wind turbine with multipole PMSG, Vensys [Jöckel 2006]

7.1.1 Steady state generator model

A DC excited synchronous generator can be electrically represented by the one phase equivalent circuit shown in Figure 7.5. In addition to that, the phasor diagram of the

synchronous generator is plotted for an arbitrary operational point. The rotor field is generated by the excitation current $\underline{I}_f$, which induces the voltage $\underline{E}$ (electromotive force EMF) in the stator windings. The total magnetic field is represented with the main inductance X_h.

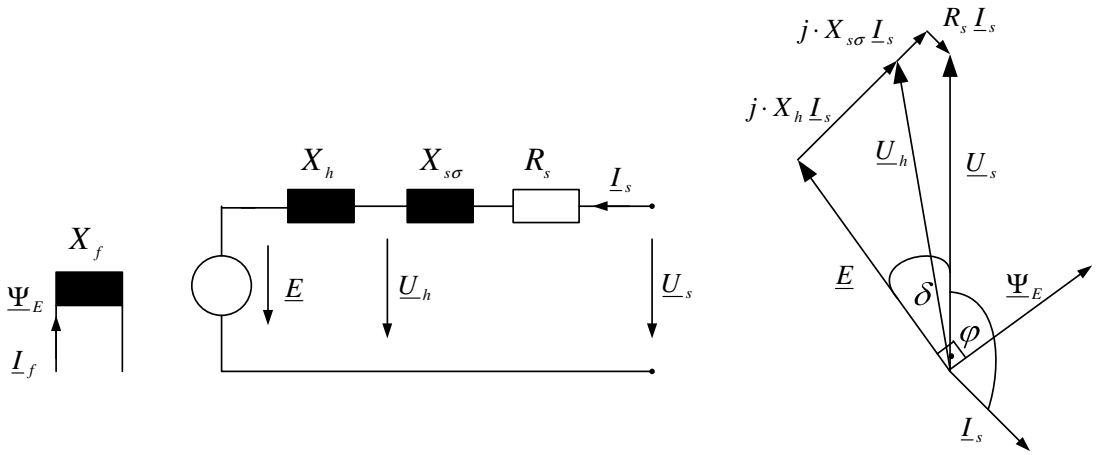

Figure 7.5: One phase equivalent circuit and phasor diagram of a DC excited synchronous generator

If the stator windings resistance R_s and the leakage reactance $X_{\sigma s}$ are neglected the equivalent circuit can be simplified. Such a simplified equivalent circuit is shown in Figure 7.6 for a permanent magnet induction generator. The voltage $\underline{E}$ is now induced by permanent magnets.

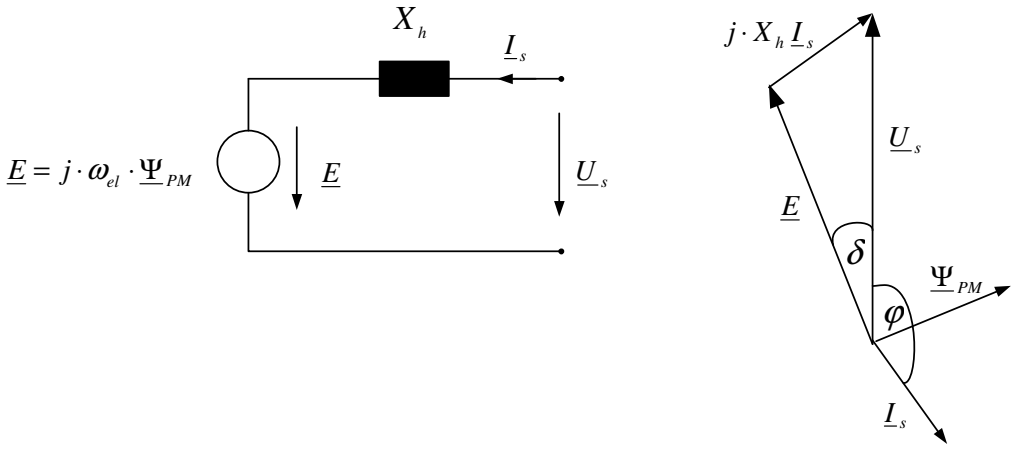

Figure 7.6: Simplified equivalent circuit and phasor diagram of a PM excited synchronous generator

$\underline{E}$	electromotive force (induced voltage)	X_f	field winding reactance
$\underline{U}_s$	stator voltage	X_h	main reactance
$\underline{U}_h$	voltage, representing the main field	$X_{s\sigma}$	stator leakage reactance
$\underline{I}_s$	stator current	R_s	stator reactance

$\underline{\Psi}_{PM}$	Permanent magnet flux	δ	load angle
$\underline{\Psi}_{E}$	DC excited flux	φ	power factor
$\underline{I}_{f}$	excitation current	ω_{gen}	generator rotational speed

Both, frequency and amplitude of the induced voltage $\underline{E}$ depend on the actual rotor speed $\omega_{gen} = p \cdot \Omega_{gen}$. The difference between the two voltage vectors $\underline{E}$ and $\underline{U}_s$, which is mainly caused by the load angle δ, drives the stator current $\underline{I}_s$. Based on this, a dependency between the machine torque, the voltages $\underline{E}$ and $\underline{U}_s$ and the load angle δ can be derived:

$$P_{gen} = m \cdot \Re\left\{\underline{U}_s \cdot \underline{I}_s^*\right\} = m \cdot \Re\left\{\underline{U}_s \cdot \frac{\underline{U}_s - \underline{E} \cdot (\cos\delta - j\sin\delta)}{-jX_h}\right\} = -m \cdot \frac{U_s \cdot E}{X_h}\sin\delta \tag{7.1}$$

$$T_e = \frac{P_e}{\Omega_{gen}} = \frac{-m}{\Omega_{gen}} \cdot \frac{U_s \cdot E}{X_h}\sin\delta \tag{7.2}$$

The reactive power of the generator is determined by:

$$Q_{gen} = m \cdot \Im\left\{\underline{U}_s \cdot \underline{I}_s^*\right\} = m \cdot \Im\left\{\underline{U}_s \cdot \frac{\underline{U}_s - \underline{E} \cdot (\cos\delta - j\sin\delta)}{-jX_h}\right\} = m \cdot \frac{U_s^2 - U_s \cdot E\cos\delta}{X_h}$$

m	number of phases	P_{gen}	Generator active power
T_e	Electromagnetic torque	Q_{gen}	Generator reactive power
p	number of pole pairs	Ω_{gen}	Mechanical generator speed

Under load conditions, the stator current $\underline{I}_s$ and the stator reactance X_h also cause a magnetic field, which is superposed to the field of the rotor. Thus, the voltage $\underline{U}_s$ corresponds to the voltage induced by the total magnetic field [Grauers 1999]. The voltage drop over the machine's reactance X_h provokes a phase delay between the electromotive force $\underline{E}$ and the stator voltage $\underline{U}_s$, which are equal only for no-load.

An increasing torque of the generator increases the load angle δ (the phase shift between $\underline{U}_s$ and $\underline{E}$) and thus also the reactive power of the machine. While electrical excited machines are controlled to be reactive neutral (reducing the converter rating to the active power value), permanent magnet machines, having a fixed excitation, work

generally underexcited [Binder 2002], [Jöckel 2002]. In this case as the converter must provide reactive power to the generator, the converter has to be oversized.

7.1.2 Dynamic model of the PMSG

Synchronous machine models for power system analysis are usually based on the assumption that the magnetic flux distribution in the rotor is sinusoidal. With this assumption the flux can entirely be described by a vector and thus the internal voltage $\underline{E}$ induced in the stator by the permanent magnets can be expressed as follows:

$$\underline{E} = j \cdot \omega_{gen} \underline{\Psi}_{PM} = j \cdot 2\pi f \cdot \underline{\Psi}_{PM} \tag{7.3}$$

where ω_{gen} is the electrical generator rotational speed, $\underline{\Psi}_{PM}$ is the flux provided by the permanent magnets of the rotor, and f is the electrical frequency. The excitation voltage $\underline{E}$ is proportional with the electrical speed of the generator.

The equations of a PMSG can be expressed directly from the equations of a DC excited SG, with the simplification that a PMSG does not have damper windings [Kundur 1994]. The voltage equations of the generator, expressed in the rotor-oriented dq-reference frame RRF (the reference frame d-axis is aligned with the vector of the permanent magnet flux), can be expressed as follows:

$$\begin{aligned} u_{sd} &= R_s\, i_{sd} - \omega_{gen}\, \psi_{sq} + \dot{\psi}_{sd} \\ u_{sq} &= R_s\, i_{sq} + \omega_{gen}\, \psi_{sd} + \dot{\psi}_{sq} \end{aligned} \quad \text{(in RRF)} \tag{7.4}$$

with the stator flux components:

$$\begin{aligned} \psi_{sd} &= L_d\, i_{sd} + \psi_{PM} \\ \psi_{sq} &= L_q\, i_{sq} \end{aligned} \quad \text{(in RRF)} \tag{7.5}$$

where u_{sd} and u_{sq} are the terminal stator voltage components, i_{sd} and i_{sq} are the stator current components, L_d and L_q are the stator inductances in the dq-reference frame. As in stability studies the stator transients can typically be neglected, the stator voltage equations can be simplified as follows:

$$\begin{aligned} u_{sd} &= R_s\, i_{sd} - \omega_{gen}\, \psi_{sq} \\ u_{sq} &= R_s\, i_{sq} + \omega_{gen}\, \psi_{sd} \end{aligned} \quad \text{(in RRF)} \tag{7.6}$$

The electrical torque of the generator can be expressed as [Achilles 2003]:

$$T_e = \frac{3}{2}\, p \cdot \mathrm{Im}\left[\underline{\psi}_s^{*}\, \underline{i}_s\right] = \frac{3}{2}\, p \cdot \left[\psi_{sd}\, i_{sq} - \psi_{sq}\, i_{sd}\right] \quad \text{(in RRF)} \tag{7.7}$$

Expressing further the stator flux components, the electrical torque can be calculated by:

$$T_e = \frac{3}{2}\, p \cdot \left[\left(L_d - L_q\right) i_{sd}\, i_{sq} + \psi_{PM}\, i_{sq}\right] \quad \text{(in RRF)} \tag{7.8}$$

If the PMSG is assumed to be a round-rotor machine where L_d=L_q, which is a reasonable approximation for this type of generator [Spooner 1996], the electrical torque of the generator results only from the permanent magnet flux and the q-component of the stator current:

$$T_e = \frac{3}{2}\, p \cdot \psi_{PM}\, i_{sq} \quad \text{(in RRF)} \tag{7.9}$$

The active and reactive power of the synchronous generator are:

$$\begin{aligned} P_{gen} &= \frac{3}{2}\left[u_{sd}\, i_{sd} + u_{sq}\, i_{sq}\right] \\ Q_{gen} &= \frac{3}{2}\left[u_{sq}\, i_{sd} - u_{sd}\, i_{sq}\right] \end{aligned} \tag{7.10}$$

As the generator is fully decoupled from the grid by the frequency converter, the reactive power expressed previously is exchanged with the generator side converter and not with the grid.

As multipole permanent magnet generators are low speed applications and generally connected to the grid through a frequency converter system, the generator has no damper winding in the rotor core. Moreover, due to the permanent excitation a PMSG has no field windings, in which transient currents could be induced or damped, respectively. Hence, in case of load changes the field windings would not contribute to damping either.

As neither a damper nor field winding exists in a PMSG, no transient or subtransient reactances, as known for wound rotor SGs, can be defined for the PMSG.

$$\begin{aligned} x_d &= x_d' = x_d'' \\ x_q &= x_q' = x_q'' \end{aligned} \tag{7.11}$$

x_d Synchronous reactance x_d' Transient reactance
x_d'' Subtransient reactance

However, as the multipole PMSG is a low speed application with slow dynamics, a damper winding is less important [Akhmatov 2003d]. Nevertheless, a damping of the system must then be applied by means of the converter control.

7.1.3 The frequency converter

In order to transfer the generator power to the grid different converter topologies are possible. Two typical topologies for the generator side converter are e.g. the diode rectifier with boost converter or the IGBT voltage source converter will be introduced here.

The passive B6-diode-bridge rectifier shown in Figure 7.7 represents a cheap and simple solution with low losses. However, the stator voltage and thus the DC voltage vary depending on the speed. This leads in turn to a low DC voltage at low speeds. Moreover, the diode rectifier cannot be controlled and cannot supply any reactive power to the generator. Hence, that stator current and stator voltage will always be in phase. When the torque and thus the load angle and the stator current increase, the stator voltage drops, which in turn leads to a decreasing DC-link voltage [Dreschinski 2005], [Grauers 1999].Due to this reason a boost converter shown in Figure 7.7 (also called “step-up converter”) in the DC-link must compensate for the drop in the DC-link voltage.

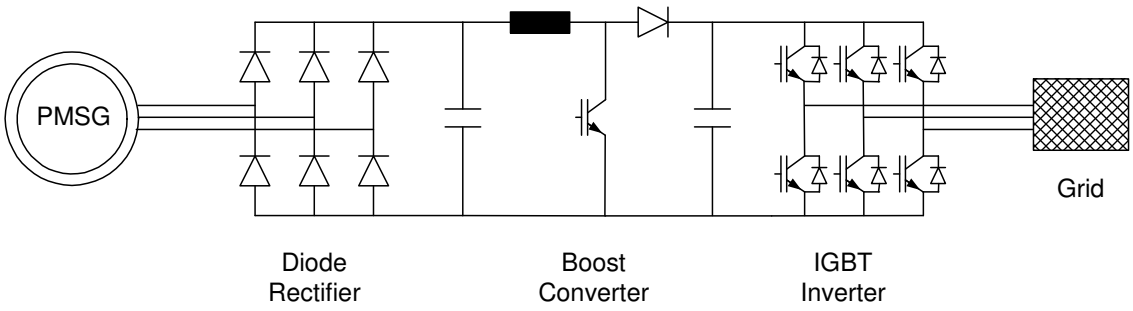

Figure 7.7: PMSG connected via diode rectifier with boost converter

A PMSG has a fixed excitation, which is only optimal for one operational point. If a diode rectifier is used, which cannot provide or consume reactive power, the PMSG is insufficiently utilized, when the operational point varies [Jöckel 2002]. A drastic drop in the efficiency compared to PMSGs with IGBT voltage source converters occurs [Jöckel 2002]. A solution, which is proposed in [Grauers 1999], is to use a series compensated diode rectifier, which compensates for the voltage drop over the generator reactance and improves the utilisation of the generator. However, the best performance of direct driven low speed permanent magnet generators is achieved with

fully controllable active inverters, e.g. the PWM controlled IGBT voltage source converter (Figure 7.8). Additional reactive power can then be provided or absorbed by the converter and a very high efficiency of the system can be achieved. However, IGBT converters are more expensive and have to be protected against overcurrents and overvoltages.

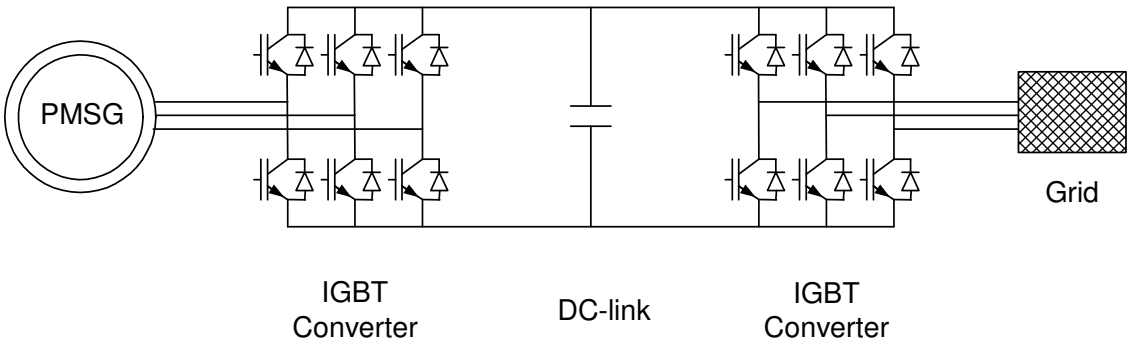

Figure 7.8: PMSG connected via IGBT voltage source converter

The DC-link capacitor current is discontinuous, as it is switched on and off with the switching frequency of the converter. This process induces voltage ripples in the DC-link. Such voltage ripples must be made small enough for the voltage to be virtually constant during a switch period and this sets on the one hand a lower limit on the capacitor size. On other hand, small voltage ripples require a larger capacitor, which has a slow response to voltage changes, but a smaller current and thus an increased lifetime. Contrarily, a small capacitor makes fast changes in the DC voltage possible, which is beneficial for control tasks, but results in higher voltage ripples and reduced lifetime. Therefore, selecting the size of the DC-link has to be a trade-off between voltage ripples, lifetime and the fast control of the DC-link [Hansen 2007c].

Considering these aspects the DC-link capacitor in the back-to-back voltage source converter system is designed based on the following equation [Bojrup 1999], [Lindholm 2004], [von Joanne 2002].

$$C = \frac{S}{U_{DC} \cdot \Delta U_{DC} \cdot 2 \cdot \omega} \tag{7.12}$$

C	capacitance of DC-link capacitor	S	apparent converter power
U_{DC}	DC-link voltage	ΔU_{DC}	allowed voltage ripple
ω	electrical frequency of the grid		

where S denotes the apparent power, which is transferred over the DC-link and ΔU_{DC} is the allowed voltage ripple of the DC-link voltage. The level of the DC-link voltage

U_{DC} is determined based on the AC voltage level of the generator [Achilles 2003], [DIgSILENT 2004]:

$$\left|U_{AC}\right| = U_{DC} \cdot \frac{\sqrt{3}}{2\sqrt{2}} m \tag{7.13}$$

where m ($0 \le m < 1$) denotes the pulse-width-modulation index.

The inverter (the grid side converter) of the PMSG wind turbine converts the DC-link voltage to the AC grid voltage with fixed frequency of the power system. The inverter must thus consist of active elements e.g. of IGBTs or GTOs. Since the converter system decouples the reactive power of grid side converter and generator side converter, the reactive power supply to the grid can be determined by the grid side converter only, independent of the reactive power operational point of the generator. The reactive power supply of the grid side converter is however limited by the converter rating and the active power flow from the turbine. Under normal operating conditions the grid side converter is operated with unity power factor. But in case of grid faults or reactive power imbalance the grid side converter can serve as a reactive power source in order to contribute to voltage stability.

7.2 Frequency converter control

Figure 7.9 shows the modelling scheme of the PMSG wind turbine and its control concept. The whole model includes models for both the aerodynamical and mechanical system, described in Chapter 4 as well as for the electrical system and its control structure. The built-in models for all electrical components (generator model, converter models, transformer model, grid model) provided in the DIgSILENT library are marked by the yellow blocks. The models for all mechanical components (wind, aerodynamics, drive train model) as well as for the total control system are developed by the user and marked in Figure 7.9 by grey blocks.

The frequency converter control of the PMSG is divided into two controllers: a control for the grid side converter and a control for the generator side converter. The frequency converter control is coordinated with the blade angle control for the rotor blades. Several control strategies are discussed and assessed in the following. However, special focus is on the control strategy implemented in this PhD work.

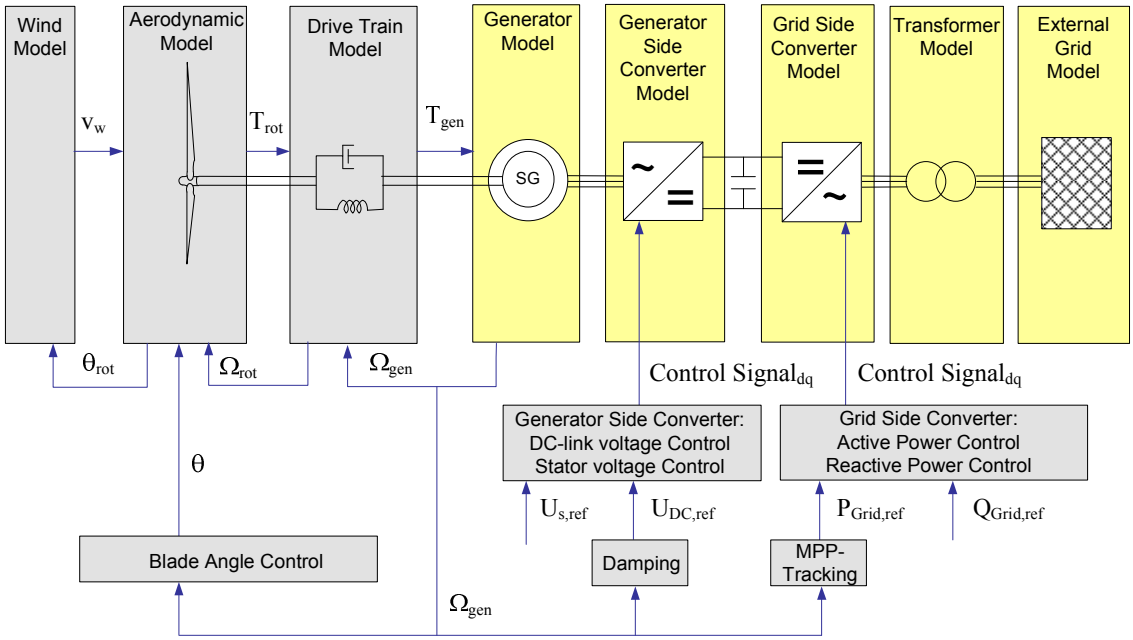

Figure 7.9: Modelling scheme and control concept of the variable speed wind turbine with PMSG

7.2.1 Reference frames for control of the PMSG

The control of any electrical machine is normally done in a reference frame, which rotates with one of the state space vectors of the generator in order to achieve steady state control signals instead of sinusoidal signals. Figure 7.10 gives an overview over the reference frames of a PMSG. In addition to that, a phasor diagram of the generator is displayed in order to illustrate the alignment of the machine vectors to the reference frames.

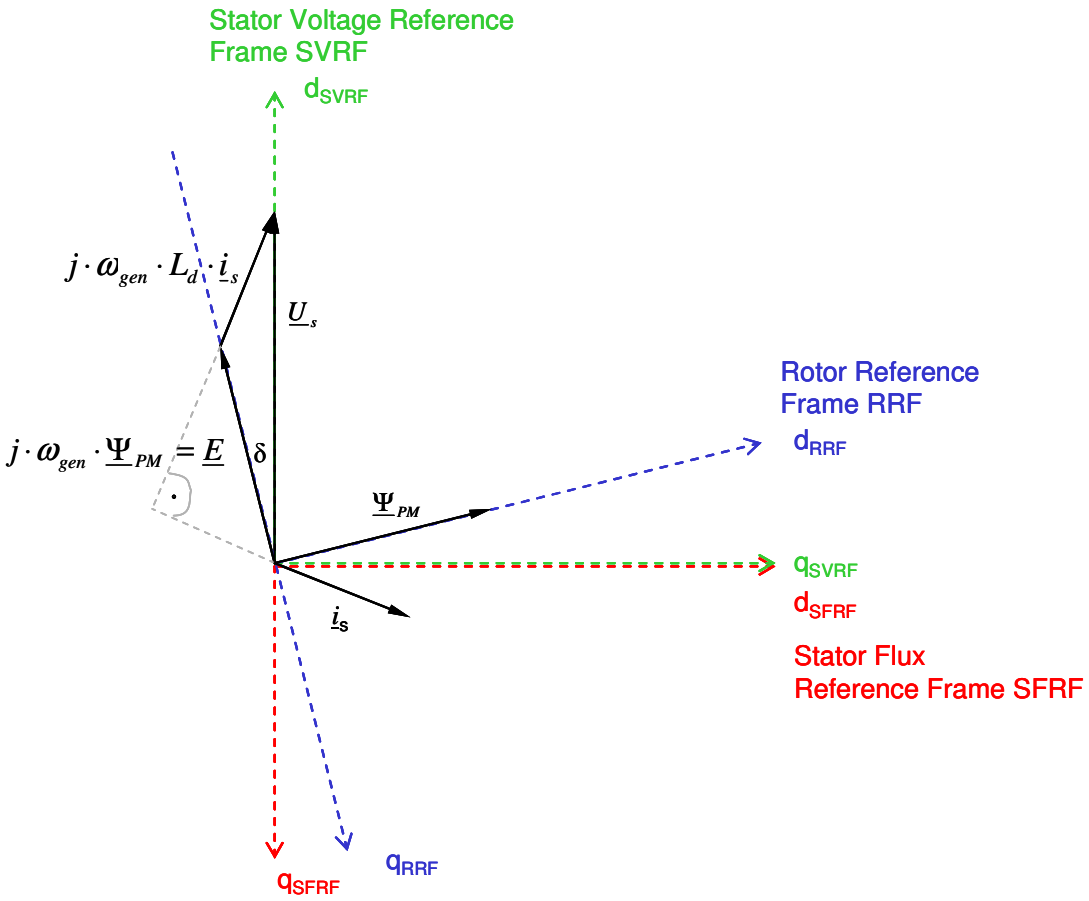

Figure 7.10: Reference frames for control

Three different reference frames for the PMSG can be considered:

- The rotor reference frame (RRF) is aligned with its d-axis to the permanent magnet flux vector Ψ_{PM}. The rotor reference frame rotates with the rotational speed ω_{gen} of the rotor flux, which is equal to mechanical generator speed Ω_{gen} times the pole pairs p:

$$\Omega_{gen} \cdot p = 2\pi f = \omega_{gen} \tag{7.14}$$

  The vector of the electromotive force E is perpendicular to the rotor flux vector.
- The stator voltage reference frame (SVRF) is aligned with its d-axis to the stator voltage vector U_s. This means, that the voltage U_s has only a d-component in the SVRF. This simplifies e.g. the equations for active and reactive power to:

$$P_{gen} = \frac{3}{2} u_{sd}\, i_{sd} \qquad \text{(in SVRF)}$$
$$Q_{gen} = -\frac{3}{2} u_{sd}\, i_{sq} \tag{7.15}$$

so that the active power is determined by the d-component of the stator current and the reactive power is determined by the q-component of the stator current. The SVRF rotates with the angular frequency of the stator voltage, which is the same rotational speed as for the RRF.

- The stator flux reference frame (SFRF) is perpendicular to the stator voltage reference frame and rotates as well with the frequency of the stator voltage. Perpendicular to the stator voltage vector is the stator flux vector, which represents the total flux linkage of the machine, the permanent magnet flux superposed to the flux generated by the stator current.

DIgSILENT Power Factory uses yet another reference frame called "system reference frame". Normally this reference frame is aligned with one reference machine (a synchronous generator) in the power system and rotates with a frequency of 50 Hz. However, if the only generator in the system is a converter controlled PMSG, which has a variable stator frequency, the definition of a system reference frame is problematic. It must then be distinguished between global (50 Hz) and local reference frame (variable generator frequency).

Different control strategies can be applied to the frequency converters [Michalke 2007b]. Four different control strategies are briefly described in the following.

Maximum torque control

The purpose of this control strategy is to use the total stator current for the production of torque (i_s=i_q, i_d=0). The control task of the generator side converter is to control the torque by means of i_q and to control i_d to zero. This implies that the generator is best utilized and the generator can be built smaller. According to equation (7.9) and (7.10) the generator torque as well as active and reactive power can be expressed in RRF as:

$$T_e = \frac{3}{2}\, p \cdot \psi_{PM}\; i_{sq} \qquad \text{(RRF)} \tag{7.16}$$

$$P_{gen} = \frac{3}{2}\, u_{sq}\; i_{sq}$$
$$Q_{gen} = -\frac{3}{2}\, u_{sd}\; i_{sq} \qquad \text{(RRF)} \tag{7.17}$$

Notice that the reactive power is not zero. This means that if the maximum torque control strategy is used, the generator side converter must be an IGBT converter in order to be able to produce Q. Figure 7.11 shows the phasor diagram of the generator in case of maximum torque control.

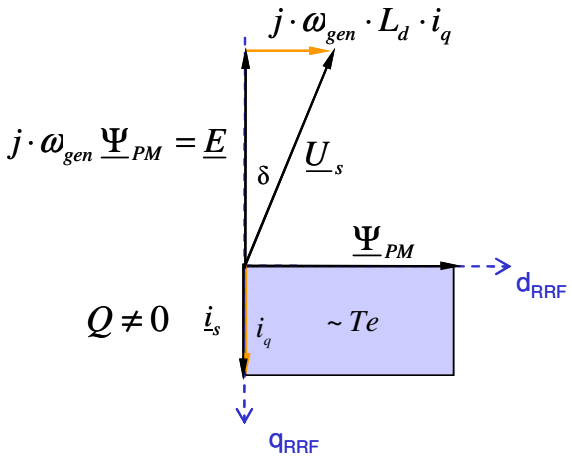

Figure 7.11: Phasor diagram for maximum torque control in rotor-oriented reference frame (RRF)

As the reference frame for this control strategy is aligned with the rotor field, this control is originally called “field oriented control”. “Field oriented control” is however used today as a general expression for vector control.

The reactive power, which is supplied to the grid, can be controlled independently from the generator reactive power operational point by means of the grid side converter. The grid side converter control must furthermore assure a constant DC link voltage, so that no energy is dissipated in the DC-link.

The advantages of this control strategy are an optimal utilization of the generator, because the total current is used for torque production. A disadvantage of this control strategy is the reactive power demand ($S > P$) of the generator, which must be provided by the frequency converter and which increases the converter rating.

Unity power factor control of the generator

The most obvious control strategy is probably to control the generator’s active and reactive power directly with the generator side converter. The control can be done in RRF or SVRF. The intention of this control is to operate the generator with unity power factor (Q=0) and to control its power according to the MPP-tracking. In order to operate the generator with unity power factor, the stator current d-component can be used to compensate the reactive power demand of the generator (Figure 7.12). In RRF the torque, expressed by equation (7.16), and thus the power depend on the q-current component.

$$P = \Omega_{gen} \cdot T_e = \Omega_{gen} \cdot \frac{3}{2} p \cdot \Psi_{PM} \cdot i_{sq} \tag{7.18}$$

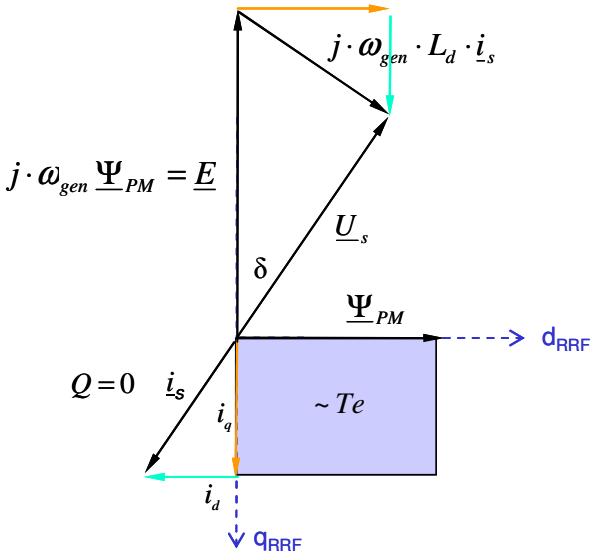

Figure 7.12: Phasor diagram for unity power factor control of the generator in rotor-oriented reference frame (RRF)

The main advantage of this control strategy is that the generator operates with unity power factor, and therefore it minimizes the converter rating. However, as the stator voltage is not directly controlled the stator voltage varies depending on the speed, which could cause overvoltages for the converter and the generator in case of overspeeds. As the reactive power supply to the grid is independent from the generator reactive power, it is less important to control the reactive power at the generator side.

The control of the grid side converter must be the same as described for the previous control strategy: the grid side converter controls the reactive power provided to the grid, which is zero in case of unity power factor control, and it maintains a constant DC-link voltage.

Constant stator voltage control

In order to avoid the risk of overvoltages due to overspeeds, the stator voltage can be controlled instead of reactive power. The stator voltage is then controlled to its rated value. The control is typically done in the stator voltage-oriented reference frame SVRF (d-axis aligned to the stator voltage vector), so that $U_s=u_d$ (Figure 7.13). This implies that the active power depends on the stator current d-component, while the reactive power depends on the q-component only.

$$P = \frac{3}{2} u_{sd}\, i_{sd}$$
$$Q = -\frac{3}{2} u_{sd}\, i_{sq} \qquad \text{(in SVRF)} \qquad (7.19)$$

While the stator current d-component is used to control the active power production of the generator, the stator current q-component is used to control the stator voltage to its rated value.

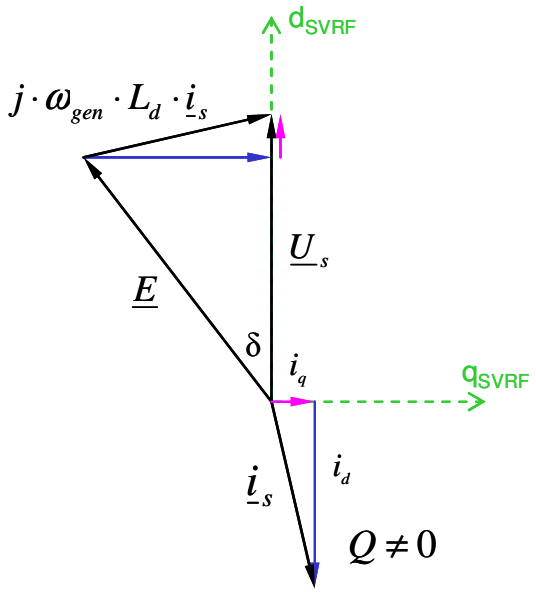

Figure 7.13: Phasor diagram for constant stator voltage control in stator voltage-oriented reference frame (SVRF)

The advantage of this P-U_s control strategy is, that generator and converter always operate at rated voltage, for which they are designed and optimized. It is furthermore beneficial if the converter has a constant rating of U_{DC}/U_{AC}. Due to the constant stator voltage there is no risk of overvoltage and saturation of the converter at high speeds. A disadvantage of the control is the reactive power demand of the generator, which increases the converter rating.

In this control the grid side converter must control Q_{grid} and U_{DC}.

P-Q control by means of the grid side converter

As in all previous mentioned control strategies for the PMSG wind turbine the reactive power, which is supplied to the grid, must be controlled with the grid side converter. The control of active power and the control of a constant DC-link voltage are closely related. The active power can only be completely fed to the grid via the DC-link, if the DC-link voltage is kept constant. If a lossless converter is assumed, the AC power is equal to the DC power.

$$P_{AC} = P_{DC} = U_{DC} \cdot I_{DC} \tag{7.20}$$

Due to this relation, the control of active power and DC voltage can be exchanged. The active power is then controlled with the grid side converter, while the DC-link voltage is kept constant by means of the generator side converter control. The control strategy is indicated in Figure 7.9. The grid side converter controls P and Q, while the generator side converter keeps U_s and U_{DC} constant. The advantages and disadvantages are the same as for the previous explained control strategy.

The control is furthermore assessed to be beneficial for fault cases. Active and reactive power supply to the power system can then directly be controlled at the wind turbine terminals, while stator voltage and DC voltage can be kept constant with the generator side converter, which is less affected by the fault due to the decoupling by the converter. This control strategy is assessed to be most advantageous for the PMSG wind turbine and is therefore implemented in the present work.

7.2.2 Control of the grid side converter

The grid side converter controls active and reactive power in a grid voltage oriented reference frame. The generic control of the grid side converter is illustrated in Figure 7.14. Each control loop has a cascaded structure: a fast inner current control loop, controlling the converter current in d- and q-axis combined with an outer slower control loop for active and reactive power, respectively. Similar to the DFIG´s rotor side converter control a maximum power point tracking (MPP) is implemented. The MPP-tracking provides the reference signal $P_{Grid,ref}$ for the active power, which is equal to the active power production of the generator. The reactive power reference $Q_{Grid,ref}$ is generally set to zero but can also be set to an imposed reference value depending on the reactive power demand of the grid. The inner current control loops provide the control signals P_{md}, P_{mq} in d- and q-axis, which are sent to the PWM-controlled frequency converter.

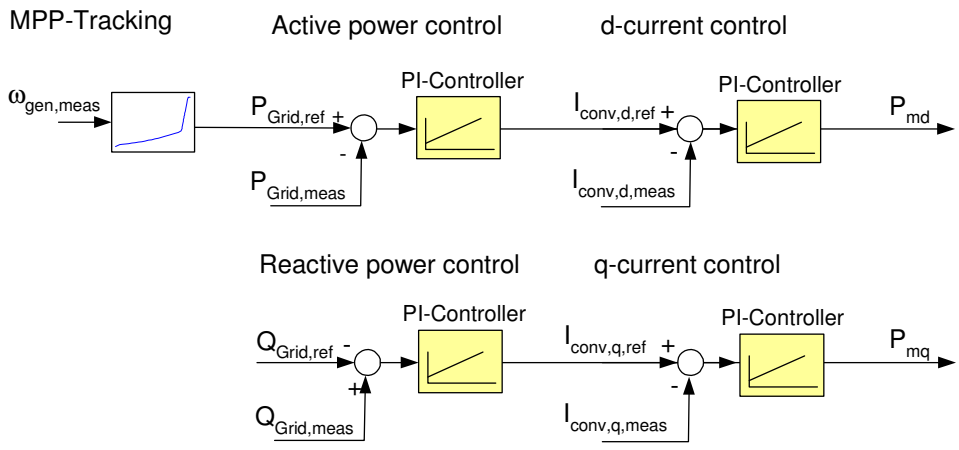

Figure 7.14: Grid side converter control

The MPP-tracking characteristic is illustrated in Figure 7.15. The principle of the control according to the MPP-tacking table is explained previously for the DFIG wind turbine presented in Section 5.2.2.

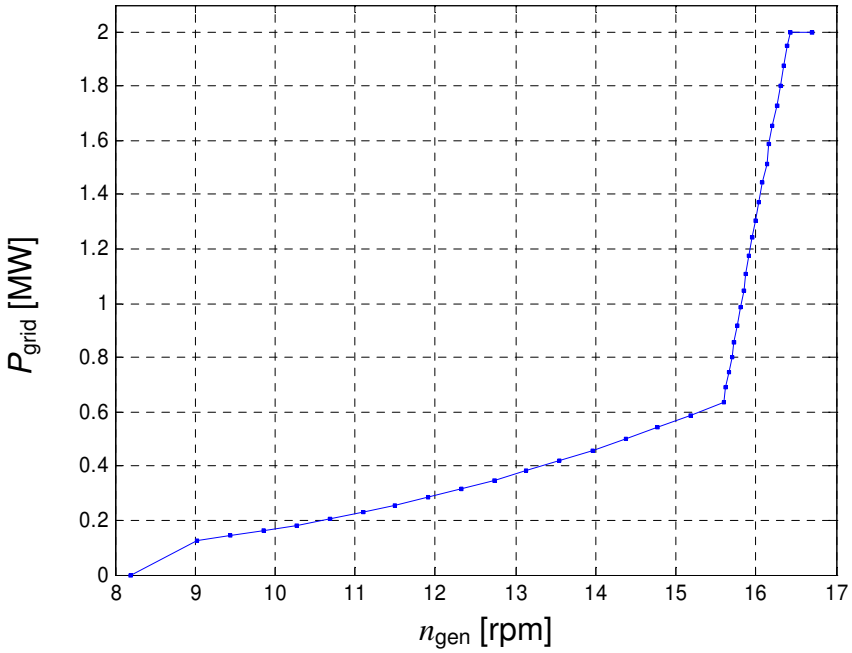

Figure 7.15: MPP-tracking characteristic

with

$$n_{gen} = \frac{\omega_{gen}}{2\pi \cdot p} \tag{7.21}$$

The parameters of the controllers are determined based on the wind turbine response to steps in deterministic wind speeds, in a similar was as it has been done for the DFIG in Chapter 5.3.

7.2.3 Control of the generator side converter

The generator side converter controls the DC-link voltage and the stator voltage in the stator voltage oriented reference frame. Both voltages are controlled to their rated values. The control is again realized with two cascaded control loops using a fast inner current control loop. The control structure is shown in Figure 7.16.

As concluded in paragraph 7.2.1, it is beneficial to control the stator voltage to its rated value in order to avoid overvoltages or saturation effects in the converter. The DC-link voltage is also kept constant in order to omit charging or discharging of the DC-link capacitor. However, small variations of the DC-link voltage are allowed, when electrical damping of the system becomes necessary. As illustrated in Figure

7.16 the DC-link voltage reference value is therefore defined by a damping control, which will be described in Section 7.3. As the generator's active power depends on the stator current d-component in SVRF, the DC voltage is controlled with the d-component of the stator current, too (equation (7.15) and (7.20)). The stator voltage is then controlled by the stator current q-component. The current control loops provide a control signal in d- and q-axis (P_{md}, P_{mq}), which is sent to the PWM-controlled frequency converter. The controller design is based on the investigations of [DIgSILENT 2007b].

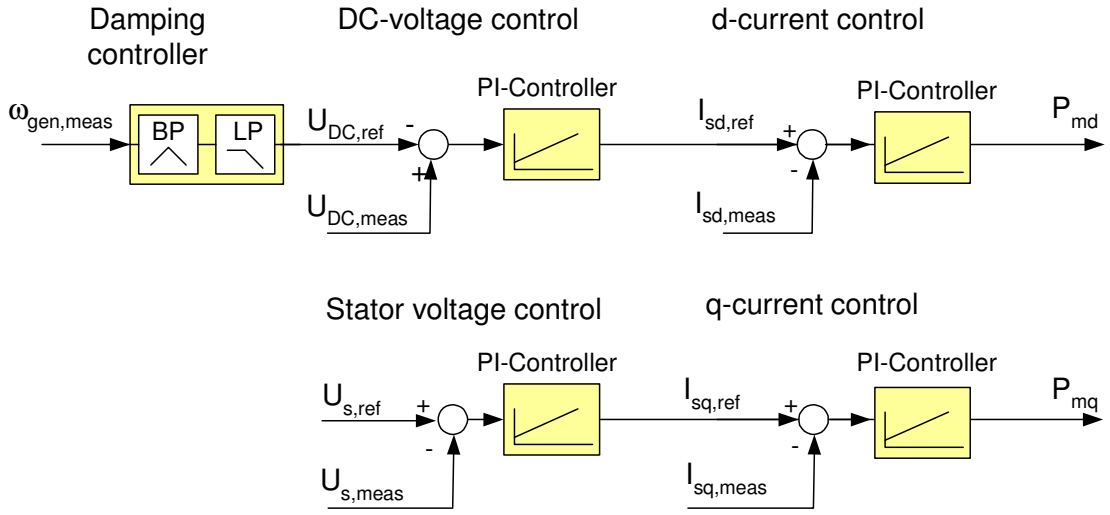

Figure 7.16: Generator side converter control

7.3 Damping of speed oscillations

The PMSG connected to a frequency converter is a system without inherent damping. This is due to the following reasons. (i) It has been mentioned before, that the PMSG has no damper windings. In case the PMSG is connected to a frequency converter, which provides a variable stator frequency according to the actual rotor speed, there is never any relative movement between stator and rotor field. Without this relative movement between stator and rotor, a damper winding would be without any impact, as no voltage would ever be induced in the damper winding [Jauch 2007]. (ii) Due to the small pole pitch of the multipole generator, a damper winding would provide insufficient damping [Grauers 1996b]. (iii) A PMSG has no field windings, which could contribute to damping either. The system has therefore no inherent damping despite the damping of the shaft. Thus, oscillations due to load changes, e.g. wind gusts, can excite oscillations, which are amplified in the system and which require an external damping of the wind turbine system.

7.3.1 Two-mass-model versus one-mass-model

Load changes due to wind gusts or grid faults can excite oscillations in the mechanical part of the wind turbine, which might be insufficiently damped. In this case it is essential to represent the mechanical system by means of a two-mass-model (see Chapter 4.3) in order to get an accurate response from the generator and the frequency converter. A representation by means of a one-mass-model would neglect such oscillations.

Furthermore, a multipole generator has a high number of poles and a large diameter, which causes a higher generator inertia compared to e.g. 2 or 4 pole generators.

It is assessed in [Akhmatov 2003a] and [Akhmatov 2003d] that the effective shaft stiffness of a generator is reduced with increasing number of poles.

$$K_{shaft,eff} = \frac{K_{shaft}}{S} \cdot \frac{\Omega_{gen}}{p} \tag{7.22}$$

where $K_{\text{shaft,eff}}$ is the effective shaft stiffness, K_{shaft} is the shaft stiffness in Nm/rad, S denotes the rated MVA-base of the generator and p is the number of pole pairs. This implies, that any mechanical torsion of the system results in larger dynamic changes of the electrical rotor angle for generators with a large number of poles. In multipole generators the same electrical angle corresponds to a much smaller mechanical angle than in generators with small pole numbers. A torsional twist of the shaft connected to a multipole generator has thus a stronger impact on the electrical system [Akhmatov 2003a]. Hence a more detailed model of the shaft system becomes necessary and a two-mass representation must be implemented [Akhmatov 2003a]. As an example a sudden change in wind speed from 12 m/s down to 11 m/s is simulated with both a two-mass-model as well as a one-mass-model. The simulations results of wind speed, generator speed and power are plotted in Figure 7.17.

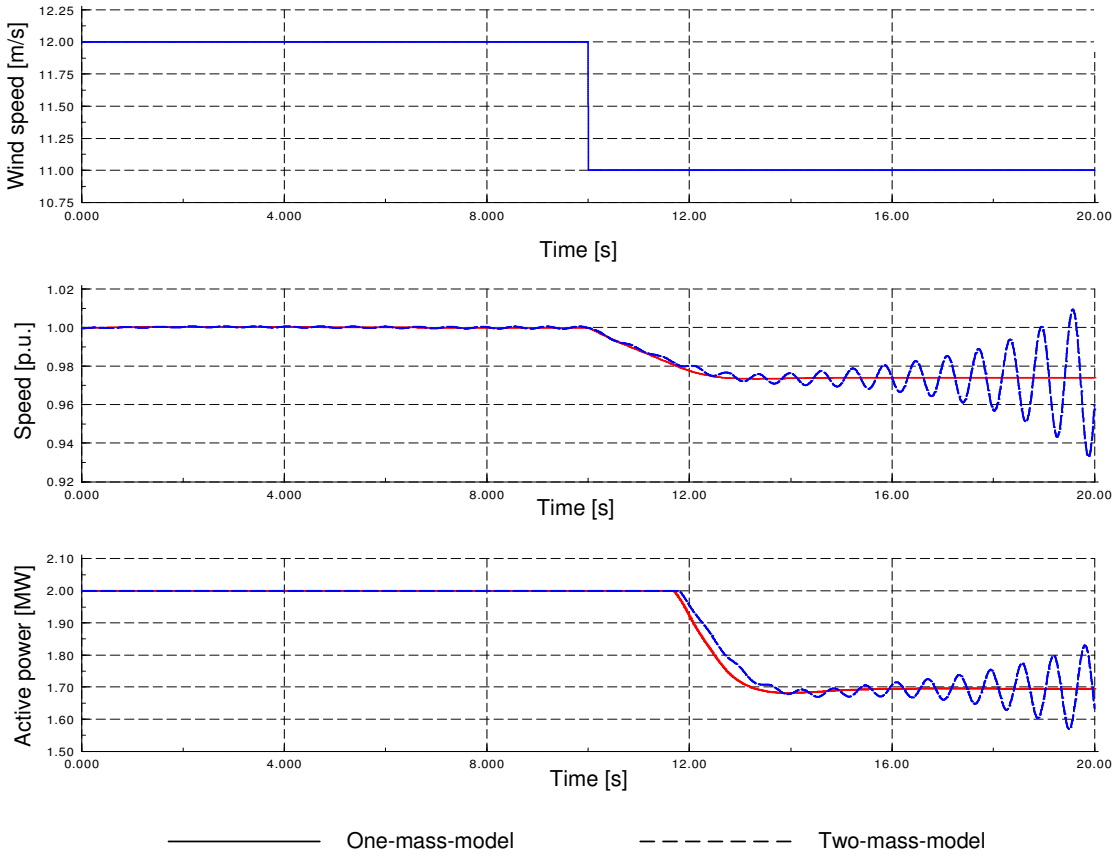

Figure 7.17: Speed and active power signal after a wind speed change from 12 m/s to 11 m/s simulated with a two-mass-model and a one-mass-model, respectively

The load change causes a drop in generator speed and active power. Notice, that the active power drop is delayed compared to the speed signal, due to the MPP-tracking characteristic. The MPP-characteristic is designed in such a way, that the active power production is kept to its rated value also in a small rage below rated generator speed in order to avoid unnecessary power fluctuations.

The oscillations in the wind turbine system, caused by load changes, can only be represented if the two-mass-model is applied. These oscillations are amplified through the wind turbine system and are insufficiently damped. Hence, an external active damping of the system (mechanical or electrical) becomes necessary. In contrast to this, the one-mass-model simplifies the system and therefore oscillations caused by load changes cannot be represented properly. In stability analysis, when the system response to heavy disturbances e.g. during grid faults is analysed, a two-mass-model is thus indispensable in order to achieve a correct prediction of the impact on the power system.

7.3.2 Damping system

In order to damp the drive train oscillations an external damping system must be implemented. Different methods for damping have been assessed and investigated, e.g.

damping by means of blade pitching [Jöckel 2001] or damping by means of a compliant mounting of the generator [Westlake 1996]. Additional or substitutional to mechanical measures, damping can also be provided by means of the electrical system.

As known from large synchronous generators in power systems a power system stabilizer (PSS) provides damping for speed and rotor angle oscillations by controlling the generator excitation. A PSS counteracts the speed oscillations by producing an electrical torque in phase with the generator speed. A similar method presented in [Jauch 2007] is also applied for wind turbines with DC excited synchronous generator and diode rectifier, where the excitation voltage is used to control and buffer transiently the power flow in the DC-link capacitor. However, since a PMSG has a fixed excitation electrical damping can only be provided by the frequency converter. Because the DC-link capacitor serves as a buffer between the generator and the grid the DC-link voltage can be used for damping. By periodically short term charging and discharging the capacitor, energy is stored in the capacitor so that the load current varies. This in turn influences the torque in such a way that it counteracts the speed oscillations and provides effective damping. The idea of the present damping controller is that, by using the DC capacitor as a short-term energy storage, the speed oscillations are buffered and reflected in an oscillating defined DC voltage reference $U_{\mathrm{DC,ref}}$. The damping controller uses the generator speed as an input signal and acts on the DC-link voltage controller of the generator side converter.

The design of the damping controller is based on a correct identification of the frequency and phase angle of the speed oscillations [Hansen 2007c]. As mentioned before, the generator speed of a wind turbine is prone to oscillations with the free-free frequency, due to the torsional spring characteristic of the wind turbine's drive train. In order to measure only the fast speed fluctuations of the drive train, the generator speed is filtered by means of a band pass filter. A bandpass filter passes a band of desired or specified frequencies, while attenuating those outside the band. In his work the band pass filter must be designed in a way, that only the free-free frequency of the system is transmitted through the filter. The free-free frequency of the drive train oscillations can be estimated according to equation (6.3). [Soerensen 2003].

Acting similar to a power system stabilizer, the damping system must produce a component of electrical torque in phase with the rotor speed oscillations [Kundur 1994]. The phase angle of the oscillations to be compensated can be identified by using a sinusoidal disturbance signal Δu_{osc} that has the frequency of the free-free frequency. This sinusoidal signal is then temporarily used as input of the DC-voltage controller instead of the generator speed (situation 1 in Figure 7.18). Moreover, a high generator inertia is necessary during simulation in order to ensure a stable operation.

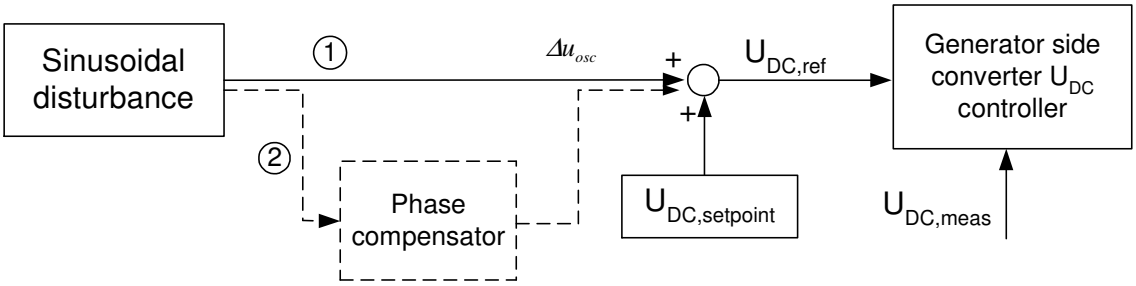

Figure 7.18: Sinusoidal disturbance signal used for phase identification

The sinusoidal signal Δu_{osc} is superimposed on the DC-voltage setpoint and defines the DC voltage reference $U_{DC,ref}$. The phase angle is found by determining the phase angle between the generator electrical torque and the sinusoidal disturbance, as exemplified in Figure 7.19. Notice that the electrical torque of the generator caused by the sinusoidal disturbance signal leads by 90 degrees, when no phase compensation is used. Therefore, a phase compensator, which introduces a –90 degrees phase, has to be applied to place the electrical torque in phase with the sinusoidal disturbance (situation 2 in Figure 7.18 and Figure 7.19).

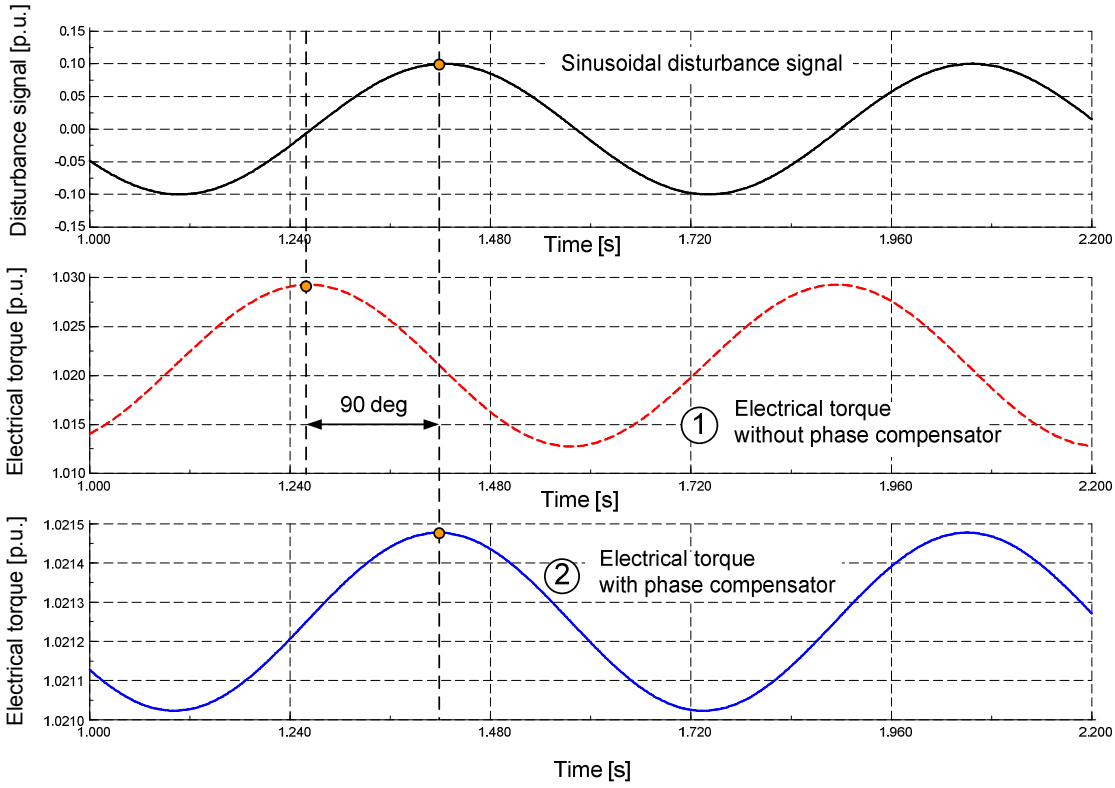

Figure 7.19: Identification of the phase to be compensated

Once the frequency and the phase angle of the oscillations are found, a damping controller can be realised, as illustrated in Figure 7.20. The damping controller consists of a bandpass filter and a phase compensator. The input in the damping controller is the

generator speed ω_{gen}, while the output is the DC voltage reference signal $U_{DC,ref}$, which is further used as input in the generator-side converter controller. The DC voltage reference signal $U_{DC,ref}$ is obtained by superimposing the output of the phase compensator on the DC voltage setpoint, as follows:

$$U_{DC,ref} = U_{DC,setpoint} + \Delta u_{damp} \tag{7.23}$$

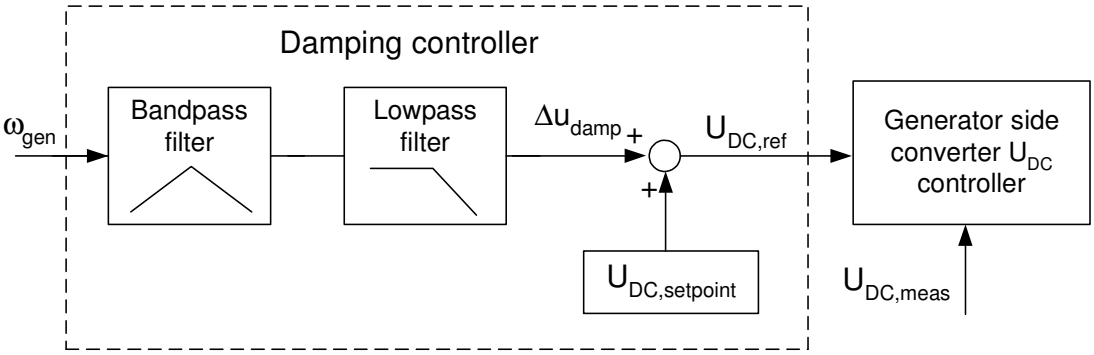

Figure 7.20: Damping controller acting on U_{DC} control of the generator side converter

As illustrated in Figure 7.19, for the considered multipole PMSG wind turbine configuration a phase compensator, which introduces a –90 deg phase at the filtered speed signal is found to be necessary. A simple solution is to use a lowpass filter as phase compensator. The design of the lowpass filter is based on the transfer function between DC voltage and electrical torque.

Figure 7.21 shows the Bode diagram of the designed bandpass and lowpass filters of the damping controller. The position of the free-free frequency to be damped (i.e. 10 rad/sec for the considered wind turbine) is outlined in the plots.

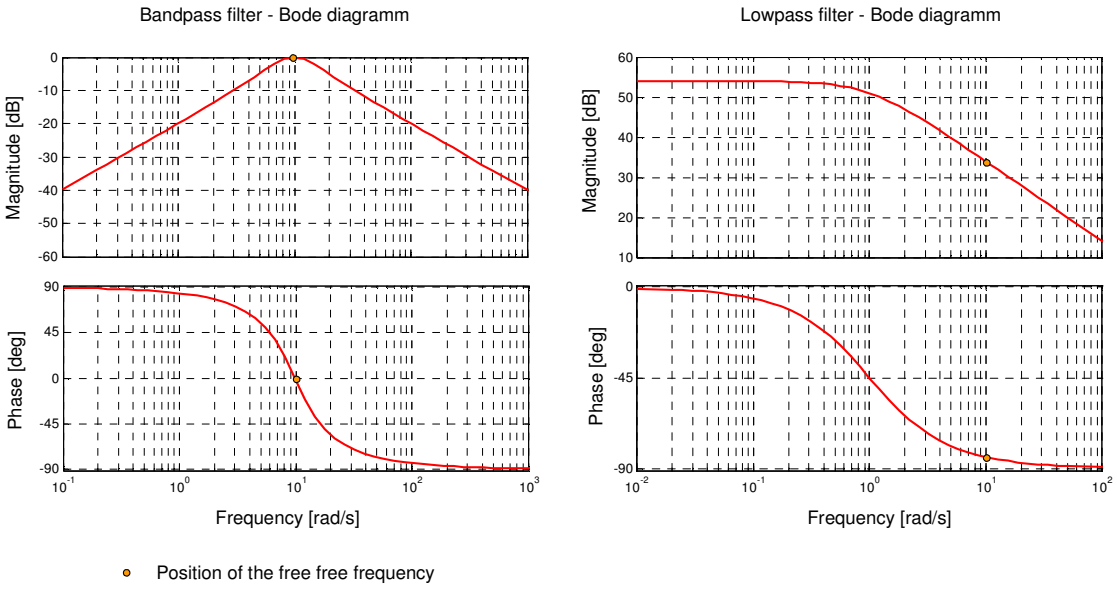

Figure 7.21: Bode diagram of bandpass filter and low pass filter

As an example Figure 7.22 shows the simulation results of wind speed, generator speed and active power production for the cases with and without damping after a wind speed change of 1 m/s. The simulation results illustrate the impact of the damping system. Without damping the wind speed change provokes large oscillations of the drive train, which are amplified in the system. In contrast to this the oscillations are suppressed effectively when the damping controller is used.

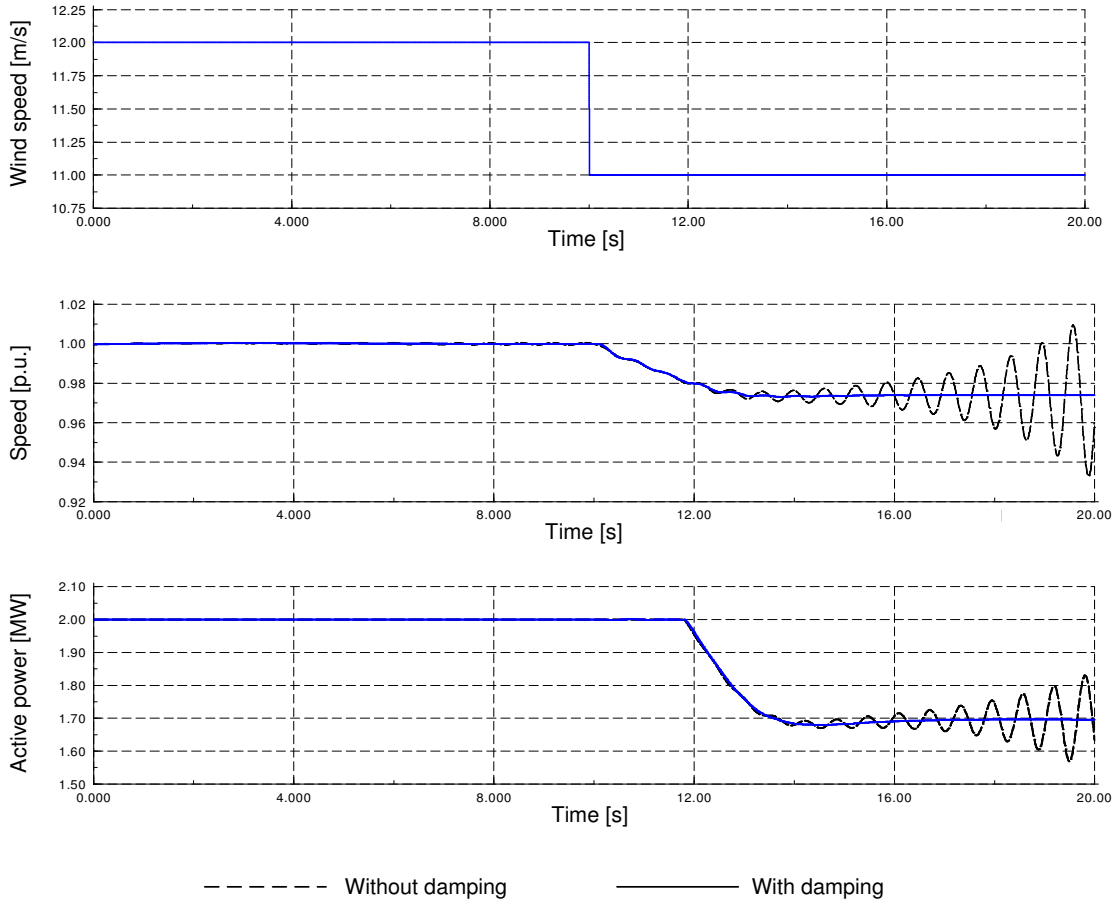

Figure 7.22: Speed and active power signal after a wind speed change of 1 m/s simulated for the cases with and without applied damping

Other methods of damping, realized by means of the converter control, can also be implemented. According to [Akhmatov 2003a] and [Hansen 2007b] the damping can instead be done by means of a PI controller. The low pass filter is then substituted by a PI controller, which actively damps the fluctuations to zero. Alternatively to the damping by means of U_{DC} the damping can also be performed by active power control [Akhmatov 2003a], [Hansen 2007b].

An overview over the total control structure of the PMSG wind turbine for normal operation conditions can be found in the appendix in Section 12.9.

7.4 Case studies

In order to evaluate the performance of the control system for the variable speed wind turbine concept with PMSG a set of step response simulations first with deterministic wind speed (no turbulence, no tower shadow) and then with stochastic wind speed are performed. For comparison, the same simulations as for the DFIG wind turbine in Section 5.3 are presented.

7.4.1 System performance under deterministic wind speeds

In Figure 7.23 typical quantities of the turbine system, as pitch angle, generator speed and active power are shown for steps in wind of 1 m/s every 20 seconds. At a wind speed of 12 m/s the turbine works at rated conditions. As the wind speed is above its rated value ($v_{w,rated}$ = 11.7 m/s), the pitch mechanism is active and limits the power and the speed to their rated values. For lower wind speeds below 12 m/s the pitch mechanism is passive and the pitch angle is kept to its optimal value (i.e. zero for the considered turbine). Under partial load the variable speed operation assures optimal energy capture. According to the P-ω table defined by the MPP-tracking, the speed and the power are adapted to their optimal values for the prevailing wind speed. Remark, that the response time of speed and power is lower at higher wind speeds, when the MPP-tracking is defined as a ramp function (see Figure 7.15), while the response time is bigger at lower wind speeds, when P and ω are defined with $P \sim \omega^3$.

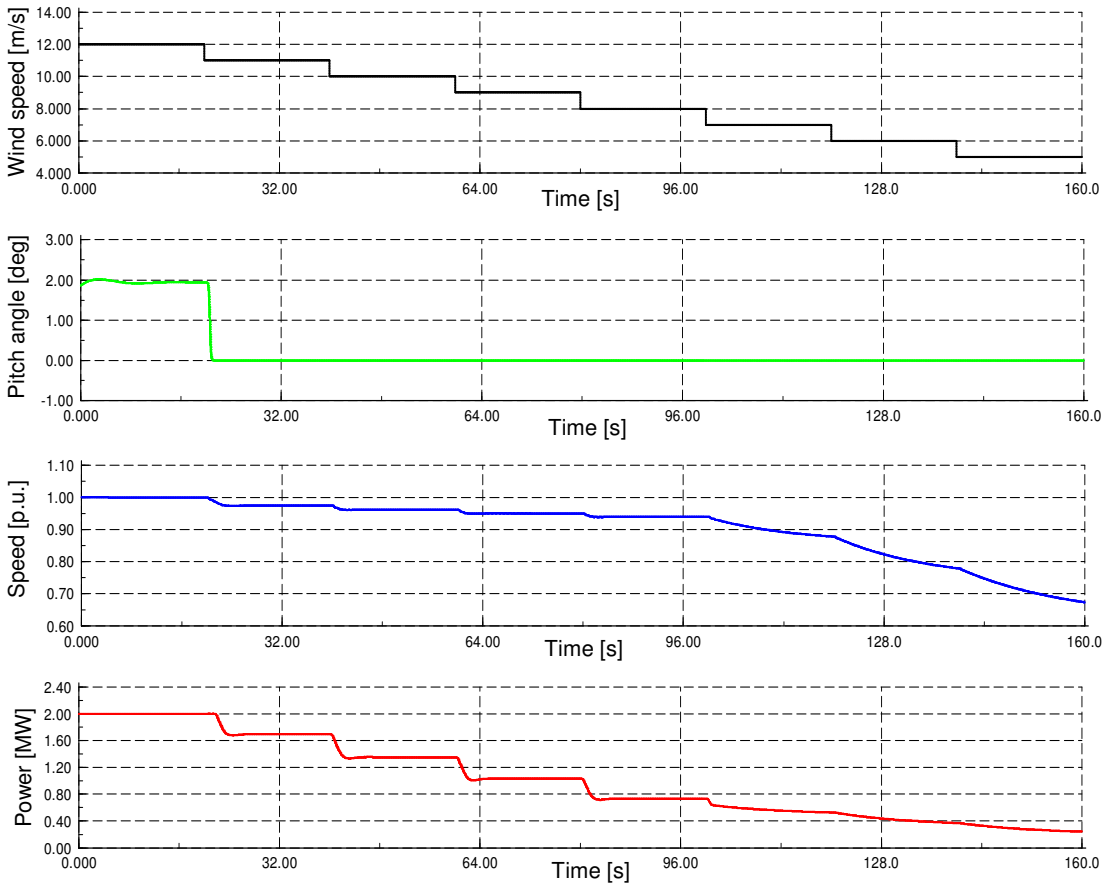

Figure 7.23: PMSG wind turbine: Wind speed, pitch angle, generator speed and active power for steps in wind of 1 m/s from 12 m/s down to 5 m/s

Figure 7.24 shows the performance of the generator side converter control during the simulated case. The DC-link voltage is kept constant to its reference value of 5.9 kV. However, the damping of the system causes small variations of the DC-link voltage around its reference value. The stator voltage is controlled to its rated value, too.

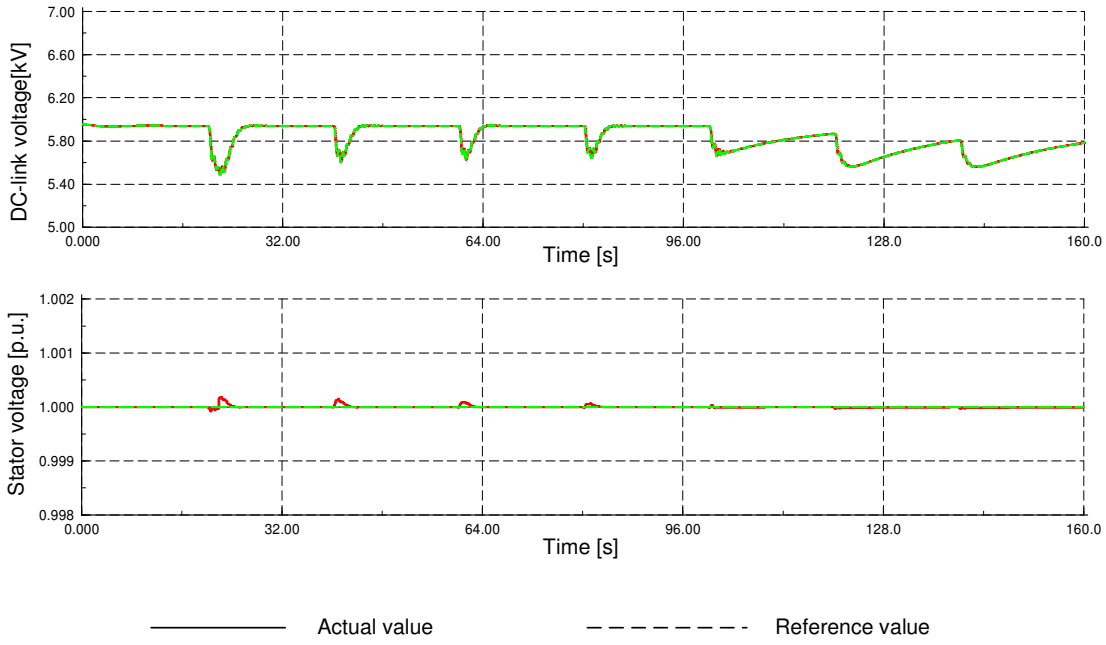

Figure 7.24: PMSG wind turbine: DC-link voltage and stator voltage for steps in wind of 1 m/s from 12 m/s down to 5 m/s

Another study case is carried out for steps in wind speed from 12 m/s up to 20 m/s. The step response of pitch angle, speed and power for wind speeds above rated wind speed is presented in Figure 7.25. In the same way as it was presented for the DFIG wind turbine the steps in wind speed yield changes in both the pitch angle and the generator speed. The pitch mechanism reacts slowly compared to the power controller. Notice thus, that dynamic variations in the generator speed occur at each step in wind speed, which facilitate, that fast wind speed changes are absorbed in rotational energy of the rotating masses. Nevertheless, the step response of the pitch angle and generator speed does not present big overshoots and oscillations and the generator power can be kept to its rated value of 2 MW. The effectiveness of the gain scheduling controller as part of the blade angle control is again visible as for the DFIG wind turbine, i.e. the response of the generator speed is identical over the whole speed range between 12 m/s and 20 m/s compensating the nonlinear aerodynamic characteristics.

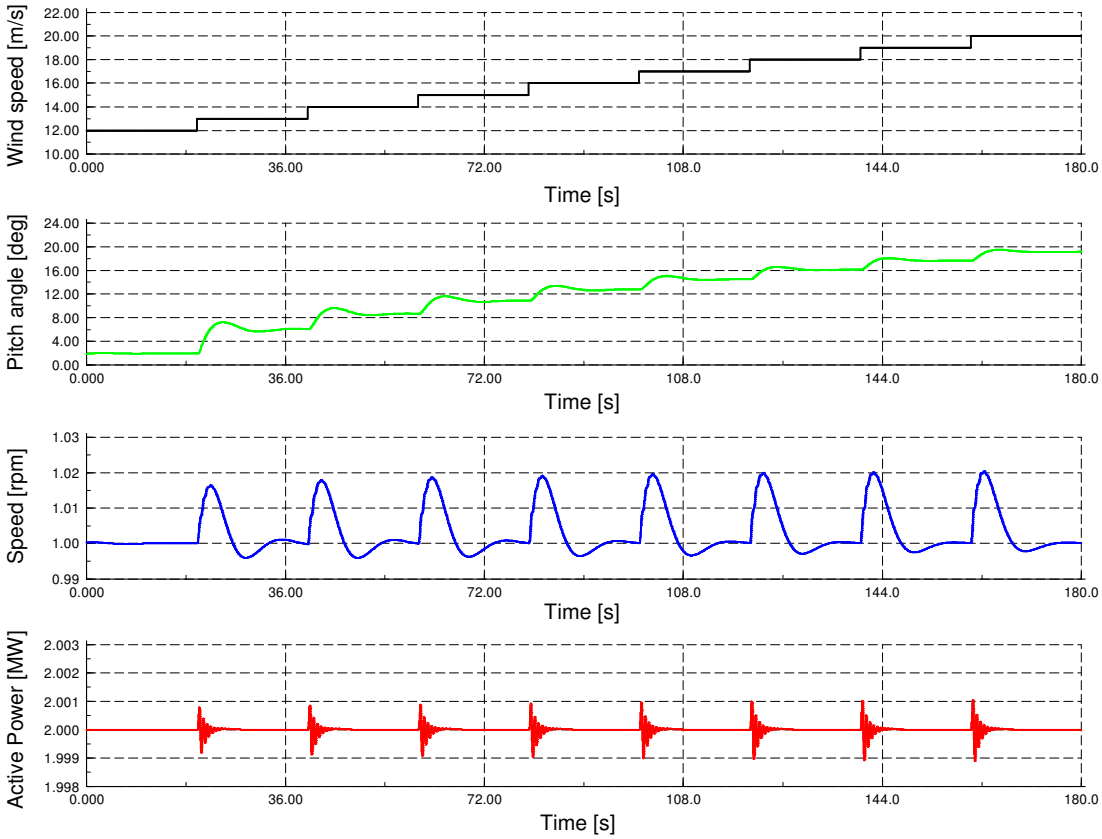

Figure 7.25: PMSG wind turbine: Wind speed, pitch angle, generator speed and active power for steps in wind of 1 m/s from 12 m/s up to 20 m/s

For the sake of completeness the results of the generator side converter control are presented in Figure 7.26. The stator voltage is kept constant, while the DC-link voltage varies according to the damping signal, which is modulated upon the reference value of U_{DC}.

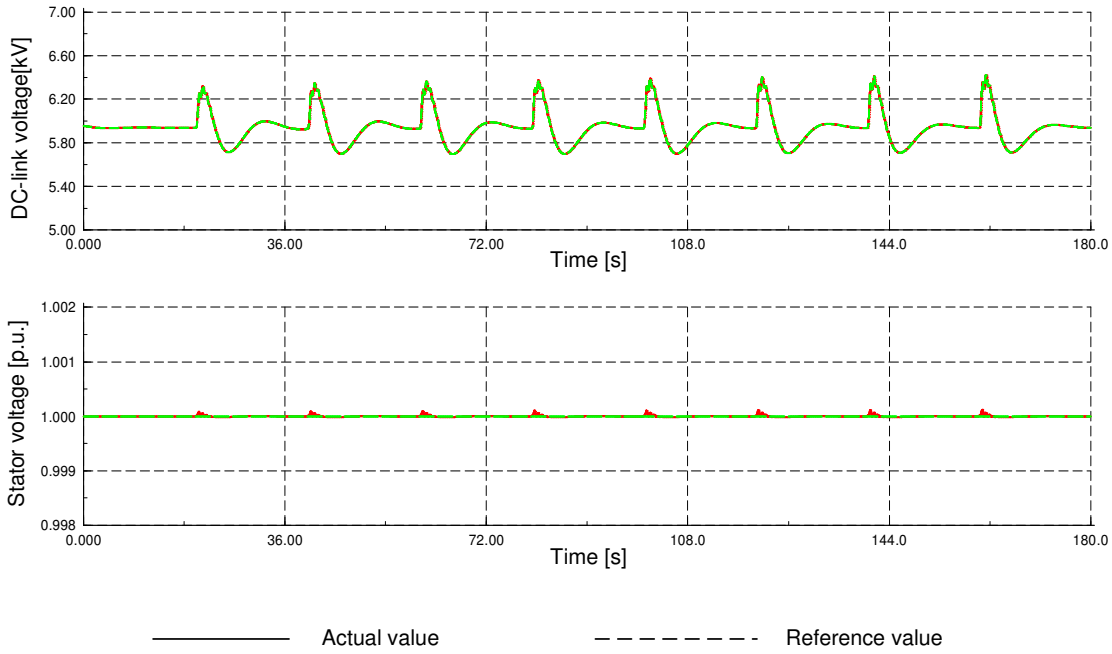

Figure 7.26: PMSG wind turbine: DC-link voltage and stator voltage for steps in wind of 1 m/s from 12 m/s up to 20 m/s

7.4.2 System performance under stochastic wind speeds

Finally, simulation results under stochastic wind conditions illustrate the ability of the control system for variable speed wind turbines with PMSG. Similarly to the case studies of the DFIG wind turbine presented in Section 5.3.2, three sets of simulations are now presented for the PMSG wind turbine under stochastic wind speed: (i) 8 m/s mean wind speed, the turbine works exclusively at partial load, (ii) 12 m/s mean wind speed, the turbine operates partly at rated and partly at partial load, (iii) 20 m/s mean wind speed, where the ability of the DFIG wind turbine to regulate its power to imposed reference values is underlined.

Simulation case (i) is shown in Figure 7.27 where wind speed, pitch angle, generator speed and active power production of the turbine system are plotted over a simulation time of 300 s. The turbine operates at partial load. Thus, the pitch angle is kept constant and the pitch control is inactive. Meanwhile, the MPP-tracking tracks the speed and the power to the turbine's optimal operational point.

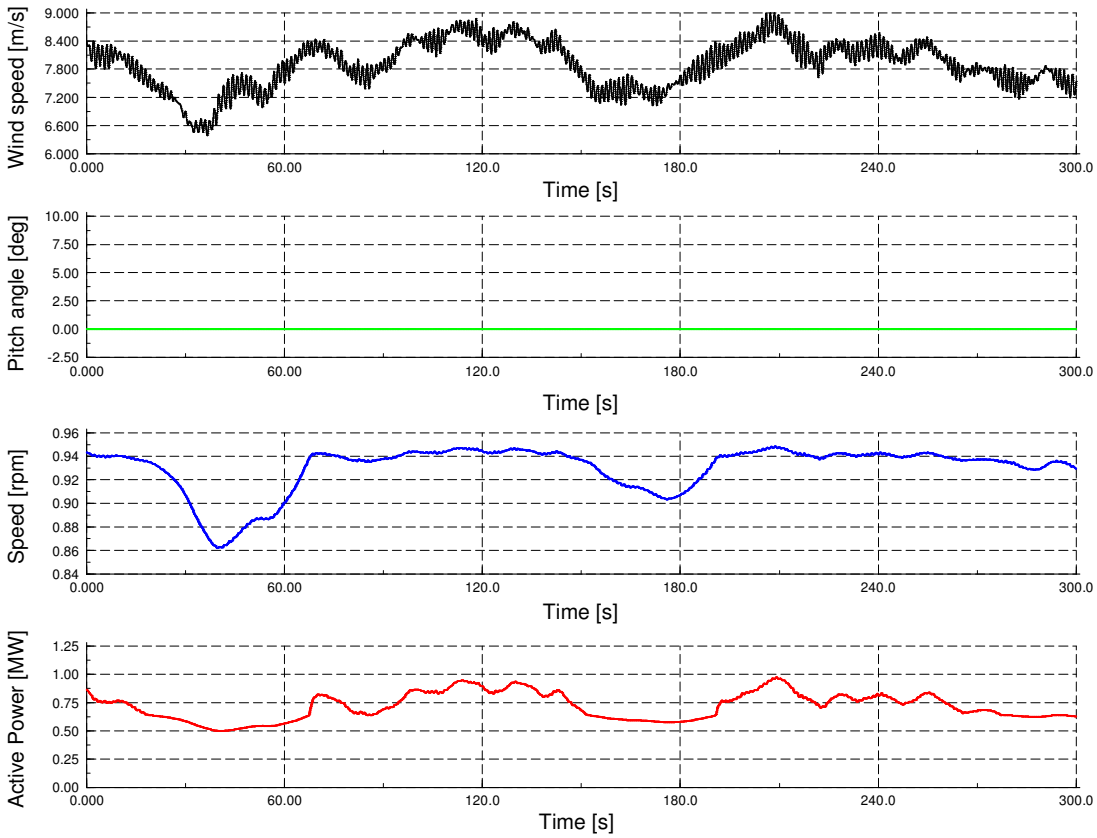

Figure 7.27: PMSG wind turbine: Wind speed, pitch angle, generator speed and active power under stochastic wind speed with a mean wind speed of 8 m/s

Figure 7.28 shows the results of simulation case (ii). As the mean wind speed is 12 m/s the turbine operates partly at rated conditions and partly at partial load. As soon as rated wind speed is exceeded, the pitch angle increases and limits the speed and indirectly also the power to their rated values. Dynamic variations of the speed above rated speed are allowed to buffer sudden changes in wind power.

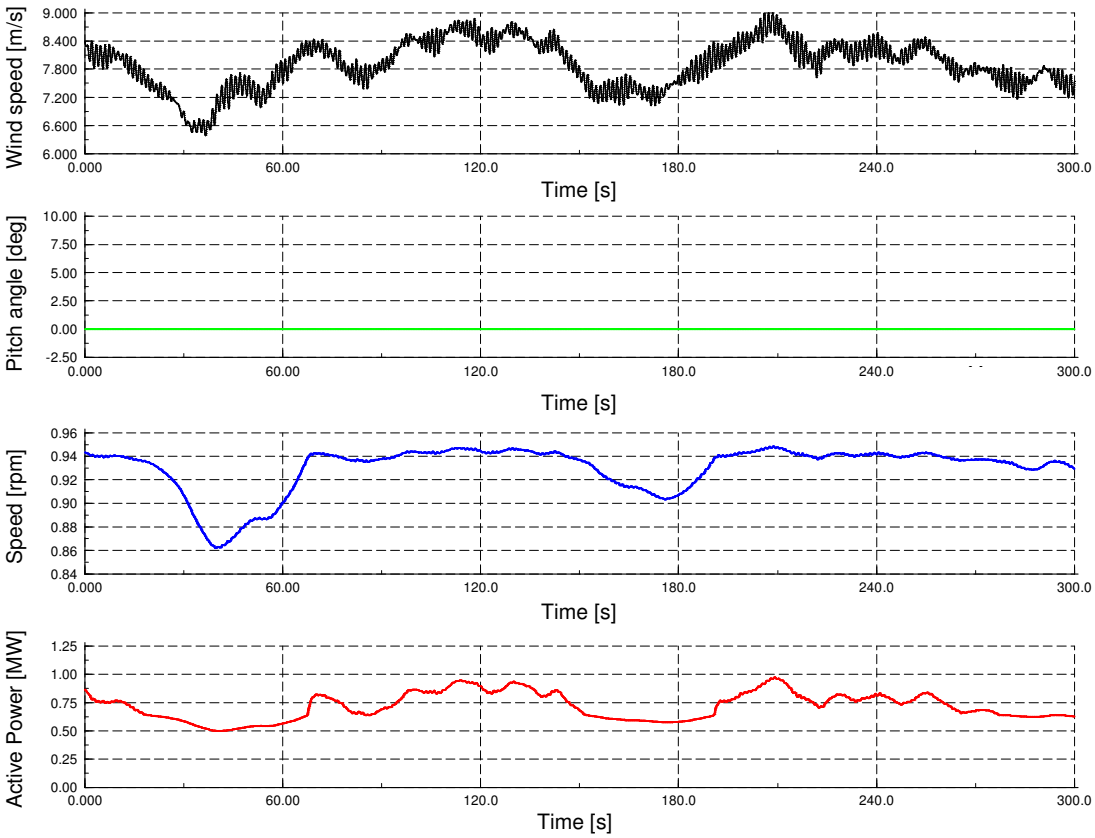

Figure 7.28: PMSG wind turbine: Wind speed, pitch angle, generator speed and active power under stochastic wind speed with a mean wind speed of 12 m/s

Simulation case (iii) presents the turbine behaviour under turbulent wind with a mean wind speed of 20 m/s and a turbulence intensity of 10 %. Figure 7.29 illustrates the pitch angle, the generator speed as well as the active and reactive power. The simulation underlines the turbine's feature of independent active and reactive power control as both are controlled independently to imposed reference values. The pitch angle is continuously adapted according to the fluctuating wind speed. Notice that dynamic speed variations are allowed to reduce the mechanical stress on the system.

The independent control of active and reactive power during fluctuating wind speed is exemplified by the following sequence: the reference power is reduced in steps of 500 kW every 30 s from 2 MW down to 1 MW and stepped up back again to 2 MW. Meanwhile, the reactive power is controlled to zero in the first 150 seconds and is then increased in steps to 1.5 MVar. 1.5 MVar denotes the maximum available reactive power of the grid side converter if rated active power (2 MW) is supplied at the same time. After 180 s the same active power control sequence is repeated now for a reactive power setpoint of 1.5 MVar. The active and reactive power output are following their references very well. However, it should be noticed that this abrupt reduction of active power would not be applied in practice to avoid sudden changes in power production. However, it is shown here only in order to underline the features of the

control system. It can be concluded that the designed control strategy of the variable speed PMSG wind turbine enables the turbine to control independently active and reactive power to specific reference values, possibly being defined by the transmission system operator.

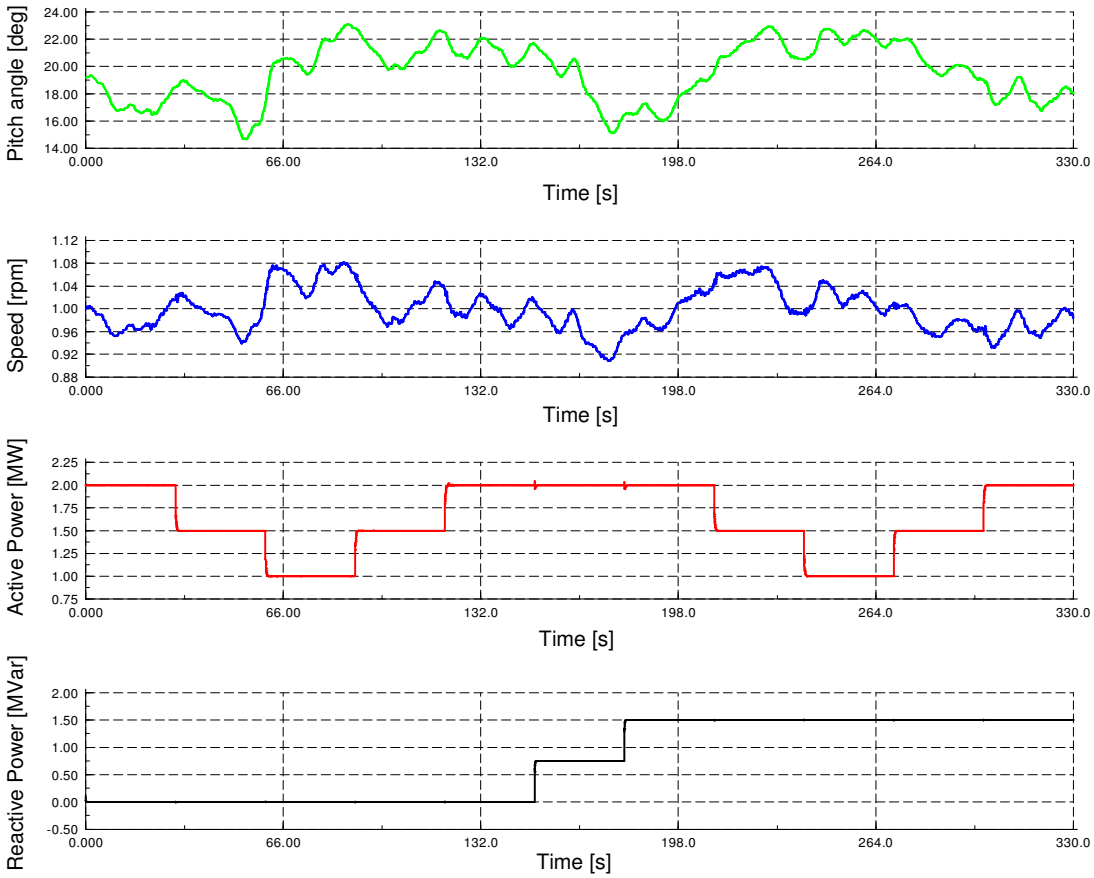

Figure 7.29: PMSG wind turbine: Pitch angle, generator speed and active and reactive power production under stochastic wind speed with a mean wind speed of 20 m/s

7.5 Summary

The present chapter focuses on modelling and control of a variable speed wind turbine with multipole permanent magnet synchronous generator and full-scale converter. Due to the gearless construction and the permanent magnet excitation the synchronous generator represents a high efficient and low maintenance solution, which can be very beneficial for offshore wind turbines.

A comprehensive dynamic simulation model is developed in the simulation tool DIgSILENT. The steady state behaviour and the differential equations used in the dynamic model are presented and analysed. Different converter topologies are discussed. For PMSG wind turbines an IGBT converter is the most appropriate solution.

The control of the PMSG wind turbine is similar to the control developed for the DFIG, i.e. the blade angle control controls the speed of the system while the power

is directly controlled by the frequency converter. A coordination between both power and speed controller is necessary. A careful assessment of different converter control strategies is carried out. The control strategy, which is found to be most advantageous for PMSG wind turbines, is implemented in the simulation model. It is based on the idea that the active and reactive power supply to the power system is directly controlled by the grid side converter, while stator voltage and DC voltage are kept constant by the generator side converter.

Different simulation studies are carried out and they confirm good performance of the presented control strategy. The converter control guarantees variable speed operation to gain optimal power production according to the MPP-tracking. Above rated wind speed the pitch angle control controls the generator speed and indirectly the power output to their rated values. A damping controller is implemented, which is necessary to damp torsional oscillations of the drive train system caused by eventual load changes. A multipole PMSG wind turbine with full-scale converter has no inherent damping and the absence of an additional damping controller might therefore lead to self-excitation and high mechanical stress of the drive train. The control strategy facilitates furthermore independent control of active and reactive power to reference values imposed externally by e.g. the transmission system operator. It is demonstrated that the PMSG wind turbine equipped with a full-scale converter and the presented control strategy, can operate in the same manner as a conventional power plant does.

8 Multipole PMSG wind turbines´ grid support capability

As the multipole PMSG wind turbine is grid connected via a full-scale frequency converter it can be presumed, that this wind turbine concept has very good grid support capability compared to any other wind turbine concept. Due to the larger converter rating the amount of reactive power, which can be provided to support the grid voltage, is larger than for any other wind turbine concept [Ackermann 2005]. Furthermore, the converter system decouples generator and turbine from the grid so that both are less subjected to the grid fault impact than turbines with direct grid connected generator. In order to approve the above made assumptions the dynamic behaviour of PMSG wind turbines under grid faults is analysed in the following. The grid fault impact on both the electrical system and on the mechanical system is investigated by means of simulations. Based on these investigations a control strategy is developed, which enhances the fault ride-through and grid support capability of PMSG wind turbines.

8.1 Dynamic behaviour of PMSG wind turbines under grid faults

In order to evaluate the dynamic behaviour of PMSG wind turbines under grid faults a selected simulation case is performed. For this simulation case a three-phase grid fault at the high voltage grid connection terminal is simulated. The turbine system and its grid connection are illustrated in Figure 8.1.

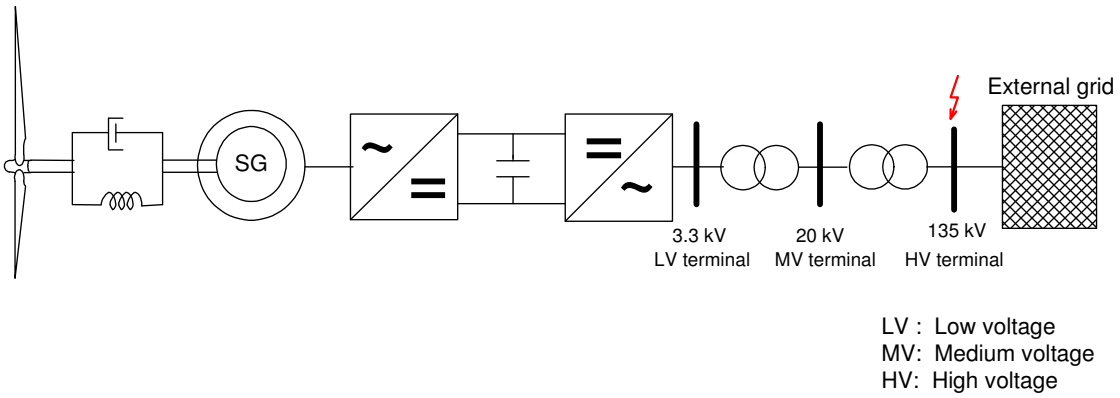

Figure 8.1: PMSG wind turbine subjected to grid fault at HV terminal

The grid is modelled by means of a Thevenin equivalent sketched in Figure 8.2 and is characterized by a short circuit power S_k of approximately 10 times the rated wind turbine power $P_{\text{wind turbine, rated}}$ and an R/X ration of 0.1. The three-phase short circuit happens at the high voltage grid connection terminal of the turbine and is represented with the short circuit impedance $R_f + j\,X_f$.

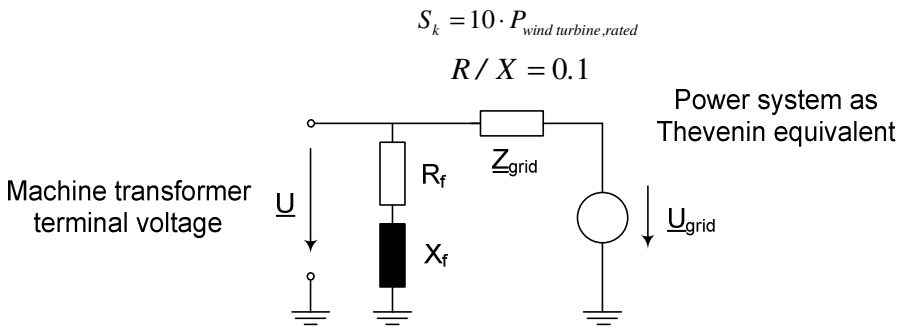

Figure 8.2: Single phase Thevenin equivalent of the external grid with short circuit impedance R_f+jX_f

8.1.1 Grid fault impact on the electrical system – simulation case

The focus of the present subsection is to analyse the grid fault impact on the electrical system of the wind turbine by means of a simulation case. In the following, simulation results of the most significant signals are presented and discussed.

In Figure 8.3 the voltage as well as active and reactive power production of the wind turbine system at the medium voltage terminal are illustrated. The symmetrical three-phase fault happens at the high voltage terminal at 0 s and lasts for 100 ms. The signals are plotted for 200 ms after the fault incident. When the fault occurs it is assumed that the turbine is operating at rated conditions. The prevailing wind speed is 12 m/s and is kept constant for the simulation as wind speed changes are little compared to the time frame of the fault.

For the presented simulation case no additional control for fault ride-through and voltage support is implemented, yet. It is assumed that in this first stage of grid fault simulation the wind turbine is equipped with the control presented in Chapter 7 (Figure 7.9) As illustrated in Figure 8.3 the simulated fault causes a voltage drop down to 40 % of the rated voltage, which is further implies a drop of the active power, too. The d-current component of the grid side converter, controlling the active power, tries to compensate for the droop in active power. However, due to the reduced voltage level, the power cannot be controlled to its reference value during the fault. Meanwhile, the grid side converter continues to control the reactive power to its reference, which is close to zero covering only the reactive power demand of the transformers. The reactive power shows two peaks at the fault incident and at fault clearing, respectively. This is due to the demagnetisation and magnetisation of the transformers, when the grid voltage drops and recovers, respectively.

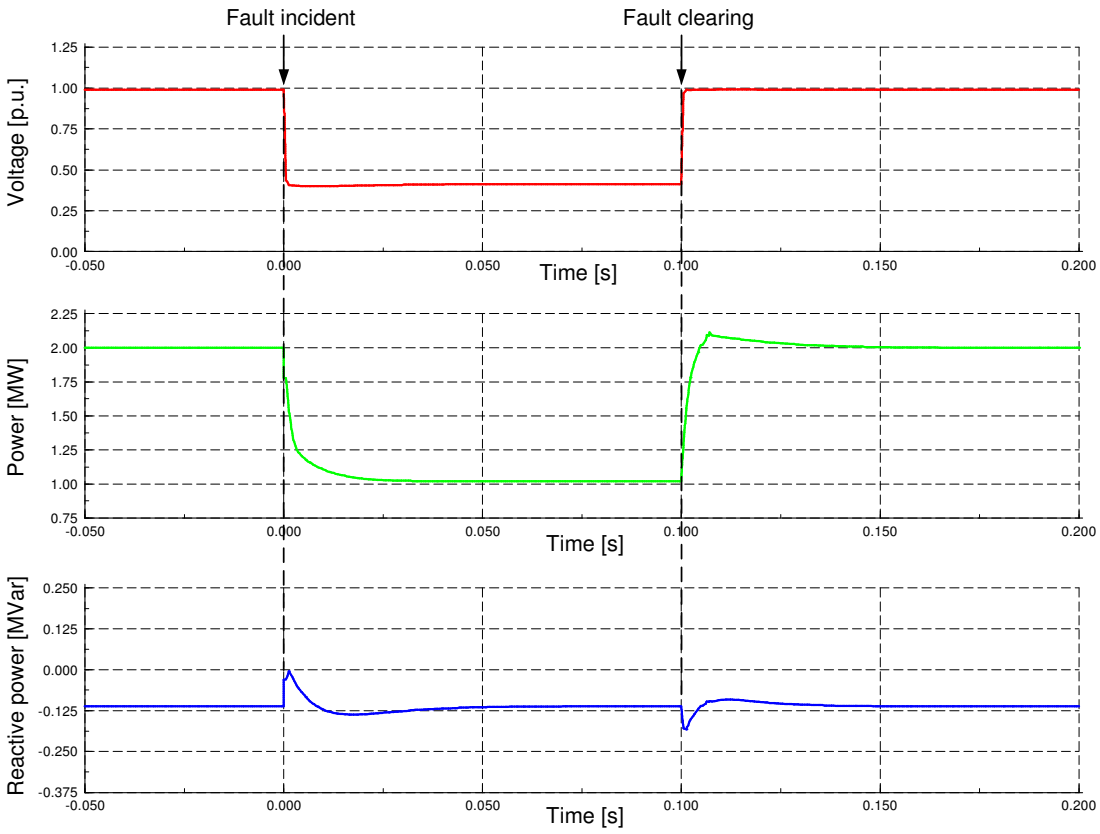

Figure 8.3: Simulation results at the medium voltage terminal: grid voltage, active and reactive power production for a three phase short circuit at the high voltage terminal, fault duration of 100 ms

Notice that on the one hand. the voltage drop causes a drop of active power, delivered to the grid by the grid side converter, while on the other hand the wind turbine continues its power production. Hence, a power imbalance in the wind turbine system occurs. The turbine produces a power surplus, which cannot be transferred to the grid. This fact is essential for the understanding of the following considerations.

If the generator side converter continues to deliver the generated power from the generator to the DC-link, the power imbalance will cause a transient charging of the DC-link capacitor. This can be represented by the following equation [Akhmatov 2006a]:

$$U_{DC}(t) = \sqrt{U_{DC}^2(0) + \frac{2}{C}\int_0^t \left(P_{GenSC}(\tau) - P_{GridSC}(\tau)\right) d\tau} \qquad (8.1)$$

P_{GenSC} power transferred by the generator side converter
P_{GridSC} power transferred by the grid side converter
U_{DC} DC-link voltage
C capacitance of DC-link capacitor

Notice that the charging of the DC-link capacitor may however cause overvoltages in the DC-link and denotes a damaging risk of the converter or the DC-link capacitor itself. The power surplus of the turbine must thus be dissipated in the system. Different possible manners for that are itemized in the following [Robles 2007]:

(i) In order to avoid the charging of the DC link capacitor a chopper can be applied to the DC link. A chopper represents a parallel resistor, which is added parallel to the capacitor in the DC-link. The chopper is switched on if the DC link voltage increases over a critical level and the surplus power is burned in the chopper resistance. The action of the chopper will be further explained in Section 8.2.2.

(ii) In the control strategy presented in this work the control task of the generator side converter is to keep the DC-link voltage constant (see Section 7.2.3). During the fault, the grid side converter can transfer less power to the grid. As a consequence the generator side converter control will decrease its active current component in order to reduce the power flow into the DC-link. This causes a decrease of the stator current, so that the generator power decreases as well. The power imbalance, which occurred in the DC-link before, is then transferred to the generator instead. When the generator power is decreased, while the turbine power stays constant, the power imbalance leads to acceleration of generator and turbine. The power surplus is then buffered in rotational energy of the rotating masses.

(iii) If a power imbalance between turbine and generator power arises, as explained under (ii), the turbine starts to accelerate. If the speed increases above its rated value the pitch control starts to counteract the acceleration and the pitch angle is increased in order to reduce the aerodynamic power. However, the response time of the pitch system is very slow compared to the time frame of the fault. The action of the pitch system and the reduction of aerodynamic power become therefore relevant in case of long faults. [Conroy 2007].

In the present simulation, the generator side converter controls the DC-link voltage to a constant value. Thus, the sequences as explained under (ii) followed by (iii) take place. Figure 8.4 and Figure 8.5 show the control signals of the generator side converter control and their reference values, i.e. DC link voltage, stator voltage and the converter currents i_d and i_q, respectively.

During the fault, the generator side converter control keeps the DC-link voltage constant (Figure 8.4). This causes a decrease of the absolute value of the d-component converter current (active current component) as illustrated in Figure 8.5.

Although the DC voltage is controlled to a constant reference value, a transient change of the DC-link voltage can be observed at the fault incident. Notice that the fault is cleared before the DC-link voltage reaches its reference value. After fault clearing the DC-link voltage oscillates. This is due to the damping controller, explained in Section 7.3.2. As a consequence of the fault, the power drop in the generator causes

speed oscillations of the drive train. The control task of the damping controller is to damp these speed oscillations. Based in the generator speed signal the damping controller adds an oscillating offset to the reference value of the DC voltage. The oscillating DC voltage provokes thus a generator torque component, which counteracts and damps the speed oscillations. Figure 8.4 illustrates the oscillations of the DC voltage.

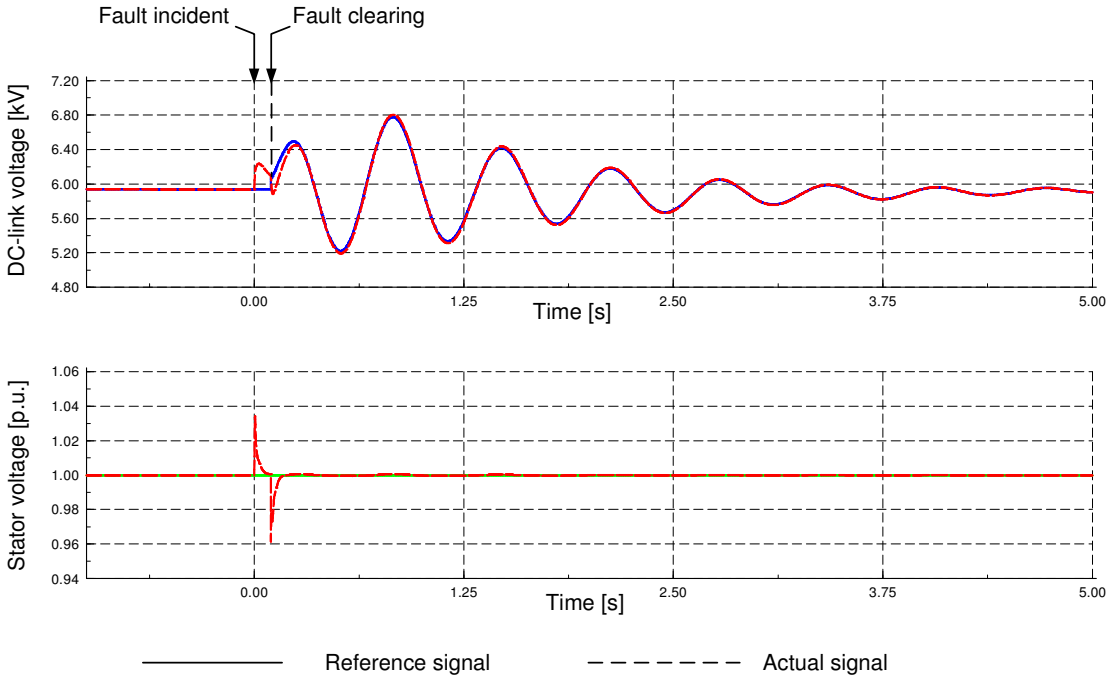

Figure 8.4: Simulation results of the generator side converter control: DC-link voltage, stator voltage for a three phase short circuit at the high voltage terminal of the PMSG wind turbine, fault duration of 100 ms

At the same time the stator voltage is controlled to its rated value. Due to the reduction of active current in the stator, the vector of the electromotive force *E* moves towards a smaller load angle. In order to keep the stator voltage constant and to compensate for the change in the load angle, the control adapts the stator current q-component, as shown in Figure 8.5. Because of this reason the reactive power setpoint of the generator changes during the fault as well (see Figure 8.6).

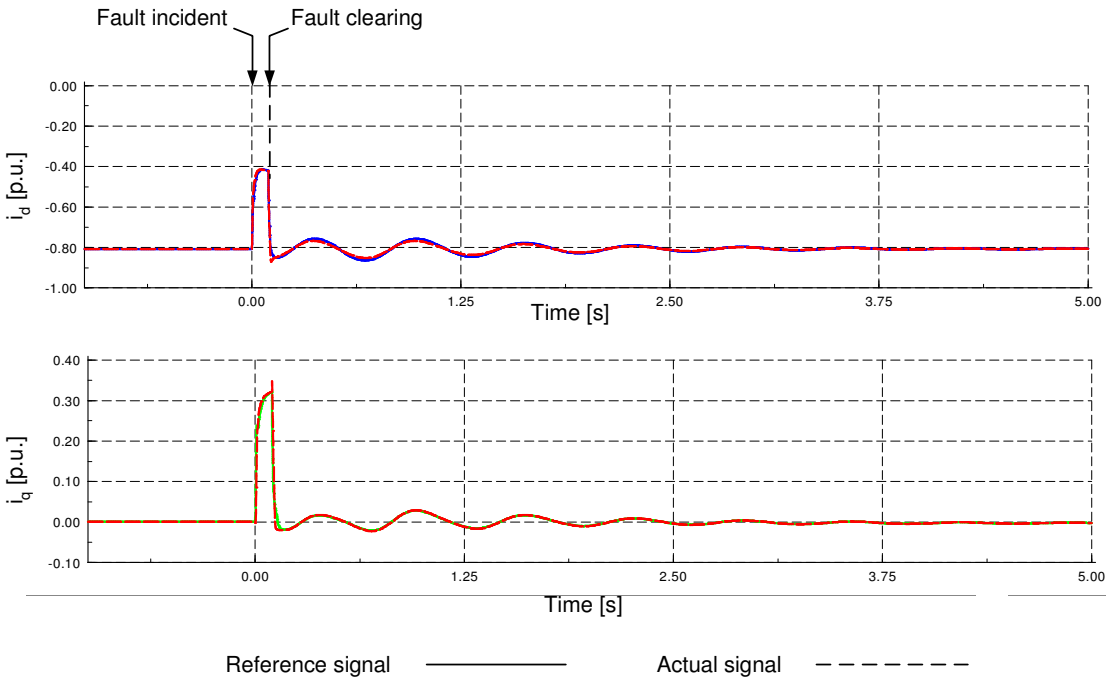

Figure 8.5: Simulation results of d- and q-current components of the generator side converter controller for a three-phase short circuit at the high voltage terminal of the PMSG wind turbine, fault duration of 100 ms

Figure 8.6 shows the simulations results of the generator's active and reactive power for the simulated grid fault. Furthermore, the active power of the grid side converter is plotted for comparison. As explained above, the drop of active power is transferred to the generator side, because the DC-link voltage is kept constant by the generator side converter control. Notice that in this simulation case the active power of grid side converter and generator have a similar characteristic during the grid fault. However, the generator power oscillates after fault clearing due to the speed oscillations excited by the fault.

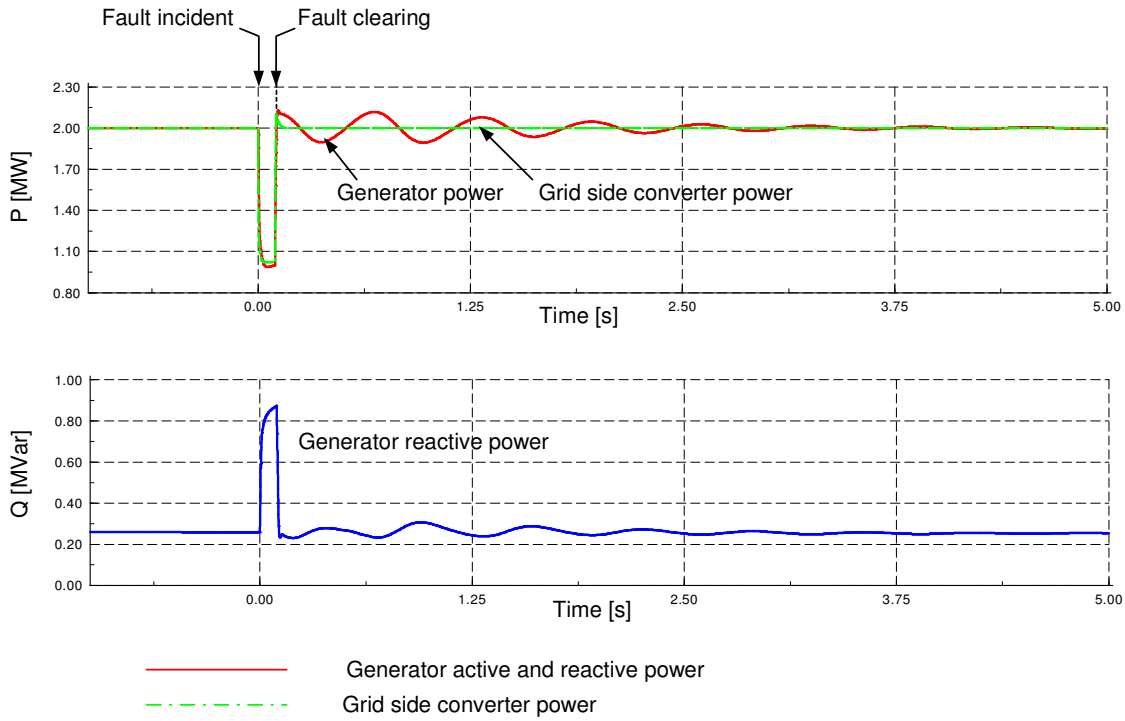

Figure 8.6: Simulation results of the generator's active and reactive power production compared to the grid side converter active power for a three phase short circuit at the high voltage terminal of the PMSG wind turbine, fault duration of 100 ms

8.1.2 Grid fault impact on the mechanical system – simulation case

As mentioned in the previous subsection, the power imbalance caused by the grid fault is transferred through the wind turbine system to the generator. Thus, the mechanical system of the turbine is subjected to fault, too. The same grid fault simulation described in Section 8.1.1 is again considered with focus now on the mechanical aspects. As the mechanical system has larger time constants than the electrical system the fault impact is longer noticeable in the mechanical system and a longer simulation time, i.e. 14 s, is needed. Representative mechanical signals as pitch angle, aerodynamic power, aerodynamic torque and shaft torque as well as the speed are plotted in Figure 8.7.

As a result of the power imbalance between turbine and generator power the generator starts to accelerate and drive train oscillations occur. The oscillations of the drive train are visible in each of the shown signals. The oscillations are damped by means of the damping controller. Depending on the speed oscillations the damping controller adds an oscillating offset signal on the reference of the DC voltage controller and causes volitional variations of the DC voltage, illustrated in Figure 8.4. However, notice that strong speed oscillations imply the risk of too strong DC-voltage variations, which could lead to overvoltages or instability. The control must avoid such critical operation conditions and the DC-link voltage must therefore be limited. This is analysed and discussed in the following Section 8.2.1.

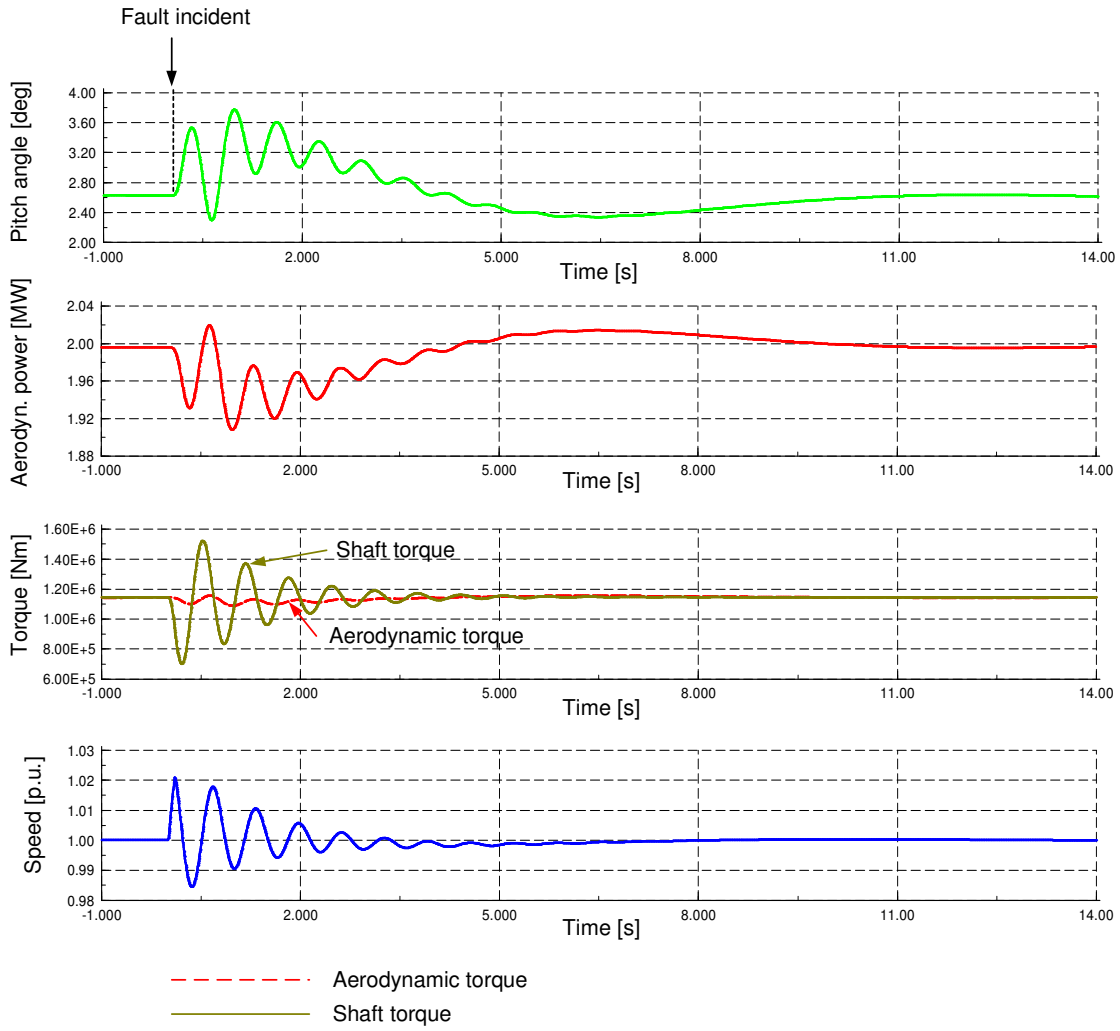

Figure 8.7: Simulation results of the mechanical system: pitch angle, aerodynamics power, aerodynamic torque and shaft torque, speed; for a three phase short circuit at the high voltage terminal of the PMSG wind turbine, fault duration of 100 ms

When acceleration of the drive train is detected, the speed control starts to act on the pitch mechanism. The pitch angle is increased and the aerodynamic power is reduced. In the simulation presented in Figure 8.7, the acceleration of the drive train is less than 2 %, which is due to the large inertia of the rotating masses. According to [Jöckel 2002] a dynamic overspeed of even 25 % in case of grid faults can occur. However, such overspeeds do not denote any mechanical risks for the turbine and generator, but overvoltages in the DC-link as a consequence of generator acceleration must be avoided [Jöckel 2002]. In the simulation case the acceleration stays thus in an acceptable range. This means that no additional control for fault ride-through is necessary and the power surplus can be buffered in the rotational power of the rotating masses.

Due to the drop of generator power during the fault the drive train acts like a torsion spring, which is untwisted. In Figure 8.7 shaft torque and aerodynamic torque acting on both sides of the drive train can be compared. Due to the large inertia of the

aerodynamic rotor the aerodynamic torque oscillates with a much lower amplitude than the shaft torque. Notice, that 5 s after the fault incident the mechanical signals are effectively damped and reach their steady state values.

8.2 Fault ride-through capability

It is concluded from the last section that fault ride-through capability is a minor problem for wind turbines with full-scale frequency converter compared to direct grid-connected generators. Direct grid connected generators imply the risk of excessive short circuit currents, which can lead to damage of power electronic devices or to tripping of turbine relays so that fault ride-through is only possible with extra control efforts and protection devices. This is however not the case for full-scale converter connected wind turbines. The simulation of the previous Subsection 8.1 confirms that the PMSG wind turbine is able to ride-through grid faults without any extra fault control strategy. This is especially due to the alternative control strategy of the PMSG wind turbine, developed in Chapter 7. The specific advantage of this alternative control strategy to accomplish fault ride-through is further emphasized in the following.

Figure 8.8 shows the converter control, which is generally applied to full converter wind turbines with IGBT converter [Akhmatov 2003d], [Deglaire 2005], [Svechkarenko 2005], [Molinas 2005], [Conroy 2007]. DC link voltage and reactive power are controlled by the grid side converter, while active power and stator voltage are controlled by the generator side converter. In contrast to this, Figure 8.9 shows the here applied control strategy. The DC link voltage is instead controlled by the generator side converter while the power is controlled by the grid side converter.

When the control strategy of Figure 8.8 is applied, a grid fault can cause the following conflict. On the one hand, a voltage drop would limit the control capability of the grid side converter, as the voltage level at the grid side converter terminals is low during the fault. This means that the converter limitations are therefore reached faster. On the other hand, grid codes often require reactive power supply during a voltage drop to support the voltage level. This means, that reactive power control has first priority, which again limits the control capability for DC voltage control. Meanwhile, the generator side converter continues to deliver power to the DC-link. Due to this reason, an additional coupling between generator side converter control and grid side converter control must be implemented to reduce the power flow from the generator side converter during the fault [Akhmavtov 2003d].

In case the alternative control strategy presented in Figure 8.9 is applied, no additional control for fault ride-through is necessary. The DC-link voltage can be kept constant during the fault by means of the generator side converter control, which has no limited control capability during the fault. This means, that fault ride-through capa-

bility is already integrated in the implemented control strategy. Notice that such control is only possible if an active rectifier e.g. IGBT converter is used.

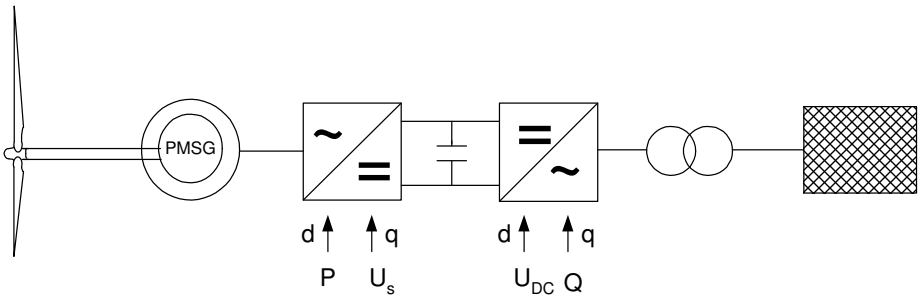

Figure 8.8: Control strategy of the PMSG wind turbine, P and U_s are controlled by the generator side converter control, U_{DC} and Q are controlled by the grid side converter control

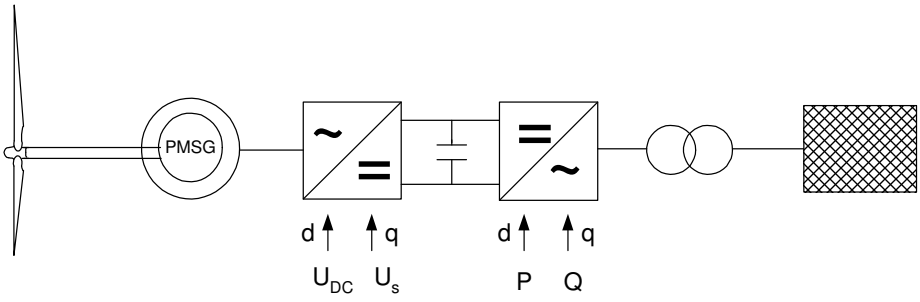

Figure 8.9: Alternative control strategy of the PMSG wind turbine, where U_{DC} and U_s are controlled by the generator side converter control, P and Q are controlled by the grid side converter control

As mentioned before, grid codes generally require voltage support and reactive power supply of the wind turbine during grid faults. For example the E.ON grid code requires that 1 p.u. reactive current is provided for voltage drops below 50 % of the rated value [E.ON 2006]. This means, that the reactive current component of the grid side converter must be prioritized, while the active current component is limited. In the worst case, when maximum reactive current is required, the active current component (d-current) is forced to zero, and then no active power can be fed to the grid during the fault. In this case the power imbalance between the turbine, continuing its power production and the grid side converter transferring no power to the grid, becomes maximum. As a consequence the acceleration and drive train oscillations are largest, too. Due to this reason two additional measures are implemented in the following, which further enhance fault ride-through capability of PMSG wind turbines.

8.2.1 Limitation of U_{DC}

In normal undisturbed operation, the control task of the DC voltage controller is to control the DC voltage to a reference value, which is provided by the damping control-

ler. As explained in Section 7.3.2, the damping controller operates similar to a power system stabilizer in a DC excited synchronous generator of large conventional power plants [Kundur 1994]. The damping controller interacts with the DC voltage controller and adds small DC voltage oscillations to the constant DC voltage reference value. These DC voltage oscillation provoke a generator torque component, which damps the speed oscillations. However, when speed oscillations become too strong under grid faults, large DC voltage variations are provoked, too.

A solution for this conflict is to limit the reference value of the DC voltage in order to avoid too high or too low values of the DC link voltage. The DC voltage must be limited in order to avoid overvoltages causing a damaging risk for the converter or to avoid undervoltages causing instability of the whole generator and converter system. Notice that although the DC voltage reference is limited the operation of the damping controller is not compromised so that the effectiveness of the damping is still guaranteed.

The simulation results, which illustrate the applied measure, are illustrated in Figure 8.10. A fault of 400 ms is applied at the high voltage terminal of the wind turbine (see Figure 8.1) causing a voltage drop down to approximately 20 %. It is assumed that at the fault incident the wind turbine is operating at rated power. In this case the power imbalance and thus the speed oscillations are largest since the turbine operates at maximum power, while the grid side converter active power production is zero. The simulation is shown for 10 s after the fault, until steady state operation is regained. The DC-voltage is limited between 5 kV and 7 kV. In the simulated fault case the speed varies with ±10 % around its rated value, but the DC-voltage is prevented to rise above the limitation so that critical operation conditions are avoided. However, although the DC-voltage is limited a damping effect of the damping controller can be achieved.

If in contrast no DC-voltage limitation is applied, too high or too low DC-voltages occur, leading to instability of the system or to a damage of power electronic components.

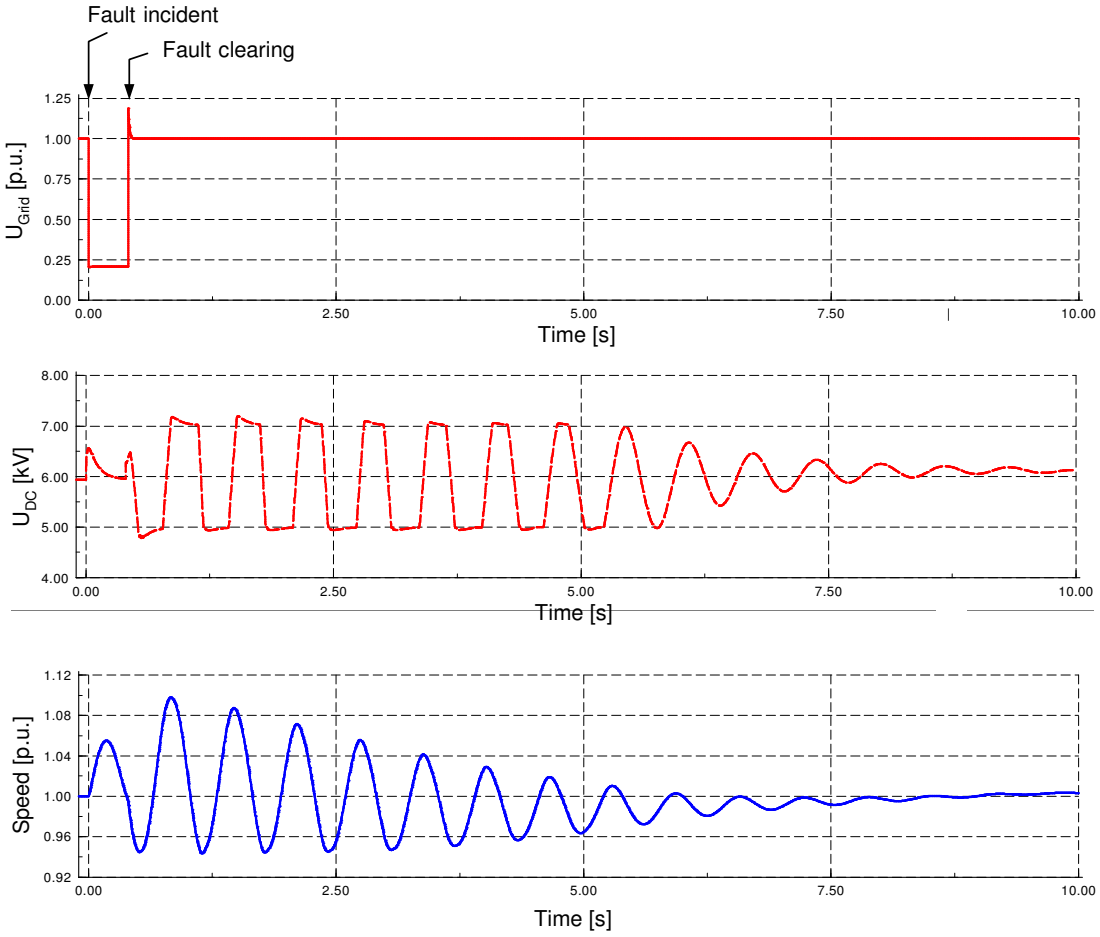

Figure 8.10: Limitation of U_{DC}. Simulation results of grid voltage, DC voltage and speed for a three-phase short circuit at the high voltage terminal of the PMSG wind turbine, fault duration of 400 ms

8.2.2 Chopper

As emphasized in the previous section the developed alternative control strategy of the PMSG wind turbine is very beneficial for fault ride-through and can be accomplished without any extra control setup. However, the implementation of a chopper can enhance the turbine's fault ride-through capability even further. This is due to the following two aspects: (i) When the grid side converter provides reactive power during a fault and it prioritizes the q-component current, the active power is forced to zero and the power imbalance in the turbine system is maximum. (ii) As the power imbalance is transferred to the generator by the control the acceleration and speed oscillations followed by DC voltage variations are maximum, too.

In order to avoid, that the power imbalance is transferred to the generator and to prohibit an acceleration of the generator a chopper can be implemented. As illustrated in Figure 8.11, the chopper is a resistance added parallel to the capacitor in the DC link. The chopper must not be mistaken for a "DC booster" or "step-up converter", which is typically applied to step up the DC voltage behind a passive diode rectifier, as shown in Figure 7.7. The chopper resistance is switched on and off by means of a

power electronic switch e.g. a single transistor with a switching frequency of 500 Hz [Brando 2004]. A chopper, also called braking resistor, is applied in the investigations of [Conroy 2007], [Hennchen 2007], [Akhmatov 2005], too. Here, the action of the chopper is essential as the power surplus inevitably accrues in the DC link, due to different control strategies or due to the use of a passive diode rectifier. However, in the here presented control strategy the chopper is only an additional measure to enhance fault ride-through capability.

When a fault happens and a power surplus in the wind turbine system occurs the DC capacitor is charged and the DC voltage rises. The chopper is switched on, if the DC voltage exceeds a certain level [Hennchen 2007], [Akhmatov 2005], [Conroy 2007]. During the time, when the chopper is switched on, it burns the surplus power so that the capacitor discharges again and the DC link voltage decreases below the threshold. This cycle is repeated with the switching frequency of the chopper. Since the surplus power is burned in the chopper both DC overvoltages and generator acceleration are avoided.

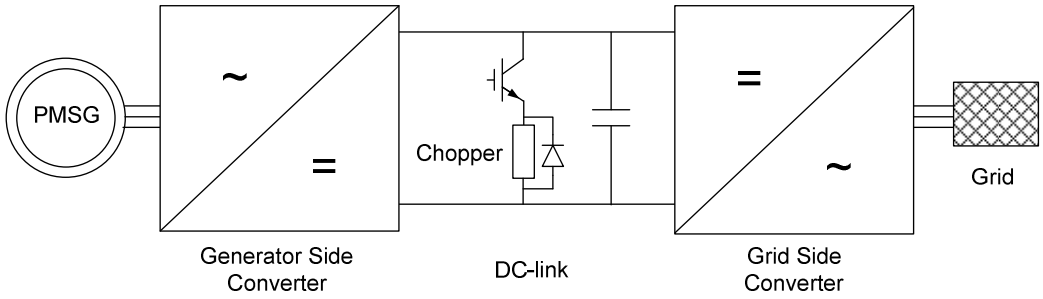

Figure 8.11: Chopper (parallel resistor) added to the DC link

In order to illustrate the effectiveness of the chopper, the same fault as illustrated in Figure 8.10 is applied in the following simulation: a three phase short circuit at the high voltage terminal of the wind turbine with a fault duration of 400 ms. Figure 8.12 and Figure 8.13 depict the performance of the chopper action. In Figure 8.12 a) the DC-voltage is plotted. The signal is shown for the two cases: with and without action of the chopper. In addition to that, Figure 8.12 b) shows a zoom of the DC-voltage signal for 600 ms after the fault. As soon as the DC-voltage rises above a certain threshold value the chopper is triggered. Due to the high frequent switching cycle of the chopper the DC-capacitor charges and discharges with the same frequency, which is visible in the DC-voltage signal (Figure 8.12 b). When the fault is cleared the chopper switching action is disabled. When the speed oscillations are damped, the DC-voltage reaches its pre-fault reference value. In contrast to the case without action of the chopper the DC-voltage signal is significantly damped.

The simulation results of grid voltage, generator power and speed are illustrated in Figure 8.13. The signals are again plotted for two cases: with and without action of

the chopper. The grid voltage has precisely the same characteristic for both cases, which proves that the action of the chopper does not affect the signals of the grid and the grid side converter, respectively. Without chopper the generator side converter control assures constant DC-voltage but transfers the power imbalance to the generator. This is visible in Figure 8.13, as the generator power drops. In this case the generator speed starts to oscillate. When however the chopper is applied to the system, the generator can continue the power production, as indicated by the power signal (red-solid line). This prevents in turn an acceleration of the generator and speed oscillation can be avoided. As the speed oscillations are prevented the influence of the damping controller on the DC voltage is substantially reduced. Besides this, the stress on the mechanical system can also be drastically reduced. The chopper reduces thus effectively the grid fault impact on the generator and on the turbine system and enhances even more the PMSG wind turbine's fault ride-through capability.

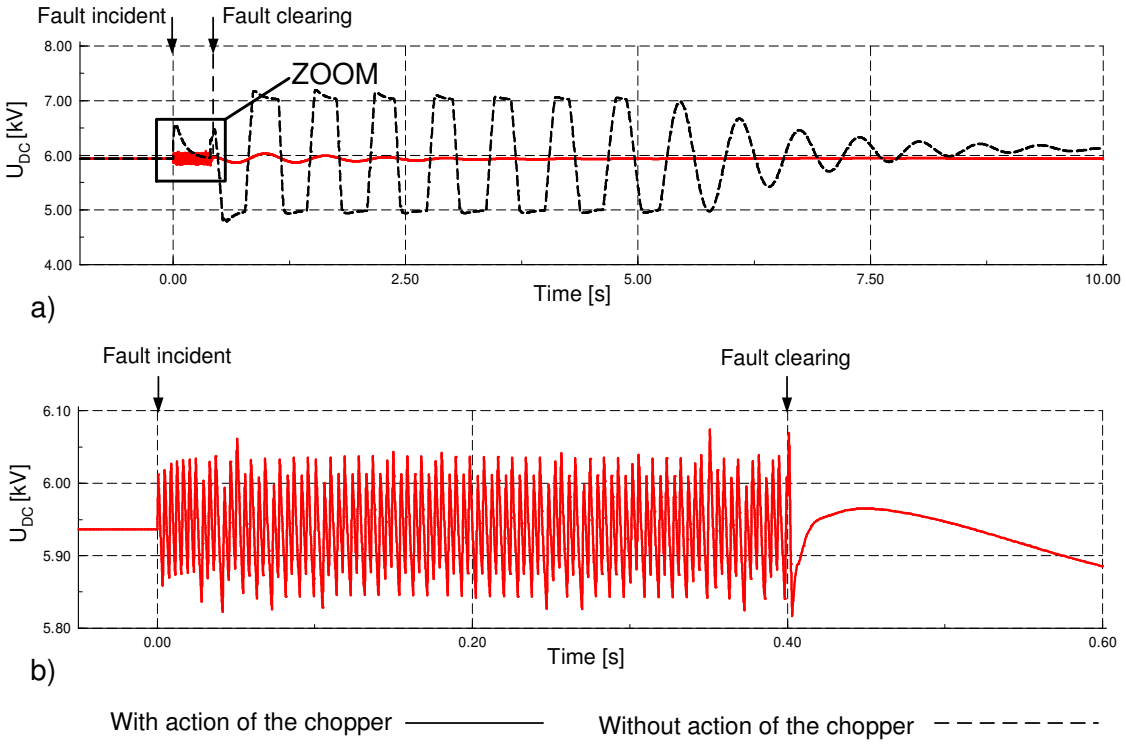

Figure 8.12: Simulation results DC voltage for a three-phase short circuit at the high voltage terminal of the PMSG wind turbine, fault duration of 400 ms

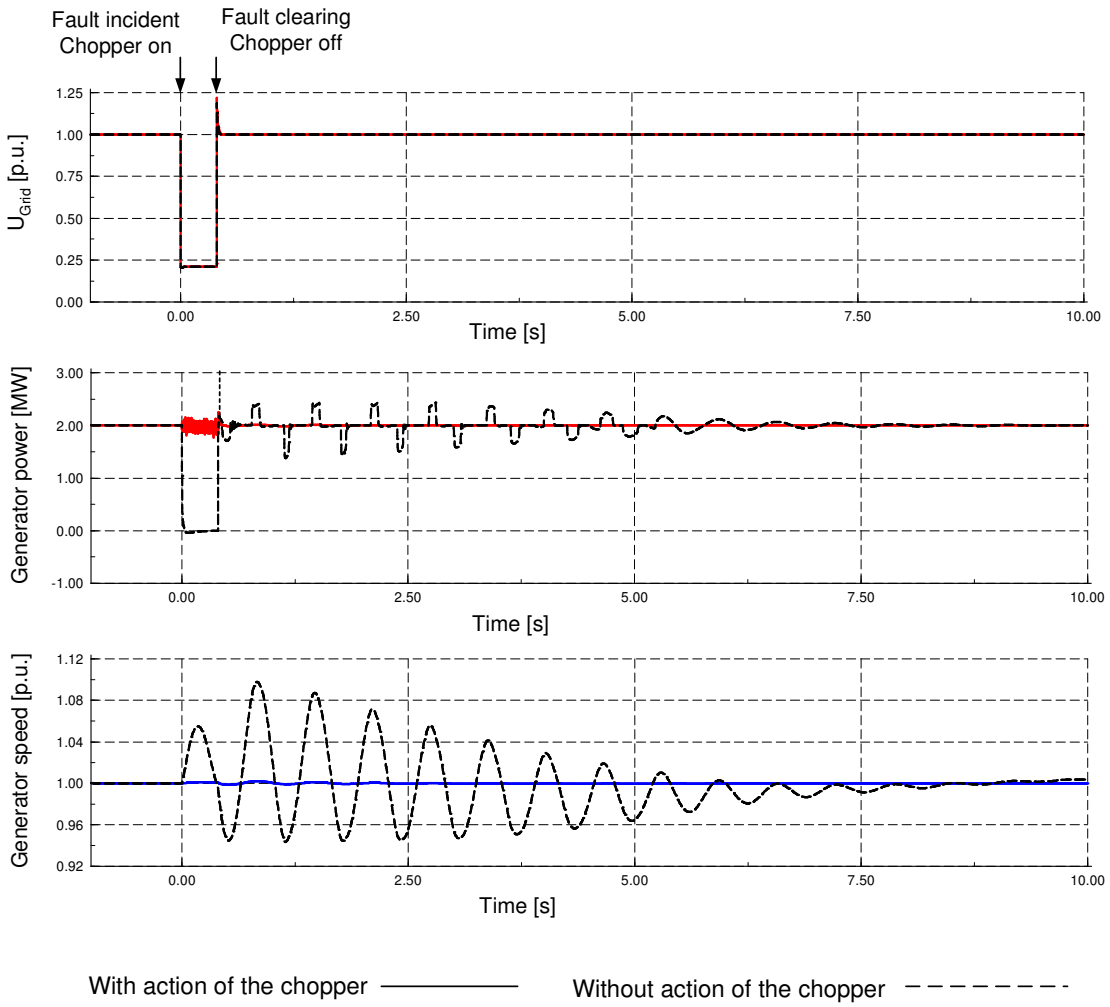

Figure 8.13: Simulation results of pitch angle, aerodynamic power, shaft torque and speed for a three phase short circuit at the high voltage terminal of the PMSG wind turbine, fault duration of 400 ms, for two cases: with and without action of the chopper

8.3 Voltage control capability

Additional to fault ride-through grid codes require reactive power supply. Due to the presence of the full-scale frequency converter system in the considered PMSG wind turbine configuration, reactive power supply can be realized by the grid side converter independently of the operational point of the generator. This is a significant difference to the DFIG wind turbine and to other wind turbine concepts with direct grid connected generator. The amount of reactive power supply is then only limited by the grid side converter rating:

$$Q_{Conv} = \sqrt{S_{Conv}^2 - P_{Conv}^2} \tag{8.2}$$

The IGBT converter of the PMSG wind turbine, applied in the present model, is designed for 2.5 MVA apparent power. The converter is slightly oversized in order to enhance the voltage control capability of the turbine.

In order to accomplish voltage support, a voltage controller is added to the grid side converter control, as illustrated in Figure 8.14. A voltage controller is implemented in cascade to the inner reactive power control loop and the converter current control loop. Dependent on the difference between the measured grid voltage and the reference voltage the voltage controller demands the grid side converter controller to provide or to consume reactive power in order re-establish the grid voltage level.

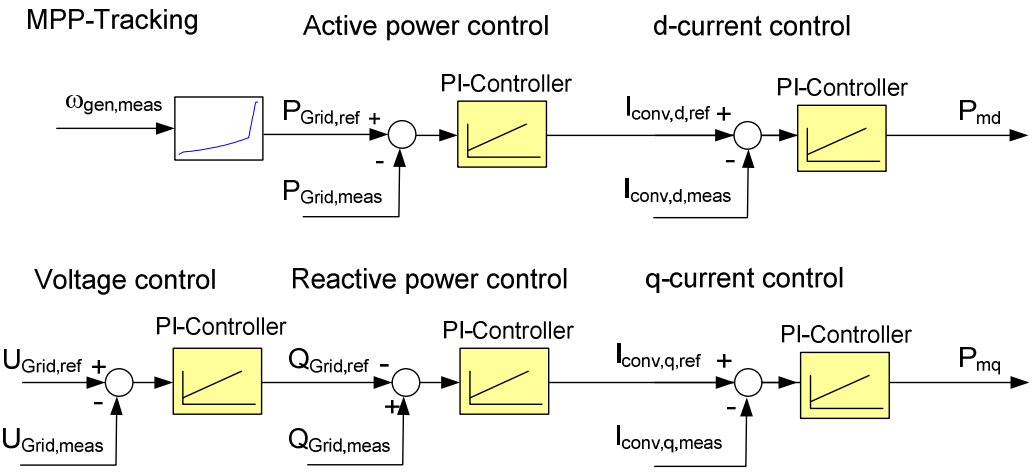

Figure 8.14: Voltage controller applied to the grid side converter control of the PMSG wind turbine

The action of the voltage controller is exemplified in Figure 8.15 by connecting e.g. an inductive load of 1.5 MVar reactive power demand for 1 s to the point of common coupling (PCC) of the wind turbine system. Two simulation cases are compared: with and without voltage controller, respectively.

The inductive load coupling causes a reactive power imbalance and therefore the voltage drops down to a level of approximately 85 %. When the voltage controller is disabled no additional reactive power is the supplied to the grid and the voltage stays at the lower level as long as the inductive load is connected. The active power can still be controlled to its reference value. After the inductive load is disconnected the voltage level recovers.

When the voltage controller is active the converter starts to supply reactive power as soon as the inductive load is connected. Due to the converter rating of 2.5 MVA the converter can provide up to 1.5 MVar reactive power without active power reduction. The voltage level can immediately be re-established to its reference value. When the inductive load is disconnected after 1 s the controller reduces the reactive power supply to its original value.

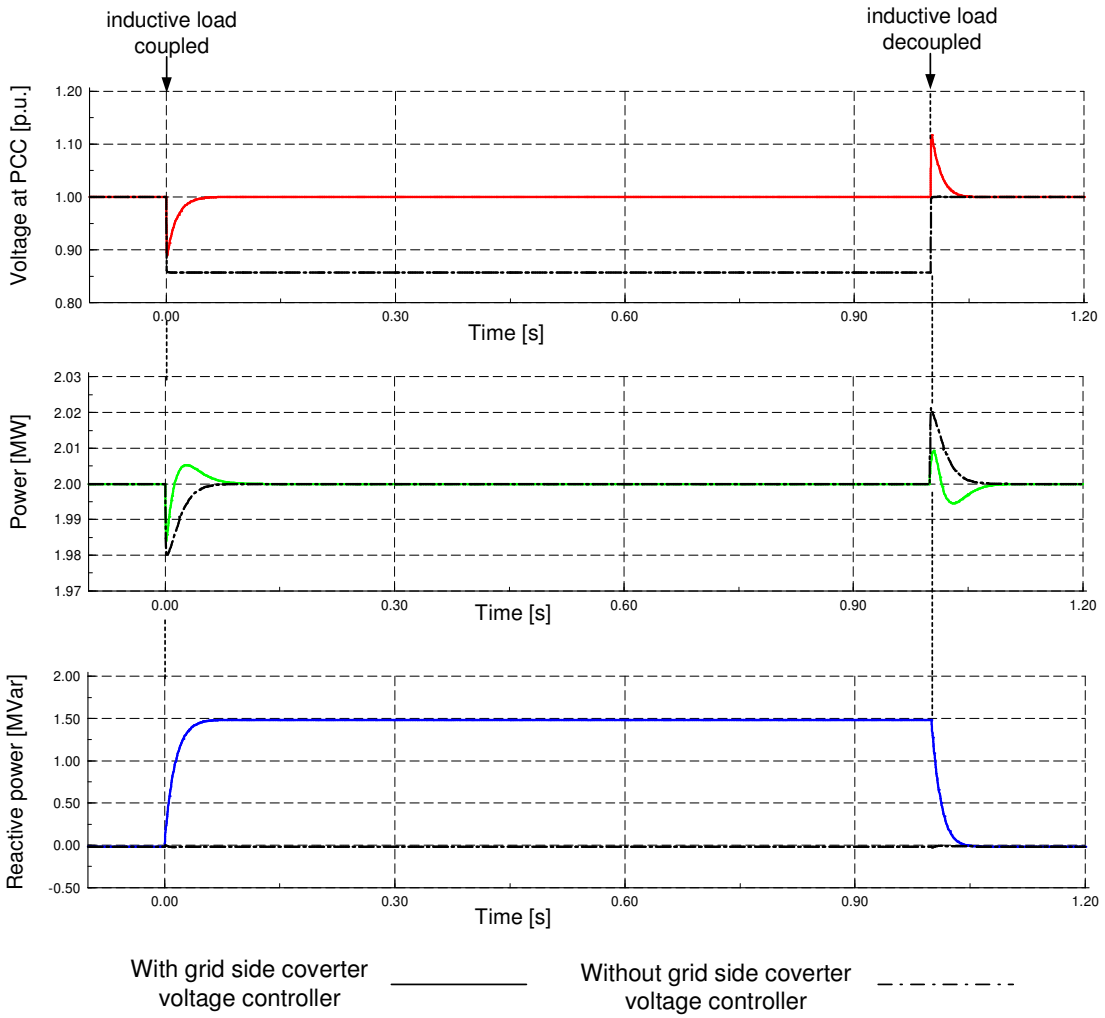

Figure 8.15: Simulation results of the PMSG generator when an inductive load is connected to the HV terminal, voltage at the HV terminal, active and reactive power production for the cases with and without voltage control of the PMSG

In a second study, the voltage control capability of PMSG wind turbines during grid faults is investigated. The same grid fault as in Figure 8.3 is simulated. The fault happens at the high voltage terminal of the wind turbine and lasts for 100 ms (see Figure 8.1). In Figure 8.16, again two cases can be compared: Case I shows the simulations results without voltage controller, which are the same as in Figure 8.3. In contrast to this, case II shows the signals when the voltage controller is active.

When the voltage controller is active the voltage level can be significantly improved during the fault. This is due to the reactive power supply of the wind turbine. In order to provide maximum reactive power during the fault, as required e.g. by the E.ON grid code [E.ON 2006], the reactive power production is prioritized over active power production. Therefore, the active power is forced to zero during the fault and the range for reactive power supply is maximized. However, due to the reduced voltage level, the reactive power reference, reaching its limitation of 2 MVar as a consequence of the large voltage droop, cannot be achieved. Nevertheless, the supply of reactive

power increases the voltage level from 40 % without voltage controller to approx. 65 % with voltage controller. This approves the effectiveness of the developed control strategy. The implemented voltage controller enables thus the PMSG wind turbine to actively support the grid during grid faults. The voltage control capability and the grid support of PMSG wind turbines is assessed to be better than for other wind turbine concepts.

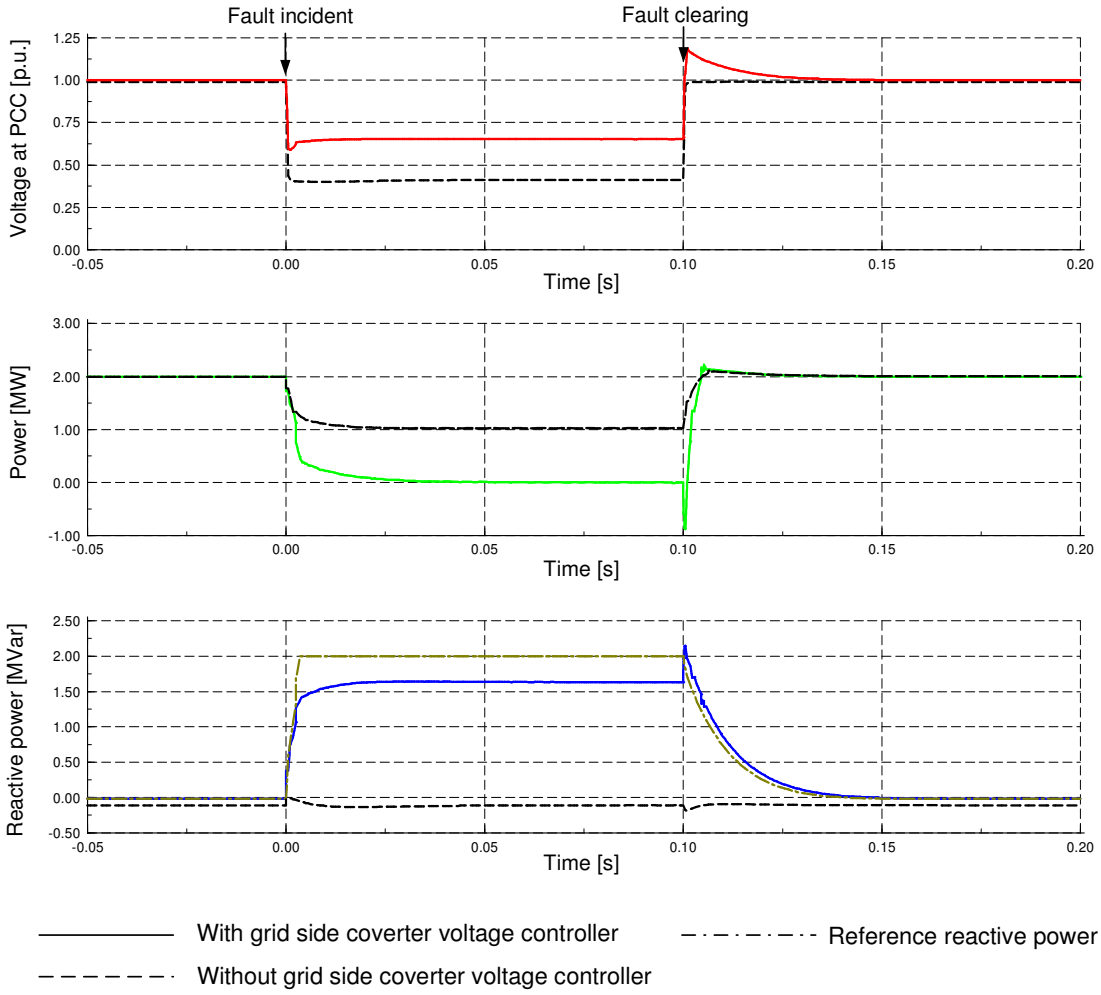

Figure 8.16: Simulation results of the PMSG wind turbine under a 100 ms three-phase short circuit, voltage at the HV terminal, active and reactive power production for the cases with and without voltage support of the PMSG

An overview over the total control structure of the PMSG wind turbine for normal operation conditions and for grid faults is given in the appendix, Section 12.9

8.4 Case studies

This subsection presents illustrates and discusses the PMSG wind turbine's compliance with grid code specifications in the same manner as it was carried out for the DFIG wind turbine in Chapter 6.4.

Two case studies are performed, simulating the E.ON and the Energinet.dk grid code requirements, presented in Chapter 2.3. The PMSG wind turbine model is connected to the Thevenin equivalent specified by the Energinet.dk grid code and illustrated in Figure 2.4. Both the voltage profiles of the E.ON and Energinet.dk grid code are applied to the voltage source of the Thevenin equivalent. Focus of the presented case study is the fault ride-through and voltage support capability of PMSG wind turbines.

8.4.1 Compliance of PMSG wind turbines with E.ON grid code

The E.ON grid code specifications were presented in Section 2.3. The voltage profile, which is applied to the voltage source shown in Figure 2.4, represents the border line above which fault ride-through must be accomplished. The voltage profile is illustrated in the uppermost plot of Figure 8.14. Furthermore, specific turbine quantities such as active and reactive power production and the reactive current supply of the PMSG wind turbine, which is subjected to the voltage drop, are also illustrated in Figure 8.14. The reference values of active and reactive power control are plotted as well.

The voltage profile represents a voltage drop down to zero lasting for 150 ms. The voltage is then ramped up to 0.9 p.u. at 1.5 s and recovers completely to its rated value of 1 p.u. According to the E.ON grid code voltage control, i.e. reactive current injection must be provided during the voltage dip. As the PMSG wind turbine is connected via a full-scale frequency converter the control is able to provide maximum reactive current to the grid. As explained in the previous Section 8.3 reactive power supply is then prioritized over active power production. The active power is reduced to zero and the surplus power of the turbine is burned in the chopper. The reactive current is increased immediately after the fault incident and is provided within the required 20 ms rise time, required by E.ON. Due to the reduced voltage level the reactive power contribution is also lessened. Nevertheless, the voltage at the wind turbine's connection point (PCC) is improved compared to the applied voltage profile. When the voltage has recovered so far, that the turbine can provide the reactive power reference of 2 MVar, the reactive current goes out of the limitation. As the voltage level is then above 50 % the grid code requires less than 1 p.u. reactive current. The active power can then be increased back to its reference. After the voltage has totally recovered the pre-fault steady state is regained.

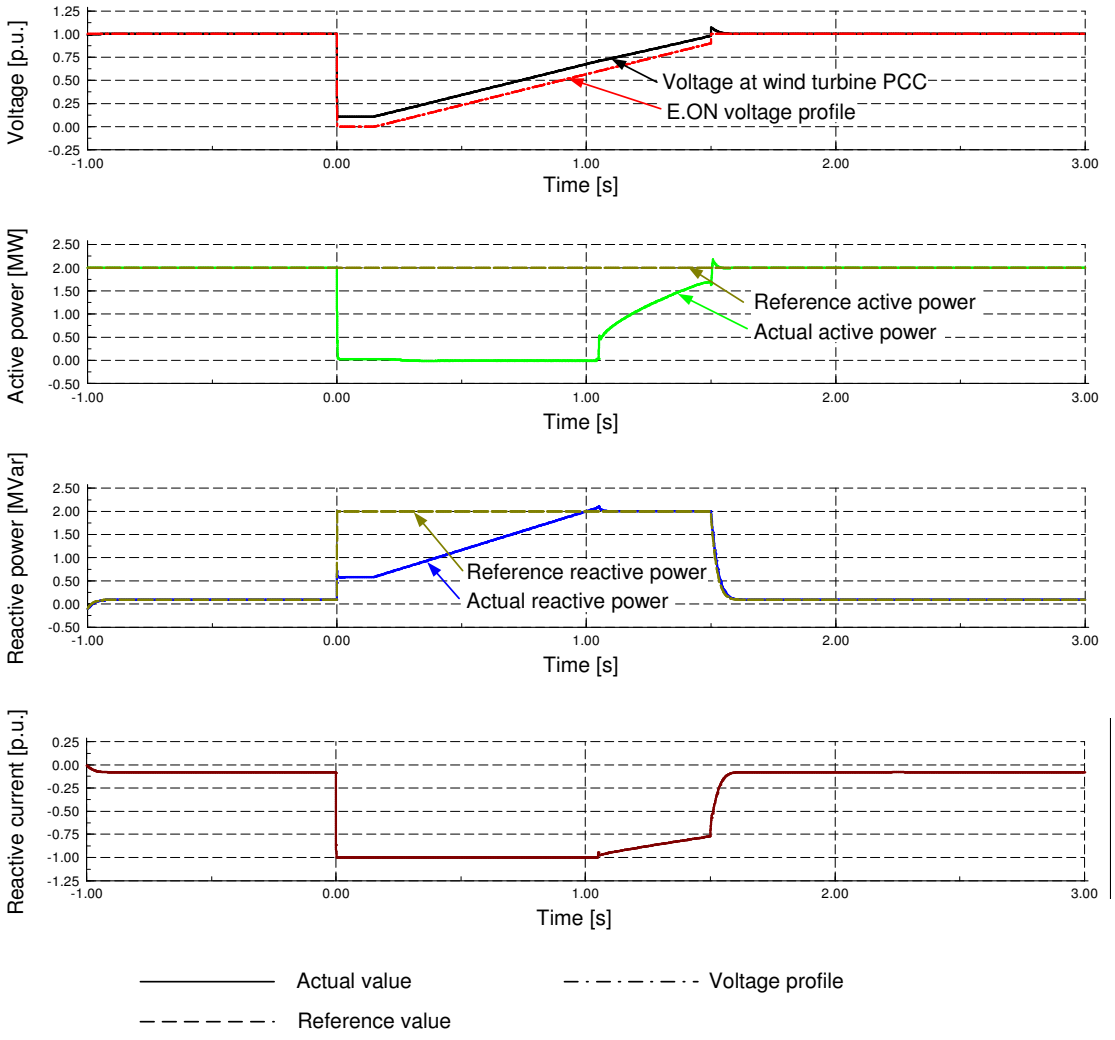

Figure 8.17: Voltage profile for fault ride-through of the E.ON grid code applied to a PMSG wind turbine: Voltage profile and voltage at PCC, active and reactive power production, reactive current supply of the PMSG wind turbine

It can be concluded that the PMSG wind turbine with full-scale frequency converter can ride-through grid faults and also complies with the reactive power supply requirements of the E.ON grid code. This means that in terms of E.ON grid code accomplishment the PMSG shows a better performance than the DFIG wind turbine, which was illustrated in Figure 6.16.

8.4.2 Compliance of PMSG wind turbines with Energinet.dk grid code

For comparison the following figure shows the simulation results achieved, when the Energinet.dk grid code is applied to the PMSG wind turbine model. The voltage profile defined by Energinet.dk is slightly different: The voltage drops down to only 25 % of its rated value for 100 ms and recovers then slowly up to 0.75 p.u. at 750 ms. The voltage level stays at 0.75 p.u. until 10 s after the fault incident, when the voltage totally recovers. In Figure 8.18 the turbine quantities, i.e. the voltage at the wind tur-

bine's PCC, its active and reactive power production together with the active and reactive power reference and the reactive current supplied by the grid side converter, are plotted for 12.5 s after the fault incident. The voltage profile is illustrated in the first plot, too.

According to the Energinet.dk grid code, active power production is required as specified in equation (2.1). The active power signal follows this reference. Due to the larger converter rating the grid side converter of the PMSG is able to provide reactive power in parallel. The reactive current is immediately increased and after a small rise time 2 MVar reactive power can be provided during the fault. The voltage level at the PCC can thus be improved.

The PMSG wind turbine is able to ride-through the applied grid fault and complies with the grid code requirements introduced by Energinet.dk.

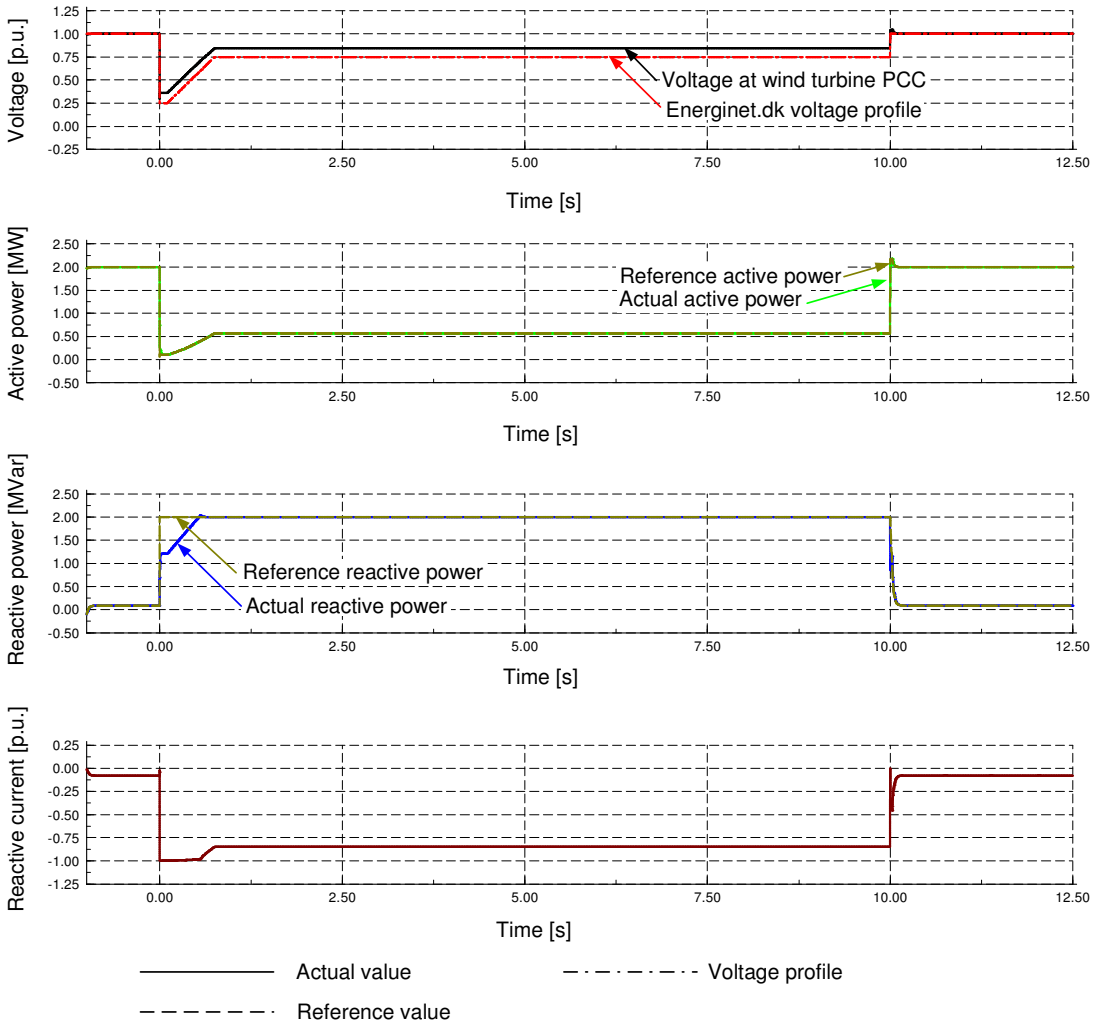

Figure 8.18: Voltage profile for fault ride-through of the Energienet.dk grid code applied to a PMSG wind turbine: Voltage profile and voltage at PCC, active and reactive power production, reactive current supply of the PMSG wind turbine

8.5 Summary

This chapter presents a control strategy of permanent magnet generator wind turbines, which enables the turbines to accomplish fault ride-through and to provide grid support during grid faults.

In a first step the dynamic behaviour of PMSG wind turbines is analysed. The impact of the grid fault on both the electrical and mechanical system of the turbine is investigated. As result of this analysis it turns out that the developed control strategy of the frequency converter is assessed to be very beneficial for fault ride-through. The DC-voltage is controlled by the generator side converter instead of the grid side converter. As the generator side converter is not coupled to the grid its control capability is not compromised during grid faults. With such control strategy the wind turbine is therefore able to ride-through faults even without any additional measures. This fact is an unique outcome of the present work and stands out against the findings of other research works.

Nevertheless, a chopper is applied to the system, in order to enhance the fault ride-through capability further. A voltage controller is also added to the grid side converter control of the PMSG wind turbine to provide reactive power supply in case of grid faults.

Simulation results in DIgSILENT Power Factory exemplify how PMSG wind farms with such control strategy participate to re-establish the voltage during grid faults. Due to the implemented control strategy the PMSG wind turbine is able to ride-through the applied grid faults and complies with grid code requirements introduced e.g. by E.ON or Energinet.dk.

9 DFIG and PMSG wind farm's impact on the power system

In the next years, wind power penetration will increase even more, which is especially due to planned installation of large offshore wind farms. Today the largest offshore wind farms with total power of up to 160 MW are installed in the North Sea and in the Baltic Sea belonging to different countries like Denmark, Great Britain and the Netherlands, e.g. the wind farms Horns Rev with 160 MW and Nysted with 158 MW in Denmark, the wind farm Kentish Flats with 90 MW in the UK or the Dutch wind farm Egmond aan Zee with 108 MW [BWEA 2007]. In Germany the first offshore project will be installed in 2008 [alpha ventus 2007]: 12 variable speed wind turbines with a power of 5 MW each will be erected in the German North Sea consisting of six DFIG wind turbines and six PMSG wind turbines, representing exactly the wind turbine concepts investigated in the present work.

Wind power, installed in such large units and consequently connected to the power transmission system, will gain a significant impact on the power system in terms of power system operation and power system stability. Wind farms are therefore required to actively support the grid, similar as conventional power plants. Focus of the present chapter is to investigate the power system impact and to verify the grid support capability of such large variable speed wind farms connected to the power system.

In the following the interaction between variable speed wind farms consisting of DFIG wind turbines or PMSG wind turbines and the power system is simulated and analysed in different case study scenarios. The considered wind farms are modelled based on the simulation models of the single wind turbines and their respective control strategies for grid support presented in the report. A power system model is used representing a generic but realistic re-scaled power system. The power system model and its components will be presented first.

9.1 Generic power transmission system model

In order to investigate the impact of large offshore wind farms on the power system, a realistic power transmission system model is required, in which voltage and frequency are not fixed to their rated values, but may be subject to fluctuations, when the power system is subjected to disturbances [Hansen 2007a]. Such a realistic model for the power transmission system is usually not easily disposable, as it is generally very complex and contains a large amount of confidential data, so that it cannot be provided by the transmission system operator. However, the Danish Transmission System Operator Energienet.dk has noted this aspect and therefore developed a small test model for the power transmission system [Akhmatov 2006b], [Akhmatov 2006c], especially

for education and research purposes. This test model is a re-scaled model of a power transmission grid, but still realistic in order to investigate the interaction between the transmission system and grid connected wind turbines in case of grid faults.

The power system model is implemented in the simulation tool DIgSILENT Power Factory and produces a realistic output when the response of a whole wind farm has to be evaluated. The simplified structure of the test model is presented in Figure 9.1. A detailed representation of the power system model can be found in [Akhmatov 2006b], [Akhmatov 2006c] and is sketched in the appendix in Section 12.10. The model was provided courtesy by the Danish transmission system operator Energinet.dk. However, the model is slightly modified for the here presented studies.

The grid model contains busbars with voltages from 0.7 kV to 400 kV, four central power plants with their control, several consumption centres, a lumped equivalent for local on-land wind turbines and a model for a 165 MW offshore wind farm, connected through a sea cable to the transmission grid at a voltage of 135 kV. The central power plants are synchronous generators with primary voltage control. The model can be easily extended with frequency controllers, but as the attention in the present work is drawn to voltage stability issues, the frequency stability in the system is assured by large generator inertia. As illustrated in Figure 9.1, the power system model is extended by a new 160 MW wind farm for different case studies. The new wind farm is a variable speed wind farm consisting of either DFIG of PMSG wind turbines.

The on-land local wind turbines are fixed-speed stall controlled wind turbines with conventional technology equipped with no-load compensated induction generators (Danish Concept). The local wind turbines illustrated in Figure 9.1 are old land-based wind turbines without any ride-through control implemented and they are therefore disconnected from the system by the protection system, to avoid over-speeding, in case of a grid fault [Hansen 2007a]. The local wind turbines are aggregated in a lumped model representing all local wind turbines spread in the system with a total power capacity of 500 MW.

The 165 MW offshore wind farm is modelled as active stall controlled wind turbines with induction generators, similar to the Danish offshore wind farm Nysted. The offshore wind farm is modelled based on aggregation technique using a one-machine approach [Akhmatov 2002b]. The wind turbine model contains models for the drive train, generator, transformer and the control, as described in detail in [Akhmatov 2006b]. As required in several grid codes [E.ON 2006], [Energinet.dk 2004], large wind farms connected to the transmission system have to be able to withstand grid faults without being disconnected in cases where the clearance of the fault does not isolate the wind farm. This is normally the case when the grid fault happens in the transmission system. Contrarily to the local wind turbines, the active stall offshore wind farm, illustrated in Figure 9.1, is equipped with a fault ride-through control for active stall wind farms. In case of a severe voltage drop, the active power production is

reduced by blade pitching to avoid uncontrolled over-speeding. The reduction of the active power production implies that the reactive power absorption is reduced, too (a "passive" reactive power control). Such power reduction control has a positive effect contributing to a better stabilisation of the wind farm, but does not participate actively in the voltage control of the system [Hansen 2007b].

Both, local wind turbines and active stall wind farm are operating at 60 % wind, which denotes that their active power production is 60 % of their rated power given in Figure 9.1 [Akhmatov 2006b]. The original power system model provided by Energinet.dk and described in [Akhmatov 2006b] comprises furthermore a Static Var Compensation (SVC) unit, to improve the voltage profile at the connection point of the active stall offshore wind farm. This SVC unit is however disabled in this study in order to verify the voltage support capability of the new variable speed wind farm connected in vicinity to the active stall wind farm.

The point of common coupling (PCC) of the connected wind turbines in the considered power system represents a very "weak" connection point. According to [Kundur 1994] the interaction between the grid and the new connected units, in this case all wind power units connected to the PCC, depends on the strength of the AC system relative to the capacity of the connected units. The short circuit ratio SCR in the PCC, as a measure to define the system strength can be computed according to [Kundur 1994]:

$$SCR = \frac{short\ circuit\ MVA\ of\ ac\ system}{wind\ power\ MW\ rating} \tag{9.1}$$

The short circuit MVA of the AC system in the PCC amounts to approximately 1570 MVA. With the MW rating of the connected wind power, the short circuit ratio is:

$$SCR_{PCC} = \frac{1571MVA}{(500MW + 165MW + 160MW)} = 1.9 \tag{9.2}$$

According to the classification of power system strength given in [Kundur 1994], the AC system strength is low, if the short circuit ratio is less than 3.

Moreover, the overhead lines connecting the PCC busbar to the rest of the grid have a very high inductance, which weakens the power system, too. The *R/X* ratio in the PCC amounts to 0.14, which corresponds to a phase angle of 82.02 deg. The *R/X* value, another parameter for system strength, confirms, that the power system is relatively weak and grid support by variable speed wind farms becomes especially impor-

tant. The study cases, performed in the following can therefore also be understood as "worst-case" scenarios.

Nevertheless, the chosen configuration represents a realistic case for future power grids. At the moment, most local wind turbines are installed in costal areas at the margin of the large network system, i.e. in a local weak power system. Moreover, it must be expected that new installed offshore wind farms will in the first place be connected to the same weak onshore connection points causing high power system control challenges in terms of stable operation. This case is exactly represented with the chosen configuration of the power system model so that the presented case studies can provide relevant conclusions for future power system operation.

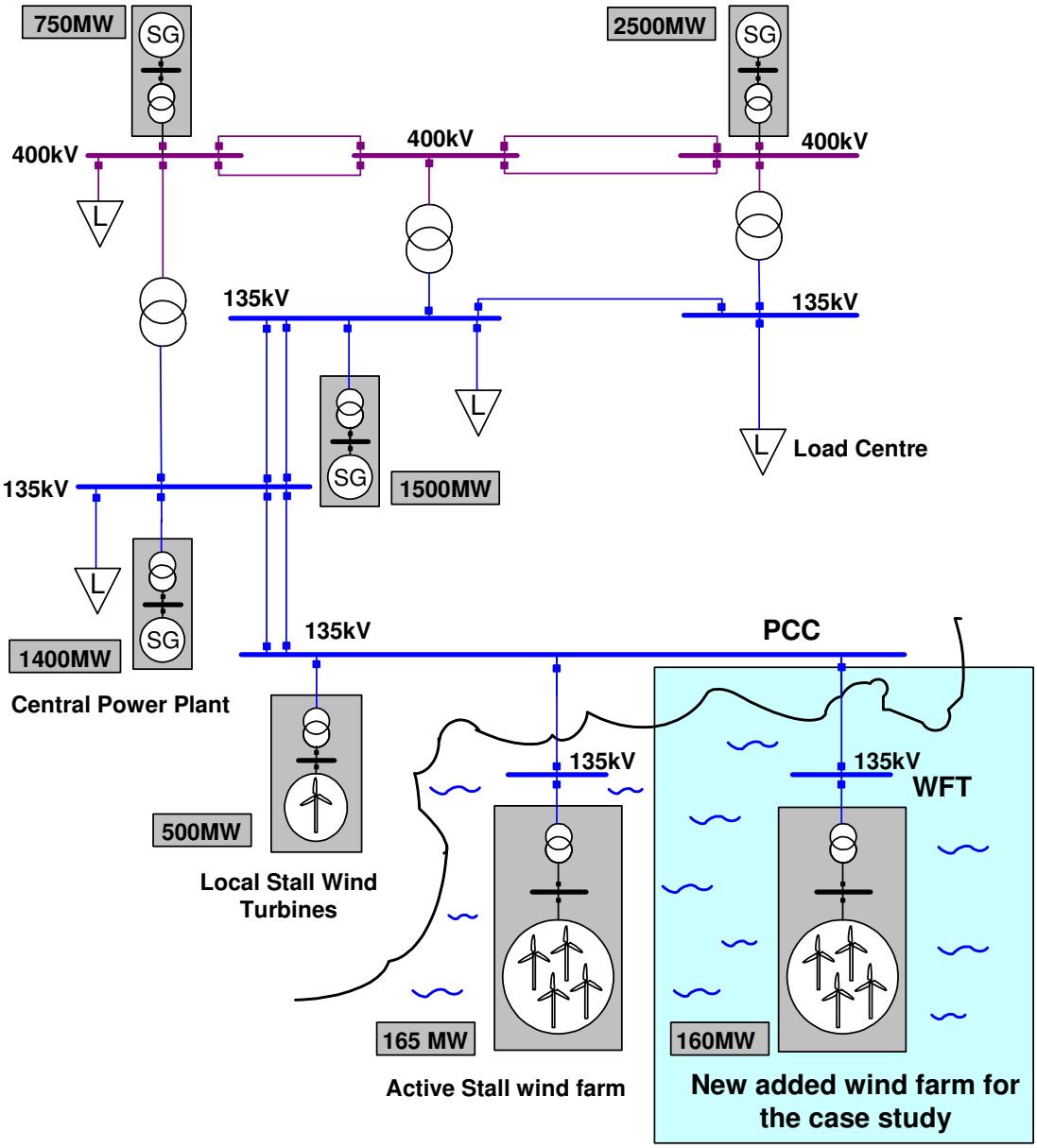

Figure 9.1: Power transmission system test model

Aggregation model of a variable speed wind farm added for case studies

The test model for the power transmission system in its original form, as described in [Akhmatov 2006b], is used for the following case studies as basis for extension. As illustrated in Figure 9.1, the test model is extended by adding a new offshore wind farm, made up exclusively of variable speed wind turbines with either DFIG or PMSG generator technology. The new wind farm model is connected to the transmission system at a 135 kV busbar through an offshore line just like in the connection case of the offshore active stall wind farm. The wind farm model consist of 80 2 MW wind turbines, in which all wind turbines are combined to an aggregated model. The aggregation method reduces the complexity and simulation time without compromising the accuracy of the simulation results [Pöller 2003] and is thus commonly used for system studies concerning the impact of large wind farms on the power system. The 80 turbines are aggregated to one equivalent lumped wind turbine with re-scaled power capacity according to the entire wind farm power. DIgSILENT Power Factory provides a built-in aggregation technique for the electrical system. The generator and the transformer can be directly modelled by a certain number of parallel machines, while the other components, as e.g. the frequency converter or the mechanical power of the turbine rotor have to be up-scaled according to the wind farm power. This method is adapted for both wind farms types, i.e. a DFIG wind farm as well as a PMSG wind farm, used in the following case studies. Both wind farms are each equipped with the respective control strategy for fault ride-through and grid support presented previously in this work.

9.2 Case study scenarios

In order to investigate and evaluate the interaction between large wind farms based on variable speed wind turbines and the power transmission system different case studies are carried out in the following. The case studies serve to assess and verify the developed control strategies for DFIG and PMSG wind turbines, respectively and their ability to support the grid in case of grid faults. Focus will especially be on the interaction between the variable speed wind farm and the conventional stall and active stall wind turbines connected in vicinity to the variable speed wind farm [Michalke 2007c], [Michalke 2007d], [Hansen 2007b], [Hansen 2007e].

Two simulation cases are performed for each wind turbine concept: Case I (DFIG wind farm) and II (PMSG wind farm) consider the variable speed wind farm interacting with the active stall wind farm and Case III (DFIG wind farm) and Case IV (PMSG wind farm) consider the variable speed wind farm interacting with the local wind turbines.

9.2.1 Case study I: DFIG wind farm and active stall wind farm

Case study I investigates the DFIG wind farm's impact on the power system [Hansen 2007a] when it is connected in vicinity to the 165 MW active stall wind farm. The power system used for this case study is again illustrated in Figure 9.2. It is assumed that the DFIG wind farm operates at its rated capacity, as this is the worst case for voltage stability. The stall wind turbines and the active stall wind farm operate at 60 % of their rated power. A severe 3-phase short circuit grid fault is considered to happen in the transmission grid at the end of an overhead line close to the wind farm's point of common coupling (PCC) – see Figure 9.2. The grid fault lasts for 100 ms and gets cleared by permanent isolation (tripping the relays) of the faulty line. Note that, by tripping of the line, the power system becomes weaker (higher impedance) and some components (e.g. the adjacent overhead line) are fully loaded. In the moment of the grid fault, it is assumed that the on-land wind turbines are disconnected from the system by their protection system. The frequency stability in the grid, in the moment of the on-land wind turbines disconnections, is assured by large generator inertia. In the following simulations the effect of the DFIG voltage control both on the power system's voltage stability and on the performance of a nearby active stall wind farm during the grid fault are illustrated.

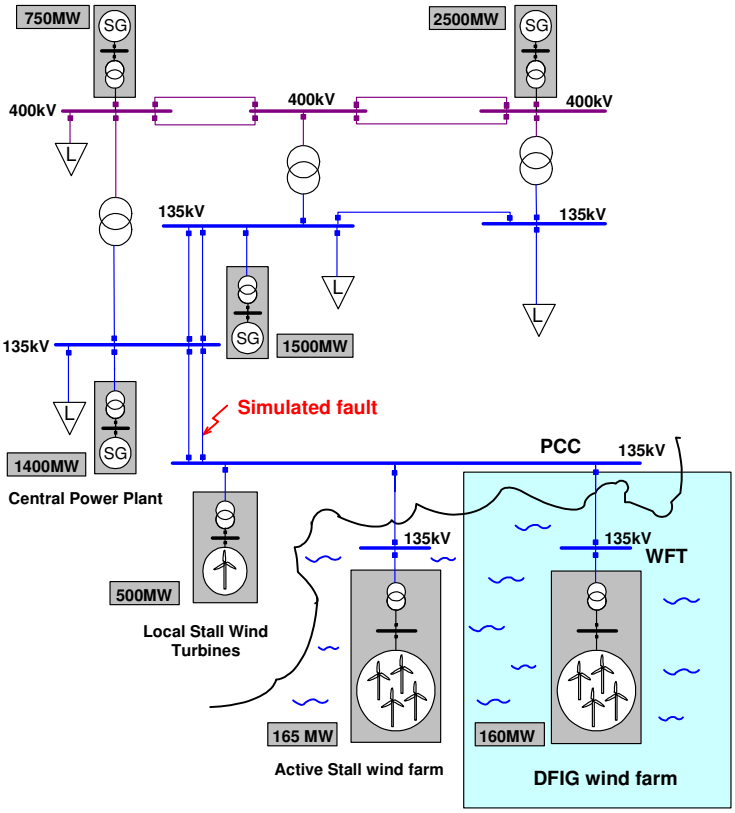

Figure 9.2: Power system model used for case study I

The voltage drop occurs at the grid fault instant. Immediately after the fault, when the DFIG´s rotor current magnitude is above the current protection limitation, the crowbar protection system of the DFIG is triggered, the rotor is short-circuited, and the rotor side converter is blocked. When the fault is cleared and the DFIG wind farm terminal voltage recovers to a certain value, the crowbar protection is disabled and the rotor side converter is restarted. Figure 9.3 illustrates the voltage, the active and the reactive power of the DFIG wind farm in the wind farm terminal (WFT), for two situations:

1. The DFIG is not equipped with voltage control capability. The turbine maintains a power factor of 1.
2. The DFIG is equipped with voltage control capability.

As mentioned before, the nearby connected active stall wind farm is typically equipped with a power reduction control for fault ride-through. For the simulations shown in Figure 9.3 this power reduction control is disabled in order to achieve the worst case for voltage stability.

As expected, in situation 2 the influence of voltage control is visible both during the fault, when the grid side converter supplies reactive power, and after the disconnection of the crowbar, when the rotor side converter controls the voltage. When no voltage control is enabled, the grid voltage oscillates and stabilizes to a higher voltage level after the fault is cleared. This can be explained both by the reactive power surplus existent in the system as result of the on-land wind turbines disconnection and by the fact that, as result of the line tripping, the transport of the active power from the wind farms to the grid is done through a higher resistance transmission line. Figure 9.3 shows that the existing reactive power surplus in the system is absorbed by the DFIG, when the voltage control is enabled. Note that the DFIG voltage control re-establishes the grid voltage to 1 p.u. very quickly without any fluctuations. No significant effect of the voltage control appears on the active power production. However, there is a slight improvement in active power when voltage control is used. The small "drops" in the power, visible in both cases just after the fault is cleared, correspond to the damped torsional oscillations in the generator speed.

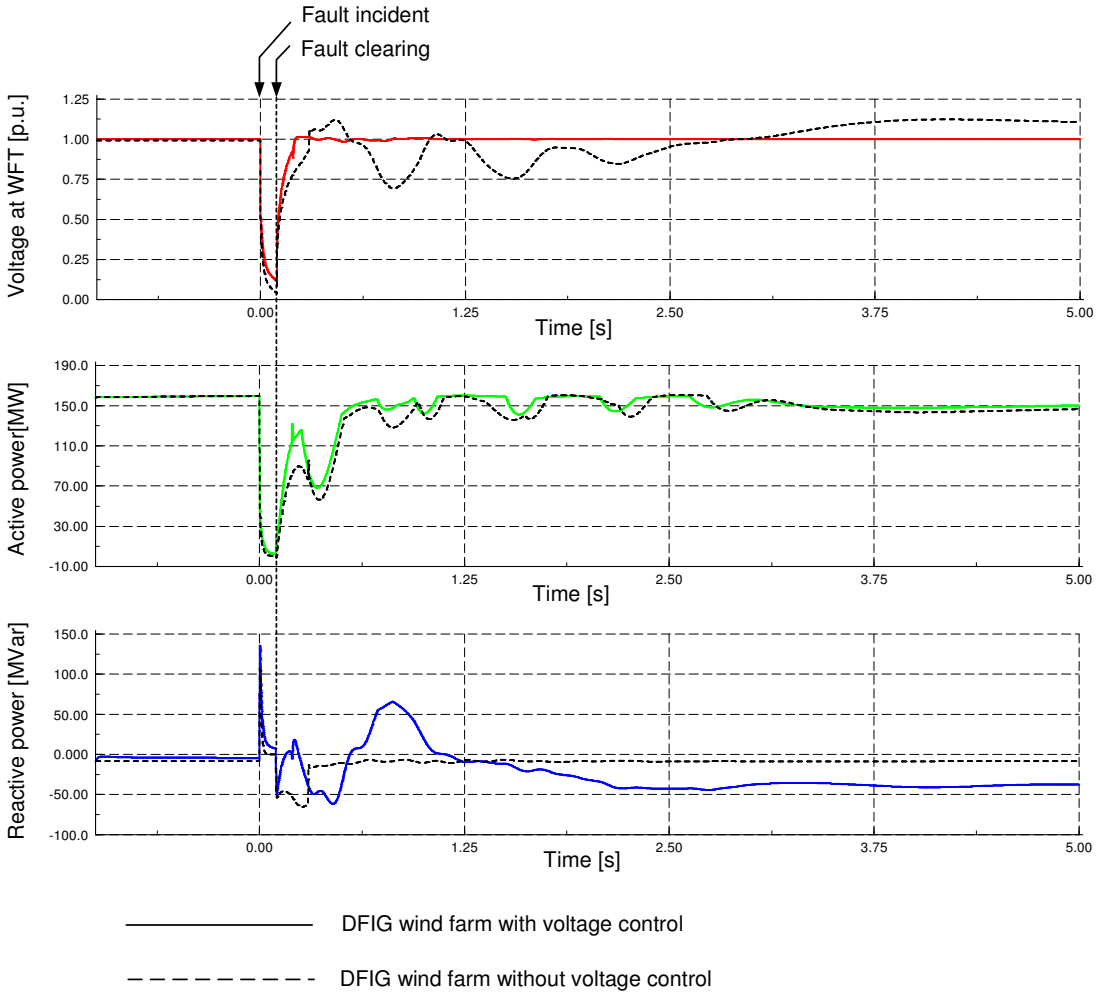

Figure 9.3: DFIG wind farm operating with or without voltage control, voltage at the wind farm terminal WFT, active and reactive power production after a 100 ms three-phase fault at the overhead line close to the wind farm´s PCC

In Figure 9.3 the attention was on the DFIG´s performance in the power system's voltage stability during grid faults. One question in mind is now how the DFIG wind farm voltage control influences the performance of a nearby active stall wind farm during a grid fault, placed as illustrated in Figure 9.2. The next two figures, i.e. Figure 9.4 and Figure 9.5, contain therefore only information concerning the active stall wind farm during the grid fault, namely the active and the reactive power in the wind farm terminal, the generator speed and the mechanical power of the active stall wind turbines, respectively. Table 9.1 gives an overview over four different control scenarios, which are considered in the following: the DFIG wind farm (DFIG WF) is equipped with or without voltage grid support and the active stall wind farm (AS WF) is equipped with or without its power reduction control.

	DFIG WF **WITHOUT** voltage grid support	DFIG WF **WITH** voltage grid support
AS WF **WITHOUT** power reduction control	**Scenario a**	**Scenario b**
AS WF **WITH** power reduction control	**Scenario d**	**Scenario c**

Table 9.1: Four control scenarios investigated in case study I

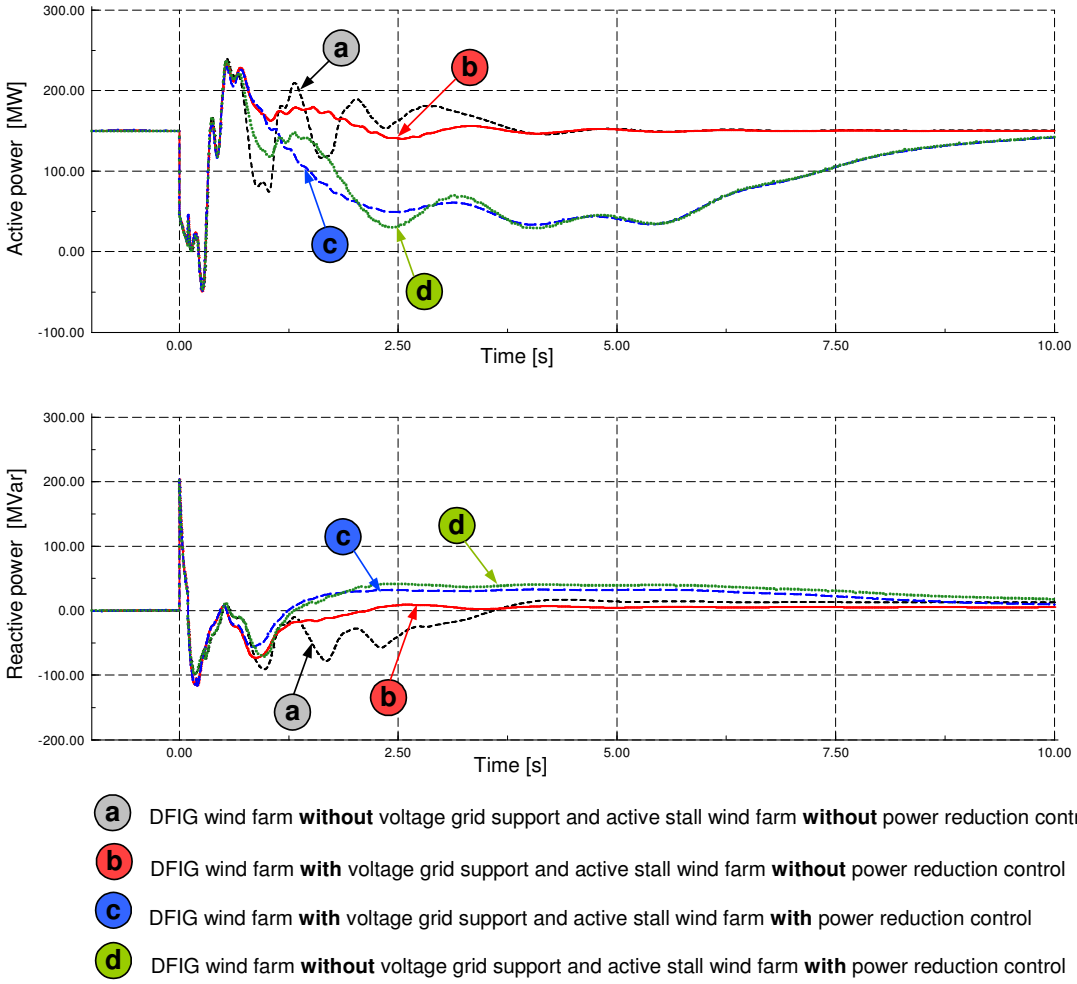

a DFIG wind farm **without** voltage grid support and active stall wind farm **without** power reduction control

b DFIG wind farm **with** voltage grid support and active stall wind farm **without** power reduction control

c DFIG wind farm **with** voltage grid support and active stall wind farm **with** power reduction control

d DFIG wind farm **without** voltage grid support and active stall wind farm **with** power reduction control

Figure 9.4: Active and reactive power of the active stall wind farm according to four different control scenarios of case study I after a 100 ms three-phase fault at the overhead line close to the wind farm´s PCC

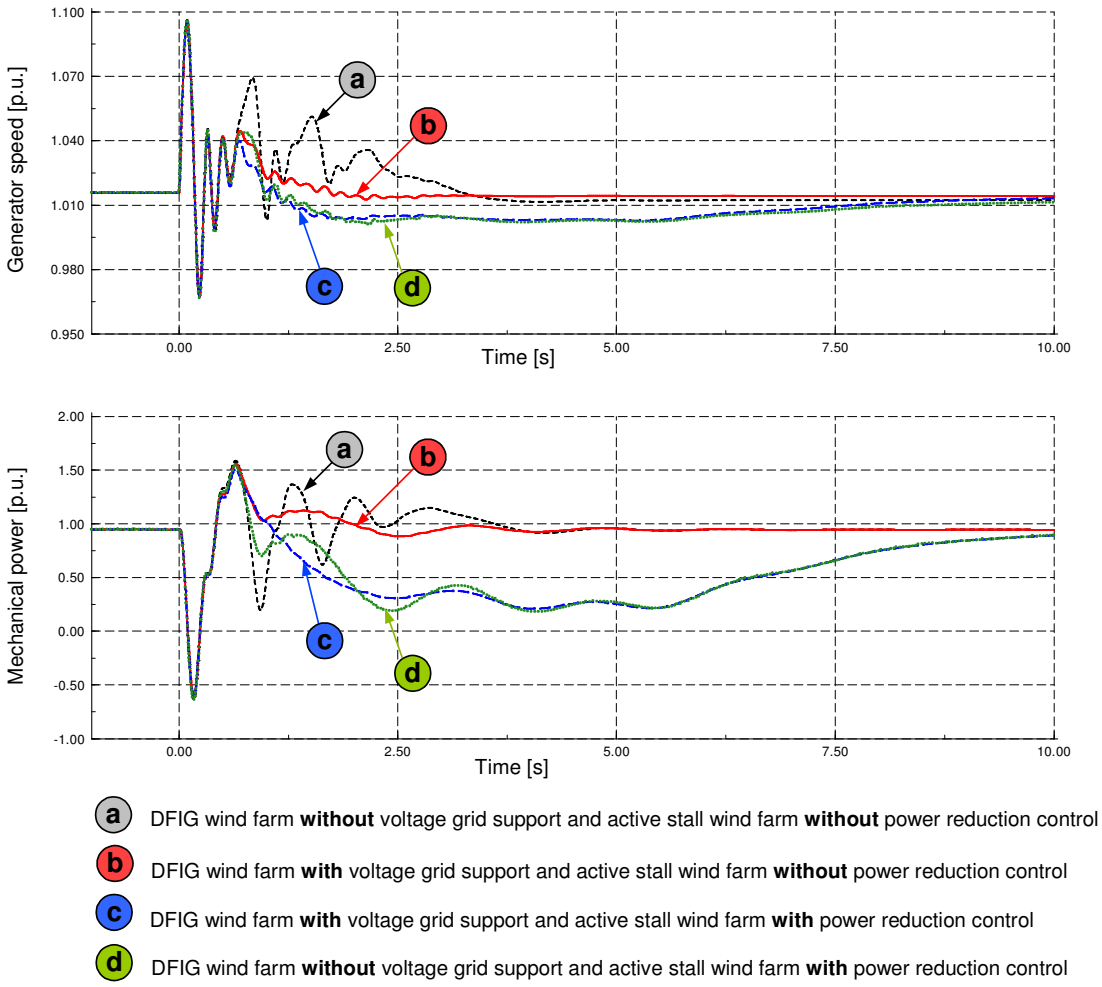

Figure 9.5: Generator speed and mechanical power of the active stall wind farm according to four different control scenarios of case study I after a 100 ms three-phase fault at the overhead line close to the wind farm´s PCC

The following remarks are concluded:

(i) The worst case for the active stall wind farm is clearly case a, when the DFIG wind farm has no voltage control and the active stall wind farm has no power reduction control.

(ii) The voltage control of the DFIG wind farm (case b and c) has a damping effect on the mentioned signals of the active stall wind farm, no matter whether this has power reduction control or not.

(iii) The active power, the generator speed and the mechanical power are almost identical *during* the grid fault, no matter which case is simulated. The fact that the mechanical power is unchanged in this period means that the drive train system is equally stressed in all 4 cases.

(iv) The best case for the active stall wind farm is clearly case b, when the DFIG wind farm is equipped with voltage control, and the power reduction control of the active stall wind farm is disabled. Note that the wind farm is not subjected

to torsional oscillations and there is no loss in the active power production. The influence of the DFIG voltage control on the active stall wind farm is thus even better when the latter does not have any special control implemented to ride-through a grid fault.

The overall conclusion from Figure 9.4 and Figure 9.5 is that the DFIG wind farm equipped with voltage control can help a nearby active stall wind farm to ride-through a grid fault, without any need to implement an additional ride-through control strategy in the active stall wind farm.

9.2.2 Case study II: PMSG wind farm and active stall wind farm

The same simulations as in case study I are now also performed in case study II using a PMSG wind farm instead. The grid support capability of the PMSG wind farm and the DFIG wind farm can then directly be compared. For the sake of completeness the power system model used in case study II is presented in Figure 9.6. Before the fault incident the PMSG wind farm operates at its rated capacity while the stall and the active stall wind turbines operate at 60 % of their rated power. As described in Section 9.2.1 a 3-phase short circuit grid fault is simulated at the end the overhead line close to the wind farm's point of common coupling (PCC) – see Figure 9.6. The grid fault lasts for 100 ms and gets cleared by permanent isolation of the faulty line and the parallel overhead line gets fully loaded. The on-land local wind turbines are disconnected from the system in the fault incident.

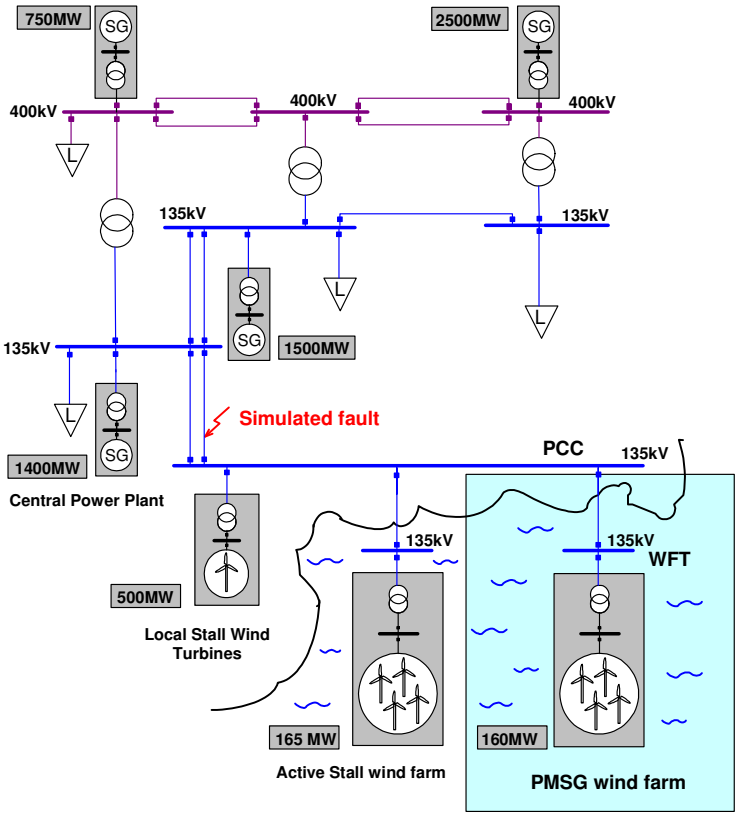

Figure 9.6: Power system model used for case study II

Figure 9.7 shows the simulation results concerning the PMSG wind farm in the simulated fault case. Two situations can be compared:

1. The PMSG is not equipped with voltage control capability. Each turbine maintains a power factor of 1.
2. The PMSG is equipped with voltage control capability.

The power reduction control of the active stall wind farm is again disabled in both situations to achieve the worst case for voltage stability.

The grid fault causes a severe voltage drop at the wind farm terminal. Immediately after the voltage drop in situation 2 the grid side converter of the PMSG wind turbines starts to provide reactive power, which improves the voltage level. When no voltage control is enabled, the grid voltage oscillates longer and stabilizes on a higher voltage level after the fault is cleared. This is again due to the reactive power surplus existent in the system as result of the on-land wind turbines disconnection and as result of the line tripping as it was explained previously in Section 9.2.1. In situation 2 when the voltage control is enabled the PMSG wind turbines can absorb the reactive power surplus in the system. The active power signal is the same for both cases, as the grid side converter prioritizes reactive power supply during the voltage dip, which limits the active power production capability.

The result is very similar to the simulation results achieved for the DFIG wind farm in case study I. However, a difference is visible in the voltage characteristic,

when both variable speed wind farms, the DFIG and PMSG wind farm, are not equipped with voltage control capability. The voltage recovers faster and oscillates less in case study II (situation 1), when the PMSG wind farm is connected to the power system. This is due to the fact, that wind turbines with DFIG have direct grid connected generators so that any oscillations of the DFIG and the grid voltage directly influence each other. Moreover, the active power signal is much smoother for the PMSG wind turbine, since the grid side converter decouples the generator from the grid and any power fluctuations can be absorbed by the damping controller in the DC-link. Nevertheless, in case study II (situation 2), when the PMSG wind farm is used, the voltage at the wind farm terminal WFT shows an overshoot above rated voltage in contrast to case study I (situation 2). As the PMSG wind farm provides a much higher amount of reactive power during the voltage drop, some time is required to reduce the reactive power after fault clearing, which causes, that the voltage shortly rises above its rated value.

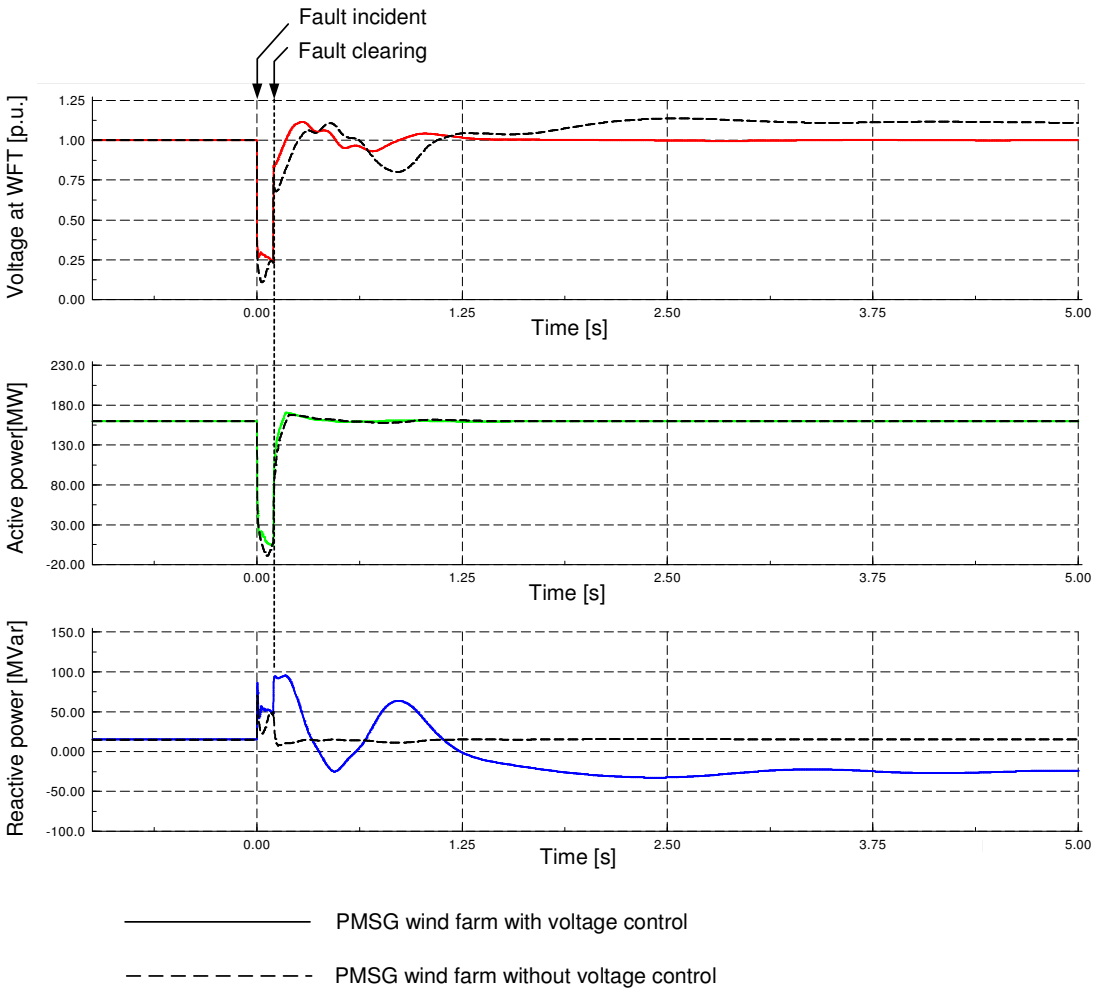

Figure 9.7: PMSG wind farm operating with or without voltage control, voltage at the wind farm terminal WFT, active and reactive power production after a 100 ms three-phase fault at the overhead line close to the wind farm´s PCC

In the following the grid support impact of the PMSG wind farm on the active stall wind farm is pointed out. In the same manner as in case study I four control scenarios are analysed. Two control cases of the PMSG wind farm (PMSG WF), when it is equipped *with* or *without* voltage grid support capability, are combined with two cases concerning the active stall wind farm, namely when the active stall wind farm (AS WF) is equipped *with* or *without* power reduction control, respectively. An overview over the four resulting control scenarios is illustrated in Table 9.2.

	PMSG WF **WITHOUT** voltage grid support	PMSG WF **WITH** voltage grid support
AS WF **WITHOUT** power reduction control	**Scenario a**	**Scenario b**
AS WF **WITH** power reduction control	**Scenario d**	**Scenario c**

Table 9.2: Four control scenarios investigated in case study II

Figure 9.8 and Figure 9.9 show the simulation results of the active stall wind farm in case of the applied grid fault. In Figure 9.8 the active and reactive power production of the active stall wind farm are plotted for all four control scenarios. Figure 9.9 presents the mechanical power of the active stall turbines as well as their generator speed.

Generally, the same conclusions as in case study I can be made. First, the PMSG has also a damping effect on the nearby connected active stall wind farm and influences its behaviour positively. Second, the PMSG wind farm equipped with voltage control can help a nearby active stall wind farm to ride-through a grid fault, so that its power reduction control becomes dispensable.

The behaviour of the active stall wind turbines is almost the same for case studies I and II. This means, that both wind farm types, a DFIG or a PMSG wind farm, have the same positive impact on power system stability in the simulated case. The only difference, which is reflected in Figure 9.7 and Figure 9.9, is that speed and grid voltage oscillations are generally more damped in the PMSG case when the voltage controller is disabled. As mentioned above, this is due to the fact, that doubly-fed induction generators are directly grid connected and speed oscillations are then transferred to the grid voltage, while permanent magnet synchronous generators are instead fully decoupled from the grid by the frequency converter. However, when both wind farms are equipped with voltage grid support, no significant difference is observed.

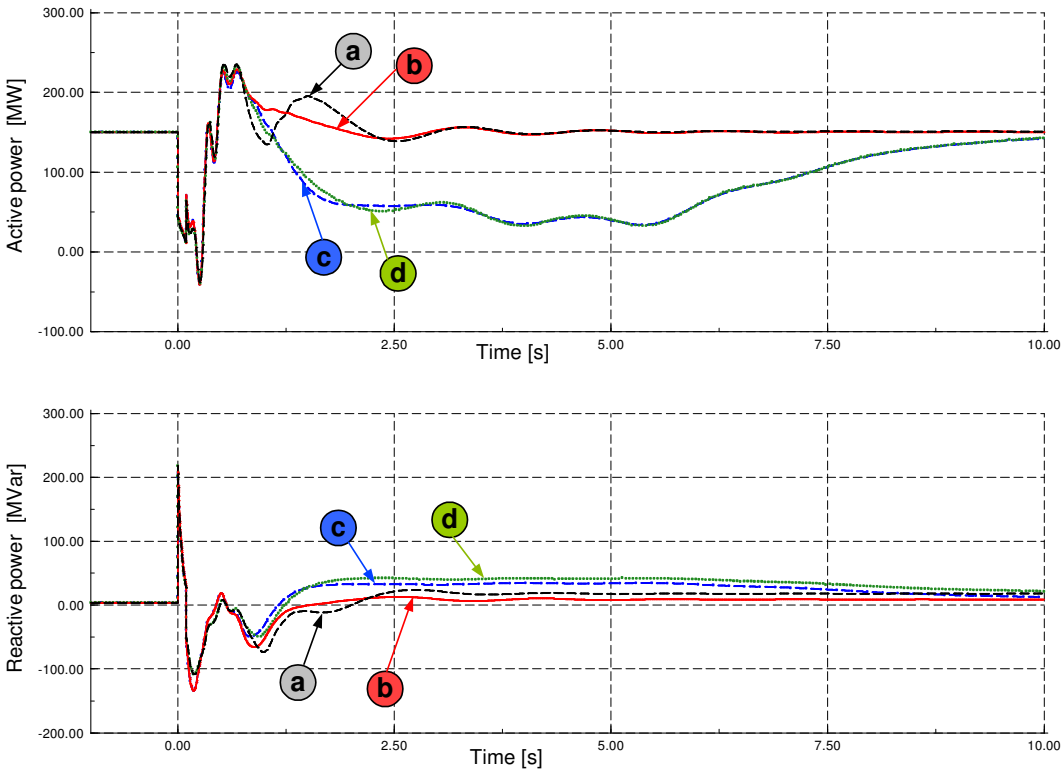

Figure 9.8: Active and reactive power of the active stall wind farm according to four different control scenarios of case study II after a 100 ms three-phase fault at the overhead line close to the wind farm´s PCC

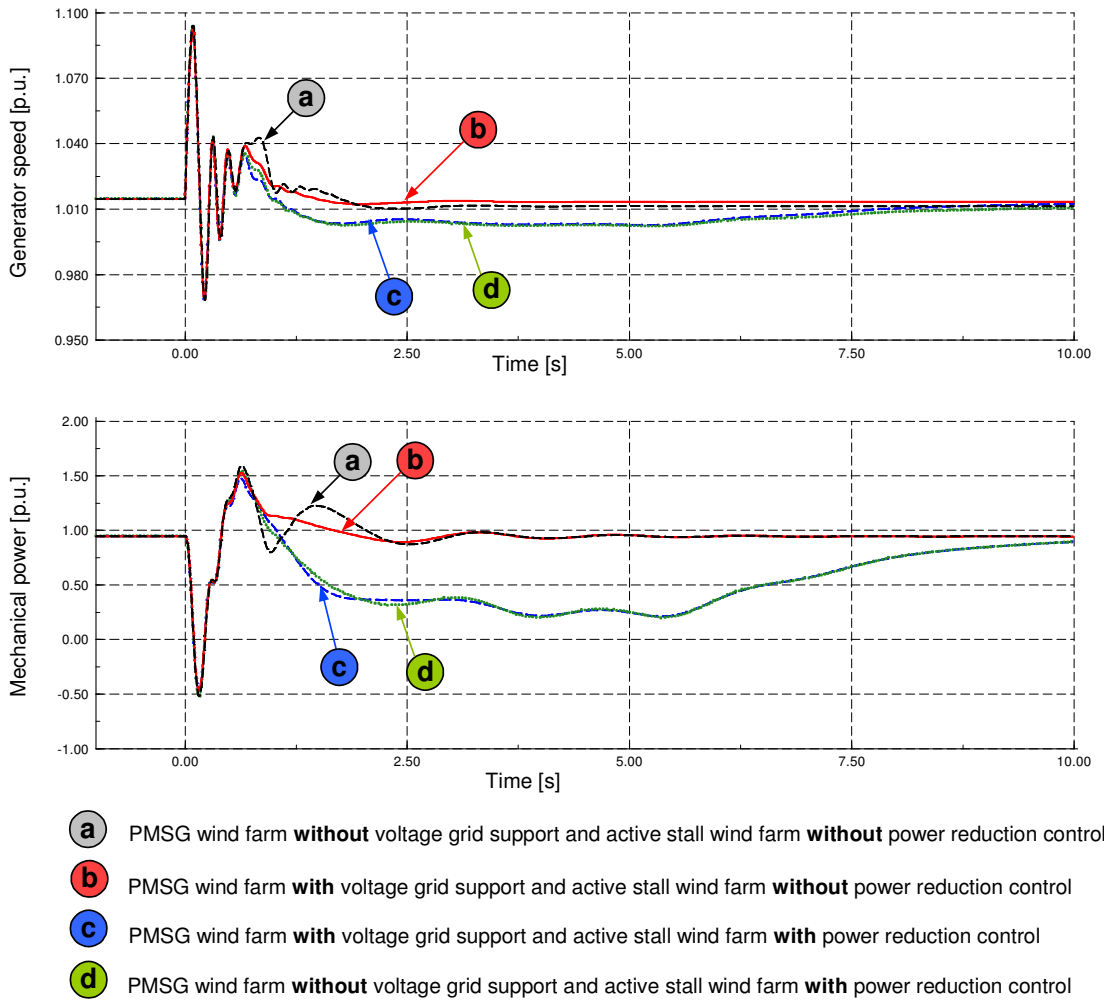

Figure 9.9: Generator speed and mechanical power of the active stall wind farm according to four different control scenarios of case study II after a 100 ms three-phase fault at the overhead line close to the wind farm´s PCC

9.2.3 Case study III: DFIG wind farm and local stall wind turbines

Case study III investigates the DFIG wind farm's impact on the nearby connected local stall wind turbines (Danish concept). The power system used for this case study is illustrated in Figure 9.10. In order to focus on the interaction between the DFIG wind farm and the local wind turbines only, the active stall wind farm is omitted. It is assumed that the DFIG wind farm operates at its rated capacity, as this is worst for voltage stability. Before the fault incident the stall wind turbines operate at 60 % of their rated power.

A 3-phase short circuit at the PCC (see Figure 9.10) with a duration of 300 ms is now performed. Due to its location close to the wind farm and its long duration, the fault scenario denotes a severe fault and critical situation for the grid and the coupled wind turbines.

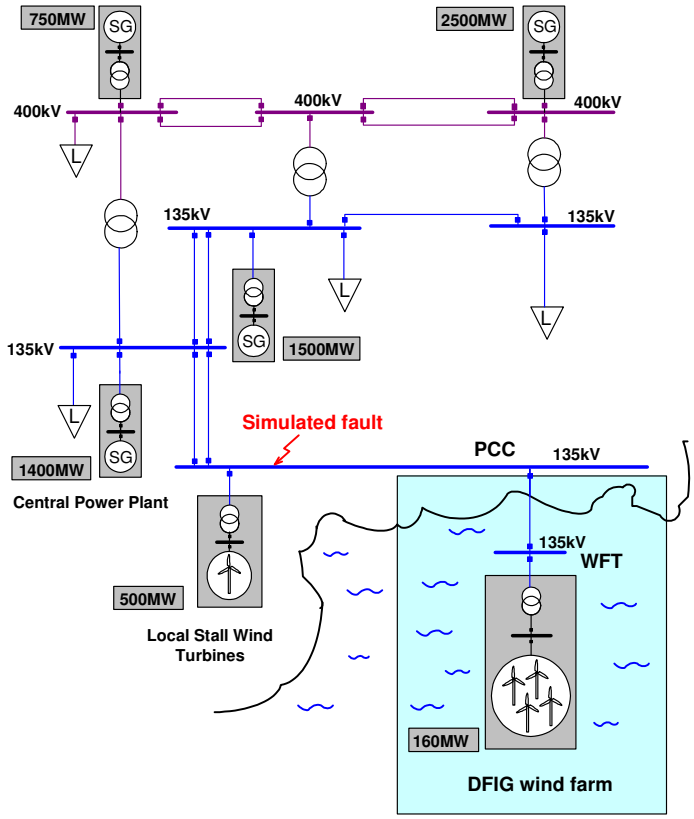

Figure 9.10: Power system model used for case study III

The simulation results of the DFIG wind farm and the local wind turbines are illustrated in Figure 9.11. The following quantities are plotted:

- The voltage at the point of common coupling (PCC)
- The voltage at the DFIG wind farm terminal (WFT)
- The active and reactive power of one representative turbine of the DFIG wind park
- The generator speed and torque of a local wind turbine

Two simulations can be compared in Figure 9.11:

- Situation 1 (dashed line) shows the results without reactive power supply of the DFIG wind farm
- Situation 2 (solid line) shows the results with reactive power supply of the DFIG wind farm

The short circuit causes a significant voltage drop at the PCC and at the wind farm terminal (WFT). This implies a drop in the generator's active power production, too. Due to the arising high transient currents the crowbar is coupled directly after the fault incident. The voltage drop causes also a reduction of the flux in the DFIG and the generator is demagnetized. In Figure 9.11 the demagnetisation is visible as a reactive

power peak in the moment of the fault. Because of the active power drop, which causes a reduction of the electromagnetic torque, the induction generators of the local wind turbines start to accelerate. In contrast to the DFIG wind turbines, where damping of torque and speed oscillations is provided by means of converter control, in situation 1 heavy generator speed and torque fluctuations are excited in the conventional (local) wind turbines. Such heavy torque and speed fluctuations imply a high mechanical stress for the local wind turbines. After the fault is cleared, the reactive power demand of the asynchronous generators of the local wind turbines has increased due to the acceleration. Moreover, also the DFIG wind park consumes reactive power during crowbar coupling, which influences the voltage reestablishment negatively. A tripping of the local wind turbines during grid faults, as it is common practice for conventional wind turbines today, is justifiable in this case. However, the tripping causes a significant loss of active power production, as the conventional wind turbines cannot immediately be reconnected after the fault is cleared.

In contrast to situation 1, situation 2 shows the results, which could be achieved, when the wind park is equipped with the new developed control strategy in the simulated fault case. As soon as the crowbar is connected, the reactive power boosting of the grid side converter is activated, which improves the voltage level during the fault. The active power signal has a similar characteristic in both cases. After crowbar decoupling, the voltage control of the rotor side converter starts to work. Due to the reactive power supply of the total wind park the voltage level can much faster be reestablished. This has a positive impact on the behaviour of the local wind turbines with conventional technique, too. The speed and torque fluctuations are significantly reduced due to the control system of the DFIG wind park.

The simulation results of situation 2 show, that a tripping of the local wind turbines is no longer necessary if the DFIG wind farm is equipped with the developed control strategy. The control system of the nearby connected DFIG wind farm facilitates so fault ride-through of the conventional wind turbines. A significant loss of active power production can then be avoided. It has thus been proven by means of the performed case study, that a large DFIG wind farm equipped with the here presented control strategy can support power system stability.

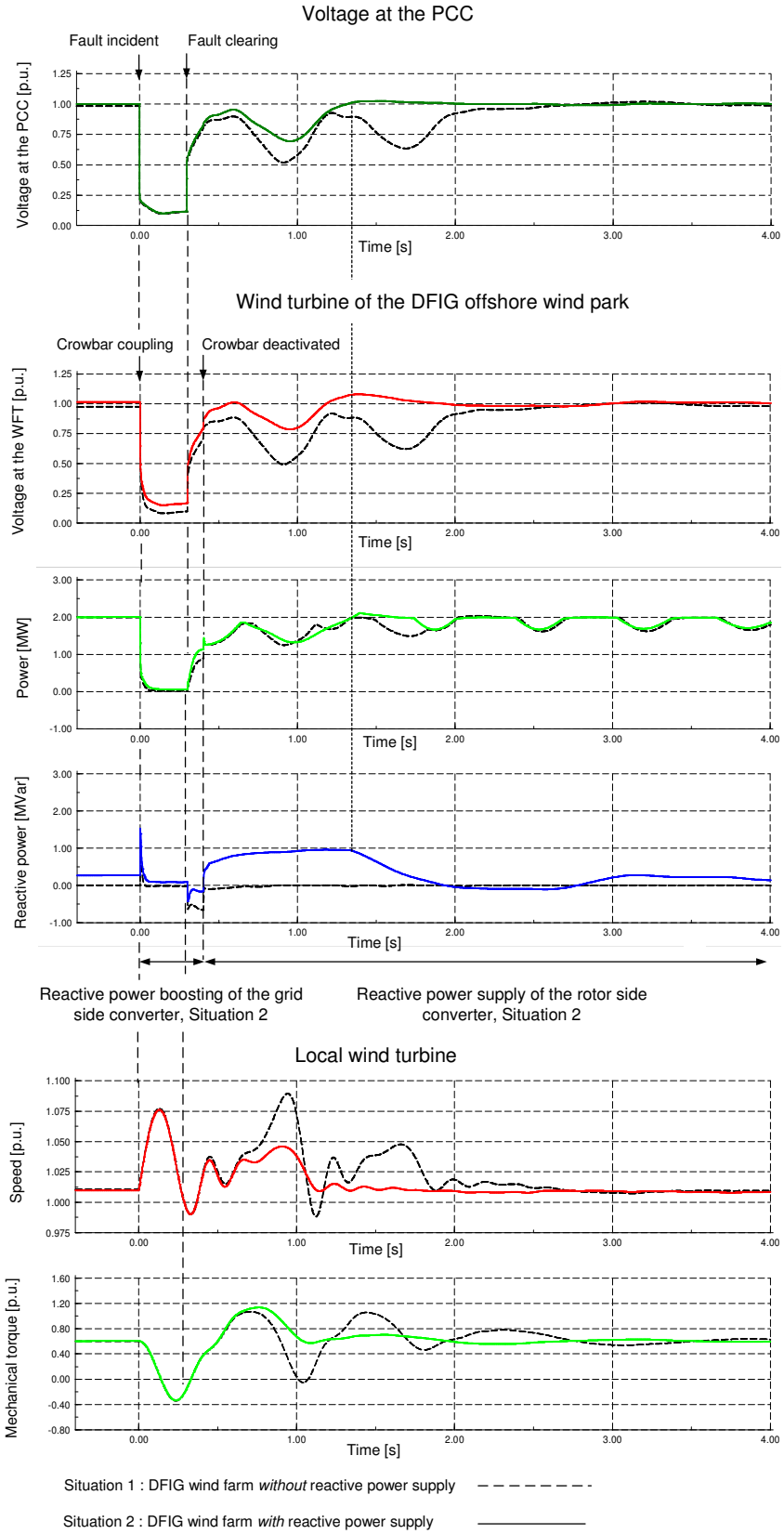

Figure 9.11: Simulation results of the DFIG wind farm and the local wind turbines after a 300 ms three-phase fault at the PCC

9.2.4 Case study IV: PMSG wind farm and local stall wind turbines

In an analogous manner as in case study III the interaction between a PMSG wind farm and the nearby connected stall wind turbines is analysed in case study IV. A 3-phase short circuit at the PCC (see Figure 9.12) with a duration of 300 ms is performed. In order to focus on the interaction between the PMSG wind farm and the local wind turbines, the active stall wind farm is again omitted. Before the fault incident the PMSG wind farm operates at its rated capacity while the stall wind turbines operate at 60 % of their rated power. The power system is sketched in Figure 9.12.

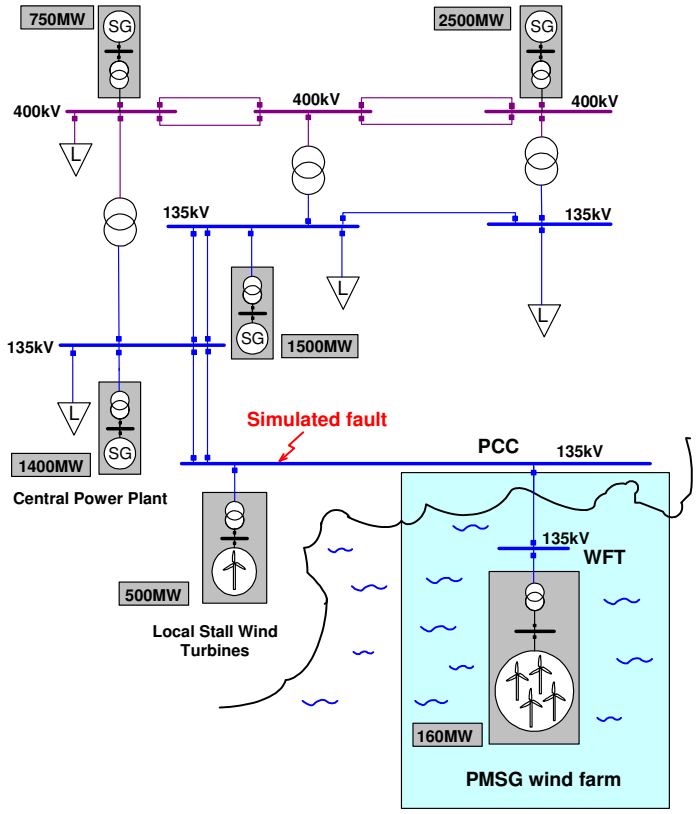

Figure 9.12: Power system model used for case study IV

The following simulation results are shown in Figure 9.13:

- The voltage at the point of common coupling (PCC)
- The voltage at the PMSG wind farm terminal (WFT)
- The active and reactive power of one representative turbine of the PMSG wind park
- The generator speed and torque of a local wind turbine

Accurately as in case study III two simulation cases are compared:

- Situation 1 (dashed line) shows the results without reactive power supply of the PMSG wind farm

- Situation 2 (solid line) shows the results with reactive power supply of the PMSG wind farm

The applied grid fault causes a voltage drop at the PCC down to approximately 10 % of its rated value. This reduces the active power production of the PMSG wind turbines and the stall wind turbines. The drop of active power provokes large speed and torque oscillations of the stall wind turbines as illustrated in Figure 9.13. Moreover, the stall wind turbines accelerate during the fault, increasing their reactive power demand especially when the fault is cleared. Due to this reason a tripping of conventional wind turbines was common practice before the fault ride-through requirement was introduced.

If however the PMSG wind farm is equipped with the developed control strategy for grid support represented in situation 2, the power system impact can significantly be improved. As soon as the grid voltage drops, the voltage controller provokes an increase of reactive power supply by the PMSG wind farm. This improves the voltage level at the wind farm terminal (WFT) considerably. The improved voltage level causes an improvement of the active power signal, too. After the fault is cleared the grid side converter provides a much higher amount of reactive power due to the increased voltage level. As soon as the voltage at the PCC reaches its rated value the reactive power supply of the grid side converter is reduced. In contrast to situation 1 voltage and system stability can much faster be regained. The grid support of the PMSG wind turbines has furthermore a noticeable positive impact on the behaviour of the local wind turbines with conventional technique. The torque and speed fluctuations are significantly reduced due to the control system of the PMSG wind farm.

Similar to case study III the simulation results show, that a tripping of the local wind turbines is no longer necessary if a nearby connected wind farm with PMSG wind turbines supports the power system stability by reactive power supply. The control system of the PMSG wind farm even facilitates fault ride-through of the conventional wind turbines. A significant loss of active power production can so be avoided.

The fault ride-through and grid support capability of PMSG wind turbines has thus been proven by means of the presented case study.

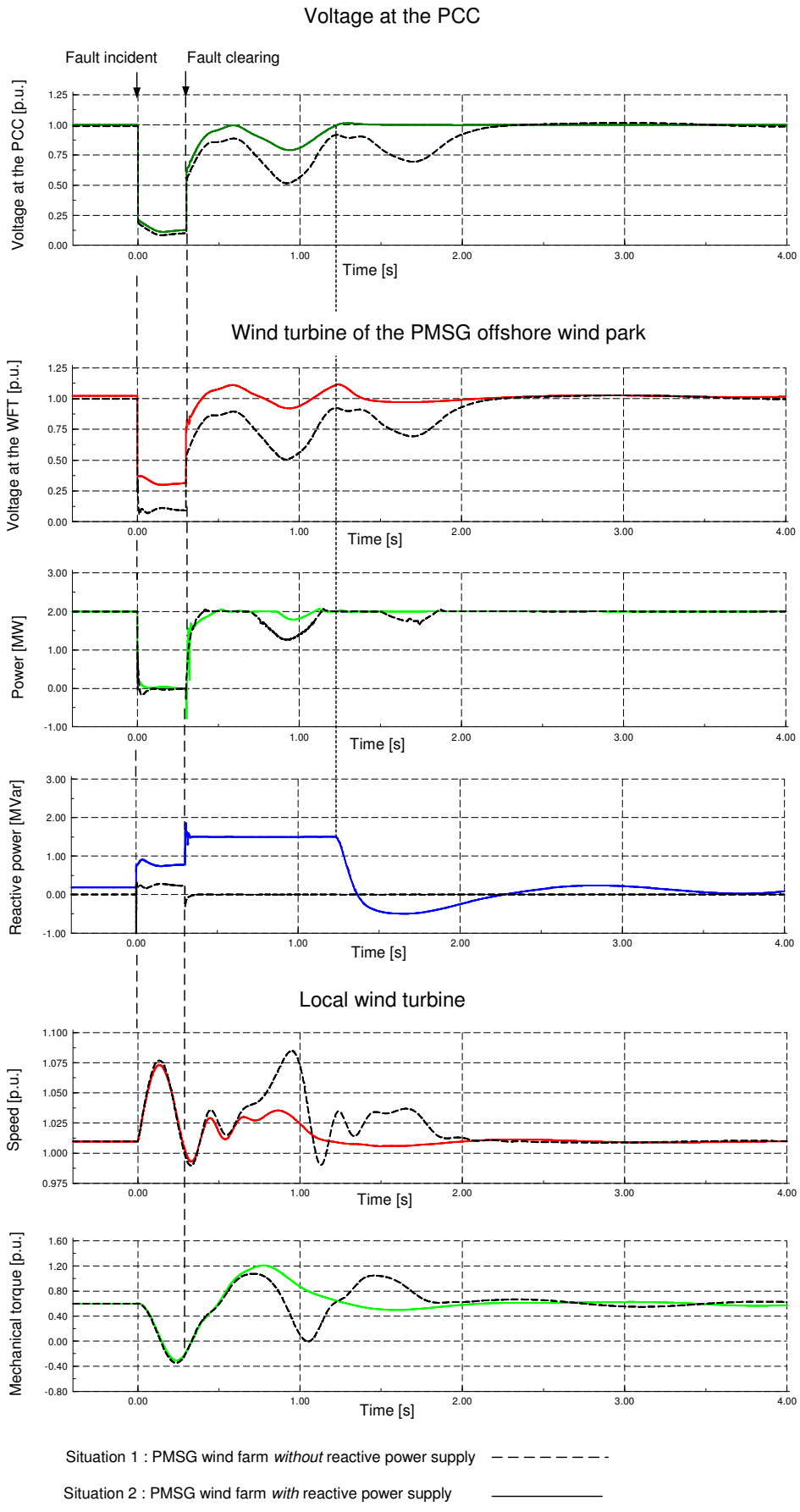

Figure 9.13: Simulation results of the PMSG wind farm and the local wind turbines after a 300 ms three-phase fault at the PCC

9.3 Comparison of DFIG and PMSG wind turbines´ grid support capability

This section presents a final evaluation and a direct comparison of DFIG and PMSG wind turbine's grid support capability. Advanced control strategies have been developed and presented, which enhance the grid support capability of both variable speed wind turbine concepts. In Chapter 5 to Chapter 9 the contribution of DFIG and PMSG wind turbines to grid support has been analysed by means of simulations. Based on this, the following conclusions can be drawn.

It has been shown, that PMSG wind turbines with full-scale frequency converter have a better grid support capability than DFIG wind turbines with partial-scale frequency converter. Due to the full converter system PMSG wind turbines can provide a higher amount of reactive power to the grid. This yields that the voltage level is supported to a higher level and recovers faster. The PMSG wind turbine itself is furthermore fully decoupled from the grid by the converter and is thus less subjected to the impact of a grid fault.

In contrast to this, DFIG wind turbines are direct grid connected generators. A disadvantage of direct grid connected generators is that the generator is demagnetized in case of a grid fault and high transient short circuit currents arise in the generator. This can on the one hand lead to a tripping of relay settings followed by disconnection of necessary supply units. On the other hand additional protective equipment, as e.g. a crowbar, has to be installed in the turbine to prevent disconnection of the turbine itself. Due to this direct grid connection, generator, converter and turbine system are directly exposed to the grid fault impact. As a consequence of a grid fault, generator speed and torque oscillations occur in the doubly-fed induction generators.

The reactive power supply capability of DFIG wind turbines is smaller compared to full converter connected wind turbines. Because of the smaller size of the partial-scale frequency converter the rotor current, which can be supplied to the DFIG, is limited. This in turn limits the amount of reactive power, which can be provided to the grid. A second disadvantage is that during severe grid faults the rotor side converter is possibly blocked by the crowbar, which temporarily reduces the reactive power supply even further. However, if the financial advantage using a cheaper partial-scale converter prevails, those disadvantages must be accepted.

In Chapter 6 and Chapter 8 both wind turbine concepts are directly examined according to existing grid code requirements (E.ON and Energinet.dk grid codes). While the PMSG wind turbine is able to fully comply with all grid code specifications, the DFIG wind turbine cannot completely provide the specified reactive current demand of 1 p.u. reactive current required by E.ON. This is due to the above mentioned

reasons, that DFIG´s reactive power supply is limited by the smaller converter or by temporary crowbar coupling. If however the converter could be dimensioned for higher power or bear transiently higher currents, the E.ON requirement could also be met by DFIG wind turbines. On the other hand, E.ON allows short-term interruption of wind turbines during faults, which means that a constraint accomplishment with the grid code specifications is tolerated anyway.

Finally, both wind turbine concepts were applied to a realistic power system model and several case studies were carried out. Considering the results of both wind turbine concepts presented in Chapter 9, both variable speed wind turbines with advanced voltage control can contribute to grid support. When both concepts are equipped with the developed control strategies no difference between PMSG and DFIG wind turbines in terms of voltage re-establishment is observed. Both concepts can equally support power system stability. Moreover, both concepts can help the nearby connected stall or active stall wind turbines to ride-through grid faults and can enable them to partly comply with grid code requirements.

Possible differences between the considered concepts can however occur because of different design of the control system. The control system must be adapted to the power system, the wind turbines are connected to. Specific transient differences due to the controller dynamics can arise but are not relevant in terms of grid support capability.

The concluding statement is thus, that DFIG wind turbines and PMSG wind turbines are able to support the power system in equal manners if they are equipped with appropriate control for grid support.

9.4 Summary

In the near future large offshore wind farms connected to the power transmission system, will gain a significant impact on the power system and its stability. In this chapter the interaction between variable speed wind farms consisting of either DFIG or PMSG wind turbines and the power system is simulated and analysed in different case study scenarios.

For each wind turbine concept an aggregated model of a large offshore wind farm, consisting of eighty 2 MW DFIG or PMSG wind turbines, is implemented. It is illustrated how the considered wind farm topologies contribute with reactive power and help to re-establish the voltage in case of a grid fault. The variable speed wind farm's fault ride-through capability and its contribution to voltage control is assessed and evaluated by means of simulations with the use of a generic but realistic transmission power system model delivered by the Danish Transmission System Operator Energinet.dk.

The simulation results illustrate how both the DFIG wind farm as well as the PMSG wind farm, each equipped with their respective voltage control, participate to re-establish properly the voltage during a grid fault. Moreover, the influence of their control strategy on the performance of an active stall wind farm placed in vicinity is also investigated. The conclusion is that a variable speed wind farm, DFIG or PMSG wind farm, equipped with voltage control can help a nearby active stall wind farm to ride-through a grid fault, without implementation of any additional ride-through control setup in the nearby active stall wind farm.

The variable speed wind farms, equipped with voltage control, can even improve the behaviour of local wind turbines with conventional technology, which are connected in vicinity to the variable speed offshore wind farm. A disconnection of the conventional wind turbines in case of grid faults is therefore not necessary anymore. This means, that significant power losses due to disconnection of conventional wind turbines during grid faults can be avoided.

A general comparison of DFIG and PMSG wind turbine's grid support capability is also presented. Main advantage of the PMSG wind turbine is its grid connection via a full-scale converter, which decouples the generator from the grid, so that it is not directly subjected to the impact of a grid fault in contrast to DFIG wind turbines with direct grid connected generator. Due to the full-scale converter, the PMSG is also able to provide a higher amount of reactive power for voltage re-establishment. Nevertheless, simulation results confirm that DFIG wind turbines and PMSG wind turbines are able to support the power system in equal manners if they are equipped with appropriate control for grid support.

10 Conclusions

This chapter summarizes the findings of the presented PhD project “Variable Speed Wind Turbines – Modelling, Control and Impact on Power Systems”. As wind power, especially offshore wind power, is expected to become one mainstream energy source and probably the largest renewable energy source in Germany and Europe in the next decades, research on the technical aspects of wind power as a part of the future power supply mix is essential.

This report focuses on the dynamic behaviour of wind turbines and their interaction with the power system. DFIG and PMSG wind turbine technologies are selected for the present investigation. The wind turbine with doubly-fed induction generator (DFIG) is the most popular wind turbine concept for modern wind turbines today, due to its good controllability and approved technology on the wind turbine market. The wind turbine concept using a multipole permanent magnet synchronous generator (PMSG) and full-scale frequency converter is assessed to be a very auspicious technology for future applications, especially offshore. Comprehensive dynamic simulation models of both of these wind turbine concepts are implemented in the power system simulation software DIgSILENT Power Factory. Furthermore advanced control strategies for the wind turbine concepts in normal and fault operation are developed.

The model of the wind turbine’s mechanical part, valid for both concepts, includes models for the rotor effective wind, the aerodynamic rotor and the drive train. It turned out in the present investigations that the drive train must be represented by at least a two-mass spring and damper model. In power system stability studies this yields a more accurate result, when the system response to heavy disturbances is analysed. The models of the electrical system, including among others the generator, the frequency converter and the transformer, are provided in the toolbox library and comprise the differential equations of the respective elements. The data for the wind turbines are not linked to a specific manufacturer but are representative for turbine and generator used in a modern 2 MW variable speed pitch controlled wind turbine.

The control of the wind turbine is achieved by two coordinated controllers: a speed controller and a power controller. The turbine power is directly controlled by the converter, while the generator speed is regulated by the pitch angle. This control principle is the same for the DFIG wind turbine concept as well as for the PMSG wind turbine concept. Simulations show that the developed control method successfully controls the variable speed wind turbines within a range of normal operational conditions. At wind speeds less than the rated wind speed the converter seeks to maximise the power according to the MPP-tracking. At large wind speeds the speed controller permits a dynamic variation of the generator speed in order to avoid mechanical stresses, while the converter keeps the power to the rated power. Moreover, the pitch controller

serves as an overspeed protection both in normal operation and during grid faults. The control strategy facilitates furthermore independent control of active and reactive power to imposed reference values at variable speed. It can thus be concluded, that modern variable speed wind turbines with power electronic interface and equipped with such control system can operate in the same manner as a conventional power plant does.

In a second step the control strategies for both wind turbine concepts are extended by an additional control, which serves to improve their performance during grid faults and enables them to contribute to power system support. Simulation results provide insight and understanding on the most significant phenomena concerning the dynamic behaviour of DFIG and PMSG wind turbines during grid faults.

The control strategy for grid faults of the DFIG wind turbine is based on the design of a proper coordination between three controllers: the damping controller, the rotor side converter voltage controller and the reactive power boosting of the grid side converter. A damping controller is implemented and tuned to damp actively torsional drive train oscillations, which might otherwise lead to self-excitation and high mechanical stress of the drive train system. The converter system is equipped with a crowbar protection system, which is triggered if high transient currents and voltages occur in the generator or converter. In case of grid faults, when the crowbar is triggered the DFIG behaves as a conventional squirrel cage induction generator. Different values for the crowbar resistance are used in order to investigate its influences on the rotor current and on the reactive power demand of the generator during grid faults. It is concluded that the crowbar resistance value is a trade of between effective reduction of transient overcurrents on the one hand and thermal heating, size and costs of the crowbar at the other hand. The grid voltage is controlled by the rotor side converter as long as it is not blocked by the protection system, otherwise the grid side converter is taking over the voltage control.

Similar to that, a control strategy for grid fault of a PMSG wind turbine is developed, which enables the turbine to accomplish fault ride-through and to provide grid support during grid faults. A damping controller is designed to actively damp the torsional oscillations in the drive train whenever the system gets excited. A multipole PMSG wind turbine with full-scale converter has no inherent damping and the absence of an additional damping controller might therefore lead to self-excitation and high mechanical stress of the drive train. The converter control designed for normal operating conditions is assessed to be very beneficial for fault ride-through. The DC-voltage is controlled by the generator side converter instead of the grid side converter. As the generator side converter is not directly coupled to the grid its control capability is not compromised during grid faults. With such control strategy the wind turbine is therefore able to ride-through faults even without any additional measures. Nevertheless, a chopper can be applied to the system, in order to enhance the fault ride-through capa-

bility even more. A voltage controller is also added to the grid side converter control of the PMSG wind turbine to provide reactive power supply in case of grid faults.

Simulation results exemplify how DFIG and PMSG wind turbines, equipped with their respective control strategy participate to re-establish the voltage during grid faults. It is furthermore illustrated that the damping controller is able to significantly reduce the oscillations of the drive train. The presented control strategies facilitate fault ride-through of the considered variable speed wind turbine concepts and enable them to comply with various grid code requirements.

Due to the grid connection via a full-scale converter the PMSG wind turbine can easier accomplish fault ride-through and provide a higher amount of reactive power to the grid than DFIG wind turbines. In contrast to full converter connected wind turbines the reactive power supply of a DFIG wind turbine is limited due to the limited size of the converter. Because of their direct grid connection, DFIG wind turbines are directly subjected to the grid fault impact. The financial advantage of using a partial-scale converter turns into a technical disadvantage in case of grid faults, as it must be protected against high transient currents and voltages. Nevertheless, with an appropriate control and protection system DFIG wind turbines can also ride-through grid faults and contribute to power system support in a satisfactory manner.

Finally, an aggregated model of a large offshore wind farm consisting of eighty 2 MW wind turbines is implemented for each wind turbine concept, a 160 MW DFIG wind farm and a 160 MW PMSG wind farm, respectively. These models serve to illustrate how such large wind farms can contribute with reactive power and help to re-establish the voltage in case of a grid fault. The wind farms´ fault ride-through capability and their contribution to voltage control is assessed and evaluated by means of simulations with the use of a generic but realistic transmission power system model delivered by the Danish Transmission System Operator Energinet.dk. Several case studies are performed in order to analyse the power system impact of both considered wind turbines concepts. The simulation results illustrate how the DFIG wind farm as well as the PMSG wind farm equipped with voltage control participate to re-establish properly the voltage during a grid fault.

The influence of the DFIG and PMSG wind farm's control setup on the performance of an active stall wind farm placed in vicinity is also investigated. The conclusion is that a variable speed wind farm equipped with voltage control can help a nearby active stall wind farm to ride-through a grid fault, without implementation of any additional ride-through control setup in the nearby active stall wind farm.

The fault ride-through and voltage control can moreover improve the behaviour of local stall wind turbines with conventional technology during grid faults, which are connected in vicinity to the DFIG or PMSG wind farm. Torque and speed oscillations of the conventional wind turbines are effectively damped and a significant loss of active power production due to tripping of such wind turbine types can be avoided. In the

performed case studies both DFIG and PMSG wind turbines could provide grid support to in equal manners.

It has been shown, that wind turbines equipped with the presented control strategy for normal operation and for grid fault operation can accomplish grid connection standards applied by the transmission system operators and can furthermore contribute to power system stability. The report presents solutions for wind turbine control and wind power grid integration. Advanced control strategies enable wind turbines to act as active components in the power system, so that a higher penetration of wind power becomes feasible.

The report at hand addresses many issues in terms of wind turbine control and the power system impact of wind power. Nevertheless, each research work can only cover a limited number of aspects related to its topic. Many other problems related to wind power grid integration and the power system impact of wind power exist. Some selected concerns for future research are mentioned in the following. For example the developed control strategies can be tested and verified against real measurements. This implies also a more elaborate validation of the developed models and control. Moreover, different other types of grid faults, as e.g. unsymmetrical fault scenarios, can be simulated with an eventual adjustment of the control for such conditions. Another aspect, which has not been focus in the present work, is the frequency response of variable speed wind turbines. Finally, future power system studies can be carried out considering an even higher wind power penetration than applied in the presented studies. The impact of large wind power units on the power system has been investigated in the present work. However, the power system impact of wind power being a major power source in the system, as expected in some decades, will originate even more new challenges, which must be addressed in future research work.

11 References

[Achilles 2003] Achilles S., Pöller M., „Direct Drive Synchronous Machine Models for Stability Assessment of Wind Farms“, Proceedings of Forth International Workshop on Large-Scale Integration of Wind Power and Transmission Networks for Offshore Wind Farms, Billund, Denmark, 2003.

[Ackermann 2005] Ackermann T., ”Wind Power in Power Systems”, John Wiley and Sons Ltd, January, 2005.

[Akhmatov 2002a] Akhmatov V., “Variable-speed wind turbines with doubly-fed induction generators. Part II: Power System Stability”, Wind Engineering, Vol. 26, No. 3, pp 171-188, 2002.

[Akhmatov 2002b] Akhmatov V., Knudsen H., “An aggregate model of a grid-connected, large-scale, offshore wind farm for power stability investigations-importance of windmill mechanical system”, International Journal of Electrical Power and Energy Systems, Volume 24, Number 9, pp. 709-717(9), November, 2002.

[Akhmatov 2003a] Akhmatov V., “Analysis of dynamic behavior of electric power systems with large amount of wind power”, PhD thesis, Ørsted DTU, Denmark, 2003.

[Akhmatov 2003b] Akhmatov V., “Variable-Speed Wind Turbines with Doubly-Fed Induction Generators Part III: Model with the Back-to-back Converters”, Wind Engineering, Volume 27, No. 2, pp 79-91, 2003.

[Akhmatov 2003c] Akhmatov V., “Variable-speed wind turbines with doubly-fed induction generators Part IV: Uninterrupted operation features at grid faults with converter control coordination”, Wind Engineering, Volume 27, No. 6, pp 519-529, 2003.

[Akhmatov 2003d] Akhmatov V., Nielsen A.H., Pedersen J. K., Nymann O., „Variable-speed wind turbines with multipole synchronous permanent magnet generators. Part I. Modelling in dynamic simulation tools”, Wind Engineering, Volume 27, No. 6, pp 531-548, 2003.

[Akhmatov 2005] Akhmatov V., “Full-load Converter Connected Asynchronous Generators for MW Class Wind Turbines”, Wind Engineering, Volume 29, No. 4, pp 341-351, 2005.

[Akhmatov 2006a] Akhmatov V., “Modelling and Ride-through Capability of Variable Speed Wind Turbines with Permanent Magnet Generators”, Wind Energy, Volume 9, Issue 4, pp 313 – 326, July/August, 2006.

[Akhmatov 2006b] Akhmatov V, Nielsen A. H., “A small test model for the transmission grid with a large offshore wind farm for education and research at Technical University of Denmark”, Wind Engineering, Volume 3, No. 3, 2006.

[Akhmatov 2006c] Akhmatov V, Lund T., Hansen A. D., Soerensen P., Nielsen A. H., ”A Reduced Wind Power Grid Model For Research and Education”, ”, Proceedings of the 6th International Workshop on Large-Scale Integration of Wind Power and Transmission Networks for Offshore Wind Farms, Delft, The Netherlands, pp 173-180, 26–28 October 2006.

[alpha ventus 2007] Offshore-Windpark alpha ventus, www.alpha-ventus.de, accessible November 2007.

[AWEA 2004] American Wind Energy Association, „Global Wind Energy Market Report 2004”, www.awea.org, accessible November 2007.

[Balzer 2001] Balzer G., “Energieversorgung Teil II”, Lecture book, Department of Electrical Power Systems, Technical University of Darmstadt, 2001.

[Balzer 2006] Balzer G., "Energieversorgung Teil I", Lecture book, Department of Electrical Power Systems, Technical University of Darmstadt, 2006.

[Bechtold 2007] Bechtold S., "Fault Ride-Through von Windkraftanlagen mit doppeltgespeisten Asynchronmaschinen", Study thesis, Technical University of Darmstadt, Department of Renewable Energies, 2007.

[Binder 2002] Binder A., "Großgeneratoren und Hochleistungsantriebe", Lecture book, Department of Electrical Energy Conversion, Technical University of Darmstadt, 2002.

[Binder 2005] Binder A., Schneider T., „Permanent magnet synchronous generators for regenerative energy conversion – a survey", European Conference on Power Electronics and Applications, EPE 2005, 11-14 September, Dresden, Germany, 2005.

[Binder 2006] Binder A., "Electrical Machines and Drives 1". Lecture book, Department of Electrical Energy Conversion, Technical University of Darmstadt, 2006.

[BMU 2007] Bundesministerterium für, Umwelt, Naturschutz und Reaktorsicherheit, Federal Ministry for the Environment, Nature Conversion and Nuclear Safety, Brochure „Erneuerbare Energien in Zahlen –nationale und internationale Entwicklung-Stand: Juni 2007", www.erneuerbare-energien.de, accessible November 2007.

[Bojrup 1999] Bojrup M., "Advanced Control of Active Filters in a Battery Charger Application", Licentiate thesis, Department of Industrial Electrical Engineering and Automation, University Lund, Sweden, 1999.

[Bolik 2003] Bolik S.M., "Grid requirements challenges for wind turbines", Proc. of the Fourth Int. Workshop on Large-Scale Integration on wind power and transmission networks for offshore wind farms, 6p, Billund, Denmark, 2003.

[Brando 2004] Brando G., Coccia A., Rizzo R., "Control method of a braking chopper to reduce voltage unbalance in a 3-level chopper", IEEE International Conference on Industrial Technology ICIT, 2004.

[BWE 2006] Bundesverband für Windenergie, www.wind-energie.de/de/statistiken, accessible in November 2006.

[BWE 2007] Bundesverband für Windenergie, " The German wind power industry The technology at a glance ", www.renewables-made-in-germany.com/de/windenergie, accessible November 2007.

[BWEA 2007] British Wind Energy Association, "Offshore Wind Worldwide", www.bwea.com, accessible December 2007.

[Co 2004] Co T.B., "Ziegler-Nichols Method", Michigan Technological University, www.chem.mtu.edu/~tbco/cm416/zn.html, accessible August 2004.

[Conroy 2007] Conroy J.F., Watson R., "Low-voltage ride-through of a full converter wind turbine with permanent magnet generator", Renewable Power Generation, IET, Volume 1, Issue 3, pp 182 – 189, September, 2007.

[Deglaire 2005] Deglaire P., Eriksson S., Solum A., "Simulation and control of a direct driven permanent magnet synchronous generator", Nordic PhD course on Wind Power, Smøla, Norway 5-11 June 2005, www.elkraft.ntnu.no/smola2005/Topics/2.pdf, accessible November 2007.

[dena 2002] dena – Deutsche Energie Agentur, „Strategie der Bundesregierung zur Windenergienutzung auf See", Januar 2002, www.offshore-wind.de, accessible in November 2006.

[dena 2005] dena – Deutsche Energie Agentur, ”dena Grid Study”, „Energiewirtschaftliche Planung für die Netzintegration von Windenergie in Deutschland an Land und Offshore bis zum Jahr 2020“, www.dena.de, accessible November 2007.

[DEWI 2006] DEWI GmbH - Deutsches Windenergie Institut, “WindEnergy Study 2006“, www.dewi.de, accessible in November 2006.

[DIgSILENT 2003] DIgSILENT GmbH, “Dynamical modelling of Doubly-Fed Induction Machine Wind-Generators - DIgSILENT Technical Documentation”, www.digsilent.com, August, 2003.

[DIgSILENT 2004] DIgSILENT GmbH, “PWM Converter – DIgSILENT Technical Documentation”, www.digsilent.com, April 2004.

[DIgSILENT 2005] DIgSILENT GmbH, www.digsilent.de, accessible June 2005

[DIgSILENT 2007a] DIgSILENT GmbH, Germany, “ DIgSILENT Power Factory User Manual” Version 13.2, November 2007.

[DIgSILENT 2007b] DIgSILENT GmbH, Germany, “Demo-Model of a Synchronous generator wind turbine with full converter”, www.digsilent.de, accessible November 2007.

[Dittrich 2005] Dittrich A., Stoev A., “Comparison of Fault Ride-Through Strategies for Wind Turbines with DFIM Generators”, EPE Conference Dresden, Germany 2005.

[Dreschinski 2005] Dreschinski A., “Comparison of Different Control Strategies for Permanent Magnet Synchronous Generators for Use in Wind Turbines“, Master thesis, Department of Renewable Energies, Technical University of Darmstadt, 2005.

[DS DS 427] Danish Standard, DS DS 472, “Conditions for the construction of wind turbines in Denmark”, June, 2007.

[E.ON 2006] E.ON. Netz GmbH, “Netzanschlussregeln, Hoch- und Höchstspannung“, www.eon-netz.com, 2006.

[Energinet.dk 2004] Energinet.dk, “Wind Turbines Connected to Grids with Voltage above 100kV“, Technical regulation TF 3.2.5, www.energinet.dk, 2004.

[Engelhard 2007] Engelhardt S., ”Regelung von Frequenzumrichtern für Windenergieanlagen mit doppelt gespeistem Asynchrongenerator“, 12. Kasseler Symposium Energie-Systemtechnik, pp 92-110, 22-23 November, 2007.

[Erlich 2006] Erlich I., Winter W., Dittrich A., “Advanced grid requirements for the integration of wind turbines into the German transmission system”, Power Engineering Society, General Meeting, 2006, IEEE, 7 pp, 18-22 June, 2006.

[Erlich 2007] Erlich I., Wrede H., Feltes C., “Dynamic Behavior of DFIG-Based Wind Turbines during Grid Faults”, Power Conversion Conference PCC '07, pp 1195-1200, Nagoya, Japan, 2-5 April, 2007.

[EU 2007] European Commission, “Communication from the Commission to the Council and the European Parliament, Renewable Energy Road Map, Renewable energies in the 21st century: building a more sustainable future”, 2007, www.ec.europa.eu/energy/energy_policy/doc/03_renewable_energy_roadmap_en.pdf, accessible November 2007.

[EWEA 2007] European Wind Energy Association, “Wind Power Installed in Europe by end of 2006 (cumulative)”, www.ewea.org, accessible November.

[Fortmann 2003] Fortmann J., “Validation of DFIG model using 1.5 MW turbine for the analysis of its behavior during voltage drops in the 110 kV grid”, Forth International Workshop on Large Scale Integration of Wind Power and Transmission Networks, 20th and 21st October, Billund, Denmark, 2003.

[Gail 2006] Gail G., Hansen A. D., Hartkopf T., "Controller design and analysis of a variable speed wind turbine with doubly-fed induction generator", European Wind Energy Conference EWEC, Athens, Greece, 2006.

[Grauers 1996a] Grauers A., "Efficiency of three wind energy generator systems", IEEE Transactions on Energy Conversion, Vol. 11, No. 3, pp. 650-657, September 1996.

[Grauers 1996b] Grauers A., "Design of Direct-driven Permanent-magnet Generators for Wind Turbines", PhD thesis, Department of Electric Power Engineering, Chalmers University of Technology, Göteborg, Sweden, 1996.

[Grauers 1999] Grauers A., Landström S., „The Rectifiers Influence on the Size of Direct-driven Generators", European Wind Energy Conference 1999, pp. 829-832, 1-5 March, Nice, France, 1999.

[Hansen 2002] Hansen A.D., Soerensen P., Blaabjerg F., Bech J., "Dynamic modelling of wind farm grid interaction", Wind Engineering, Volume 26, No. 4, pp. 191-210, July, 2002.

[Hansen 2003] Hansen A.D., Jauch C., Sørensen P., Iov F., Blaabjerg F., "Dynamic wind turbine models in power system simulation tool DIgSILENT", Risoe Report R-1400(EN), Risø National Laboratory, Denmark, 2003.

[Hansen 2004a] Hansen A.D., Iov F., Blaabjerg F., Hansen L.H., "Review of Contemporary wind turbine Concepts", Wind Engineering, Volume 28, No. 3, 2004.

[Hansen 2004b] Hansen A.D., Iov F., Sørensen P., Blaabjerg F., "Overall Control Strategy of variable speed induction generator wind turbine", Nordic Wind Power Conference, 1-2 march, Chalmers University of Technology, Göteborg, 2004.

[Hansen 2004c] Hansen A.D., Sørensen P., Iov F., Blaabjerg F., "Control of variable speed wind turbines with doubly-fed induction generators", Wind Engineering, Volume 28, No. 4, 2004.

[Hansen 2005] Hansen M.H., Hansen A.D., Larsen T. J., Øye S., Sørensen P., Fuglsang P., "Control design for a pitch regulated, variable speed wind turbine", Risø report R-1500, Risø National Laboratory, Denmark, 2005.

[Hansen 2007a] Hansen A.D., Hansen L., "Wind Turbine Concept Market Penetration over 10 Years (1995-2004)", Wind Energy, Volume 10, Issue 1, pp 81 – 97, January/February 2007.

[Hansen 2007b] Hansen A. D., Michalke G., Soerensen P., Lund T., Iov F., "Co-ordinated voltage control of DFIG wind turbines in uninterrupted operation during grid faults", Wind Energy, Volume 10, Issue 1, Pages 51-68, January/February 2007.

[Hansen 2007c] Hansen A.D., Michalke G., "Modelling and control of variable speed multi-pole PMSG wind turbine", submitted to Wind Energy, 2007.

[Hansen 2007d] Hansen A. D., Michalke G., "Fault ride-through capability of DFIG wind turbines", Renewable Energy, Volume 32, Issue 9, pp 1594-1610, July, 2007.

[Hansen 2007e] Hansen A. D., Michalke G., "Voltage grid support of DFIG wind turbines during grid faults", European Wind Energy Conference EWEC, Milan, Italy, 2007.

[Hennchen 2007] N. Hennchen, "Wind turbine converter fits E.ON Regulation", Frisia Schaltanlagen GmbH, www.frisia-schaltanlagen.de/data/grid_integration_of_wind_turbines.pdf, accessible November 2007.

[Holdsworth 2004] Holdsworth L., Charalambous I., Ekanayake J.B., Jenkins N., "Power system fault ride through capabilities of induction generator based wind turbines", Wind Engineering, Vol. 28, No 4, pp 399-412, 2004.

[Holttinen 2007] Holttinen H., "State-of-the-art of design and operation of power systems with large amounts of wind power – summary of IEA Wind collaboration", Workshop on Integration Studies, Tuesday 8th May, 2007, Power Point Presentation, European Wind Energy Conference EWEC, Milan–Italy, 7th –10th May 2007.

[Horns Rev 2007] DONG Energy, Vattenfall AB, "Horns Rev Offshore Wind Farm", www.hornsrev.dk, accessible November 2007.

[IEC 61400-1] International Standard IEC 61400-1, "Wind turbine generator systems – Part 1: Safety requirements" Second Edition 1999.

[Infineon 2007] Infineon Technologies AG, www.infineon.com, accessible November 2007.

[Iov 2004] Iov F., Hansen A.D., Sørensen P., Blaabjerg F "Wind Turbine Blockset in Matlab/Simulink General Overview and Description of the Models", Aalborg University, Denmark 2004.

[ISET 2007] ISET – Institut für Solare Energieversorgungstechnik, „Entwicklung der Windenergienutzung in Deutschland", http://reisi.iset.uni-kassel.de, accessible November 2007.

[Jauch 2004] Jauch C., Sørensen P., Bak-Jensen B. "International review of grid connection requirements for wind turbines". Nordic wind Power Conference, 6p., Chalmers University of Technology, 1-2 March, 2004.

[Jauch 2007] Jauch C., "Transient and Dynamic Control of a Variable Speed Wind Turbine with Synchronous Generator", Wind Energy, Volume 10, Issue 3, pp 247 – 269, May/June, 2007.

[Jöckel 2001] Jöckel S., Hagenkort B., Hartkopf T., Schneider H., "Direct-Drive Synchronous Generator System For Offshore Wind Farms with Active Drive Train Damping by Blade Pitching", European Wind Energy Conference EWEC 2001, 2nd-6th July, Copenhagen, Denmark, pp. 991-994, 2001.

[Jöckel 2002] Jöckel S., "Calculations of Different Generator Systems for Wind Turbines with Particular Reference to Low-Speed Permanent-Magnet Machines", PhD thesis, Technical University Darmstadt, 2002.

[Jöckel 2006] Jöckel S., VENSYS Energiesysteme GmbH, Germany, „High energy production plus built-in reliability – The new Vensys 70 / 77 gearless wind turbines in the 1.5 MW class", Paper no. 0583, European Wind Energy Conference EWEC, Athens, 2006.

[Kayikçi 2005] Kayikçi M., Anaya-Lara O., Milanović J. V., Jenkins N., "Strategies for DFIG voltage control during transient operation", 18th International Conference on Electricity Distribution, Turin, Italy, 6-9 June, 2005.

[Kayikçi 2006a] Kayikçi M., Milanović J. V., "Contribution of DFIG based wind plants to voltage and frequency recovery following system disturbances", Proceedings of the 6th International Workshop on Large-Scale Integration of Wind Power and Transmission Networks for Offshore Wind Farms, Delft, The Netherlands, pp 211-220, 26–28 October 2006.

[Kayikçi 2006b] Kayikçi M., Milanović J. V., "Assessing Transient Responses Of DFIG Based Wind Plants – The Influence Of Model Parameters And Simplifications", accepted for publication in the IEEE Transactions on Power Systems, TPWRS-0013-2006 (15/06/06), 2006

[Krause 2002] Krause P.C., Wasynczuk O., Sudhoff S. D., „Analysis of Electric Machinery and Drive Systems", 2nd Edition, IEEE Press, John Wiley and Sons, 2002

[Kundur 1994] P. Kundur, "Power System Stability and Control". McGraw Hill, 1994.

[Langreder 1996] Langreder W., "Models for Variable Speed Wind Turbines", Master thesis, CREST, Loughborough University, UK, Risø National Laboratory, Denmark, 1996.

[Leonhard 2001] Leonhard W., "Control of electrical drives", Springer Verlag Stuttgart, ISBN: 3-540-41820-2, 3rd edition, 2001.

[Lindholm 2004] Lindholm M., "Doubly Fed Drives for Variable Speed Wind Turbines - A 40kW laboratory setup", PhD thesis, Ørestad-DTU, Denmark, 2004.

[Lund 2007] Lund T., Sørensen P., Eek J., "Reactive power capability of the DFIG", Wind Energy, Volume 10, Issue 4, pp 379 – 394, July/August, 2007.

[Michalke 2007a] Michalke G., Hansen A., Hartkopf T., "Dynamic behaviour of a DFIG wind turbine subjected to power system faults", European Wind Energy Conference EWEC, Milan, Italy, 2007.

[Michalke 2007b] Michalke G., Hansen A., Hartkopf T., "Control strategy of a variable speed wind turbine with multipole permanent magnet synchronous generator", European Wind Energy Conference EWEC, Milan, Italy, 2007.

[Michalke 2007c] Michalke G., Hansen A., Hartkopf T., "Control of a wind park with doubly fed induction generators in support of power system stability in case of grid faults", European Wind Energy Conference EWEC, Milan, Italy, 2007.

[Michalke 2007d] Michalke G., Hansen A., Hartkopf T., "Fault ride-through and voltage support of permanent magnet synchronous generator wind turbines", ", Nordic Wind Power Conference NWPC, 1-2 November, Roskilde, Denmark, 2007.

[Milborrow 2003] Milborrow D., "Going Mainstream at the grid face", Windpower Monthly, pp 47-50, September, 2005.

[Mohan 1989] Mohan N., Undeland T. M., Robbins W. P., "Power Electronics: converters, application and design", John Wiley and Sons, 1989.

[Molinas 2005] Molinas M., Naess B., Gullvik W., Undeland T., "Control of Wind Turbines with Induction Generators Interfaced to the Grid with Power Electronics Converters", International Power Electronic Conference IPEC 2005, Niigata, Japan, 4 - 8 April, 2005.

[Morales 2007] Morales A., "Advanced Grid Requirements for the Integration of Wind Farms into the Spanish Transmission System", Power Point Presentation, European Wind Energy Conference EWEC, Milan–Italy, 7th –10th May 2007.

[Niiranen 2004] Niiranen J., "Voltage dip ride through of a doubly-fed generator equipped with an active crowbar", Nordic Wind Power Conference NWPC, 1-2 March, Chalmers University, Sweden, 2004.

[Niiranen 2006] Niiranen J., "Second Generation Active Crowbar for Doubly Fed Generators", Nordic Wind Power Conference NWPC, 22-23 May, Espoo, Finland, 2006.

[Novotny 1998] Novotny D. W., Lipo T. A., "Vector control and dynamics of AC drivers", Oxford University Press, 1998.

[Pena 1996] Pena R., Clare J. C., Asher G. M., "Doubly-fed induction generator using back-to-back PWM converters and its application to variable speed wind energy generation", IEE proceedings on electronic power application, 143(3), pp. 231-241, 1996.

[Pierik 2004] Pierik J., Morren J., de Haan S., van Engelen T., Wiggelinkhuizen E., Bozelie J., "Dynamic models of wind farms for grid-integration studies", Nordic Wind Power Conference NWPC, 1-2 March, Chalmers University, Sweden, 2004.

[Polinder 2004] Polinder H., de Haan S. W. H., Dubois M. R., Slootweg J., "Basic Operation Principles and Electrical Conversion Systems of Wind Turbines", NORPIE / 2004, Nordic Workshop on Power and Industrial Electronics, Paper 069, Trondheim, Norway, 14-16 June, 2004.

[Pöller 2003] Pöller M., Achilles S., "Aggregated Wind Park Models for Analyzing Power System Dynamics", Forth International Workshop on Large Scale Integration of Wind Power and Transmission Networks, 20th and 21st October, Billund, Denmark, 2003.

[Risø/DNV 2007] Risø National Laboratory, Det Norske Veritas, " Guidelines for Design of Wind Turbines", 2nd edition, 2007.

[Robles 2007] Robles E., Villate J.L., Ceballos S., Gabiola I., Zubia I., "Power electronics solutions for grid connection of wind farms", European Wind Energy Conference EWEC, Milan–Italy, 7th –10th May 2007.

[Rodriguez 2005] Rodriquez M., Abad G., Sarasola I., Gilabert A., "Crowbar control algorithms for doubly fed induction generator during voltage dips", European Conference on Power Electronics and Applications, 11-14 September, 2005.

[Seman 2006a] Seman S., "Transient performance analysis of wind-power induction generators", PhD thesis, Helsinki University of Technology, Department of Electrical and Communications Engineering, Laboratory of Electromechanics, Espoo, Finland, 2006.

[Seman 2006b] Seman S., Niiranen, J. Arkkio, A., "Ride-Through Analysis of Doubly Fed Induction Wind-Power Generator Under Unsymmetrical Network Disturbance", IEEE Transactions on Power Systems, Volume 21, Issue 4 pp 1782-1789, November, 2006.

[Semikron 2007] SEMIKRON International GmbH Deutschland Germany, www.semikron.de, accessible November 2007.

[Soens 2003] Soens J., De Brabandere K., Driesen J., Belmans R., "Doubly fed induction machine: Operating regions and dynamic simulation", 10th European Conference on Power Electronics and Applications (EPE 2003), 10 pages, Toulouse, France, September 2-4, 2003.

[Soerensen 2001] Sørensen P., Hansen A.D., Rosas P.A.C., "Wind models for prediction of power fluctuations from wind farms", Proc. The Fifth Asia-Pacific Conference on Wind Engineering (APCWEV), Kyoto, Japan, Journal of Wind Engineering no.89, pp. 9-18., 2001.

[Soerensen 2003] Soerensen P., Hansen A. D., Christensen P., Mieritz M., Bech J., Bak-Jensen B., Nielsen H., "Simulation and Verification of Transient Events in Large Wind Power Installations", Risø National Laboratory, Risø Report Risø-R-1331(EN), Denmark, October, 2003.

[Soerensen 2007] Soerensen P., Cutululis, N. A., Lund T., Hansen A. D.; Soerensen T., Hjerrild J., Donovan M. H., Christensen L., Kraemer Nielsen H, "Power Quality Issues on Wind Power Installations in Denmark", Power Engineering Society, General Meeting, 2007. IEEE Volume, Issue 24-28, pp 1 – 6, June 2007.

[Spooner 1996] Spooner E., Williamson A.C., "Direct coupled, permanent magnet generators for wind turbine applications", IEE Proceedings, Electr. Power Appl., Vol. 143, No. 1, January 1996.

[Sun 2005] Sun T., Chen Z., Blaabjerg F., "Transient Stability of DFIG Wind Turbines at an External Short-circuit fault", Wind Energy, Volume 8, Issue 3, pp 345 – 360, July/September, 2005.

[Svechkarenko 2005] Svechkarenko D., "Simulations and Control of Direct Driven Permanent Magnet Synchronous Generator", Nordic PhD course on Wind Power, Smøla, Norway 5-11 June 2005, www.elkraft.ntnu.no/smola2005/Topics/18.pdf, accessible November 2007.

[Tande 2003] Tande J. O. G., "Grid Integration of Wind Farms", Wind Energy, Volume 6, Issue. 3, pp. 281-295, 2003.

[Van der Hoven 1957] Van der Hoven I., "Power Spectrum of Horizontal Wind Speed in the Frequency Range from 0.0007 to 900 Cycles per Hour", Journal of Atmospheric Sciences, vol. 14, Issue 2, pp.160-164, 1957.

[von Joanne 2002] von Joanne A., Dai S., Zhang H., „A Multilevel Inverter Approach Providing DC-Link Balancing, Ride-Through Enhancement, and Common-Mode Voltage Elimination", IEEE transactions on Industrial Electronics, Vol. 49, No 4., August 2002.

[Westlake 1996] Westlake A. J. G., Bumby J.R., Spooner E., "Damping the power-angle oscillations of a permanent-magnet synchronous generator with particular reference to wind turbine applications", IEE Proceedings, Electr. Power Appl., Vol 143, No 3, May, 1996.

[Woodward 2007] Woodward SEG GmbH & Co KG, "CONCYCLE® Wind - Modular frequency converters with enhanced dynamic grid fault performance", www.woodward-seg.com, www.seg-pq.com, accessible November 2007.

12 Appendix

12.1 List of figures

12.2 List of tables

12.3 Abbreviations

AC	Alternating current
AS WF	Active stall wind farm
BP	Bandpass
DC	Direct current
DCSG	DC excited synchronous generator
DFIG	Doubly-fed induction generator
DFIG WF	Doubly-fed induction generator wind farm
DSL	DIgSILENT dynamic simulation language
EMT	Electromagnetic transients
GSC	Grid side converter
GTO	Gate-turn-off thyristor
GVRF	Grid voltage reference frame
HV	High voltage
IGBT	Insulated gate bipolar transistor
LP	Lowpass
LV	Low voltage
MPP	Maximum Power Tracking
MV	Medium voltage
PCC	Point of common coupling
PM	Permanent magnets
PMSG	Permanent magnet synchronous generator
PWM	Pulse width modulation
RMS	Root mean square
RRF	Rotor reference frame
RSC	Rotor side converter
SCIG	Squirrel cage induction generator
SFRF	Stator flux reference frame
SG	Synchronous generator
STI	Short term interruption
TSO	Transmission system operator
WFT	Wind farm terminal
WRIG	Wound Rotor induction generator

12.4 Nomenclature and Indices

Symbol	Unit	Quantity
a		Amplitude
C	F	Capacitance of DC-link capacitor
c_p		Power coefficient
$c_{p,opt}$		Optimal power coefficient
c_q		Torque coefficient
D_{shaft}	Nm/rad	Damping coefficient of the shaft
E	V	Electromotive force
f	Hz	Frequency
f_{osc}	Hz	Free-free-frequency
i	A	Space vector of the current
I_{AC}	A	AC current
$i_{conv,d}$	A	Converter current d-component
$I_{conv,d,meas}$	A	Measured d-current in grid side converter
$I_{conv,d,ref}$	A	Reference d-current in grid side converter
$i_{conv,q}$	A	Converter current q-component
$I_{conv,q,meas}$	A	Measured q-current in grid side converter
$I_{conv,q,ref}$	A	Reference q-current in grid side converter
I_d	A	d-component current
I_{DC}	A	DC-link current
I_f	A	Excitation current
I_m	A	Magnetizing current
im		Imaginary part
I_N	A	Rated current
I_Q	A	Reactive current
I_q	A	q-component current
I_{Q0}	A	Reactive current before the fault
I_{Qmax}	A	Maximum available reactive current
I_r	A	Rotor current
i_{rd}	A	Rotor current d-component
$I_{rd,meas}$	A	Measured rotor current d-component
$I_{rd,ref}$	A	Reference rotor current d-component
i_{rq}	A	Rotor current q-component
$I_{rq,meas}$	A	Measured rotor current q-component
$I_{rq,ref}$	A	Reference rotor current q-component
I_s	A	Stator current

Symbol	Unit	Quantity
i_{sd}	A	Stator current d-component
i_{sq}	A	Stator current q-component
ΔI_Q	A	Additional reactive current
J_{eq}	kg m^2	Equivalent inertia
J_{gen}	kg m^2	Generator inertia
J_{rot}	kg m^2	Aeordynamic rotor inertia
K_0		Sinusoidal PWM factor
K_{basis}		Basis gain of gain-scheduling
k_{gear}		Gearbox ratio
K_{PI}		PI controller gain
K_{shaft}	Nm/rad	Shaft stiffness
$K_{shaft,eff}$	Nm/rad	Effective shaft stiffness
K_{system}		Gain of the total pitch system
L	m	Length scale in prevailing wind direction
L_d	H	Stator inductance d-component
L_m	H	Main inductance of the DFIG
L_q	H	Stator inductance q-component
L_r	H	Rotor inductance
$L_{r\sigma}$	H	Rotor leakage inductance
L_s	H	Stator inductance
$L_{s\sigma}$	H	Stator leakage inductance
m		Number of phases
m		Pulse with modulation index
n	rpm	Speed
n_{rated}	rpm	Rated speed
n_{syn}	rpm	Synchronous speed
P	W	Power
p		Pole pairs
P_δ	W	Airgap Power
P_{AC}	W	AC-side power
P_{conv}	W	Active power of the converter
$P_{current}$	W	Actual active power measured in the connection point (during fault)
P_{DC}	W	DC-side power
P_e	W	Electrical power
P_{GenSC}	W	Active power of the generator side converter
P_{Grid}	W	Active grid power

Symbol	Unit	Quantity
$P_{\text{Grid,meas}}$	W	Measured grid power
$P_{\text{Grid,ref}}$	W	Reference grid power
P_{GridSC}	W	Active power of the grid side converter
P_{loss}	W	Losses
$P_{\text{loss,r}}$	W	Rotor winding losses
$P_{\text{loss,s}}$	W	Stator winding losses
P_{md}		PWM signal d-component
P_{mech}	W	Mechanical Power
P_{mq}		PWM signal q-component
P_{r}	W	Rotor Power
P_{rot}	W	Aerodynamic power
P_{s}	W	Stator Power
$P_{\text{t=0}}$	W	Power measured in the connection point immediately before the fault
$P_{\text{windturbine,rated}}$	W	Rated wind turbine power
PWM		PWM factor
PWM_{i}		Imaginary part of the PWM factor
PWM_{r}		Real part of the PWM factor
Q	Var	Reactive power
Q_{conv}	Var	Reactive power of the converter
$Q_{\text{conv,meas}}$	Var	Measured reactive power of the converter
$Q_{\text{conv,ref}}$	Var	Reference reactive power of the converter
Q_{Grid}	Var	Reactive grid power
$Q_{\text{Grid,meas}}$	Var	Measured reactive grid power
$Q_{\text{Grid,ref}}$	Var	Reference reactive grid power
Q_{s}	Var	Stator reactive power
R	m	Wind turbine radius
$R_{Crowbar}$	Ω	Crowbar resistant
re		Real part
R_{f}	Ω	Fault resistance
R_{r}	Ω	Rotor resistant
R_{s}	Ω	Stator resistant
S	VA	Apparent power
S	m/s	Spectral energy distribution
s		Slip
S_{conv}	VA	Apparent power of the converter
SCR		Short circuit ratio

Symbol	Unit	Quantity
SCR_{PCC}		Short circuit ratio in point of common coupling
S_k	VA	Short circuit power
s_L		No-load slip
T	Nm	Torque
t	s	Time
T_e	Nm	Electromagnetic torque
T_{gen}	Nm	Mechanical generator torque
t_p	s	Time of one period
T_{rot}	Nm	Aerodynamic torque
T_{Servo}	s	Servo time constant
T_{shaft}	Nm	Shaft torque
U	V	Voltage
u	V	Space vector of the voltage
U_0	V	Voltage before the fault
U_0	m/s	Mean wind speed
U_{AC}	V	AC-voltage
$U_{AC,i}$	V	AC-voltage imaginary part
$U_{AC,r}$	V	AC-voltage real part
$u_{conv,d}$	V	Converter voltage d-component
$u_{conv,meas}$	V	Measured converter voltage
$u_{conv,q}$	V	Converter voltage q-component
$u_{conv,ref}$	V	Reference converter voltage
$U_{current}$	V	Actual voltage measured in the connection point (during fault)
U_d	V	d-component rotor voltage
U_{DC}	V	DC-link voltage
$U_{DC,meas}$	V	Measured DC-link voltage
$U_{DC,ref}$	V	Reference DC-link voltage
$U_{DC,setpoint}$	V	DC-voltage setpoint
U_{grid}	V	Grid voltage
$u_{grid,meas}$	V	Measured grid voltage
$u_{grid,ref}$	V	Reference grid voltage
U_h	V	Voltage representing the main field
U_q	V	q-component rotor voltage
U_r	V	Rotor voltage
$U_{r,real}$	V	Real part of rotor voltage
U_s	V	Stator voltage

Symbol	Unit	Quantity
u_s	V	Stator voltage
$U_{s,meas}$	V	Measured stator voltage
$U_{s,ref}$	V	Reference stator voltage
u_{sd}	V	Stator voltage d-component
u_{sq}	V	Stator voltage q-component
$U_{t=0}$	V	Voltage in the connection point immediately before the voltage fault
Δu_{damp}	V	Oscillating DC-voltage offset
ΔU_{DC}	V	Allowed DC-link voltage ripple
Δu_{osc}	V	Sinusoidal disturbance signal
v_w	m/s	Wind speed
x_d	Ω	Synchronous reactance d-component
x_d'	Ω	Transient synchronous reactance d-component
x_d''	Ω	Subtransient synchronous reactance d-component
X_f	Ω	Fault reactance
X_f	Ω	Field winding reactance
X_h	Ω	Main reactance of the PMSG
X_m	Ω	Main reactance of the DFIG
x_q	Ω	Synchronous reactance q-component
x_q'	Ω	Transient synchronous reactance q-component
x_q''	Ω	Subtransient synchronous reactance q-component
$X_{r\sigma}$	Ω	Rotor leakage reactance
$X_{s\sigma}$	Ω	Stator leakage reactance
Z_{grid}	Ω	Grid impedance
λ		Tip speed ratio
λ_{opt}		Tip speed ratio at optimal c_p
δ		Logarithmic decrement
δ	deg	Load angle
θ	deg	Pitch angle
θ_{gen}	deg	Generator shaft angular position
θ_{opt}	deg	Pitch angle at optimal c_p
θ_{ref}	deg	Reference pitch angle
θ_{rot}	deg	Aerodynamic rotor shaft angular position
φ		Power factor
ρ	kg/m^3	Air density

Symbol	Unit	Quantity
ψ	Vs	Space vector of the flux
ψ_f	Vs	DC excited flux
ψ_{PM}	Vs	Permanent magnet flux
ψ_r	Vs	Rotor flux
ψ_s	Vs	Stator flux
ψ_{sd}	Vs	Stator flux d-component
ψ_{sq}	Vs	Stator flux q-component
σ^2	m^2/s^2	Variariance
ξ		Damping ratio
ω_{gen}	rad/s	Rotational generator speed
$\omega_{gen,meas}$	rad/s	Measured rotational generator speed
$\omega_{gen,ref}$	rad/s	Reference rotational generator speed
ω_r	rad/s	Electrical frequency of the rotor
ω_s	rad/s	Electrical frequency (angular velocity) of the stator
ω_{syn}	rad/s	Generator synchronous speed
Ω_{gen}	rad/s	Generator mechanical speed
Ω_{rot}	rad/s	Rotational speed of the aerodynamic rotor
Ω_{syn}	rad/s	Generator synchronous speed

Indices	Quantity
0	Mean
0	Immediately before the fault
AC	Alternating current
basis	Basis gain of gain-scheduling
conv	Converter
Crowbar	Crowbar
current	Actual value
d	d-component
damp	Damping
DC	Direct current
e	Electrical
eff	Effective
eq	Equivalent
f	Field
f	Fault
gear	Gearbox

Indices	**Quantity**
gen	Generator
GenSC	Generator side converter
Grid	Grid
GridSC	Grid side converter
h	Main field
i	Imaginary
L	No-load
loss	Losses
m	Main field
max	Maximum
meas	Measured
mech	Mechanical
N	Rated
opt	Optimal
osc	Oscillating
p	Power
PCC	Point of common coupling
PI	PI-Controller
PM	Permanent magnets
q	Torque
q	q-component
Q	Reactive
r	Rotor
r	Real
rated	Rated
real	Real
ref	Reference
rot	Aerodynamic Rotor
s	Stator
Servo	Servo mechanism
setpoint	Setpoint
shaft	Shaft
syn	Synchronous
system	Total gain of the system
w	Wind
δ	Airgap
σ	Leakage

12.5 Design of the mechanical system of the 2 MW wind turbine

The most relevant data of the aerodynamical and mechanical system of the wind turbine is given in Table 12.1. The data is valid for both wind turbine concepts, the DFIG wind turbine as well as the PMSG wind turbine.

Rotor diameter	80 m
Rotor inertia	8.6 10^6 kg m^2
Air density	1.225 kg/m^3
Tip speed ratio	70 m/s
Rotational rotor speed	9...16.7 rpm dyn. 19 rpm
Optimal pitch angle	0 deg
Servo time constant	0.1 s
Pitch angle limits	0....30 deg
Pitch angle rate of change limitation	10 deg/s

Table 12.1: Data of the wind turbine´s mechanical system

12.6 Design of the electrical system of the DFIG wind turbine

The single line diagram of the DFIG wind turbine implemented in the simulation software DIgSILENT Power Factory is shown in Figure 12.1.

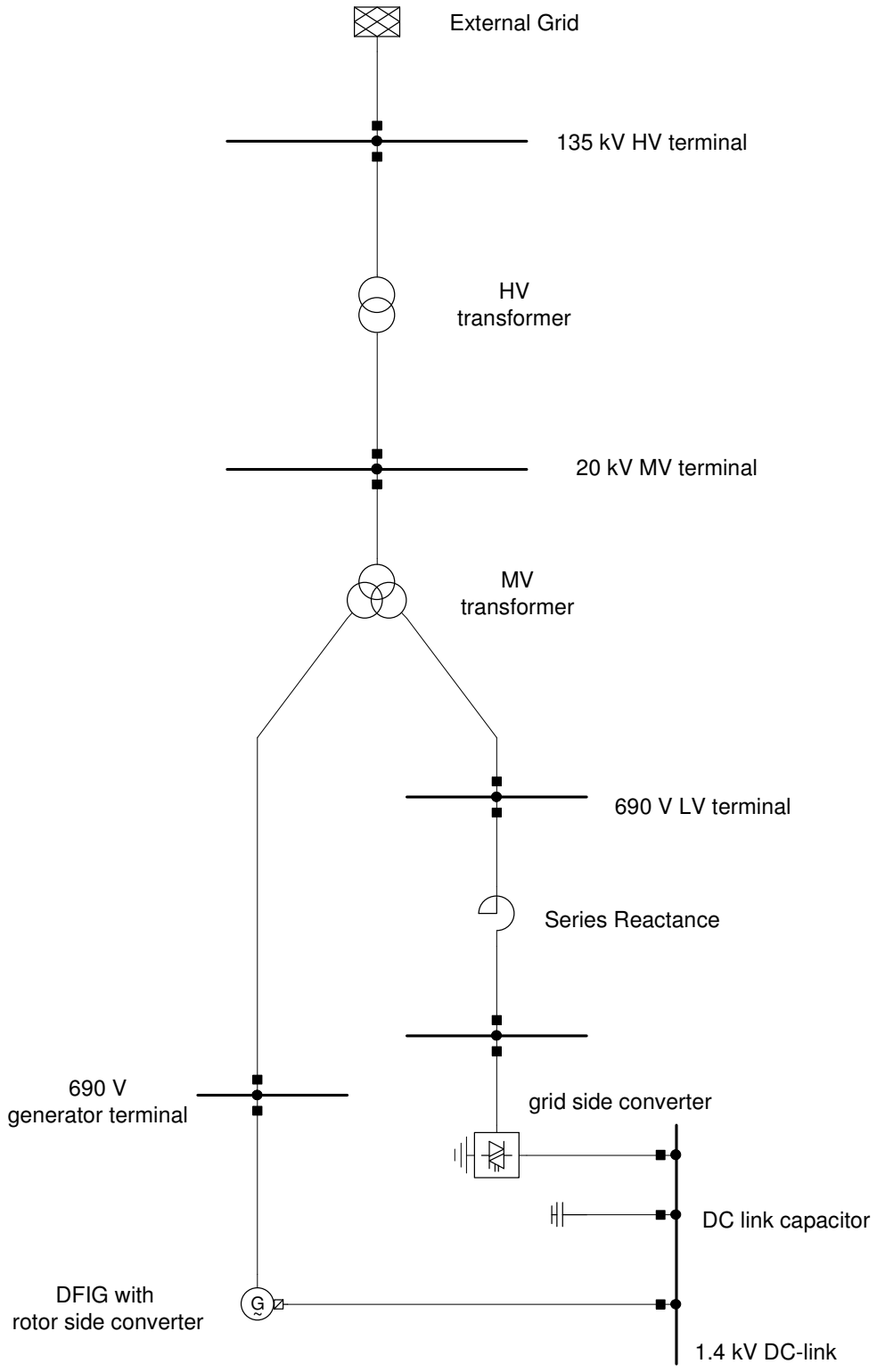

Figure 12.1: Single line diagram of the DFIG wind turbine in DIgSILENT Power Factory

The most relevant data of the DFIG wind turbine´s electrical system is given in Table 12.2.

Apparent power	2.21 MVA
Generator active power (p.u. base)	2 MW
Rating of the IGBT back-to-back voltage source converter	0.9 MVA
Stator voltage	690 V
Rated speed	1686 rpm
Pole pairs	2
Synchronous speed (p.u. base)	1500 rpm (= 1p.u.)
Speed range	800 rpm...1686 rpm dynamic limit 1920 rpm
Generator inertia	150.9 kg m^2
Gear ratio	101
DC-link voltage	1.4 kV
DC-link capacitor	1461 µF

Table 12.2: Data of the DFIG wind turbine´s electrical system

12.7 Total control structure of the DFIG wind turbine

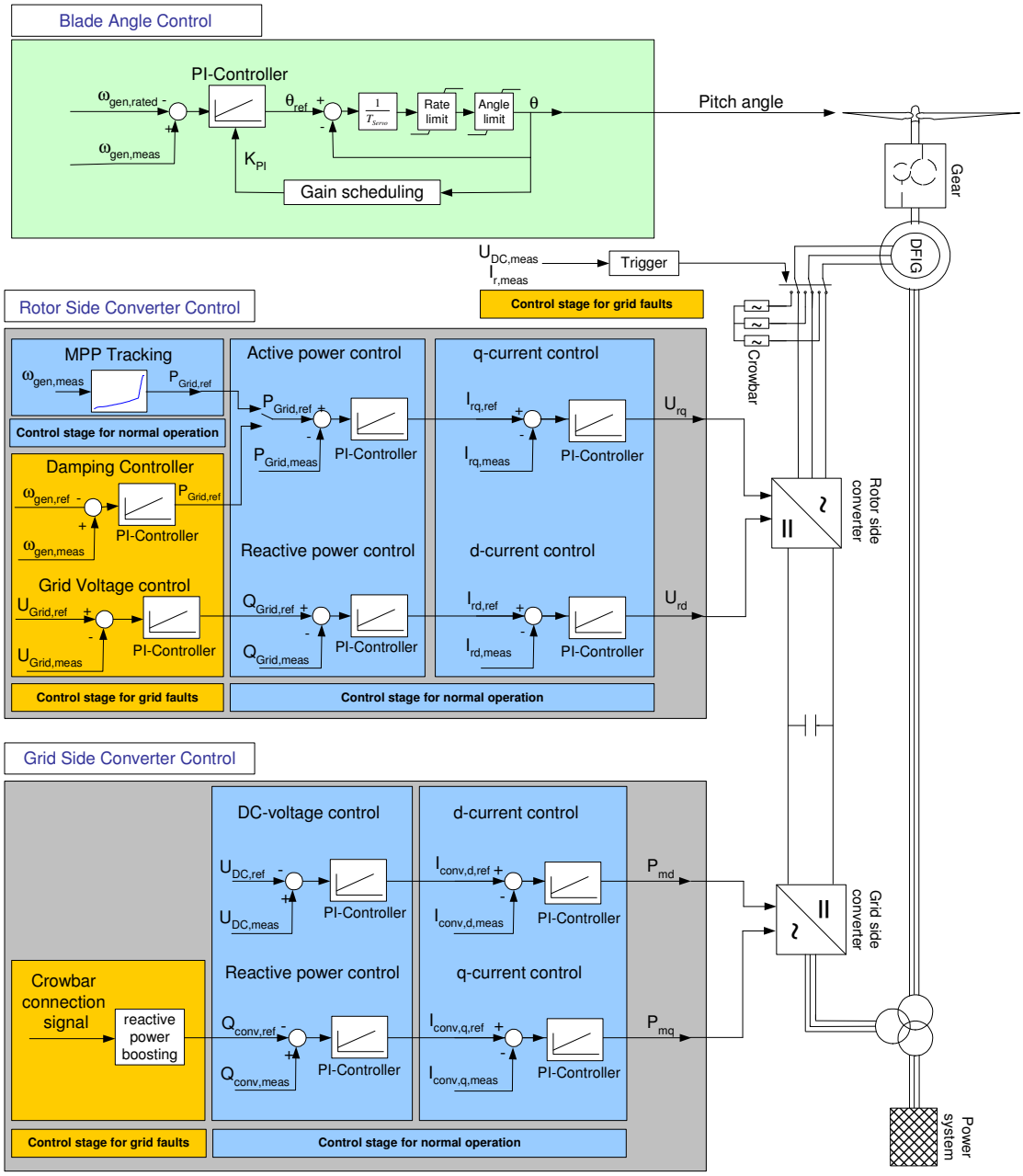

Figure 12.2: Total control structure of the DFIG wind turbine: control stage for normal operation and for grid faults

12.8 Design of the electrical system of the PMSG wind turbine

The single line diagram of the PMSG wind turbine implemented in the simulation software DIgSILENT Power Factory is shown in Figure 12.3.

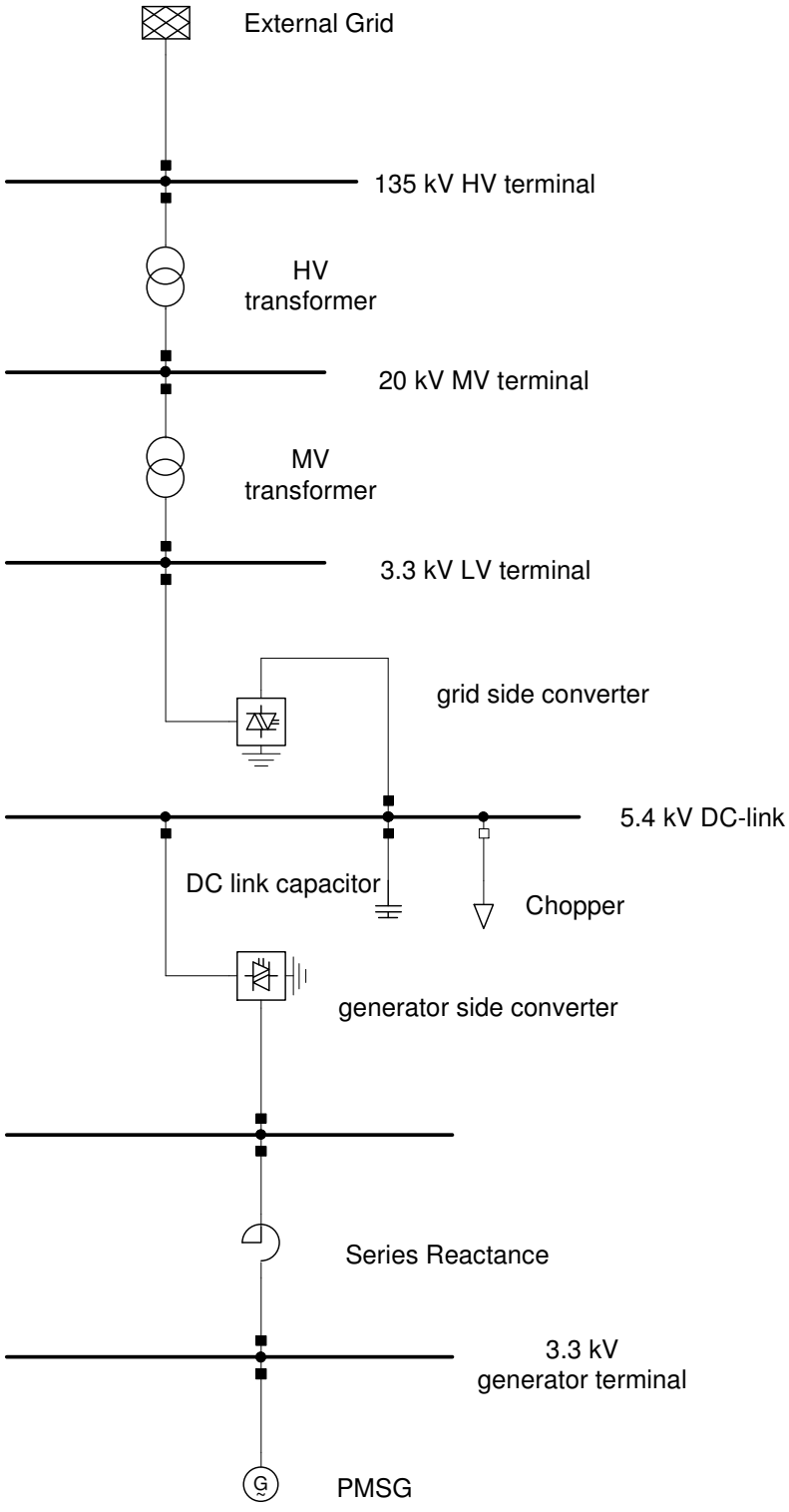

Figure 12.3: Single line diagram of the PMSG wind turbine in DIgSILENT Power Factory

The most relevant data of the PMSG wind turbine´s electrical system is given in Table 12.3.

Apparent power	2.2 MVA
Generator active power (p.u. base)	2 MW
Rating of the IGBT back-to-back voltage source converter	2.5 MVA
Stator voltage	3.3 kV
Pole pairs	48
Speed range	9...16.7 rpm dynamic limit 19 rpm
Frequency range generator side converter	5.7...13.37 Hz
Rated speed (p.u. base)	16.7 rpm (=1 p.u.)
Generator inertia	$1.3\ 10^6$ kg m^2
DC link voltage	5.4 kV
DC-link capacitor	2400 µF

Table 12.3: Data of the PMSG wind turbine´s electrical system

12.9 Total control structure of the PMSG wind turbine

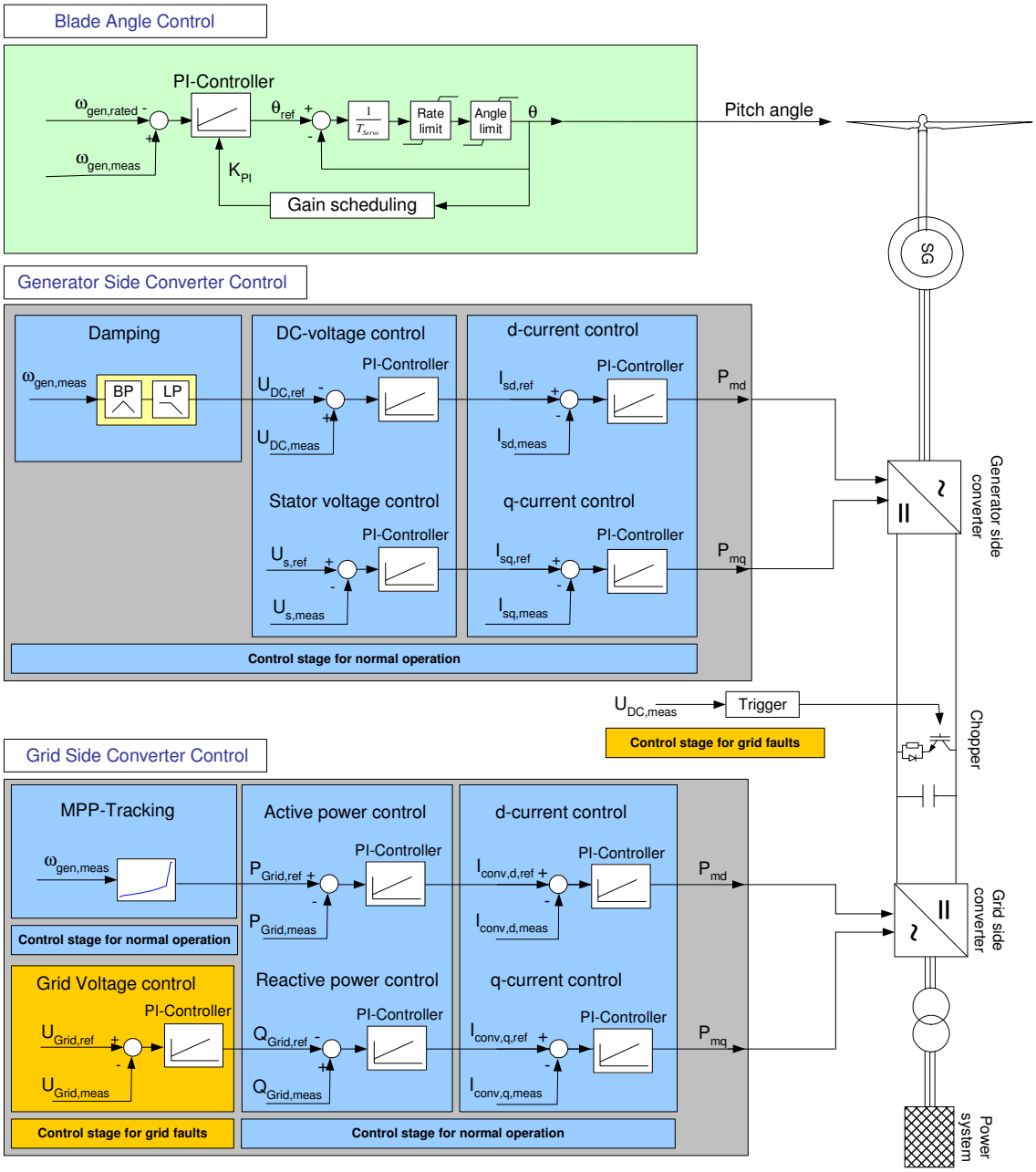

Figure 12.4: Total control structure of the PMSG wind turbine: control stage for normal operation and for grid faults

12.10 Detailed line diagram of the generic power transmission system model

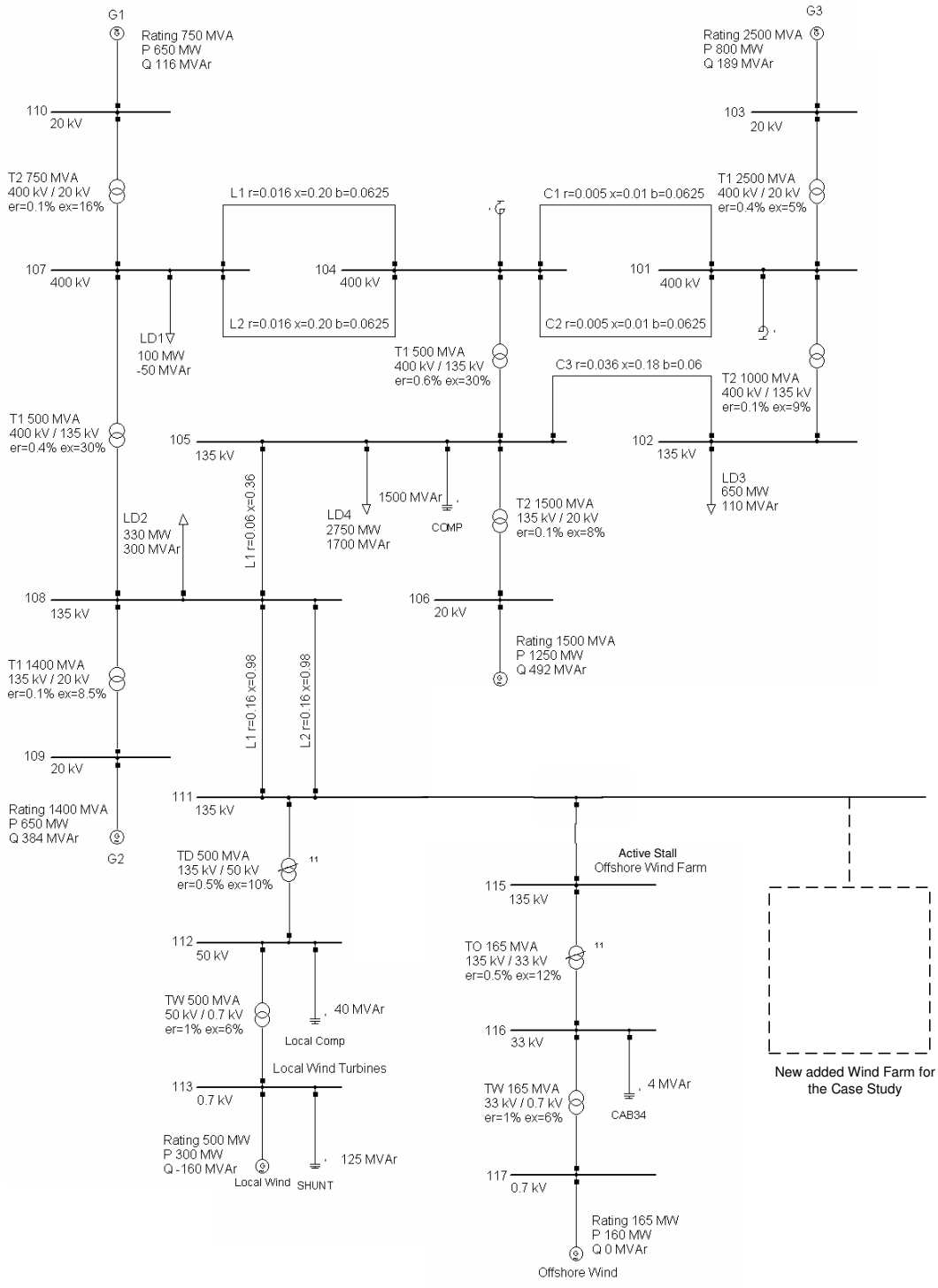

Figure 12.5: Single line diagram of the generic power transmission system model in DIgSILENT Power Factory [Akhmatov 2006b]

Publications

Peer-reviewed papers and articles

G. Michalke, A. Hansen, “Variable Speed Wind Turbines - Modelling, Control and Impact on Power Systems”, European Wind Energy Conference EWEC, Brussels, Belgium, March-April 2008.

A. Hansen, G. Michalke, “Modelling and control of variable speed multi-pole PMSG wind turbine”, accepted for Wind Energy, submitted in September 2007.

A. Hansen, G. Michalke, “Fault ride-through capability of DFIG wind turbines”, Renewable Energy 2007, Volume 32, Issue 9, pp 1594-1610, July 2007.

A. Hansen, G. Michalke, “Voltage grid support of DFIG wind turbines during grid faults”, European Wind Energy Conference EWEC, Milan, Italy, 7. – 10. May 2007.

A. Hansen, G. Michalke, P. Soerensen, T. Lund, F. Iov, “Co-ordinated voltage control of DFIG wind turbines in uninterrupted operation during grid faults”, Wind Energy, Volume 10, Issue 1, pp 51-68, January/February 2007.

G. Gail, E. Tröster, T. Hartkopf, “Static and Dynamic Measurements of a Permanent Magnet Induction Generator: Test Results of a New Wind Generator Concept”, Recent Developments of Electrical Drives, Best Papers from the International Conference on Electrical Machines ICEM´04, Springer 2006, Editors: Slawomir Wiak, M. Dems and K.Komeza

Article and conference papers

G. Michalke, A. Hansen, T. Hartkopf, “Variable speed wind turbines – fault ride-through and grid support capabilities”, awarded with the ewec2008 Power Award, European Wind Energy Conference EWEC, Brussels, Belgium, March-April 2008.

A. Hansen, G. Michalke, “Modelling and fault ride-through capability of a full converter wind turbine with multi-pole PMSG “,European Wind Energy Conference EWEC, Brussels, Belgium, March-April 2008.

G. Michalke, A. Hansen, T. Hartkopf, G. Scheuermann, “Windparkregelung zur Unterstützung der Netzstabilität im Fehlerfall“, Zwölftes Kasseler Symposium Energie-Systemtechnik, November 2007.

G. Michalke, A. Hansen, T. Hartkopf, “Fault ride-through and voltage support of permanent magnet synchronous generator wind turbines”, Nordic Wind Power Conference NWPC, Roskilde, Denmark, November, 2007.

G. Michalke, A. Hansen, T. Hartkopf, “Control strategy of a variable speed wind turbine with multipole permanent magnet synchronous generator”, European Wind Energy Conference EWEC, Milan, Italy, 7. – 10. May 2007.

G. Michalke, A. Hansen, T. Hartkopf, “Control of a wind park with doubly fed induction generators in support of power system stability in case of grid faults”, European Wind Energy Conference EWEC, Milan, Italy, 7. – 10. May 2007.

G. Michalke, A. Hansen, T. Hartkopf, “Dynamic behaviour of a DFIG wind turbine subjected to power system faults”, European Wind Energy Conference EWEC, Milan, Italy, 7. – 10. May 2007.

E. Spahic, J. Morren, G. Balzer, G. Michalke, “Mathematical Model of the Double Fed Induction Generator for Wind Turbines and its Control Quality”, International Conference on Power Engineering, Energy and Electrical Drives, Setúbal, Portugal, 12. – 14. April, 2007.

G. Michalke, “Erfahrungsbericht zum Auslandsaufenthalt am Forschungsinstitut Risø in Dänemark gefördert durch den Herbert-Kind-Preis“, ETG Mitgliederinformation, Nr. 1, Energietechnische Gesellschaft im VDE 2007.

G. Michalke, A. Hansen, T. Hartkopf, “Regelung eines Windparks mit doppelt gespeisten Asynchronmaschinen zur Unterstützung der Netzstabilität im Fehlerfall“, VDE Kongress, Aachen, Germany, 23.-25. October 2006.

G. Michalke, A. Hansen, T. Hartkopf, “Regelung eines Windparks mit doppelt gespeisten Asynchronmaschinen zur Unterstützung der Netzstabilität im Fehlerfall“, ETG Mitgliederinformation, Energietechnische Gesellschaft im VDE, Nr. 2, 2006.

G. Gail, A. Hansen, T. Hartkopf, “Controller design and analysis of a variable speed wind turbine with doubly-fed induction generator”, European Wind Energy Conference EWEC, Athens, Greece, February-March 2006.

E. Tröster, G. Gail, T. Hartkopf, “A New Control Concept for Offshore Wind-Parks - Constant Speed Turbines on a Grid with Variable Frequency“, European Wind Energy Conference EWEC, London, UK, 22.-25. November 2004.

E. Tröster, G. Gail, T. Hartkopf, “Analysis of the Equivalent Circuit Diagram of a Permanent Magnet Induction Machine“, 16th International Conference on Electrical Machines, ICEM, Cracow, Poland – Paper No. 664, 5.-8. September 2004.

G. Gail, E. Tröster, T. Hartkopf, “Static and Dynamic Measurements of a Permanent Magnet Induction Generator: Test Results of a New Wind Generator Concept“, 16th International Conference on Electrical Machines, ICEM, Cracow, Poland – Paper No. 666, 5.-8. September 2004.

Unpublished reports

1. – 6. Progress report of the project „Investigation of the Technical Aspects of Grid Connection of Offshore Windparks“, Stiftung Energieforschung Baden-Württemberg, 11/2003-07/2006

Supervised student projects

K. Healey, “Simulation of Wind Conditions for Offshore Wind Farms”, Bachelor thesis, Technical University Darmstadt, June 2004.

A. Dreschinski, “Comparison of Different Control Strategies for Permanent Magnet Synchronous Generators for Use in Wind Power Plants”, Diploma thesis, Technical University Darmstadt, July 2005

S. Geisen, “Bestimmung der Stromgestehungskosten eines Offshore-Windparks bestehend aus Anlagen mit doppelt gespeister Asynchronmaschine“, Study thesis, Technical University Darmstadt, April, 2006.

J. Andresen, “Bestimmung der Stromgestehungskosten eines Offshore-Windparks bestehend aus Anlagen mit permanenterregter Synchronmaschine”, Study thesis, Technical University Darmstadt, April, 2006.

K. Kolharkar, “Grid Integration of Decentralized Power Plants”, Master thesis, Technical University Darmstadt, July 2006.

G. Scheuermann, “Erfüllung der Netzanschlussregeln von Windkraftanlagen“, Study thesis, Technical University Darmstadt, October, 2007.

S. Bechtold, “Fault Ride-Through von Windkraftanlagen mit doppeltgespeisten Asynchronmaschinen“, Study thesis, Technical University Darmstadt, October, 2007.

Acknowledgements

This PhD work was carried out during the years 2003 to 2007 while I was working as a PhD student at the Department of Renewable Energies of Darmstadt Technical University in Germany and the Wind Energy Department of Risø National Laboratory in Denmark. In many ways I am deeply indebted to all the people, who contributed to this work.

Especially, I want to thank my supervising professor, Prof. Dr.-Ing. Thomas Hartkopf, the head of the Department of Renewable Energies, for all his advisory help and his unremitting belief in the success of this work. I would like to thank all my colleagues at the Department of Renewable Energies for all their technical, professional and administrative support. I want in special thank my colleague Eckehard Tröster for many inspiring discussions, encouragement and professional help as well as for the proofreading of this work.

I want to express my gratitude to all students, who participated in projects related to my PhD work. My thanks go to Kathryn Healey, Stefan Rotenbücher, Andreas Schiffler, Kedar Kolharkar, Stephan Geisen, Julia Andresen, Sebastian Bechtold and Garvin Scheuermann.

My PhD work was furthermore co-supervised at Risø National Laboratory. During my PhD project I was able to visit Risø National Laboratory in Denmark for four longer research periods. It is a pleasure for me to take the opportunity to thank all my colleagues in the research group “Wind Energy Systems” at the Wind Energy Department of Risø. I want to thank for their hospitality and the really good working atmosphere I experienced at Risø. My colleagues at Risø made me feel entirely integrated as an equal colleague as if I worked there continuously. Especially, I want to thank Poul Sørensen for initiating the co-supervision of my PhD at Risø. I also thank Søren Larsen for the co-ordination of the educational program at Risø.

My greatest thanks go to the person, who aided me most during my PhD work. I would like to express my deepest gratitude to Dr.-Ing. Anca Hansen, my co-supervisor at Risø National Laboratory, for all her guidance and support as well as teaching me numerous skills of doing scientific work. I thank for all her critics, encouragement, patience and also for teaching me the Danish language. Moreover, I want to thank Anca Hansen´s family for all their hospitality during my stays in Denmark.

A special acknowledgement is given to Vladislav Akhmatov for his advisory help and support.

I want to thank all other people, who have followed and contributed to the project, which I cannot all name separately here.

Finally, I owe my gratitude to my family, my brothers and sisters, my parents, grandparents and parents-in-law, for all their support during my personal and professional education.

I am mostly indebted to the person being closest to me, my husband Thomas Michalke, for his unremitting encouragement, approvals, acknowledgements and his love.

I want to thank God for his help and his mercy.
“God gave not to us the spirit of dread, but of virtue, and of love, and of soberness” (Tim. 1,7)

Curriculum Vitae

Name:	Gabriele Michalke, née Gail
Date of birth:	September 21 1978
Place of birth:	Dillenburg
Family status:	Married

School:

1985 – 1989	Grundschule Nanzenbach (grammar school)
1989 – 1998	Gymnasium Wilhelm-von-Oranien-Schule Dillenburg
22.06.1998	Abitur

Studies:

1998 – 2003	Darmstadt Technical University, Germany Electrical Engineering
06/2003 – 09/2003	Diploma thesis at ELIN EBG Motoren GmbH, Austria
09/2003	Diploma

PhD

11/2003-10/2007	Research assistant at Darmstadt Technical University, Institute of Electrical Power Systems, Department of Renewable Energies
08/2004 - 10/2004	Research periods at Risø National Laboratory, Denmark
08/2005 - 10/2005	
08/2006 - 10/2006	
04/2007 – 06/2007	

Awards and Scholarships

11/2002	Carl-Schenck-Preis, 5000 Euro
10/2006	Herbert-Kind-Preis of the VDE, 8000 Euro
07/2006	Scholarship of the German Academic Exchange Service